

Elucidating the Role of Antigen-presenting Cells in the Immunopathogenesis of the Porcine Reproductive and Respiratory Syndrome Virus

A thesis submitted to the
College of Graduate and Postdoctoral Studies
In partial fulfillment of the Requirements
For the Degree of Doctor of Philosophy
In the Department of Veterinary Microbiology, WCVM,
University of Saskatchewan,
Saskatoon

By

Joseph Andikpeme Darbellay

Copyright Joseph Andikpeme Darbellay, May, 2019.

All right reserved

PERMISSION TO USE

In presenting this thesis/dissertation in partial fulfillment of the requirements for a Postgraduate degree from the University of Saskatchewan, I agree that the Libraries of this University may make it freely available for inspection. I further agree that permission for copying of this thesis/dissertation in any manner, in whole or in part, for scholarly purposes may be granted by the professor or professors who supervised my thesis/dissertation work or, in their absence, by the Head of the Department or the Dean of the College in which my thesis work was done. It is understood that any copying or publication or use of this thesis/dissertation or parts thereof for financial gain shall not be allowed without my written permission. It is also understood that due recognition shall be given to me and to the University of Saskatchewan in any scholarly use which may be made of any material in my thesis/dissertation.

Requests for permission to copy or to make other uses of materials in this thesis/dissertation in whole or part should be addressed to:

Dean of the Western College of Veterinary Medicine
52 Campus Drive, S7N 5B4
University of Saskatchewan,
Saskatoon

OR

Dean
College of Graduate and Postdoctoral Studies
University of Saskatchewan
116 Thorvaldson Building, 110 Science Place
Saskatoon, Saskatchewan S7N 5C9 Canada

ABSTRACT

The porcine reproductive and respiratory syndrome virus (PRRSV) is a positive sense single-stranded RNA virus of the *arteriviridae* family and is one of the most economically devastating pathogens in the swine industry today. The PRRSV was discovered in the early 1990s in Europe and the United States, with strains being divided into Type 1 and Type 2 genotypes, respectively. Disease outcomes range from being asymptomatic to upwards of 100% mortality in herds, being attributable to the pathogenicity of the PRRSV strain, to co-infections with opportunistic pathogens, and to the age and breed of the pig. Animals subject to infection with PRRSV exhibit an array of clinical symptoms, including but not limited to, respiratory difficulty and pneumonia, weight loss, immune suppression leading to secondary bacterial infections, and spontaneous abortions/fetal mummification, from which the majority of the economic losses stem. Immunization with modified live vaccines are the most popular intervention to control disease, and although they are effective in improving health status of animals, the currently distributed vaccines pose a risk of reversion to virulence and afford limited cross protection amongst circulating strains of the virus. Thus, there is a high demand for a safe and effective vaccine.

The goal of this study was to investigate the role of specific antigen-presenting cell (APC) subsets during the pathogenesis of PRRSV and to further understand the progression to T cell immunity in response to PRRSV. To accomplish this, we chose to investigate the susceptibility of bone marrow-derived dendritic cells (BMDCs), monocyte-derived dendritic cells (MoDCs), and monocyte-derived macrophages (MoMΦs). After successfully differentiating and characterizing BMDCs from hematopoietic stem cells isolated from the sternum of animals, we demonstrated that PRRSV infection is restricted only to APCs that express CD163. Furthermore, we showed that PRRSV replicates more quickly in MoMΦ cell cultures than in CD163+ BMDC cultures and potentially in MoDCs. We continued to investigate PRRSV infection of APCs and discovered that in non-infected MoDCs, the cellular protein gamma actin 1 associates closely with MHCII. When MoDCs were infected with PRRSV, gamma actin 1 was no longer associated with MHCII. We hypothesize that PRRSV could be

manipulating the actin cytoskeleton, potentially interfering with MHCII peptide presentation.

Ultimately, we were interested in the interaction of APCs with T cells. In order to study this interaction, we developed an assay utilizing a mixed leukocyte reaction (MLR). Our hypothesis was confirmed in the MLR that showed M1 MoMΦs (IFN- γ stimulated) are more potent inducers of cytotoxic lymphocyte (CTLs) and CD4 α^+ T cell proliferation than M2 MoMΦs (IL-4 stimulated) or M0 MoMΦs (non-stimulated). In addition, our results indicated that gamma delta ($\gamma\delta$) T cells did not participate in the MLR. Next we proceeded with an animal trial investigating the interaction of APCs with T cells in a PRRSV-antigen specific manner.

The objective of the trial was to investigate the progression to T cell immunity during a PRRSV infection. We used a commercial swine-influenza vaccine as a positive control antigen, and as a comparative measure for the T cell immune response to PRRSV. Our results indicated that PRRSV infection of APCs does not interfere with the ability of APCs to promote T cell proliferation. We detected IFN- γ secreting cells in PBMCs two weeks post infection, and T cell proliferation was evident in all lymphoproliferative cell cultures two weeks post infection. A comparison between MoMΦ-T cell co-cultures and MoDC-T cell co-cultures indicated that MoDCs may be more potent stimulators of central memory Th cell proliferation. Lastly, PRRSV infected animals showed a higher capacity to promote the proliferation of T cells specific for swine-influenza A virus, potentially signifying that the general monocyte population from PRRSV infected animals acquired an activated state as a result of the infection.

Overall, the work in this thesis allowed us to formulate a theory regarding the dysregulated immune response to PRRSV. A characteristic adaptive immune response to PRRSV includes the early appearance of non-neutralizing antibodies (within a week), a delayed induction of T cell immunity (2-3 weeks post infection), with neutralizing antibodies becoming detectable roughly 4 weeks post infection, correlating to the resolution of illness. We believe that specific subsets of DCs are responsible for the induction of T cell immunity, and the rarity of this DC population(s) causes a delay in the induction of the T cell immune response. Furthermore, the delayed induction of T cell

immunity would affect the humoral immune response. In the absence of CD4⁺ follicular T helper cells, B cells would not be able to undergo proper somatic hypermutation and the result would be a state of hypergammaglobulinemia, similar to what is observed early during a PRRSV infection with non-neutralizing antibodies and auto-antibodies. The results herein support our theory, and contribute to the general knowledge surrounding the immunopathogenesis of PRRSV. Future work investigating the mechanisms by which PRRSV hinders the progression to adaptive immunity could prove to be fundamental in the development of a novel vaccine.

ACKNOWLEDGEMENTS

I would like to express my gratitude to my supervisor Dr. Volker Gerdts for providing me with the opportunity to work in his lab. Furthermore, I'd like to thank Volker for giving me the freedom to explore different aspects of immunology and for his encouragement, and lending his knowledge, throughout my time in graduate school. I would also like to thank the members of my advisory committee, Drs. John Gordon, Francois Meurens, Suresh Tikoo, and Baljit Singh for their encouragement, sense of direction, and invaluable advice over the years. I would like to thank the graduate chairs Drs. Janet Hill and Joe Rubin for their support and encouragement as well.

I would like to thank my lab members and friends, particularly Jill Van Kessel and Stacy Strom, for all of their patience, help, and encouragement over the years. I'd like to extend my gratitude to Drs. Vladi Karniychuk, Klaus Osterrieder and Crystal Loving for allowing me to visit their labs and learn from them. Also thank you to my good friend and former colleague Dr. Tobias Käser for his advice and for the countless discussions regarding immunology and PRRSV. I'd also like to thank Dr. Heather Wilson, her lab members, and the animal care staff for their help and encouragement. Lastly, I would like to thank my close friends and family for their invaluable support and encouragement throughout my time in school.

TABLE OF CONTENTS

PERMISSION TO USE.....	i
ABSTRACT.....	ii
ACKNOWLEDGEMENTS	v
TABLE OF CONTENTS	vi
LIST OF FIGURES	viii
LIST OF TABLES	xii
LIST OF ABBREVIATIONS	xiii
Chapter 1 LITERATURE REVIEW	1
1.1 Introduction:	1
1.1.1 <i>PRRSV Structure and genomic organization</i>	1
1.2 Transmission and pathogenesis	2
1.2.1 <i>Tropism</i>	2
1.3 PRRSV pathogenicity characteristics	4
1.3.1 <i>Low virulent strains</i>	4
1.3.2 <i>High virulent strains</i>	5
1.4 Innate immunity.....	6
1.4.1 <i>Innate Immune Response</i>	6
1.4.1.1 <i>Cytokines associated with PRRSV infection</i>	7
1.4.1.2 <i>PRRSV mechanisms of innate immune regulation</i>	8
1.5 Dendritic cells.....	12
1.5.1 <i>PRRSV and dendritic cells</i>	12
1.5.2 <i>Plasmacytoid dendritic cells</i>	13
1.5.3 <i>Antigen processing and presentation</i>	14
1.6 Humoral immunity	17
1.6.1 <i>Humoral immune response to PRRSV</i>	17
1.6.2 <i>Antibody mediated enhanced uptake</i>	19
1.6.3 <i>Targets for antibody intervention</i>	20
1.6.4 <i>Hypergammaglobulinemia</i>	21
1.7 Cell-mediated immunity	22
1.7.1 <i>CD4⁺ T helper cells</i>	22
1.7.2 <i>CD8β⁺ cytotoxic T cells</i>	25
1.7.3 <i>Porcine T lymphocytes</i>	26
1.7.4 <i>Gamma delta-T cells and natural killer cells</i>	26
1.7.5 <i>Cell-mediated immunity to PRRSV</i>	28
1.7.5.1 <i>Natural killer cells and PRRSV</i>	32
1.7.5.2 <i>Regulatory T cells and PRRSV</i>	32
1.8 Discussion	34
Chapter 2 HYPOTHESIS AND OBJECTIVES	36
2.1 Rationale	36
2.2 Objectives and hypotheses	36
2.2.1 <i>Objective 1: Characterization of Flt3L derived bone marrow dendritic cells</i>	36
2.2.2 <i>Objective 2: Comparison of antigen-presenting cell susceptibility to PRRSV infection</i> 37	
2.2.3 <i>Objective 3: Investigate the maturation of the invariant chain</i>	37

2.2.4 Objective 4: Investigate the T cell response to PRRSV infection.....	37
----------------------------------------------------------------------------	----

Chapter 3 ANTIGEN-PRESENTING CELL SUSCEPTIBILITY TO PORCINE REPRODUCTIVE AND RESPIRATORY SYNDROME VIRUS INFECTION.....	39
3.1 Abstract.....	39
3.2 Introduction.....	39
3.3 Materials and methods	41
3.4 Results	46
3.5 Discussion	56
3.6 Supplementary figures	59
3.7 Conclusion	66
Chapter 4 PRRSV INFECTION ALTERS THE ASSOCIATION OF GAMMA ACTIN 1 WITH MHCII IN MONOCYTE-DERIVED DENDRITIC CELLS	67
4.1 Abstract.....	67
4.2 Introduction.....	67
4.3 Materials and methods	69
4.4 Results	73
4.5 Discussion	75
4.6 Conclusion	81
Chapter 5 PORCINE M1 MACROPHAGES ARE MORE POTENT INDUCERS OF LYMPHOCYTE PROLIFERATION THAN M2 OR M0 MACROPHAGES ..	82
5.1 Abstract.....	82
5.2 Introduction:	82
5.3 Materials and methods	84
5.4 Results	86
5.5 Discussion	89
5.6 Supplementary Figures	92
5.7 Conclusion	93
Chapter 6 T-CELL IMMUNE RESPONSE TO PRRSV INFECTION	94
6.1 Abstract.....	94
6.2 Introduction:	94
6.3 Materials and methods	97
6.4 Results:.....	105
6.4 Discussion:	127
6.5 Conclusion:	134
6.6 Supplementary Figures:	136
Chapter 7 GENERAL DISCUSSION	154
7.1 Future work.....	160
REFERENCES.....	161

LIST OF FIGURES

Figure 1-1: <i>Mechanisms of innate immune regulation by PRRSV</i>	11
Figure 3-1: <i>BMDC infection with VR-2385 over 72 hours</i>	47
Figure 3-2: <i>Sorted BMDC (CD163⁺ and CD163⁻) susceptibility to PRRSV</i>	48
Figure 3-3: <i>APC cell susceptibility to PRRSV infection</i>	50
Figure 3-4: <i>Antigen-presenting cell viability post infection.</i>	50
Figure 3-6: <i>MHCII Cell surface expression on APCs infected with PRRSV</i>	52
Figure 3-7: <i>MHCI Cell surface expression on APCs infected with PRRSV</i>	53
Figure 3-8: <i>Cell surface expression of MHCII (A) and MHCI (B) on M0 MoMΦs infected with PRRSV VR-2332 and VR-2385</i>	54
Figure 3-9: <i>T cell recall-response from immunized animals via macrophage- T cell co-culture.</i>	55
Figure 3-10: <i>Bone marrow dendritic cell (BMDC) characterization.</i>	59
Figure 3-11: <i>Summary of flow cytometry staining to characterize BMDC derived population</i>	59
Figure 3-12: <i>Light microscopy of BMDCs from 1 pig on day 7 of culture (6 well plates, 5.0x10⁵ cells/mL).</i>	60
Figure 3-13: <i>BMDC infection with VR-2385 over 72 hours</i>	60
Figure 3-14: <i>PRRSV replication in the supernatant.</i>	61
Figure 3-15: <i>Fluorescence activated cell-sorting images to show gating strategy for the CD163⁺ sort of the BMDC population.</i>	61
Figure 3-16: <i>BMDCs sorted for CD163 expression were infected with PRRSV and stained intracellularly for PRRSV N protein.</i>	62
Figure 3-17: <i>MoDC forward scatter/side scatter plots demonstrating cell viability 24 and hours post infection with PRRSV VR-2332.</i>	62
Figure 3-18: <i>Standard curve utilized to demonstrate primer efficiency and quantification of PRRSV transcripts. Y = -2.704ln(x) + 62.863. R² = 0.99971</i>	63
Figure 3-19: <i>Representation of the flow cytometry staining of antigen-presenting cells for cell surface marker expression.</i>	63
Figure 3-20: <i>Flow cytometry demonstrating MFI of MHCI and MHCII expression on CD163- BMDCs treated with PRRSV.</i>	64
Figure 3-21: <i>Flow cytometry data demonstrating MHCI and MHCII expression from the 48 hour time points of PRRSV infected CD163⁺ BMDCs</i>	65
Figure 3-22: <i>Interferon-gamma ELISpots from PRRSV immunized animals on day 0</i>	65
Figure 3-23: <i>Interferon-gamma ELISpots from PRRSV immunized animals on day 16 post immunization.</i>	66
Figure 4-1: <i>Silver stained SDS-PAGE-Gel of immunoprecipitated MHCII samples from PRRSV infected and non-infected APCs.</i>	74
Figure 4-2: <i>Schematic summarizing the replication and assembly of PRRSV, and the potential association of PRRSV with the maturation of the invariant chain and MHCII antigen processing and presentation.</i>	77
Figure 5-1: <i>Figure demonstrating the plating schematic utilized in co-culturing APCs with an enriched T cell population for the MLRs.</i>	85
Figure 5-2: <i>M0 mixed leukocyte reaction T cell proliferation.</i>	87
Figure 5-3: <i>M2 mixed leukocyte reaction T cell proliferation.</i>	87

Figure 5-4: <i>M1 mixed leukocyte reaction T cell proliferation</i>	88
Figure 5-5: <i>CD4α T cell proliferation</i>	88
Figure 5-6: <i>CD8β T cell proliferation</i>	89
Figure 5-7: <i>FlowJo schematic demonstrating the purity of the enriched T cell population</i>	92
Figure 5-8: <i>Schematic representing the gating strategy for analysis of T cell proliferation in the MLR co-culture assay</i>	92
Figure 5-9: <i>Schematic demonstrating T cell proliferation in response to ConA stimulation in the MLR</i>	93
Figure 6-1: <i>Schematic demonstrating the gating strategy applied for the analysis of CD4α⁺ CD8α⁺ T cells (red), CD4α⁺ CD8α⁻ T cells (blue), and CD4α⁻ CD8α⁺ T cells (orange) (6-1A) from a PBMC cell culture treated with PRRSV</i>	102
Figure 6-2: <i>Serum ELISAs measured utilizing the commercial IDEXX ELISA kits for PRRSV (Fig 2a) or swIAV (Fig 2b) to demonstrate seroconversion and compare the humoral immune response amongst the treatments</i>	106
Figure 6-3: <i>Peripheral blood mononuclear cell (PBMC) interferon-gamma ELISPOTs from the different treatment groups over the course of the trial</i>	107
Figure 6-4: <i>The level of total lymphocyte proliferation in PBMC cell culture assays in response to PRRSV (MOI 1.0), swIAV (MOI 1.0), or co-infected treatments on day 0 from their respective animal groups</i>	109
Figure 6-5: <i>The percentages of total lymphocyte proliferation from PBMC, MoMΦ-T cell co-cultures, and MoDC-T cell co-cultures in response to PRRSV (MOI 1.0), swIAV (MOI 10.0), or co-infected treatments from their respective groups on the indicated days post PRRSV challenge</i>	111
Figure 6-6: <i>The percentages of CD3⁺ T cell proliferation from PBMC, MoMΦ-T cell co- cultures, and MoDC-T cell co-cultures in response to PRRSV (MOI 1.0), swIAV (MOI 10.0), or co-infected treatments from their respective groups on the indicated days post PRRSV challenge</i>	113
Figure 6-7: <i>The percentages of total CD4α⁺ CD8α⁻ T cell (naïve) proliferation from PBMC, MoMΦ-T cell co-cultures, and MoDC-T cell co-cultures in response to PRRSV (MOI 1.0), swIAV (MOI 10.0), or co-infected treatments from their respective groups on the indicated days post PRRSV challenge</i>	115
Figure 6-8: <i>The percentages of total CD4α⁺ CD8α⁺ T cell (activated) proliferation from PBMC, MoMΦ-T cell co-cultures, and MoDC-T cell co-cultures in response to PRRSV (MOI 1.0), swIAV (MOI 10.0), or co-infected treatments from their respective groups on the indicated days post PRRSV challenge</i>	117
Figure 6-9: <i>The percentages of total CD3⁺ CD4α⁻ CD8α⁺ T cell (CTL) proliferation from PBMC, MoMΦ-T cell co-cultures, and MoDC-T cell co-cultures in response to PRRSV (MOI 1.0), swIAV (MOI 10.0), or co-infected treatments from their respective Groups, on the indicated days post-PRRSV infection</i>	119
Figure 6-11: <i>The percentages of CD4α⁺ CD8α⁺ CD27⁺ Th cell (central memory T helper cell) proliferation from PBMC, MoMΦ-T cell co-cultures, and MoDC-T cell co- cultures in response to PRRSV (MOI 1.0), swIAV (MOI 10.0), or co-infected treatments from their respective groups at the indicated time points post-PRRSV infection</i>	121

Figure 6-12: <i>The percentages of CD4α⁺ CD8α⁺ CD27⁺ T cell (effector memory T helper cell) proliferation from PBMC, MoMΦ-T cell co-cultures, and MoDC-T cell co-cultures in response to PRRSV (MOI 1.0), swIAV (MOI 10.0), or co-infected treatments from their respective groups at the indicated time points post PRRSV-challenge</i>	123
Figure 6-13: <i>The percentages of CD3⁺ T cells (right y-axis) that proliferated within the total lymphocyte population (left y-axis) of the PBMC (Figure 14A), MoMΦ-T cell co-culture (Figure 14B), and MoDC-T cell co-culture (Figure 14C), from Group B, in response to either media, ConA, Co-infected, PRRSV, or swIAV treatments</i>	126
Figure 6-14: <i>Figure representing the peripheral blood mononuclear cell (PBMC) interferon-gamma ELISPOTs from the different treatment groups in the fifth week of PRRSV infection</i>	136
Figure 6-15: <i>Figure indicating the percentage of CD3⁺ T cells that proliferated within the total lymphocyte population of the PBMC cultures from all of the groups over the course of the trial</i>	140
Figure 6-16: <i>Figure indicating the percentage of CD3⁺ T cells that proliferated within the total lymphocyte population of the MoMΦ-T cell co-cultures from all of the groups over the course of the trial</i>	141
Figure 6-17: <i>Figure indicating the percentage of CD3⁺ T cells that proliferated within the total lymphocyte population of the MoDC-T cell co-cultures from all of the groups over the course of the trial</i>	141
Figure 6-18: <i>Figure indicating the level of CD3⁺ T cell proliferation from PBMC cultures in response to PRRSV (MOI 1.0), swIAV (MOI 10.0), or co-infected treatments from their respective groups during the fifth week of infection</i>	142
Figure 6-19: <i>Representation of the FMIA cytokine ELISAs measuring IFN-α during the 2nd week post-PRRSV infection</i>	142
Figure 6-20: <i>Representation of the FMIA cytokine ELISAs measuring IFN-α during the 3rd week post-PRRSV infection</i>	143
Figure 6-21: <i>Representation of the FMIA cytokine ELISAs measuring IFN-γ during the 2nd week post-PRRSV infection</i>	144
Figure 6-22: <i>Representation of the FMIA cytokine ELISAs measuring IFN-γ during the 3rd week post-PRRSV infection</i>	145
Figure 6-23: <i>Representation of the FMIA cytokine ELISAs measuring IL-10 during the 2nd week post-PRRSV infection</i>	146
Figure 6-24: <i>Representation of the FMIA cytokine ELISAs measuring IL-10 during the 3rd week post-PRRSV infection</i>	147
Figure 6-25: <i>Representation of the FMIA cytokine ELISAs measuring IL-12 during the 2nd week post-PRRSV infection</i>	147
Figure 6-26: <i>Representation of the FMIA cytokine ELISAs measuring IL-13 during the 2nd week post-PRRSV infection</i>	148
Figure 6-27: <i>Representation of the FMIA cytokine ELISAs measuring IL-13 during the 3rd week post-PRRSV infection</i>	149
Figure 6-28: <i>Representation of the FMIA cytokine ELISAs measuring IL-17α during the 2nd week post-PRRSV infection</i>	150
Figure 6-29: <i>Representation of the FMIA cytokine ELISAs measuring IL-17α during the 3rd week post-PRRSV infection</i>	151

Figure 6-30: *Schematic demonstrating the gating strategy utilized for CD4 α ⁺ CD8 α ⁺ CD27⁺ T cells from a PRRSV treated PBMC cell culture (pig 343)..* 152

Figure 6-30: *Comparison between the immunostimulatory capacity of MoDCs and MoM Φ s to stimulate central memory Th cell proliferation during the later time point of the animal trial to the specific treatments within their respective groups.....* 153

LIST OF TABLES

Table 1.1: <i>Strains of PRRSV according to pathogenicity.</i>	6
Table 4.1: <i>Mass spectrometry identified proteins from the MHCII immunoprecipitation.</i>	75
Table 6.1: <i>Table indicating the primary and secondary antibodies, including their clone numbers and suppliers, utilized for the multicolour flow cytometry staining.</i>	100
Table 6.2: <i>Table indicating the primary and secondary antibodies, including their concentrations and suppliers, utilized in the FMIA.</i>	104
Table 6.3: <i>Table indicating the standards utilized in the FMIA along with the suppliers.</i>	104
Table 6.4: <i>Table indicating the groups and their immunization with the FluSure-XP vaccine of exposure to PRRSV strain VR-2385</i>	105
Table 6.5: <i>The mean percentage of CD3⁺ lymphocytes that proliferated in response to the indicated administered treatments in the PBMC or APC-T cell co-culture assays from Group B animals.</i>	127
Table 6.6: <i>Mean percentage of lymphocyte proliferation in the indicated treatments, groups, cell cultures, on specific days post infection (DPI).</i>	136
Table 6.7: <i>Mean percentage of CD3⁺ T cell proliferation in the indicated treatments, groups, cell cultures, on specific days post infection (DPI).</i>	137
Table 6.8: <i>Mean percentage of naïve (CD3⁺ CD4α⁺ CD8α⁻) T cell proliferation in the indicated treatments, groups, cell cultures, on specific days post infection (DPI).</i>	137
Table 6.9: <i>Mean percentage of activated (CD3⁺ CD4α⁺ CD8α⁺) T helper cell proliferation in the indicated treatments, groups, cell cultures, on specific days post infection (DPI).</i>	138
Table 6.10: <i>Mean percentage of cytotoxic lymphocyte (CD3⁺ CD4α⁻ CD8α⁺) proliferation in the indicated treatments, groups, cell cultures, on specific days post infection (DPI).</i>	138
Table 6.11: <i>Mean percentage of gamma delta T cell (CD3⁺ $\gamma\delta$⁺) proliferation in the indicated treatments, groups, cell cultures, on specific days post infection (DPI).</i>	139
Table 6.12: <i>Mean percentage of central memory T helper cell (CD3⁺ CD4α⁺ CD8α⁺ CD27⁺) proliferation in the indicated treatments, groups, cell cultures, on specific days post infection (DPI).</i>	139
Table 6.13: <i>Mean percentage of effector T helper cell (CD3⁺ CD4α⁺ CD8α⁺ CD27⁻) proliferation in the indicated treatments, groups, cell cultures, on specific days post infection (DPI).</i>	140

LIST OF ABBREVIATIONS

Analysis of variance	ANOVA
Antibody	Ab
Antigen-presenting cells	APC
Bone Marrow	BM
Bovine serum albumin	BSA
C-X-C chemokine receptor type	CXCR
CC-chemokine ligands	CCL
Chemokine receptor	CCR
Chinese	Ch
Cluster of differentiation	CD
Concavalin A	ConA
Cytotoxic lymphocyte	CTL
Danger associated molecular pattern	DAMP
Dendritic cell	DC
Deoxyribonucleic acid	DNA
Double stranded	Ds
Envelope protein	E
Enzyme-linked immunosorbent assay	ELISA
Enzyme-linked immunospot assay	ELISpot
Flow cytometry	FCM
Fluorescent activated cell sorting	FACS
FMS-related tyrosine kinase 3 ligand	Flt3L
Forkhead Box P3+	FoxP3
Gamma delta	$\Gamma\delta$
Granulocyte-macrophage colony-stimulating factor	GM-CSF
Hematopoietic stem cells	HSCs
IFN-regulatory factor	IRF
Interferon	IFN
Interleukin	IL
Lipopolysaccharide	LPS
Lymph node	l.n.
Macrophage	M Φ
Magnetic activated cell sorting system	MACS
Major histocompatibility complex	MHC
Mass Spectrophotometry	mass spec
Melanoma differentiation-associated protein 5	MDA5
Membrane protein	M
Mesenteric lymph node	MLN
MHCII compartment	MIIC
Mixed lymphocyte reaction	MLR
Monocyte-derived dendritic cell	MoDC

Monocyte-derived macrophage	MoMΦ
Multiplex fluorescent microsphere immunoassay	FMIA
Natural killer	NK
Neutralizing antibody	nAb
Non-neutralizing antibody	non-nAb
Non-structural protein	Nsp
North American	NA
Nuclear factor	NF
Nucleocapsid protein	N
Open reading frame	ORF
Pathogen associated molecular pattern	PAMP
Pattern recognition receptors	PRR
Peripheral blood mononuclear cells	PBMCs
Plasmacytoid DCs	pDCs
Polyacrylamide gel electrophoresis	PAGE
Polymerase chain reaction	PCR
Porcine reproductive and respiratory syndrome virus	PRRSV
Post-infection	P.I.
Real time quantitative PCR	RT-qPCR
Recombinant porcine	Rp
Regulatory T cells	Treg
Respiratory syncytial virus	RSV
Retinoic acid-inducible gene I	RIG-I
Ribonucleic acid	RNA
Sialoadhesin	Sn
Single stranded	Ss
Swine leukocyte antigen	SLA
Swine-influenza virus	swIAV
T helper	Th
Toll-like receptor	TLR
Transforming growth factor	TGF
Tumor necrosis factor	TNF

Chapter 1 LITERATURE REVIEW

1.1 Introduction:

Porcine reproductive and respiratory syndrome virus (PRRSV) is a positive sense, single-stranded, enveloped RNA virus that causes disease in swine worldwide. The virus is classified under the order Nidovirales from the *Arteriviridae* family and was first identified in the early 1990s (Shi et al., 2010). Today, PRRSV is the most significant pathogen in the swine industry causing yearly losses upwards of \$650 million dollars in the United States alone (Butler et al., 2014; Holtkamp, 2012). Outcomes of disease include respiratory difficulty, spontaneous abortions and fetus mummification in sows, weight loss, and death under certain circumstances (Butler et al., 2014; Reeth, 1997; Tong et al., 2007). The demand for an efficacious vaccine and the development of strategies for disease control are top priorities for producers and consumers alike (Nan et al., 2017).

1.1.1 *PRRSV Structure and genomic organization*

Two main species of PRRSV exist, the North American (Type 1) and the European (Type 2) between which a roughly 63% nucleotide identity is shared (Allende et al., 1999; Nelsen et al., 1999; Stadejek et al., 2013). The genome consists of 15.1-15.5 kb and can be divided into 9 open reading frames (ORF). The entire viral RNA transcript codes for ORF1a and ORF1b, which are translated into separate polyproteins. The polyproteins translate into 14 non-structural proteins (nsp) possessing protease (nsp1 α , nsp1 β , nsp2, nsp4), endonuclease (nsp11), helicase (nsp10), and RNA-dependent RNA polymerase (nsp9) activities. The structural proteins are encoded in ORFs 2-7. The glycosylated membrane proteins (GP2-GP5) are translated from ORFs 2-5, a small non-glycosylated protein (E) is resolved from ORF2b within ORF2, the membrane protein (M) is coded for in ORF6, and ORF7 codes for the nucleocapsid protein (N) (Dokland, 2010). High genetic variability, due to spontaneous mechanisms of mutation and recombination

between strains, has been observed in the Type 1 and Type 2 genotypes. As a result, numerous strains have been identified conferring variable levels of pathogenicity (Murtaugh et al., 2010; Wang et al., 2007).

1.2 Transmission and pathogenesis

1.2.1 Tropism

The tropism of PRRSV is thought to be restricted to cells that express the hemoglobin/haptoglobin scavenger molecule CD163, which was identified as a necessary cellular receptor for viral entry into the cytoplasm (Calvert et al., 2007). In addition to CD163, sialoadhesin 1 (CD169) and heparan sulfate residues have been identified as attachment factors for PRRSV (Van Breedam et al., 2010; Van Gorp et al., 2008).

Although it has been widely accepted that porcine alveolar macrophages (PAMs) are the main target cells for PRRSV infection and replication, it has been proposed that certain dendritic cell (DC) subsets, and likely monocyte-derived macrophages, may also be prone to infection (Calzada-Nova et al., 2010; Calzada-Nova et al., 2011; Chang et al., 2008; Chaung et al., 2010; Peng et al., 2009; Rodriguez-Gomez et al., 2012; Rodriguez-Gomez et al., 2015; Silva-Campa et al., 2009). It is also possible that DC susceptibility to infection is strain dependent (Bordet et al., 2018). Thus, it remains unclear which cells are involved in spreading PRRSV throughout the blood and into peripheral lymphoid organs. Because DCs are the professional APC of the immune system, the modulation of their antigen-presenting ability, or their being targets of PRRSV replication, would have major implications on the transition from innate to adaptive immunity (Mildner and Jung, 2014; Randolph et al., 2005). Whether or not DCs are susceptible to infection is under debate and must be resolved.

1.2.2 Transmission and Pathogenesis

PRRSV is highly communicable and is transmitted via aerosols, on fomites, through direct contact, and in seminal fluids (Kristensen et al., 2004; Pitkin et al., 2009; Swenson et al., 1994; Wills et al., 1997). Different stages of illness have been described in pigs; acute with resolution of viremia, viremia and persistence in lymphoid organs, or a

resolution of viremia with a rebound and re-established viremic state as a result of viral persistence in peripheral lymphoid organs (Chen et al., 2016; Petry et al., 2007). The course of disease is likely dependent on the pathogenicity of the virus in addition to the immune status, age, and genetics of the pig. Age seems to be a significant contributor to the outcome of an infection as older animals seem to fare better than younger animals potentially being attributable to a more developed immune response in adults (Butler et al., 2014). In the field, the most likely routes of a PRRSV infection would be intranasally, via direct contact and from respiratory droplets, or through semen during intercourse. The initial targets of PRRSV infection are likely PAMs, which reside in the alveolar space in the lungs. After replicating in PAMs, PRRSV becomes viremic roughly 6-12 hours post infection, allowing it to spread to peripheral lymphoid organs, infecting and replicating in macrophages and potentially dendritic cells (DCs). The immunosuppressive qualities of the PRRSV and compromisation of the macrophage population render animals susceptible to secondary bacterial and viral infections (porcine circovirus, swine-influenza A virus (swIAV), *S. suis*, *H. parasuis*, *Actinobacillus suis*), which lead to an exacerbation of the disease resulting in the porcine respiratory disease complex. Pathology associated with disease includes pneumonia, respiratory difficulty, and weight loss (Brockmeier et al., 2017b; Lunney et al., 2016). Additionally, PRRSV infection of tissue macrophages in peripheral lymphoid organs and the thymus leads to the apoptosis of bystander lymphocyte populations. It's possible that the apoptosis and atrophy that has been documented in these peripheral lymphoid organs could lead to an overall depletion of the lymphocyte population, resulting in a delayed induction of immunity (Gomez-Laguna et al., 2013a; He et al., 2012).

The majority of economic losses associated with PRRSV stem from the complications that arise during gestation. Rowland showed that late during gestation (70-90 days), if a sow becomes infected, PRRSV is able to cross the maternal/fetal barrier and productively infect the fetus (Rowland et al., 2003). Viral replication primarily occurs in the thymus, but virus is also detectable in the heart, lungs, kidney, spleen, and liver. Furthermore, it appeared that the fetus was able to launch an independent immune response, in which elevated pro-inflammatory cytokines (IFN- γ and TNF α) were detected in the placenta (Rowland, 2010). Until recently, the mechanism by which PRRSV crossed the maternal-

fetal interface was unknown. Karniychuk *et al.* hypothesized that infection of the fetus being restricted to late gestation is attributable to the level of CD163⁺/Sn⁺ cells (endometrial macrophages) during late gestation, otherwise present in lower numbers throughout earlier periods. This led to their theory that PRRSV most likely enters the placenta via infected endometrial macrophages, which are able to traverse the maternal/fetal interface. Although replication occurred in the fetus, there was a lack of lesions surrounding internal organs, leading the authors to believe that pathological effects are of maternal origin. Overall, it seems that maternal CD8β⁺ and NK T cell mediated immunity at the endometrium, in addition to PRRSV replication within the placenta and fetal mesenchyme, which would result in apoptosis of surrounding cells, lead to the detachment of the trophoblast layer and ultimately the degradation of the placenta (Nauwynk, 2013). There have been few investigations surrounding the PRRSV infection of the fetus. Focusing future research efforts on both the fetal and the maternal response to infection in the placenta could prove to be beneficial in developing a vaccine.

1.3 PRRSV pathogenicity characteristics

The outcome of a PRRSV infection is largely dependent on the pathogenicity of the causative strain. Strains of Type 2 PRRSV can be categorized as being avirulent/moderately virulent, North American highly pathogenic (NA-HP), or Chinese HP (Ch-HP). Observations under lab conditions are subject to variation and are dependent on, but not limited to, route of inoculation, dosage, age, strain and sex of the pig. But for the most part, the syndromes of the animals subjected to RPRSV infection under controlled conditions correlate to those in the field.

1.3.1 Low virulent strains

Two of the first isolated strains of PRRSV became the prototypes for the Type 1 and Type 2 genotype designation, they were VR-2332 and Lelystad (LV), respectively (Murtaugh *et al.*, 2010). Although significant genetic variation exists between the two strains (40%), the clinical signs and outcome of infection are fairly similar (Guo *et al.*,

2013; Hanada et al., 2005; Weesendorp et al., 2013). Generally, pigs are asymptomatic in response to infection with either strain. Fever development and weight loss are minimal, if they occur at all, and symptoms occur later during infection in comparison to virulent strains. Mortality in response to infection with either strain is attributable to secondary co-infections (Guo et al., 2013; Weesendorp et al., 2013).

1.3.2 High virulent strains

Highly virulent strains of PRRSV have arisen in North America and Europe causing rates of mortality ranging from 50-100% in herds (Zhou and Yang, 2010). Clinical symptoms in pigs are more pronounced and occur early during infections with the virulent strains upon comparison to the Type 1 and Type 2 prototypes. Classical symptoms indicating PRRSV infection such as blue ears, respiratory difficulty, and weight loss have been observed amongst the experimentally infected pigs. Strains typically studied include Type 1 VR-2385, MN184, SDSU73, VFL-12, SD-23983, SD01-08 and Type 2 Lena. (Guo et al., 2013; Karniychuk et al., 2010; Miguel et al., 2010; Weesendorp et al., 2013). The previously listed strains have been placed into the NA-HP category. Lastly, we are left with the highly pathogenic Chinese strains, which have been documented to cause upwards of 100% mortality in herds as well as under laboratory conditions. Infected animals have similar symptoms to the NA-HP challenged pigs except more acute and pronounced (Guo et al., 2013; Tong et al., 2007).

Table 1.1: *Strains of PRRSV according to pathogenicity.*

Strain	Virulence	Genotype
VR2332	Avirulent	Type 2
LV	Avirulent	Type 1
01NP1	Avirulent	Type 2
BS/AL2011	Avirulent	Type 2
HF6-2	Moderate	Type 2
NVSL-97-7895	Moderate	Type 2
SD-23983	Moderate	Type 2
VR2385	High	Type 2
HuN4	High	Type 2
MN184	High	Type 2
Lena	High	Type 1
vFL12	High	Type 2
SD01-08	High	Type2
rJXwn06	Ch High	Type 2
CH-1a	Ch High	Type 2
07HBEZ	Ch High	Type 2
WUH3	Ch High	Type 2
SY0608	Ch High	Type 2

List of the various strains mentioned in the review according to their genotype and pathogenicity.

1.4 Innate immunity

1.4.1 Innate Immune Response

The innate immune response is critical for not only host defense, but also in providing a foundation for and influencing the adaptive immune response. In regards to PRRSV, the RNA genome is recognized by endosome bound TLR-3, TLR-7, and TLR-8 and by RIG-I/MDA-5 in the cytoplasm (Calzada-Nova et al., 2010; Chaung et al., 2010; Miguel et al.,

2010; Miller et al., 2009; Sang et al., 2011). Detection of the viral genome leads to the stimulation of type 1 interferons (IFN- α , IFN- β) and other pro-inflammatory cytokines (TNF α , IL-6, IL-8, IL-1 β , etc) resulting in the establishment of an anti-viral state in neighboring cells, in addition to recruiting other immune cells to the site of infection. One of the more important cells recruited are DCs, the professional antigen-presenting cells (APC) of the immune system (Akira et al., 2006). It comes as no surprise that PRRSV is able to regulate the expression of the innate cytokines, and may also play a role in altering the activity of DCs, which would have dramatic implications on the progression of the adaptive response (Yoo et al., 2010). There has not been any clear correlation attributing increased pathogenicity to differential levels/mechanisms of immune regulation.

1.4.1.1 Cytokines associated with PRRSV infection

The activation of pro-inflammatory cytokine expression and type 1 IFNs occurs as a result of the recognition of pathogen associated molecular patterns (PAMPs). In regards to PRRSV, viral RNA would trigger a response. As a result, levels of type 1 IFNs and TLR expression have been analyzed in PAMs upon challenge with different strains of PRRSV. Miller *et al.* analyzed the induction of IFN- α in porcine alveolar macrophages (PAMs) infected with VR2332 upon stimulation with poly IC. Their results indicated that the low virulent PRRSV strain was able to inhibit the synthesis of IFN- α over the 48 hour time period. Although IFN- α was detected 20 and 48 hours post stimulation, the concentration was negligible (Miller et al., 2009). In a later study, PRRSV VR-2332 infected pigs were shown to suppress pro-inflammatory cytokines in both the lungs and the serum (Guo et al., 2013). Chaung *et al.* infected AMs with a moderately virulent PRRSV strain (HF6-2) and assessed the level of TLR expression 6 and 24 hours post infection, and in response to poly IC (a TLR3 agonist) 24 hours post infection (PI). Their results indicate that TLR4 and TLR7 were downregulated upon poly IC stimulation while TLR3 expression was upregulated. In non-stimulated cells, TLR3 and TLR7 were consistently downregulated at 6 and 24 hours PI, on the other hand TLR8 was downregulated at 6 hours PI but returned to normal after 24 hours. No difference was observed in TLR2, TLR3, TLR4, or TLR9 (Chaung et al., 2010). Miguel *et al.* were

interested in TLR and cytokine expression in response to the high virulent VR2385 strain. Interestingly, they found that TLR3, TLR4, and TLR7 expression were downregulated in the lungs of infected pigs, which coincided with suppressed IL-1 β , TNF α , and IL-6. But the opposite was observed in the tracheobronchial lymph nodes, in which all of the TLRs and pro-inflammatory cytokines were induced (Miguel et al., 2010). Guo *et al.* pigs infected with an Ch-HP strain showed high levels of IFN- α , TNF α , IL-6, IL-8, IL-2, IL-12, IL-10, and IFN- γ in both the lungs and serum, which seems to indicate that a cytokine storm could potentially provide an explanation for the HP-PRRSV increased mortality rates (Guo et al., 2013). Overall, there appears to be a correlation between increased pathogenicity and the induction of pro-inflammatory cytokines. Lastly, although PRRSV seems to inhibit type 1 IFN synthesis, it has been shown that administration of IFN- α inhibits PRRSV replication *in vivo*, lending to the potential therapeutic applications of administered IFN- α as a resolution for PRRSV infection (Brockmeier et al., 2017a). For the most part, mechanisms by which PRRSV modulates the innate immune response have been elucidated.

1.4.1.2 *PRRSV mechanisms of innate immune regulation*

Non-structural protein 1 (nsp1) is a polyprotein that possesses a papain-like cysteine protease domain, which is responsible for its resolution into its two separate components, nsp1 α and nsp1 β . In addition to participating in viral replication, nsp1 is responsible for a significant portion of type 1 IFN inhibition. Song *et al.* investigated the properties of nsp1 α , derived from VR-2332, in HeLa cells. They observed that nsp1 α was able to localize to both the nucleus and the cytoplasm. Upon further analysis, they determined that nsp1 α acted by suppressing I κ B phosphorylation, inhibiting NF- κ B translocation to the nucleus (Song et al., 2010). Conflicting results were obtained later that year by Kim *et al.* when they were unable to replicate the inhibition of IRF3 phosphorylation. This may have been attributable to their using MARC-145 and HeLa cells or that nsp1 was derived from VR-2332. They concluded that nsp1 β was able to translocate into the nucleus and stimulate the poly-ubiquitination of CBP, which prevents the stabilization and transport of IRF3 to the IFN- β promoter (Kim et al., 2010). Nsp1 β has been shown to possess multiple mechanisms by which it regulates both the expression of type 1 IFNs and IFN

regulatory factors (IRFs). Beura *et al.* observed that IRF3 phosphorylation was inhibited in HEK293-TLR3 cells that were transfected with PRRSV nsp1 β (vFL-12) and subsequently challenged with dsRNA. Inhibition of IRF3 phosphorylation would prevent its nuclear translocation, thus inhibiting the activation of IFN- β (Beura et al., 2010). Patel *et al.* continued to research the activity of nsp1 β in which they observed a completely different mechanism. Patel *et al.* observed the inhibition of STAT1 transportation to the nucleus in HEK293 and HeLa cells, but were unable to deduce the exact mechanism by which its translocation is inhibited (although they proved that it was not due to suppressed phosphorylation). Unlike the previous two studies, they went on to demonstrate STAT1 translocation inhibition in primary PAMs by infecting cells with VR-2385 and the MLV. Interestingly, the MLV was not able to suppress STAT1 translocation (Patel et al., 2010). Although conflicting results exist, it is apparent that nsp1 β plays a role in type 1 IFN regulation. Once again, it seems that the activity is strain dependent. In addition to nsp1 β inhibition of type 1 IFN expression, nsp2 has also been implicated in its inhibition.

Highly pathogenic strains of PRRSV that have arisen in China all have a similar 90 base pair deletion in nsp2, which is a unique feature not observed in North American or European strains. Nsp2 is the largest viral protein and possesses a papain like cysteine protease domain, typically associated with deubiquitinase activity (Dokland, 2010). Sun *et al.* were able to demonstrate that the cysteine protease domain of nsp2 from the avirulent SD01-08 strain is able to prevent the polyubiquitination of I κ B α , which in turn prevents the translocation of NF- κ B to the nucleus. The end result is an inhibition of type 1 IFN stimulated genes (ISGs), pro-inflammatory cytokines, and may also play a role in the inhibition of apoptosis (Sun et al., 2010). In addition to preventing IRF3 and NF- κ B translocation, nsp2 has been shown to antagonize IFN stimulated gene 15 (ISG15) activity. ISG15 is an important innate antiviral response protein and its activity is referred to possess “ISGylation” activity. Although its exact mechanism is being investigated, the conjugation of ISG15 to viral proteins has been hypothesized to either target viral proteins for degradation or disrupt protein activity (Durfee and Huibregtse, 2010). It has been theorized that the 30 amino acid deletion present in the HP-PRRSV strains does not contribute to virulence (Zhou et al., 2009). Zhi Sun *et al.* demonstrated that PRRSV strain

SD01-08 inhibits ISGylation in PAMs and more specifically, nsp2 inhibition of ISGylation in HeLa cells (Sun et al., 2012). Another study found that nsp2 (Ch-HP) was also able to inhibit the translocation of IRF3 across the nucleus, preventing the transcription of ISGs. Whether this inhibition is due to deubiquitinase activity or not remains to be determined (Li et al., 2010). Ying Fang *et al.* observed that the nsp2 from Ch-HP strains induces the degradation of I κ B α in HeLa cells, thus activating the NF- κ B pathway. They were able to determine that the hypervariable region in nsp2 is responsible for the NF- κ B translocation and that the 30-amino acid deletion has no influence on activity (Fang et al., 2012). Recently, nsp2 was identified as being a structural component of the PRRSV virion, likely integrating into the viral envelope. This provides a potential explanation for high antibody titres against nsp2 *in vivo*. Furthermore, the study highlights the potential significance that nsp2 variation amongst strains could be playing a further role in immune evasion than what had been considered in the past (Kappes et al., 2013). Overall, past studies indicate that more than one domain exists in nsp2, resulting in multiple immunoregulatory properties such as interfering with proinflammatory cytokine synthesis, preventing IFN stimulated gene expression, and potentially having a structural role. Although nsp2 mechanisms have only been demonstrated in continuous cells lines, it's possible that nsp2 could play a significant role in determining virulence. In addition to the a-fore mentioned nsps, the nucleocapsid protein (N), nsp4, and nsp11 appear to participate in modifying the innate response as well.

PRRSV nsp11 contains an endoribonuclease (NendoU) domain, which is also found in other Nidoviruses (Ulferts and Ziebuhr, 2011). Xibao Shi *et al.* investigated the properties of nsp11 and compared its NendoU domain sequence to those of SARS-CoV and EAV. The amino acids essential for the NendoU activity (His-129, His-144, Lys-173) were subjected to mutagenesis to elucidate the properties of the domain. They found that nsp11 was able to inhibit the phosphorylation of IRF3 in MARC-145 cells, preventing its nuclear translocation. This resulted in the suppression of IFN- β induction. Knocking out the amino acids listed previously dramatically decreased the IRF3 suppression (Shi et al., 2011). Zhitao Ma et al. were able to demonstrate in both MARC-145 cells and PAMs, that nsp4 is able to induce apoptosis, which is highly dependent on its serine protease

activity. Previously, GP5 had been associated with the potential induction of apoptosis, but this activity was not observed during their study (Ma et al., 2013). In regards to the N protein, its translocation to the nucleus and nucleolus during infection has been documented (Rowland et al., 1999; Rowland and Yoo, 2003). Rui Luo *et al.* investigated the potential activity of the N protein and discovered that it activated the NF- κ B pathway. Their study was performed in MARC-145 cells and they observed that the DNA binding activity of NF- κ B increased in a dose dependent manner (Luo et al., 2011). Overall PRRSV has multiple mechanisms by which it suppresses type 1 IFNs and ISGs and is able to suppress or activate the induction NF- κ B associated genes.

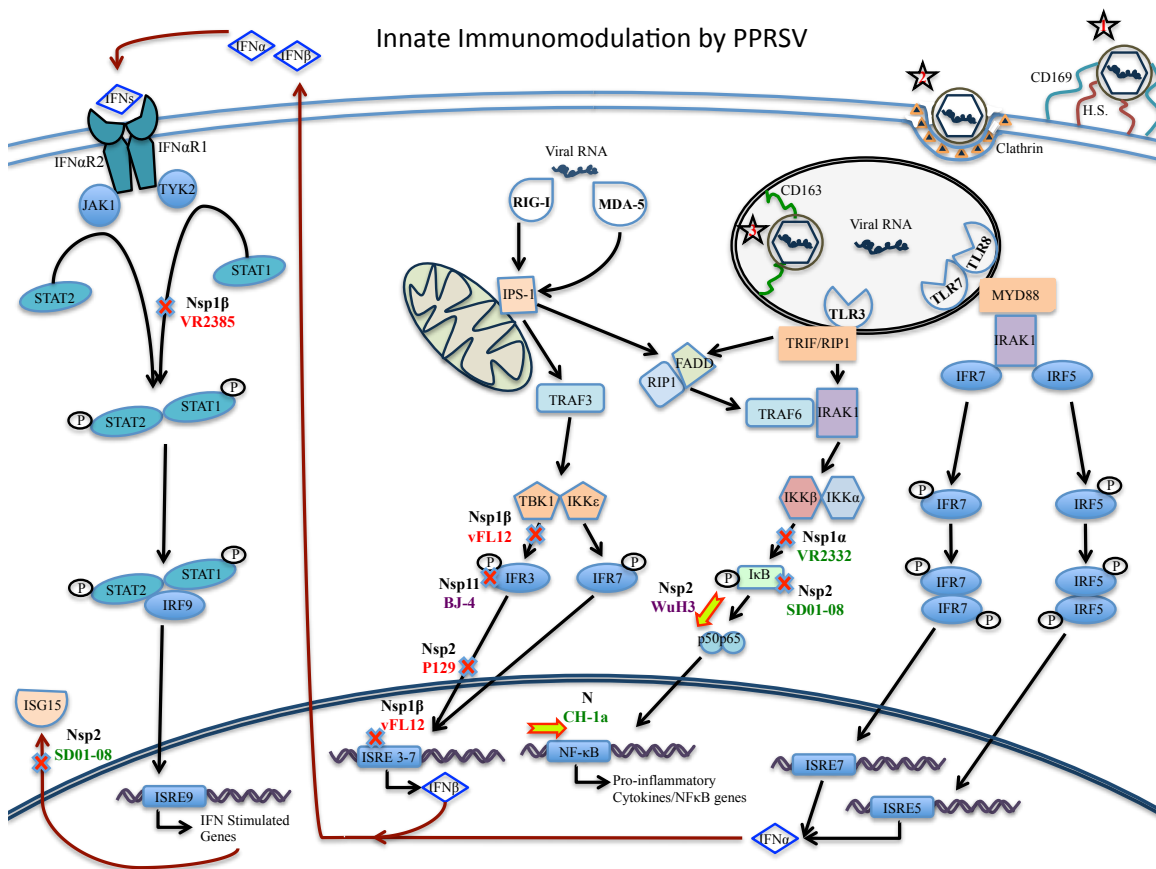


Figure 1-1: Mechanisms of innate immune regulation by PRRSV. The strains have been color coordinated according to their virulence. Stars with numbers = steps of PRRSV entry into the cell. Red = Highly Pathogenic. Green = Avirulent. Purple = Chine Highly Pathogenic. Red X = inhibition. Green arrow = activation.

There appears to be a significant amount of information indicating that mechanisms of innate immune regulation act in either a synergistic or antagonistic manner (Figure 1-2). The activities of specific viral proteins are highly dependent on individual strain pathogenicity. A prime example of this can be seen in studies performed on nsp2. Nsp2 derived from a low virulent strain (SD01-08) was observed to deubiquitinate I κ B α , preventing NF- κ B activation, whereas nsp2 from a HP-PRRSV strain activates the translocation of NF- κ B. The question then arises as to whether the former activity of nsp2 is abolished or whether there is a secondary interaction with a different PRRSV protein that causes the phenomenon to occur.

1.5 Dendritic cells

1.5.1 PRRSV and dendritic cells

Dendritic cells are the professional APCs of the immune system, providing a direct link between innate and adaptive immunity. They are responsible for transporting antigen to peripheral lymphoid organs to directly stimulate naïve T cells to mount a specific response. Cytokines produced during this process influence the type of response subsequently raised (Bousoo, 2008). In 2007, Wang *et al.* were one of the first groups to demonstrate DC infection *in vitro*. Their results indicated that a moderately virulent strain of PRRSV (SD-23983) targeted monocyte-derived DCs (MoDCs) specifically and the rates at which PRRSV replication was detected was similar to those observed in MARC-145 cells. They went on to demonstrate that SD-23983 kills DCs by both necrosis and apoptosis. More importantly, they observed a decrease in antigen-presenting ability in the infected DC population. Lastly, infected MoDCs did not produce Th1 cytokines or IL-10 but low levels of TNF α were present (Wang *et al.*, 2007). Later, Zhang *et al.* infected MoDCs with the moderately virulent strain SD-23983. Their results indicate that PRRSV is able to induce the transcription of IFN- α via the phosphoinositide 3-Kinase (PI3K) pathway. But, levels of IFN- α in the supernatant were negligible upon ELISA analysis. They concluded that PRRSV possesses a post-transcriptional method of IFN- α inhibition that is replication dependent, as heat inactivated virus did not possess the same immunomodulatory capability (Zhang *et al.*, 2012). Mendoza *et al.* obtained different

results upon analyzing the infection of mature MoDCs (mDCs) with a NA virulent strain of PRRSV (vFL12). Similar to the previous study, PRRSV was able to infect and achieve similar rates of replication in the mDCs as those in observed in PAMs. Apoptosis was detected in the cells 24 hours PI and a downregulation of MHCII occurred. On the other hand, they observed a major upregulation of IL-10 and little IFN- α (Flores-Mendoza et al., 2008). In 2011, Subramaniam *et al.* published a paper utilizing the same viral strain as Mendoza that showed levels of IL-10 were not up-regulated in DCs. A potential explanation for the difference to Mendoza's past results could be attributable to LPS treatment (stimulating DC maturation) inducing high levels of IL-10 production in MoDCs before infecting the DCs (Subramaniam et al., 2011). PRRSV strain HF6-2 was utilized to infect GM-CSF/IL-4 derived BMDCs. The results were consistent in demonstrating decreased levels of MHC-I and CD80/86 expression in infected cells and apoptosis in cell cultures. Interestingly, bystander, uninfected cells showed an upregulation of CD80/86. There appeared to be a significant induction of IL-1, IL-6, IL-8, and more importantly IL-10. Levels of TNF α and IL-12 were negligible (Chang et al., 2008; Peng et al., 2009). More recently, Rodriguez-Gomez *et al.* found that MoDCs infected with either Type 1 or Type 2 PRRSV showed an upregulation of SLA-DR and CD80/86. They investigated whether IL-10 secretion resulted in the induction of regulatory T cells and determined that PRRSV infection of MoDCs did not result in the stimulation of regulatory T cells (Rodriguez-Gomez et al., 2015). The variable results obtained from different studies could be attributable to the strain of virus used, the MOI of the infection, and the breed or age of the pigs.

1.5.2 *Plasmacytoid dendritic cells*

Plasmacytoid DCs (pDCs) have been identified in humans to be a specific subset of DCs responsible for the majority of the IFN- α production observed *in vivo*. Calzada-Nova *et al.* were able to isolate and characterize a pDC population from pigs based on their CD4 α^{hi} CD172a $^{\text{lo}}$ cell surface morphology utilizing cell sorting (Calzada-Nova et al., 2010). They went on to investigate whether pDCs were susceptible to PRRSV infection *in vitro*. Plasmacytoid DCs were treated with PRRSV 4468 and subsequently challenged with ODN D19 (TLR9 agonist) or transmissible gastroenteritis virus (TGEV), which on

their own induce IFN- α , TNF α , IL-8, IL-6, and IL-2. The cells were found to be non-permissive to PRRSV infection, but only moderate levels of IL-2 were detected. Upon closer examination, they found that PRRSV (live or inactivated) suppressed levels of IRF7 upon challenge with ODN D19 or TGEV. Similarly, they observed a decrease in STAT1 translocation to the nucleus. Although the exact mechanism by which PRRSV acts to modulate the response in pDCs was not determined, the authors hypothesize that the immune suppression is occurring as a result of an extracellular interaction of a viral protein with a pDC cell surface receptor (Calzada-Nova et al., 2011). Results obtained by Zhang *et al.* demonstrated a lack of IFN- α production in MoDCs after Poly I:C stimulation, which could be attributed to pDCs not being present in MoDC populations. Later, Baumann *et al.* investigated the IFN- α response of pDCs upon challenge with various strains of PRRSV. They found that all PRRSV isolates, both type 1 and 2, were able to induce IFN- α , but the levels of IFN- α were considered negligible. Furthermore, there appeared to be a strain dependent variation as the Ch-HP strain (SY0608) suppressed 51% of IFN- α compared to VR2332's 31% suppression upon stimulation with CpG (Baumann et al., 2013). During early stages of infection, IFN- α has been detected systemically in PRRSV infected animals (Guo et al., 2013). A group investigated the source of IFN- α in pigs infected with Lena virus and found that pDCs were responsible for the secretion of IFN- α . Their results indicate that pDCs detected PRRSV virions in association with infected macrophages, and PRRSV virion on its own was unable to induce IFN- α (Garcia-Nicolas et al., 2016). Overall, it doesn't seem that pDCs are targets of PRRSV replication, but pDCs play a prominent role in the synthesis of IFN- α . Furthermore, past investigations would suggest that the induction levels of IFN- α appear to be dependent of the viral strain, which could provide some insight into the pathogenesis of PRRSV.

1.5.3 *Antigen processing and presentation*

The recognition of a peptide sequence in association with an MHC molecule by an $\alpha\beta$ T cell receptor (TCR) is arguably the most important step towards stimulating a cell mediated immune response against the antigen from which the peptide sequence was derived. Although every nucleated cell *in vivo* is capable of presenting antigen on MHCI

molecules, antigen presentation is typically associated with those cell that express MHCII in addition to MHCI, which are MΦs, B cells, and DCs (and thymic epithelial cells). The pathways by which antigen is processed can be divided into the endogenous or the exogenous pathway (Klein et al., 2014; Vyas et al., 2008b). Antigens being processed and presented by APCs are not always foreign, as the majority are likely self-derived peptide sequences. Surveying self-derived peptide sequences aids in maintaining tolerance in addition to providing a means to survey for potentially oncolytic cells expressing abnormal proteins. As its name implies, the endogenous pathway involves the processing of antigen found within the cytoplasm of a cell. Essentially, this pathway provides a means by which cells are able to recycle amino acids from mis-folded proteins that have been polyubiquitinated and targeted for degradation into short peptide sequences (8-10 amino acids in length) by the proteasome (Blum et al., 2013). In regards to pathogens, the endogenous pathway provides a means by which intracellular pathogen's proteins can be presented on MHCI molecules for recognition by CD8β⁺ T cells. On the other hand, the exogenous pathway involves the processing of antigen that has been encountered extracellularly. Of note is the premise of cross-presentation, which is essentially antigen processed via the exogenous pathway that results in peptide sequences being loaded onto MHCI molecules in the endoplasmic reticulum. Cross-presentation explains how the stimulation of naïve CD8β⁺ T cells occurs when the APC is not susceptible to infection by an intracellular pathogen, therefore the pathogen's antigens would need to be processed exogenously (Embgenbroich and Burgdorf, 2018).

Antigens acquired from the external environment of an APC are processed through the exogenous pathway. In brief: antigen is phagocytosed and the phagosome eventually fuses with a lysosome (forming the phagolysosome), which results in the degradation of the antigen into short peptide sequences. After MHCII has undergone post-translational modification, it is transported to the phagolysosome where peptide sequences are loaded in the binding groove of MHCII so that it can be transported to the cell surface for antigen presentation to CD4α⁺ T cells (Vyas et al., 2008a). Unlike its MHCI counterpart, the length of peptide sequences bound the groove of MHCII can range from 10-51 amino acids in length. Furthermore, it has been shown that some of these longer peptide sequences may possess higher immunogenicity than some of the shorter peptides

(Niebling and Pierce, 1993). Variations in the length of peptide sequences bound to MHCII, in regards to immunogenicity, are likely antigen specific. Given that 10-12 amino acids may be bound to the groove of MHCII at one time, any peptides longer than this would have interactions outside the groove of MHCII which would alter the interaction of the MHC molecule with a TCR. Before the MHCII molecule binds to a peptide sequence, it must go through a series of steps during its translation to ensure that it acquires a peptide sequence efficiently. Shortly after translation in the endoplasmic reticulum, the MHCII binding groove is occupied by the invariant chain (Iip31). The invariant chain serves to prevent self peptide sequences from occupying the binding groove before the MHCII molecule has been transported to a phagolysosome (Sercarz and Maverakis, 2003). Non-cysteine proteases are responsible for the initial trimming of the invariant chain before the MHCII-Iip31 complex is transported to the endosomal compartments. A crucial step in the maturation of the invariant chain is the processing of Iip31 into the class II-associated invariant chain peptide (CLIP). After being processed into CLIP, the accessory proteins HLA-DM/HLA-DO are able to exchange CLIP for a nascent peptide sequence within the endosome/phagolysosome. Cysteine proteases have been shown to be indispensable to the maturation of the invariant chain, particularly Cathepsin S. In mice, studies have demonstrated that Cathepsin S is responsible for the final processing of the Iip31 into CLIP. Furthermore, inhibition of Cathepsin S in DCs essentially eliminates their ability to present antigen to CD4 α ⁺ T cells and may even have an effect on germinal center development (Riese et al., 1998; Shi et al., 1999). Other cysteine proteases of interest, when considering the maturation of Iip31, are Cathepsin F and Cathepsin L. Considering there are multiple antigen-presenting cells, it doesn't surprise that cysteine protease expression varies within specific cell types. Cathepsin F activity in MΦs has been shown to be higher than in B cells and DCs, and Cathepsin L activity seems to be indispensable for thymic epithelial cells antigen presentation during positive and negative selection process of thymocytes (Shi et al., 2000); (Turk et al., 2012). Currently there is no information regarding the expression or role of cysteine proteases in pigs, nor has there been any research on the maturation of the invariant chain in pigs. Considering the variation in cysteine protease expression amongst APC populations in mice, it would seem plausible that this variation could have an effect on

the peptide sequences being presented within those specific APC populations. It has been demonstrated that PRRSV may be forming a replication complex in association with endoplasmic reticulum derived double membrane vesicles in infected cells (Kappes and Faaberg, 2015). If this is the case, PRRSV could be interfering with antigen processing.

1.6 Humoral immunity

1.6.1 Humoral immune response to PRRSV

Humoral immunity involves antigen recognition by specific B cell receptors (BCRs) on the surface of B cells, which have been germline encoded. B cell activation can occur independently of T cell help, or with the aid of helper T cells. Upon antigen recognition, the BCR undergoes affinity maturation via isotype switching and somatic hypermutation within germinal centers. In the case of a viral infection, the primary mechanisms by which antibodies (ab) act would be through virus neutralization and opsonization (Hangartner et al., 2006). Regarding PRRSV, a robust ab response is detectable in serum 7 days post infection, although they are non-neutralizing antibodies (non-NA) and do not aid in the subversion of the infection. Roughly 4 weeks post infection, the appearance of NA in serum and in mucosal secretions becomes apparent eventually leading to the resolution of viremia (Loving et al., 2015). Furthermore, the passive transfer of serum containing NA to naïve pigs protected them from infection when challenged with a homologous strain of PRRSV. Thus, it's safe to conclude that NA provide sufficient protection from infection, although the role that cell mediated immunity plays in protection, in addition to influencing the humoral response, should not be dismissed (Osorio et al., 2002). In the past, research areas focused predominantly on identifying neutralizing epitopes within glycoprotein 5 (GP5) and the membrane (M) protein of PRRSV, but recently the GP2-GP3-GP4 trimer have gained increasing attention. The ideal vaccine candidate will stimulate a NA response within 2 weeks of immunization and have broad cross-protection across different strains of PRRSV. Difficulty in achieving NA induction stem mainly from the masking of neutralizing epitopes on the surface of virions by glycan shields, and the unusually high mutation rates seen in PRRSV make it difficult to identify conserved epitope motifs (Lopez and Osorio, 2004;

Loving et al., 2015; Lunney et al., 2016). Multiple questions arise when considering the humoral response to PRRSV, which include the following: What antibody isotypes correlate to the highest level of protection and how do they function? What is the role of non-NA and how do they influence disease progression? And lastly, why is there a delay in the appearance of NA?

A kinetic of the ab response to PRRSV has indicated that immunoglobulins are detectable in oral fluids of infected animals as early as 3 days post infection. Secreted IgM (sIgM) was detected from days 3-10, sIgG from days 7-10, and sIgA from days 8-14.

Immunoglobulins in serum are detected on similar days with (IgM>IgG>IgA concentrations), increasing until day 21 at the end of the trial (Kittawornrat et al., 2013).

Classically, IgM is associated with a primary B cell response in humans and mice.

However, the fetal pig does not rely on its mother for passive immunity *in utero*. Instead, the immune status of the pig begins to develop *in utero*. As such, it has been shown that isotype switching in pigs occurs during gestation. Additionally, it has been shown that isotype switching is able to occur in the absence of encountering antigen specific for its specific B cell receptor. This may be advantageous as it could speed up the process of developing an antibody repertoire conferring higher affinity for antigen by skipping the isotype switch process seen in humans and mice (Butler et al., 2001). But, somatic hypermutation will only occur in the presence of antigen, so the overall period of time of B cell affinity maturation may not be impacted that significantly (Butler et al., 2002).

Regarding PRRSV, ab isotypes involved in protection include IgM, IgG, and IgA. Early during infection, B cells encounter their antigen inducing the secretion of IgM and proliferation of plasma cells. IgM is the first line of ab defense, in that it has a lower affinity for specific epitopes, but has 10 potential binding regions conferring a high avidity. Three main mechanisms by which IgM can function include: a) opsonization of antigen resulting in the recruitment of the C1 complex from complement; b) opsonization of antigen leading to increased uptake by APCs; and c) antigen neutralization. It is generally found in serum, but can also be detected in oral fluids (Burton, 2002), (Hangartner et al., 2006). IgG is found mainly in serum and tissues and possesses similar mechanisms to IgM. Primary mechanisms include virus neutralization and opsonization. Binding of IgG to viral antigen can prevent attachment of the virus to cells or inhibit viral

membrane fusion, preventing entry of the viral genome into the cell's cytosol. Opsonization of the virus results in the recruitment of macrophages, dendritic cells, and neutrophils, mediating phagocytosis via an interaction with the Fc portion of the ab with the Fc γ R on the surface of the cells. Furthermore, a potential mechanism would be the binding of ab to viral antigen on the plasma membrane of an infected cell. This would in turn activate antibody-dependent cell-mediated cytotoxicity by NK cells, ultimately leading to the death of the cell (Hangartner et al., 2006). Although, this mechanism may not be as prevalent during PRRSV infection as viral proteins typically localize to the endoplasmic reticulum, and budding occurs at the golgi, not the plasma membrane. Viral particles are transported out of the cell via exocytosis, making it unlikely for PRRSV proteins to associate with the plasma membrane of cells (Veit et al., 2014). Lastly, IgA is commonly found as a secreted form in the mucosa, although it is also detectable in serum. The primary role of secreted IgA (sIgA) is neutralization of toxins or in the prevention of pathogen attachment to their target cells. Thus, an ideal vaccine candidate will elicit a strong IgA response in mucosal tissues in order to prevent the infection from breaching the mucosal epithelium, halting the establishment of a potential infection (Burton, 2002; Hangartner et al., 2006). The major hurdle that exists in the immune response to PRRSV is the robust non-NA response and the delay in NA induction, which is discussed below.

1.6.2 Antibody mediated enhanced uptake

As mentioned previously, NAs don't appear until 4 weeks post infection. This could be attributable to immune evasion and the immune dysregulation in both the innate and adaptive branches of immunity. As such, the non-NAs have shown specificity for GP5, M, N, and multiple non-structural proteins (nsps). This begs the question as to what role non-NAs play during infection. It has been hypothesized that antibody dependent enhanced uptake (ADE) exists, which would result in a heightened rate of infection with potentially severe clinical outcomes if an animal were to be infected with a heterologous strain of PRRSV. But the evidence surrounding ADE has been sketchy, and likely is not occurring (Loving et al., 2015). Taking into consideration how quickly PRRSV disseminates to multiple organs throughout the body, it seems plausible that non-NA could be enhancing the rate of dissemination. The mechanism of dissemination would be

comparable to ADE, in that opsonization of viral particles with serum immunoglobulins (via interactions with FcR γ on the surface of APCs and the recruitment of C1 from complement) would result in increased uptake into APCs, particularly macrophages (M Φ s). In addition to the early viremic state associated with PRRSV infection, enhanced uptake by APCs, and their subsequent infection, would provide a potential explanation for the rapid spread of virus throughout the body. The difficulty in demonstrating ADE upon challenging pigs with a heterologous strain of PRRSV could be attributed to ADE occurring in a primary challenge in naïve animals. Essentially, the mutation rates are so high within non-neutralizing epitopes of PRRSV that upon encountering a heterologous strain of PRRSV, the immune system would be unable to recognize it as being related to the primary strain. But this doesn't mean that non-NA don't enhance the rate of infection and dissemination. If anything it's the opposite, in that a state of ADE occurs during every PRRSV infection, excluding challenges with homologous strains in the presence of NAs. Thus, a potential role for non-NA in PRRSV infection could be the enhancement of dissemination through the body via opsonization of viral particles, leading to enhanced uptake by APCs (the targets of viral replication). In terms of usefulness, non-NAs are not entirely useless as they can be utilized for diagnostic purposes. It is also possible that non-NA could play a role in virus neutralization, as discussed in the following paragraph.

1.6.3 Targets for antibody intervention

Antigenic epitopes associated with neutralization are buried beneath glycan shields and potentially within quaternary protein structures (the GP2-GP3-GP4 trimer) on the surface of the PRRSV virion. Furthermore, the principal neutralizing epitopes (NE) are flanked by non-neutralizing decoy epitopes (Loving et al., 2015; Lunney et al., 2016). It begs the question as to how NAs are able to circumvent the glycan shields (as glycan shields have been shown to be indispensable for PRRSV replication, they can't be deleted or modified) to gain access to the NEs that are buried and hidden. It's plausible that upon binding to their antigenic epitopes, non-NA could alter the conformation of adjacent viral proteins. Alterations in the conformation of proteins surrounding NEs could theoretically expose the NE. This could potentially explain how NAs are able to gain access to the hidden and buried NE, in addition to the NAs undergoing rigorous somatic hypermutation

(Burton, 2002; Hangartner et al., 2006). It's clear that NAs are a necessary component in overcoming infection. Thus, the main issue that exists is the delay in the induction of NA and the preferential synthesis of non-NA during the viremic period of infection.

1.6.4 *Hypergammaglobulinemia*

The robust non-NA response seen early during infection with PRRSV may be attributable to hypergammaglobulinemia. Butler *et al.* were able to demonstrate that the amount of immunoglobulin present in bronchoalveolar lavages (BAL) during a PRRSV infection was increased more than 10 fold in comparison to pigs infected with swine-influenza virus (swIAV) and porcine circovirus-2 (PCV-2). They essentially showed that the majority of the B cells, during the viremic state of a PRRSV infection, express different isotypes (IgM, IgG, IgA) but nearly identical sequences in their 3rd complementarity determining region (HCDR3) of the antibody heavy chain. In other words, the authors showed that the non-NA response to PRRSV originated from similar B cell clones that had not undergone somatic hypermutation. Furthermore they argued that the amino acids within the HCDR3 region (the central binding domain of the hypervariable region) were of hydrophobic nature, resembling a non-specific, polyvalent repertoire of antibodies characteristics of a naïve ab repertoire in infants (Schroeder et al., 1998). The authors hypothesized there is a PRRSV antigen that acts similar to a superantigen, stimulating the proliferation of a population of B cells derived from a nearly identical clone. There has been no evidence of a super antigen that PRRSV secretes. But it's plausible that early during PRRSV infection B cells are activated independently of T cell help. In this case, ab-ag complexes could interact with B cells in peripheral lymphoid organs and stimulate a robust antibody response. Without the aid of T helper cells, somatic hypermutation would be delayed resulting in an ab repertoire with relatively low affinity for PRRSV antigens, and potentially even auto-reactive abs (Butler et al., 2008). Taking into consideration the timeline of the adaptive immune response to PRRSV, it seems that IFN- γ cells appear in the periphery before NAs. Therefore, it is plausible that B cells proliferate independently of T cell help early during infection. Then once T cells have been activated, they interact with B cells driving somatic hypermutation, eventually resulting in NA synthesis. Overall, it seems likely that in order for B cells to undergo

somatic hypermutation, leading to the synthesis of NA, they must communicate with CD follicular T helper cells. Unfortunately, the cell-mediated immune response to PRRSV seems to be suppressed or dysregulated in some way. Knowledge surrounding the cell-mediated immune response to PRRSV is lacking, and the information that does exist is relatively conflicting. Particularly whether regulatory T cells are being induced to suppress the progression to an effective T cell response must be addressed. In order to discover answers regarding the immune dysregulation that occurs during PRRSV infection, both cell-mediated immunity and humoral immunity warrant further attention.

1.7 Cell-mediated immunity

1.7.1 CD4⁺ T helper cells

The initial stages of T lymphocyte development occur in the thymus, in which T cells undergo a process of positive and negative selection. During positive selection, CD4 α /CD8 β double positive thymocytes migrate to the thymic cortex and interact with thymic epithelial cells. If the double positive thymocytes interact more strongly with MHCII they become CD4 α ⁺ and if they interact more with MHCI they acquire a CD8 β ⁺ lineage. If the thymocyte has undergone a poor rearrangement of its T cell receptor (TCR) and does not interact with either MHCI or MHCII, that thymocyte undergoes apoptosis and is eliminated from the T cell repertoire. The negative selection of T cells eliminates those lymphocytes that have acquired a T cell receptor (TCR) that is reactive against self-MHC molecules in association with its peptide complex. Those T cells that are self reactive, for the most part, undergo apoptosis and are eliminated from the repertoire, in turn preventing self-reactivity and auto-immunity (Colf et al., 2007; Singer et al., 2008). Once a thymocyte has acquired markers towards a specific lineage (CD4 α ⁺, CD8 β ⁺, or $\gamma\delta$ ⁺) it then migrates to secondary lymphoid organs for further development (Klein et al., 2014).

CD4⁺ T helper (Th) cells can be described as the directors of the adaptive immune response. As their name implies, the primary role of CD4⁺ Th cells is to aid in the development of both the cell-mediated and the humoral arms of immunity (Bevan, 2004; Crotty, 2015). A naïve CD4⁺ Th cell resides within peripheral lymphoid organs awaiting

its encounter with the antigen for which its $\alpha\beta$ TCR has been rearranged to recognize. Upon acquiring antigen, APCs migrate towards the draining lymph node to stimulate T lymphocyte maturation. This step of T cell maturation is dependent on multiple factors during antigen presentation that include the following: First, the successful recognition and interaction of the TCR with the MHCII peptide bound molecule. Secondly, the induction of CD80/86 expression on the APC and its interaction with CD28 on the T cell. And lastly, the cytokines expressed by the APC to which the T cell is directed towards differentiating into a specific lineage (Pennock et al., 2013). In regards to PRRSV, the most effective lineage to combat the viral infection would be a Th1 type immune response. In order for this to occur, APCs presenting antigen to T cells would be expressing IL-12 and potentially IFN- α . The cytokines delivered by the APC stimulate the expression of different transcription factors that influence the type immune response the Th cell will be geared towards. In the case of a Th1 type immune response, the transcription factor T-bet would be activated in the lymphocyte (Luckheeram et al., 2012a). Whether or not this is occurring during PRRSV infection is unknown. Multiple subsets of CD4⁺ Th cells exist and they will be discussed in the following paragraphs. For simplicity's sake, this review will focus primarily on Th1 differentiated CD4⁺ Th cells as they are the major effectors when considering viral infections. CD4⁺ Th cells can thus be characterized as having an effector or a memory phenotype.

Upon stimulation, a naïve CD4⁺ Th cell clone differentiates towards a specific lineage (eg: Th1) from which it undergoes cell division into effector T cells. The effector T cells acquire homing receptors that enable their migration towards sites of inflammation, resulting in their activity to clear the antigen to which they have been stimulated. Once antigen has been cleared, roughly 90% of the effector population dies leaving the residual population to undergo memory cell differentiation. T cells acquiring a memory phenotype can be categorized as central memory T cells (T_{CM}) or effector memory T cells (T_{EM}). The purpose of the memory cell population confers the ability to mount a secondary response to a previously encountered antigen. Although the mechanisms by which a CD4⁺ Th cell undergoes memory differentiation are not completely understood, marked differences between T_{CM} and T_{EM} cells are known. Central memory T cells reside within peripheral lymphoid organs, expressing the homing receptor CCR7 that permits their

migration between secondary lymphoid organs, surveying and sampling for their particular antigen. Furthermore, the T_{CM} population seems to have a lower expression of the lineage committed transcription factors (eg T-bet) in comparison to their T_{EM} counterparts. It's likely that T effector clones arise from the T_{CM} populations. The T_{EM} population have higher expression of their lineage committed transcription factors and reside within specific organs or tissues, likely associated with their original homing destination (where the antigen was encountered at its highest concentration). Thus, the T_{EM} population lends the ability to mount a quick and effective an immune response at the site of infection (Pepper and Jenkins, 2011a).

As mentioned previously, the major role of $CD4\alpha$ T cells is to direct the immune response, given their “helper” T cell designation. Once stimulated, Th cells differentiate into different subsets. One important subset of $CD4^+$ Th cells is the follicular T helper (T_{FH}) cells. As their name implies, T_{FH} are $CD4^+$ Th cells that up-regulate the expression of CXCR5, which enables their migration to germinal centres. Within germinal centres T_{FH} , in conjunction with follicular DCs, direct somatic hypermutation and isotype switching. They have been shown to be crucial in generating long lasting neutralizing antibody responses to certain viruses. In addition to aiding the activation of B cells, $CD4^+$ Th cells also play a role in the stimulation of naïve $CD8\beta^+$ CTLs. The activation of $CD8\beta^+$ can be accomplished via stimulation and antigen presentation by APCs, but $CD4^+$ Th cells seem to be crucial in forming a memory $CD8\beta^+$ T cell response. An interaction of co-stimulatory molecules between $CD4^+$ Th cells and $CD8\beta$ T cells, particularly CD40-CD40L, results in a downregulation of TNF-related apoptosis inducing-ligand (TRAIL) within $CD8\beta^+$ T cells, conferring long lived memory cells via inhibition of apoptosis (Swain et al., 2012b). In addition to helping, $CD4^+$ T cells possess effector mechanisms that directly combat infection by influencing the cytokine environment at the sites of immune activation and infection.

As mentioned previously, the activation of a $CD4^+$ T cell clone results in its division into lymphoblast $CD4^+$ effector T cells. These effector T cells migrate towards sights of inflammation in order to aid in clearing antigen to which they have been primed.

Arguably, the major contribution of $CD4^+$ effector T cells when combatting a viral infection is via the secretion of IFN- γ . The secretion of IFN- γ aids in the establishment of

an anti-viral response amongst cells surrounding the area in which the CD4⁺ effector T cell is located (eg: activation of MΦs to an M1 phenotype). Additionally, some CD4α⁺ effector T cells may possess some cytolytic activity, either through perforin secretion or FasL induced apoptosis of target cells (Swain et al., 2012a). After the resolution of an infection, T lymphocyte numbers return to base levels with the help of CD4⁺ regulatory T cells (T_{Reg}). Regarding a viral infection, it's likely that regulatory T cells are induced in an antigen specific manner. A hallmark for regulatory T cell identification in pigs is the expression of Forkhead box P3 (FOXP3) and CD25, in addition to CD4α (Kaser et al., 2015). Regulatory T cells possess potent anti-inflammatory mechanisms, mainly through secretion of IL-10 and tissue-growth factor β (TGF-β). These cytokines are also able to induce apoptosis in effector T lymphocytes that are no longer needed, in the case of antigen clearance. Regulatory T cells may also possess some cytolytic activity, through the secretion of granzyme A/B and perforin, which would also aid in the induction of apoptosis in lymphocytes that are no longer needed. Whether or not these inducible T_{Regs} acquire a memory phenotype is unknown, but it's possible that some of the natural T_{Regs} that are more involved in self-tolerance and tissue homeostasis could be found to acquire a memory phenotype (Vignali et al., 2008).

1.7.2 *CD8β⁺ cytotoxic T cells*

The endogenous pathway of antigen presentation has been discussed previously. To recap, cytoplasmic antigen is processed via proteasomal degradation and presented as peptide sequences bound to MHCI molecules on the surface of cells. This provides the immune system with a mechanism to combat intracellular pathogens through the activation of CD8β⁺ CTLs. As such, an optimal Th1 type immune response mounted against a virus will involve the induction of CD8β CTLs (Rosendahl Huber et al., 2014). Similar to CD4⁺ Th cells, CTLs can acquire memory of effector phenotypes. The memory cell phenotype of CTLs follows similar principles to CD4⁺ induction, thus only effector mechanisms of CTLs will be discussed here. Viral infected cell recognition by CTLs results in their targeted apoptosis through multiple mechanisms. The main effector mechanism of CTLs would be through secretion of perforin, which punches holes in the membranes of cells, and the delivery of granzyme A/B to induce apoptosis. In addition to

perforin/granzyme secretion, CTLs can induce apoptosis via Fas-FasL interactions on cell surfaces. And lastly, similar to CD4⁺ effector T cells, CTLs are capable of influencing the immune environment through the secretion of inflammatory cytokines such as IFN- γ and TNF α (Barry and Bleackley, 2002).

1.7.3 Porcine T lymphocytes

Taking into consideration the porcine immune system, a study was performed to identify cell surface markers associated with T memory cell (T_{Mem}) differentiation and variation in T cell subsets over the first 6 months of a pig's life. A portion of porcine CD4 α ⁺ Th cells are found to express CD8 α , which seems to correlate with age. The authors went on to theorize that CD8 α expression was associated with antigen-experienced memory Th cells. As a result, they noted an absence of CD4 α ⁺ CD8 α ⁺ T cells that were CD27⁻, early in life. Over time, as pigs would encounter antigen and begin to develop a memory Th cell pool, the CD4 α ⁺ Th cells began to express CD8 α and were CD27⁺. Therefore, in pigs, it seems that CD4 α ⁺CD8 α ⁺CD27⁺ Th cells are an indicator of a memory cell phenotype and CD4 α ⁺CD8 α ⁻CD27⁻ would account for the naïve CD4 α ⁺ Th cell population. The CD8 β cytotoxic lymphocytes (CTL) seemed to follow a similar path of maturation as the CD4 α Th cells. Essentially, the authors found that the expression of CD27 correlated with a naïve CTL phenotype. In the first week after birth, perforin expression was limited to NK cells. Perforin expressing CD8 β T cells occurred in conjunction with the gradual loss of CD27 expression. The authors theorized that during the early stages of activation, effector CTLs begin to lose CD27 expression while up-regulating perforin. Therefore, the memory CTL pool can be described as CD3⁺CD8 β ⁺CD27⁺. Lastly, it should be mentioned that a major constituent to the T cell pool in pigs is the $\gamma\delta$ T cell population (Talker et al., 2013).

1.7.4 Gamma delta-T cells and natural killer cells

Gamma delta-T cells ($\gamma\delta$ T cells) are a CD3⁺ lymphocyte population that share properties characteristic of both the innate and adaptive arms of immunity. Found both in tissue and peripheral blood, multiple subsets possessing different qualities have been identified.

Their recognition of antigen occurs via interactions between the $\gamma\delta$ TCR and CD1d molecule on APCs and T cells, which presents the antigen. Whether or not $\gamma\delta$ T cells can acquire a memory phenotype, being specific for a particular antigen, is still under investigation (Lalor and McLoughlin, 2016). It appears that this may be pathogen specific and it is also possible that different subsets of $\gamma\delta$ T cells exist in which some may be more innate and others more adaptive. The innate aspect of $\gamma\delta$ T cells has received more attention and the mechanisms of $\gamma\delta$ antigen recognition have been identified.

Phosphoantigens, which are host-derived and presented on CD1d molecules, have been shown to possess $\gamma\delta$ T cell stimulatory capacity. Additionally, certain pathogen-associated proteins can be recognized by $\gamma\delta$ T cells to activate their anti-viral mechanisms. And lastly, $\gamma\delta$ T cells have been shown to be sensitive to TLR stimulation, lending another method for activation in response to an infection (Vantourout and Hayday, 2013). Regarding their mechanisms to combat pathogens, $\gamma\delta$ T cells exhibit similar cytotoxic qualities to NK cells and CTLs. Being capable of perforin and granzyme B secretion, in addition to utilizing the Fas-FasL pathway, $\gamma\delta$ T cells are potent inducers of apoptosis in target cells. Furthermore, $\gamma\delta$ T cell secretion of pro-inflammatory cytokines play an important role early during infections to promote the recruitment of leukocytes and the activation of phagocytes, in addition to influencing APC maturation. Lastly, in mice it has been shown that $\gamma\delta$ T cells may act in the stimulation of $\alpha\beta$ T cells through antigen presentation, as studies have demonstrated their expression of MHCII in addition to CD80/86. Their function as APCs warrants further investigation. Overall, $\gamma\delta$ T cells possess numerous functions to influence the outcome of an infection, resulting in their classification within the innate and adaptive branches of immunity (Zheng et al., 2013).

Natural killer cells (NK) are a branch of the innate immune system and were originally identified based on their anti-tumor properties. The recognition of stress or damage associated molecules on the surface of a cell is one mechanism that initiates NK cell cytotoxicity. In addition to this, tumor cells, and sometimes virally infected cells, often have down-regulated expression of MHCI molecules, which is also a primary mechanism utilized by NK cells for targeted apoptosis (Topham & Hewitt, 2009). Similar to CTLs, NK cells induce apoptosis via perforin/granzyme B secretion and the Fas-FasL pathway.

The expression of CD16 on NK cells confers the capability of inducing antibody dependent cell cytotoxicity (ADCC). Essentially, a virally infected cell could have viral proteins incorporated into its cell membrane that would be recognized by antibodies. The opsonization of the virally infected cell could then be recognized by CD16, through binding to the Fc portion of the antibody, which would in turn mediate the apoptosis of the infected cell. Lastly, NK cells are capable of secreting pro-inflammatory cytokines, such as IFN- γ and TNF α . Secretion of cytokines could lead to the activation of phagocytes, aid in the recruitment of leukocytes to the site of infection, and potentially influencing the adaptive arm of immunity. Their capabilities of cell cytotoxicity and their influence on the cytokine environment mirror those of CTLs, albeit in a primarily non-antigen specific manner (Vivier et al., 2008).

As mentioned previously, a large proportion of CD3⁺ T cells in the peripheral blood of pigs consist of $\gamma\delta$ T cells. It was found that the amount of $\gamma\delta$ T cells increased as a result of age, reaching upwards of 50% of the entire CD3⁺ T cell population. Furthermore, CD8 α was expressed on the majority of the $\gamma\delta$ T cell population, indicating their likelihood in thymic development. In addition to CD8 α , the expression of CD27 on the surface of $\gamma\delta$ T cells seems to decrease with age, potentially indicating antigen encounter. If this is the case, CD27 on $\gamma\delta$ T cells could be utilized to address maturation stages for $\gamma\delta$ T cells. In addition to $\gamma\delta$ T cells, the study investigated proportions of NK cells. Of note, NK cells can be identified as CD8 α ⁺ and CD3⁻ and the expression of perforin seems to be prominent immediately after birth, which is unlike other species. Proportions of NK cells seemed to vary and there was not a clear course in which their constitution to the T cell population could be identified (Talker et al., 2013). Further investigation into the roles of the $\gamma\delta$ and the NK cell populations of pigs is warranted.

1.7.5 *Cell-mediated immunity to PRRSV*

It appears to be widely accepted that both cell-mediated and humoral immunity are necessary components in overcoming PRRSV infection. Yet, evidence regarding the type of immune response conferring resistance has not been clearly defined. The research surrounding cell-mediated immunity in particular has been quite confusing. Variability in results are attributable, but not limited, to the routes/dosage of inoculation, viral strains

utilized, controlled vs. field conditions, and the breed/age/sex of the pigs. Fortunately, there appears to be a trend near the end of the viremic stage in pigs when IFN- γ expression is highly up-regulated. Unfortunately, the period of viremia varies not only in a strain specific manner, but also according to breed, and SLA haplotype of individual pigs. Additionally, a subject of continuing debate is the role that regulatory T lymphocytes (Tregs) play in PRRSV pathogenesis, if they are induced at all. The following section hopes to resolve some of the conflicting research surrounding cell-mediated immunity and PRRSV.

A major hurdle for controlling PRRSV is identifying the stage of infection a herd is currently in, albeit acute or chronic. In 2008, Molina *et al.* inoculated pigs via the intramuscular route (IM) with the avirulent VR2332 strain and observed infected animals over the course of 193 days in a controlled environment. Overall, pigs became moderately ill showing non-specific symptoms. In order to assess cell-mediated immunity, IFN- γ was detected in serum over the course of the trial. At day 42 post infection (PI) the levels of IFN- γ spiked and slowly declined thereafter. It should be noted that the point at which IFN- γ was highest occurred in correlation with a decline in viremia, which led to half of the pigs resolving the infection (Molina *et al.*, 2008). Overall, their results seemed to support that both cell-mediated immunity and humoral immunity were important for viral clearance. Similarly, Weesendorp *et al.* investigated the response of 5-week old pigs to Lelystad virus (LV) and found that IFN- γ also played an essential role in viral clearance. Furthermore, they observed an increase in NK cells and CTLs 26-33 days post infection (Weesendorp *et al.*, 2013). Overall, it seems likely that CTLs and potentially NK cells are playing an important role in resolving the viremic state in response to avirulent strains of PRRSV. On the other hand, highly virulent strains have been able to suppress these activities, which could provide an explanation for increased virulence. However, these results were obtained in experimental trials and may need to be confirmed in trials mimicking field conditions. For example, Dotti *et al.* performed a trial under field conditions with a moderately virulent NA clinical isolate (BS/AL2011). Briefly, their results indicate that the levels of IFN- γ observed under controlled conditions did not occur in the field. The levels of IFN- γ they detected in the sera were comparable to the controls stimulated with PBS. This seems to indicate that

observing PRRSV immunopathogenesis in a controlled environment may not be applicable to what is occurring naturally (Dotti et al., 2013).

As mentioned previously, confusion regarding PRRSV immunology could be due to strain specific virulence. Wang *et al.* was interested in the response of 1-month old piglets to NA highly pathogenic HuN4. In addition, they tested the efficacy of the currently available CH-1R vaccine. Piglets were inoculated intranasally (i.n.) with HuN4 on day 28. The vaccinated group was immunized on day 0, boosted on day 14, and infected on day 28. Sera was collected over the 56 day trial for cytokine analysis. On day 33 levels of IL-10 and IFN- γ increased significantly in the non-vaccinated group, peaked around day 38, and declined to normal levels by day 49. The vaccinated group had stable levels of IL-10 and IFN- γ in comparison to mock-infected pigs throughout the experiment. Of particular note, the vaccinated piglets had increased serum levels of IL-4 at day 33 P.I., decreasing gradually by day 42. This occurred in conjunction with decreased levels, and eventual loss, of viremia. Unsurprisingly, IL-4 was not detected in the non-vaccinated group which remained viremic until day 56. Overall, it seems that high levels of IL-10 and low levels of IL-4 aided in the establishment of the persistence of the virus. The authors believed that the vaccine induction of IL-4 resulted in prevention of disease, although the virus was still detectable in peripheral lymphoid organs (Wang et al., 2011). Yet, the levels of IFN- γ in the non-vaccinated group did not correlate with clearance of virus, which seems strange. In this case, it appears that humoral immunity could be playing a more important role than cell-mediated immunity. But, the delayed protection from infection could have occurred as a result of partial cell-mediated immunity, exhibiting the inefficiency of the vaccine. It can therefore be assumed that the most effective and safe vaccine will evoke both cellular and humoral immune responses.

Manickam *et al.* performed a thorough analysis of infection by NA highly virulent MN184. One month-old pigs were inoculated i.n. and the response in the blood, mucosal tissues, and lymphoid organs was assessed over 63 days. The cytokine profile showed an upregulation of IL-12 early during infection, a peak of IL-6 at day 42 until day 57, and high levels of IFN- γ at day 35, gradually decreasing by day 49. Resolution of infection appeared to coincide with increased expression of IL-6 and IFN- γ . Similar to Molina *et*

al., IFN- γ secreting cells were low in PBMCs, the lungs, and TBLN until day 30 at which point they increased significantly, but levels returned to normal at day 60. Levels of memory T cells and T helper (Th) cells increased in response to the infection in the lungs and lymphoid tissue. Levels of CD8 β^+ T cells only increased in the lungs. Interestingly, $\gamma\delta$ T cells increased in lymphoid tissue and in the lungs throughout the infection. Two unique phenomena were observed during the trial. The first of which was the upregulation of TGF β but low levels of IL-10 (although slightly increased). As a result, Treg cell proliferation was detected in PBMCs, lung tissue, and peripheral lymphoid organs until day 60. The second occurrence was a decrease in the proportion of natural killer (NK) cells. Further analysis of the NK cell population indicated that their cytotoxic activity had decreased by 50% in the blood and the lungs. Overall the authors wanted to demonstrate that a new vaccine is needed. Viral titres were still high in the lungs at day 60 days PI but had decreased in lymph nodes, although PRRSV was still detectable (Manickam et al., 2013). In comparison to the Lena virus (Eu high virulent), the results are surprisingly different. Overall, Th cell levels decreased, there was a very weak IFN- γ response, $\gamma\delta$ T cells didn't increase, CD8 β^+ T cells remained the same, and the NK cell population increased (Weesendorp et al., 2013). The Lena virus is often compared to NA highly virulent strains, but it seems that their immunomodulatory capabilities are significantly different.

More recently, a group developed an assay to measure cytotoxicity of PRRSV infected target cells from animals that had been exposed to PRRSV and subsequently recovered from the infection. Their results indicate that CD4 α^+ CD8 α^+ double positive T cells were capable of killing PRRSV infected macrophages 3-6 hours post infection. Furthermore, they found that CD4 α^+ CD8 α^- T cells possessed cytotoxic properties, killing infected macrophages 16-24 hours post infection. Interestingly, they noted that CD4 α^- CD8 α^+ T cells did not contribute to cytotoxicity. In addition, the authors noted that neutralizing antibodies were not detected in the infected animals. These results indicate the importance of cytotoxic T cells in the resolution of a PRRSV infection (Chung et al., 2018). An investigation into the T cell response to a Type 1 PRRSV infection indicated that there is a delayed induction of memory T cells as CD4 α^+ CD8 α^+ and CD4 α^- CD8 α^+ CD8 β^+ detected roughly three weeks post infection in PBMCs. The kinetics of the T cell

response seem to indicate that regulatory T cells decrease upon infection in PBMCs as do CD21⁺ B cells, until roughly three weeks post infection at which point the levels of both regulatory T cells and CD21⁺ B cells begin to increase. Lastly, roughly one-week post infection there was a marked increase in the levels of natural killer T cells (NKT) and gamma delta ($\gamma\delta$) T cells (Ferrari et al., 2018). This may be an indication of the potential importance of $\gamma\delta$ T cells and NKT early during a PRRSV infection.

1.7.5.1 *Natural killer cells and PRRSV*

Research surrounding the role of natural killer (NK) cells in PRRSV immunopathogenesis is in the early stages. Recently Cao *et al.* performed analysis utilizing the avirulent Lelystad virus to assess the immunomodulation of NK cells. Essentially, NK cells were enriched and cultured in the presence of IL-2 to spurn the population into an activated state. Using K652 cells (NK cell targets) and Pseudorabies virus (PrV) as positive controls to demonstrate NK cell lysis, the group infected PAMs with PRRSV and co-cultured them with the activated NK cells. Their results demonstrate that PRRSV infected PAMs were able to suppress the NK cell activity. Upon comparison to the mock-infected PAMs, NK cell activity in PRRSV infected PAMs was still lower. They hypothesized that PRRSV is able to modulate a receptor molecule on the surface of PAMs that is able to suppress the degranulation process in NK cells, which would inhibit perforin and granzyme secretion (Cao et al., 2013). Results obtained previously seemed to indicate that this was only occurring in highly virulent strains of PRRSV. Furthermore, the result obtained by Weesendorp are contradictory considering he saw a proliferation of NK cell activity. Further investigation into NK cell modulation by PRRSV is warranted.

1.7.5.2 *Regulatory T cells and PRRSV*

Shortly afterwards, Wongyanin *et al.* performed a similar analysis using an avirulent strain (01NP1) *in vitro*. They found that after 48 hours in co-culture with infected MoDCs, a similar Treg population had proliferated, which they characterized as being FoxP3⁺CD4 α ⁺CD25^{high} which are similar to those in humans and mice. They continued to perform an *in vivo* analysis by which they infected pigs and harvested blood on day 0, 5,

and 10. Observations confirmed the *in vitro* results as a FoxP3⁺CD4⁺CD25^{high} population had proliferated. Lastly, they too agreed that TGFβ and not IL-10 was responsible for the proliferation, although it was mentioned that IL-10 could contribute to proliferation (Wongyanin et al., 2010). Regulatory T cell induction by PRRSV is under debate. Silva-Campa *et al.* (2009) was the first group to demonstrate Treg induction by PRRSV strains NVSL 97-7895 and CIAD008. Essentially, they infected MoDCs with the PRRSV strains and co-cultured them with PBMCs over a 5-day period. Their results indicate that Foxp3⁺CD25⁺ Tregs proliferated significantly in response to infection. Furthermore, upon treatment with IFN-α (either during MoDC infection or during co-culture) Treg proliferation was inhibited. Upon closer analysis, they found that IL-10 expression did not play a role as it was not up-regulated. They found that TGFβ was solely responsible for the differentiation. They defined the population as Th3 Tregs, and concluded that proliferation was occurring as a direct result of PRRSV infection (Silva-Campa et al., 2009). More recently in 2012, Wongyanin published results that are conflicting to those obtained previously. Briefly, the N protein from PRRSV 01NP1 was transfected into PAMs, which resulted in the induction of IL-10. It should be noted, that Hou *et al.* had previously demonstrated that the GP5 protein was able to induce IL-10 synthesis in transfected PAMs (Hou et al., 2012). Transfected PAMs were then co-cultured with PBMCs, but no Treg induction occurred. Interestingly, when MoDCs were transfected and then co-cultured with PBMCs, Treg proliferation was prominent. Upon the addition of IL-10 antibody, the proliferation was suppressed. The authors concluded that IL-10 was responsible for Treg induction and failed to mention TGFβ (Wongyanin et al., 2012). Recently, a group demonstrated that Tregs were detected in the tracheobronchial lymph nodes and lung tissue of PRRSV infected animals. Furthermore, the authors demonstrated that mononuclear cells infected with PRRSV induced Treg differentiation from PRRSV negative animals, which is contradictory to what Rodriguez-Gomez published previously (Rodriguez-Gomez et al., 2015). Lastly, the authors concluded that the induction of Tregs was likely attributable to the increased levels IL-10 secretion (Nedumpun et al., 2018). The pathogen load of PRRSV, the breed and age of the animal, in addition to the strain of PRRSV are all potential contributors in the induction of Tregs and T cell immunity in general. The debate as to whether Tregs are

induced during a PRRSV infection and the potential role that Tregs have in the delayed induction of the cytotoxic T cell response, ultimately leading to the resolution of an infection, continues.

1.8 Discussion

Developing a vaccine for PRRSV has proven to be extremely difficult. The major issues encountered thus far stem mainly from unusually high mutation rates, which has resulted in the divergence of PRRSV into countless variants between the Type 1 and Type 2 PRRSV genotypes (Brar et al., 2015; Lu et al., 2017). Although multiple strategies have been employed, efforts have been met with limited success, as the induction of cross-reactive neutralizing antibodies seems to be nearly impossible. Shedding light upon unknown aspects of PRRSV immunology and viral pathogenesis, particularly those surrounding the regulation of cell mediated immunity and humoral immunity, will aid in future vaccine development strategies.

Based on current research, it is likely that both cytotoxic T cell mediated immunity and the induction of neutralizing antibodies are necessary components to provide protection and overcome a PRRSV infection. Currently distributed live attenuated vaccines for PRRSV are relatively efficacious, conferring cross protection and improving the overall health status of immunized animals in comparison to non-immunized animals (Canelli et al., 2018; Haiwick et al., 2018). A recent study demonstrates that MLV variants improve the health of challenged animals and provide differential protection, depending on the strain that animals were challenged with (Huang et al., 2019). A major challenge will be the development of a universal PRRSV vaccine for both Type 1 and Type 2 strains. Another recent study showed that immunization of gilts with a Type 2 MLV conferred increased overall health and a significant decrease in stillborn piglets when late-term pregnant gilts were challenged with a Type 1 PRRSV strain. The authors noted that T cell mediated immunity was the likely contributor to improved health status and decreased viremia in the challenged gilts, as neutralizing antibody titres were low (Jeong et al., 2018). In contrast, a recent study demonstrated that pigs infected with a Type 2 PRRSV strain possessed cross-reactive IFN- γ secreting T cells to other Type 2 strains, but not

with a Type 1 PRRSV strain. Additionally, the authors noted that neutralizing antibodies were not cross-reactive amongst any of the challenge strains (Correas et al., 2017). The discrepancy between the studies could be attributable to methods utilized in the assay. It would be surprising if a Type 2 PRRSV immunization offered cross-protection against a Type 1 PRRSV strain. Although the currently available MLVs are beneficial towards improving health status amongst PRRSV challenged animals, immunization with a live virus is not without risk. Major issues associated with the currently available MLVs include the risk of reversion to virulence and the immunosuppressive attributes associated with PRRSV itself, resulting in animal susceptibility to opportunistic pathogens (Liu et al., 2018; Niederwerder et al., 2015). Therefore, given the high mutation rates observed amongst strains of PRRSV, the ideal vaccine candidate would not be attenuated. Utilizing inactivated, vector delivered, DNA, or conjugate vaccine platforms are potential options for future vaccine formulations. In order for one of the previously listed strategies to be effective, viral epitopes leading to the induction of both cytotoxic T cells and neutralizing antibodies must be determined. Based on previous studies, it seems that T cell epitopes are relatively well conserved, as demonstrated by cross-reactive IFN- γ secreting T cells within the Type 2 genus (Correas et al., 2017). Theoretically, supplementing a peptide vaccine with an appropriate adjuvant platform will elicit a T cell mediated response. Therefore, shedding light upon the delayed induction of neutralizing antibodies to PRRSV, and identifying epitopes associated with PRRSV neutralization, will be crucial for future vaccine development efforts.

Chapter 2 HYPOTHESIS AND OBJECTIVES

2.1 Rationale

The tropism of PRRSV has been shown to be restricted to cells that express CD163. The majority of these cells are of myeloid origin and are responsible for the stimulation of both naïve and memory T cell responses. There is a delayed adaptive immune response to PRRSV and the cause(s) surrounding the delay are unknown. Thus, we chose to investigate the influence that PRRSV infection has on specific antigen-presenting cell (APC) subsets. Furthermore, we chose to investigate the stimulatory capacity of PRRSV infected APCs when co-cultured with T cells, in order to assay the progression to T cell immunity over the course of a PRRSV infection. We hypothesize that a specific subset of DCs is critical for the induction of T cell mediated immunity. The delayed induction of T cell immunity could be attributable to the relative rarity of this specific DC population and the dysregulated humoral immune response can be attributable to a lack of follicular T helper cell directing somatic hypermutation.

2.2 Objectives and hypotheses

2.2.1 Objective 1: Characterization of Flt3L derived bone marrow dendritic cells

Dendritic cells are the professional APCs of the immune system, directly linking the innate and adaptive immune response. They are responsible for antigen presentation to naïve T cells and the cytokines that DCs secrete play a significant role in directing T cell lineage (Th1, Th2, Th17, Th22, Treg). Multiple DC subsets exist *in vivo*, but their rarity makes it difficult to obtain the different subsets for *in vitro* assays. As such, we chose to differentiate DCs from bone marrow hematopoietic stem cells in order to obtain a population of DCs consisting of multiple subsets. We characterized the successful differentiation of our bone marrow DC populations using flow cytometry.

2.2.2 Objective 2: Comparison of antigen-presenting cell susceptibility to PRRSV infection

Antigen presentation to naïve T cells is not restricted to DCs, as macrophages (MΦs) and potentially B cells are also capable of presenting antigen to stimulate a naïve T cell. Because PRRSV infects MΦs and DCs, we were interested in susceptibility of different APCs to infection and how they responded to the infection. We hypothesized that PRRSV replicates more efficiently in MΦs than in DCs, making DCs more properly equipped to stimulate naïve T cell activation.

2.2.3 Objective 3: Investigate the maturation of the invariant chain

The maturation of the invariant chain is a critical step during antigen processing that ensures an antigen-derived peptide sequence is loaded into the binding groove of an MHCII molecule. This process of maturation occurs within endosomes. Coincidentally, it has been demonstrated that PRRSV forms a double membrane vesicle replication complex, reminiscent of endosomes. Given the importance that invariant chain maturation has during antigen processing and presentation, we hypothesized that PRRSV infection interferes with the maturation of the invariant chain. By immunoprecipitating MHCII from infected and non-infected APCs, we aimed to demonstrate that PRRSV infection prevents maturation of the invariant chain. This could provide a potential explanation for the delayed induction of cell-mediated immunity to PRRSV.

2.2.4 Objective 4: Investigate the T cell response to PRRSV infection

Studying the susceptibility of APCs to PRRSV infection, and their subsequent response, does not provide information regarding the effect that infection has on the interaction of APCs with T cells. In order to study the interaction of APCs with T cells, we established an APC-T cell co-culture assay using a mixed leukocyte reaction (MLR). The MLR confirmed our hypothesis that specific APC populations possess differential immunostimulatory capacities to promote T cell proliferation. This allowed us to perform an animal trial analyzing the progression of the T cell response over the course of a PRRSV infection, comparing the antigen-presenting capability of either monocyte-

derived MΦs or monocyte-derived DCs. We hypothesized that DCs were more potent stimulators of CD4⁺ T helper cells, contributing directly to the initiation of the T cell immune response, whereas MΦs, still possessing the capability to stimulate T cells, are more involved during the recall of cytotoxic lymphocyte responses during the resolution of an infection.

Chapter 3 ANTIGEN-PRESENTING CELL SUSCEPTIBILITY TO PORCINE REPRODUCTIVE AND RESPIRATORY SYNDROME VIRUS INFECTION

Joseph Darbellay, Jill Van Kessel, Volker Gerdtz

3.1 Abstract

Porcine reproductive and respiratory syndrome virus (PRRSV) has a worldwide distribution and is the most economically devastating virus in the swine industry today. The tropism of PRRSV has been shown to be restricted to antigen-presenting cells (APC) that express CD163. Furthermore, a characteristic of PRRSV disease is the delayed induction of T cell immunity. Given their roles in the stimulation of both naïve and memory T cell responses, we chose to investigate the rates of viral replication within APC populations using flow cytometry (FCM) and rt-qPCR. The susceptibility of monocyte-derived macrophages (MoMφs), monocyte-derived DCs (MoDCs), and Flt3L-derived bone-marrow DCs (BMDCs) to PRRSV infection were compared *in vitro*. Intracellular detection of PRRSV was comparable and prominent 24 hours post infection in MoDCs and Mφs. Furthermore, using rt-qPCR we found that viral copies in the supernatants of Mφs increased at a higher rate than the DC populations. In comparison to the Mφs, the rate of PRRSV replication in CD163⁺ BMDCs was much lower. Additionally, we investigated the expression of cell surface molecules associated with antigen presentation in PRRSV infected APCs with FCM. The levels of MHCI and MHCII expression on the surface of infected non-stimulated Mφs were both down-regulated. Although it is difficult to conclude why DCs are less susceptible to infection, our study allows for speculation on the potential role that DCs may have in the induction of T cell immunity.

3.2 Introduction

Porcine reproductive and respiratory syndrome virus (PRRSV) is a positive sense, single-stranded, enveloped RNA virus that causes disease in swine worldwide. The virus was

first identified in the early 1990s and is thought to have emerged during the early-mid 1980s (Shi et al., 2010). Today, PRRSV is the most significant pathogen in the swine industry causing losses upwards of \$650 million dollars in the United States alone (Holtkamp, 2012). Outcomes of disease include respiratory difficulty, spontaneous abortions and fetus mummification in sows, weight loss, and death under certain circumstances (Reeth, 1997; Tong et al., 2007). The demand for an efficacious vaccine and the development of strategies for disease control are top priorities (Kimman et al., 2009).

Two main species of PRRSV exist, the North American (Type 1) and the European (Type 2) in which a roughly 40% nucleotide identity is shared (Shi et al., 2010). It is classed under the order Nidovirales from the *Arteriviridae* family. The tropism of PRRSV is restricted to cells that express the hemoglobin/haptoglobin scavenger molecule CD163, which was identified as the main cellular receptor for viral entry into the cytoplasm (Calvert et al., 2007). Although it has been widely accepted that porcine alveolar macrophages (PAMs) are the main target cells for PRRSV infection and replication, it has been proposed that dendritic cell (DC) are also targets of infection (Calzada-Nova et al., 2010; Calzada-Nova et al., 2011; Chang et al., 2008; Chaung et al., 2010; Peng et al., 2009; Rodriguez-Gomez et al., 2012; Silva-Campa et al., 2009). Because DCs are the professional antigen-presenting cell (APC) of the immune system, the modulation of their antigen-presenting ability, or their being targets of PRRSV replication, would have major implications on the transition from innate to adaptive immunity (Randolph et al., 2005). A major interest in the field of PRRSV virology and immunology is the transition to adaptive immunity. PRRSV specific antibodies can be detected in animals within days of being exposed to the virus, although the antibodies are non-neutralizing. The virus continues to spread unchecked, as non-neutralizing antibody titres increase steadily, until 4+ weeks post infection when neutralizing antibodies become apparent in serum (Loving et al., 2015). Although numerous investigations have been undertaken to understand why there is a delayed induction of neutralizing antibodies, there has not yet been a concrete explanation. On the other side of adaptive immunity, very little is known about the T cell response to PRRSV. It seems that there is a similar delay in the induction of T cell immunity as is seen with the neutralizing antibodies. The majority of what is known

about T cell immunity has been collected through analyses using IFN- γ ELISpots, which have essentially indicated that IFN- γ secreting cells in PBMCs of infected animals become apparent around the same time as neutralizing antibodies (Loving et al., 2015). Future investigations into the induction of T cell immunity by PRRSV may contain long sought after answers. In this study, we focus on antigen-presenting cell susceptibility to PRRSV in order to obtain information regarding the first step towards inducing T cell immunity.

We feel the confusion surrounding DC susceptibility to PRRSV has arisen as a result of utilizing DC models subject to monocyte/macrophage contamination. Studies carried out thus far have been performed with GM-CSF bone marrow-derived DC (BMDC) or monocyte-derived DC (MoDC) populations. These populations are often subject to macrophage contamination, making them inaccurate for elucidating the DC response to PRRSV. We have thus chosen to utilize FMS-like tyrosine kinase 3 ligand (Flt3L) BMDCs to study PRRSV infection of DCs *in vitro*. We hypothesize that specific subsets of DCs, and not the entire population, are susceptible to PRRSV. Furthermore, we hope to demonstrate that immune modulation in this DC subset occurs in a strain specific manner according to pathogenicity of the particular strain being investigated. Overall, we aim to shed light upon the immunopathogenesis of PRRSV and the evasion strategies it possesses. Understanding its mechanisms of immune evasion will be crucial for developing new methods of control in addition to establishing strategies for immunization.

3.3 Materials and methods

Animals:

Six-eight week old Dutch Landrace pigs were purchased from the pathogen free herd at the Prairie Swine Centre (Saskatchewan). A group of 8 pigs was immunized with the Fostera® PRRS modified live virus (MLV) intramuscularly to measure T lymphocyte proliferation in a co-culture assay. All experiments were conducted in accordance with

the ethical guidelines of the University of Saskatchewan and Canadian Council of Animal Care.

Cells and viruses:

Flt3L bone marrow-derived dendritic cells (BMDCs) were prepared as described previously (Guzylack-Piriou *et al.*, 2010). Briefly, the sternums were removed from 6-8 week old Dutch Landrace pigs. Bone marrow was flushed from the sternum with PBS (supplemented with 0.7% EDTA, 1% Antibiotic/antimycotic (Gibco®-BRL), and 0.5% Gentamycin (Gibco®-BRL)) using an 18-gauge syringe. Hematopoietic stem cells (HSCs) were removed from a buffy coat, using a FICOLL-PAQUE® Plus gradient (GE Healthcare, Uppsala Sweden) centrifuging at 1000 x g, 40 minutes. Cells were cultured in 6 well, non-tissue culture treated plates, at a concentration of 5.0×10^5 cells/mL in RPMI-1640 complete (Gibco®-BRL) (1% Antibiotic/antimycotic, 0.5 mM β -mercaptoethanol, 1% MEM non-essential amino acids (Gibco®-BRL), 1% HEPES (Gibco®-BRL), and 10% FBS) supplemented with 20 ng/mL huFlt3L (R&D Systems). Every third day, 1.0 mL of media was removed and replaced with fresh media. Cells were harvested on day 7 for analysis. Monocytes were isolated from whole blood as previously described (Auray *et al.*, 2013). Briefly, PBMCs were isolated on a FICOLL-PAQUE® Plus gradient (GE Healthcare, Uppsala Sweden). Monocytes were labeled with anti-human CD14 beads and selected for on LS columns using a magnetic isolated cell sorter (Miltenyi Biotec, Auburn, CA). To obtain MoMΦs, monocytes were plated at 1.0×10^6 cells/mL in RPMI complete supplemented with rpGM-CSF (20 ng/ml - Biosource, Camarillo, CA) for 3 days at 37 °C with 5% carbon dioxide. To obtain MoDCs, monocytes were plated at 1.0×10^6 cells/mL in RPMI complete with recombinant porcine (rp) IL-4 (100 ng/mL – R&D 654-P4) and rpGM-CSF (20 ng/mL – R&D 711-PG) for 6 days at 37 °C with 5% carbon dioxide, and media was changed every 3rd day as shown previously (Facci *et al.*, 2010). PRRSV strains VR2332 and VR2385 (ATCC, Manassas, VA, USA) were used in the study. Virus was grown up on MARC-145 cells and titers were calculated as the TCID_{50/mL} (Reed and Muench, 1938).

BMDC Characterization:

BMDCs were harvested on day 6 and resuspended in cold 1 x PBS (pH 7.2, 0.2% gelatin, 0.03% Na Azide at 1.0×10^6 cells/mL). BMDCs were characterized by staining with each antibody for 20 min at 4° C, washed three times (1 x PBS), and fixed with 2% paraformaldehyde. Cells (>10,000 events) were analyzed using FACScalibur™, Becton Dickinson, BD Biosciences and CELLQUEST™ software. The following antibodies were used for BMDC characterization: CD172a (BL1H7, Bio-Rad), CD90 (F15-42-1, Bio-Rad), CD3 (PPT3, Southern Biotech), CD14 (MIL-2, Bio-Rad), CD163 (2A10/11, Bio-Rad), CD16 (G7, Bio-Rad), CD21 (BB6-11C9.6, Southern Biotech), Swc9 (PM18-7, Bio-Rad), MHC II (K274.3G8, Bio-Rad), and MHC I (JM1E3, Bio-Rad). FITC anti-mouse immunoglobulins IgG1 (1072-07) and IgG2b (1092-02, Southern Biotech) were used as secondary antibodies.

Microscopy:

Cells were fixed, permeabilized and stained with the FITC-SR30 ab as indicated previously at 1.0×10^6 cells/mL. Cells were pipetted (10 μ L) onto glass slides, air dried, and 1 drop of ProLong® Gold antifade reagent with DAPI (Life Technologies) was applied to sample according to the manufacturer's instructions. Immunofluorescence was visualized with the Zeiss Axiovert 200m Inverted microscope (Carl Zeiss Light Microscopy, Germany) under 20x magnification. Images were captured with the AxioCam (Zeiss, 1069-414) and analyzed using AxioVision Rel. 4.6 (Carl Zeiss Light Microscopy).

Antigen presenting cell infections:

Antigen presenting cells were infected with PRRSV strain VR-2385 at a 0.1 MOI for 3 hours at 37°, 5% CO₂. Cells were centrifuged at 350 g, resuspended in fresh media, and seeded on 12 well plates. Cells and supernatant were harvested at 8, 24, 48, and 72 hours post infection for flow cytometry analysis and rt-qPCR. Monocyte-derived macrophages were either non-stimulated (M0), or stimulated with IL-4 (100 ng/mL) or with recombinant porcine IFN- γ (20 ng/mL, R&D 985-PI) for 24 hours to mimic an M2 or M1 phenotype, respectively before being infected with the PRRSV as previously.

Flow cytometry:

At 24 or 48 hours post infection, DCs and MoMΦs were harvested and resuspended in 1× phosphate buffered saline (PBS) pH 7.3 containing sodium azide (0.03%) and gelatin (0.02%) (staining media) and stained to assess cell surface marker expression by flow cytometry. Briefly, cells were incubated 20 min at 4°C with primary antibodies, then washed twice before incubation with their respective secondary antibody. The primary antibodies utilized are as follows: CD163 (2A10/11, Bio-Rad), MHC II (K274.3G8, Bio-Rad), and MHC I (JM1E3, Bio-Rad). Cells were incubated for 20 min at 4°C with a goat-anti mouse IgG1-APC secondary antibody (Southern Biotech 1070-11s). For PRRSV nucleocapsid staining, cells were fixed and permeabilized with the Fixation/Permeabilization Kit (eBioscience) according to the manufacturer's instructions. At least 10000 events were collected on a FACSCALIBUR™ (BD Biosciences, Mountain View, CA) using the CELLQUEST™ software. Changes in mean fluorescence intensity (MFI) were calculated by subtracting the MFI from the infected cells by the MFI of the non-infected cells.

Reverse transcription-quantitative real-time polymerase chain reaction (RT-qPCR):

To measure PRRSV replication, 180 µl of supernatant was collected from infected cell cultures and stored at -80. RNA was extracted using a QIAmp Viral RNA Mini Kit (Qiagen) according to the manufacturer's instructions. A 2-step reverse transcription PCR was performed to determine levels of PRRSV in the supernatant. Complementary DNA was synthesized (High Capacity cDNA Reverse Transcription Kit, Invitrogen) and then quantitative-PCR was performed using 2 µL of each cDNA reaction with the KAPA SYBR® Fast qPCR kit according to the manufacturer's instructions (Kapa Biosystems). Analysis was performed using a Bio-Rad iCycler iQ 5 (Bio-Rad, Hercules, CA). Primers were selected based on previous publication (S-GGCCAGCCAGTCAATC; AS-CACACGGTCGCCCTAATTG) (Calzada-Nova et al., 2011).

Interferon-gamma ELISpots:

A group of 8 animals was immunized with the Foster® PRRS modified live virus (MLV). Peripheral blood mononuclear cells (PBMCs) were isolated on day 0 and day 16

for IFN- γ ELISpots. ELISpots were performed as demonstrated previously (Dar et al., 2012). Briefly, nitrocellulose microtiter plates (UNIFILTER[®] 350, Whatmann, Florham Park, NJ, USA) were coated with 0.5 $\mu\text{g}/100 \mu\text{l}$ of anti-porcine IFN- γ monoclonal antibodies solution (Thermo Fisher Scientific, Inc., Nepean, ON, Canada). 5.0×10^5 PBMC were added to each well and cells were stimulated with PRRSV or inactivated PRRSV (VR-2385, MOI 1.0). After 24 hr incubation at 37 °C, rabbit anti-porcine IFN- γ antibody solution (0.2 $\mu\text{g}/100 \mu\text{l}$ in phosphate buffer saline with 0.05% tween[®] 20) was added and plates were incubated for 4 hours at room temperature. Biotin-conjugated goat anti-rabbit IgG (Invitrogen-Zymed, Burlington, ON, Canada) was added (1/5000 dilution) for 2 hours at room temp before the addition of 1/5000 diluted streptavidin alkaline phosphatase solution for 1.5 hours at room temp. Lastly, spots were developed with NBT/BCIP (Sigma-Aldrich, St. Louis, MO, USA). Spots were counted with an AID ELISpot Reader Classic.

Monocyte-derived macrophage – T cell co-cultures and lymphocyte proliferation assay: Monocyte-derived macrophages and T cells were co-cultured to investigate the stimulatory capacity of PRRSV infected M0 MoMΦs, to promote T lymphocyte proliferation. Animals were immunized with the MLV and 14 days post immunization, monocytes were isolated from PBMCs of MLV immunized animals. After 3 days in culture monocytes had differentiated into MoMΦs. On the same day, T cells were isolated from PBMCs of the MLV immunized animals. To isolate T cells, PBMCs were stained with anti-CD172a and anti-CD21 for 15 minutes at 4° C, then washed twice. Cells were then incubated with IgG1 MACS beads for 15 minutes at 4° C before passing the cells through LS columns (Miltenyi Biotec). The enriched T cell population was stained with CFSE according to the manufacturer's protocol (Cell Trace CFSE, Thermo Fisher) to monitor proliferation, before being plated at 3.0×10^5 cells/well on a 96 well U bottom plate. The M0 MoMΦs were infected with PRRSV VR-2385 for 3 hours, or mock-infected, before being washed and plated with T cells at a ratio of 1:10. After the addition of M0 MoMΦs, the MoMΦ-T cell co-culture was incubated at 37° C, 5% CO₂ for 4 days before assessing proliferation with FCM.

Statistical Analysis:

All data points on graphs are representative of genetically unrelated individual animals. All the data were statistically analysed using GRAPHPAD PRISM™ 7 software (GraphPad Software, Inc., La Jolla, CA). Differences between groups were assessed using the Mann-Whitney U test for non-paired, non-Gaussian data. When $P \leq 0.05$, differences were considered significant.

3.4 Results

Characterization of bone marrow-derived dendritic cells:

Flow cytometry (FCM) was carried out on day 7 of culture to demonstrate successful differentiation of HSC precursors into BMDCs. The relative purity of DCs in the culture can be seen by the lack of macrophages (Swc9), lymphocytes (CD3/CD21), and fibroblasts (CD90). Furthermore, the BMDCs were consistently CD172a^{high} and MHCII^{mid/high} (Supplementary Figure 3-10 and 3-11). Supplementary Figure 3-12 demonstrates the clustered arrangement of DCs in culture after they have differentiated. Cells were non-adherent, further indicating purity of DCs in the cultures. Based on previously published data, we are confident in confirming successful differentiation of the BMDC populations (Guzylack-Piriou et al., 2010), (Facci et al., 2010).

Susceptibility of BMDCs to PRRSV:

A preliminary investigation was launched in order to determine the susceptibility of BMDCs to PRRSV infection using VR-2385. Figure 3-1 demonstrates that over a 72-hour period of time, cells became gradually infected with PRRSV, as the level of staining against the viral nucleocapsid protein increased (FCM schematic shown in supplementary Figure 3-13). Lastly, RT-qPCR for PRRSV transcripts in the supernatant indicated a roughly 400-fold increase after 72 hours (Supplementary Figure 3-14).

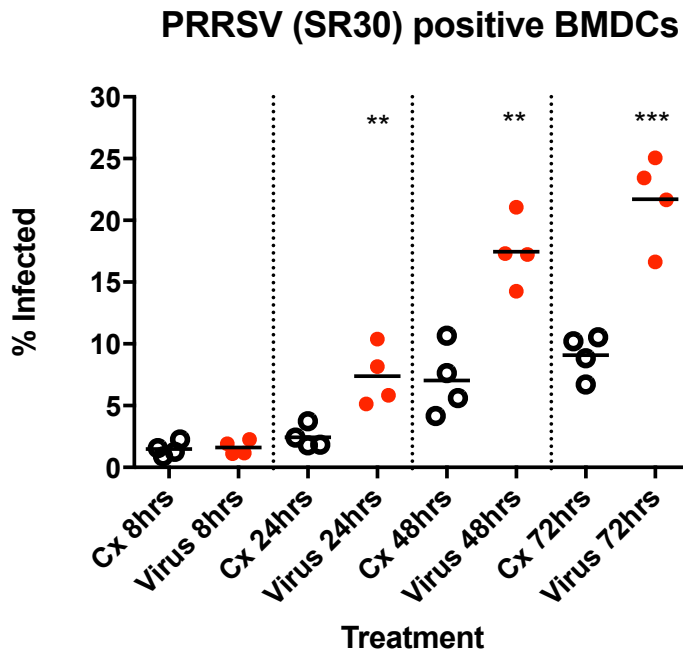


Figure 3-1: BMDC infection with VR-2385 over 72 hours. BMDCs were infected at an moi of 0.1 and harvested at the indicated time points. Cells were subsequently fixed, permeabilized, and stained with the SR30-FITC to detect the PRRSV N protein. Data points are representative of genetically unrelated animals, performed as single samples. The figure demonstrates flow cytometry (FCM) data showing individual pigs (dots) and the percentage of infected cells (bars); Cx = non-infected cells. $P < 0.05 = *$; $P < 0.005 = **$; $P < 0.0005 = ***$.

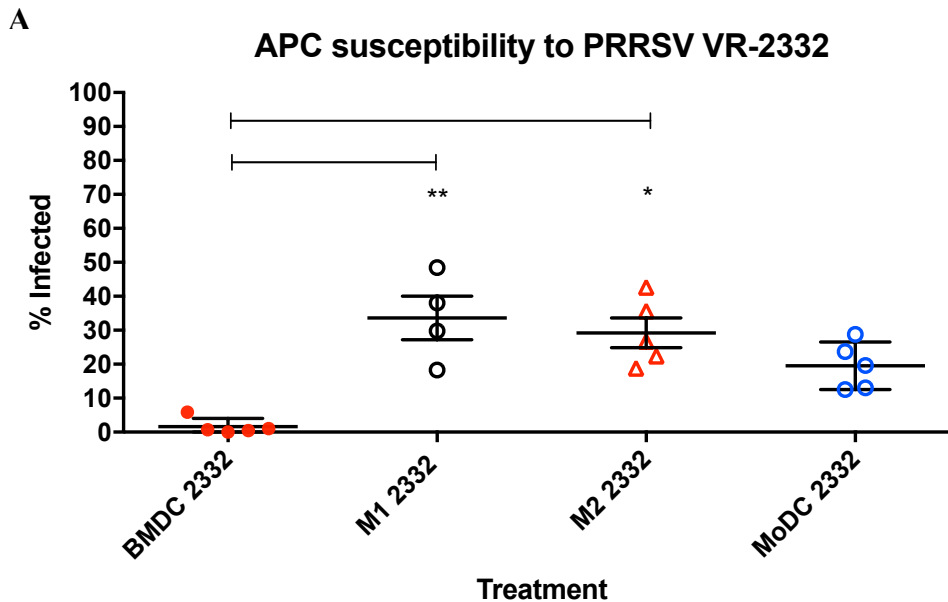
CD163⁺ and CD163⁻ BMDC susceptibility to PRRSV:

BMDCs were sorted using a fluorescence activated cell sorter (MoFlo XDP Cell Sorter, Beckman Coulter) according to CD163 expression (Supplementary Figure 3-15). The BMDC populations were exposed to the PRRSV and stained intracellularly for the viral N protein (Supplementary Figure 3-16). Based on the FCM results, CD163⁺ BMDCs are susceptible to infection and CD163⁻ BMDCs are not susceptible to infection (Figure 3-2).

Antigen presenting cell susceptibility to PRRSV:

MoMΦs were stimulated with IL-4 or IFN- γ for 24 hours to mimic and M2 or M1 phenotype respectively. M1 and M2 MoMΦs and MoDCs were infected with two strains of PRRSV (VR-2385 and VR-2332). The susceptibility of the MoMΦs and MoDCs was compared to that of the BMDCs (Figure 3-3). There was no difference amongst the susceptibility of MoMΦs, regardless of stimulation and the MoDCs seem share a similarity in susceptibility to MoMΦs. The CD163⁺ BMDCs were not as susceptible to infection in comparison to the other APC populations.

As shown in Figure 3-4, upon comparing forward scatter (FSC) / Side scatter profiles (SSC) of the infected APCs, it became apparent that MoDCs (Supplementary Figure 3-17) and MoMΦs were no longer viable 48 hours post infection, in comparison to the BMDCs which still appear to be healthy. The assessment of cell viability is based on the relative diameter of the cell (FSC). As cells begin to die they appear lower on the FSC axis where debris is normally located on FSC/SSC dot plots.



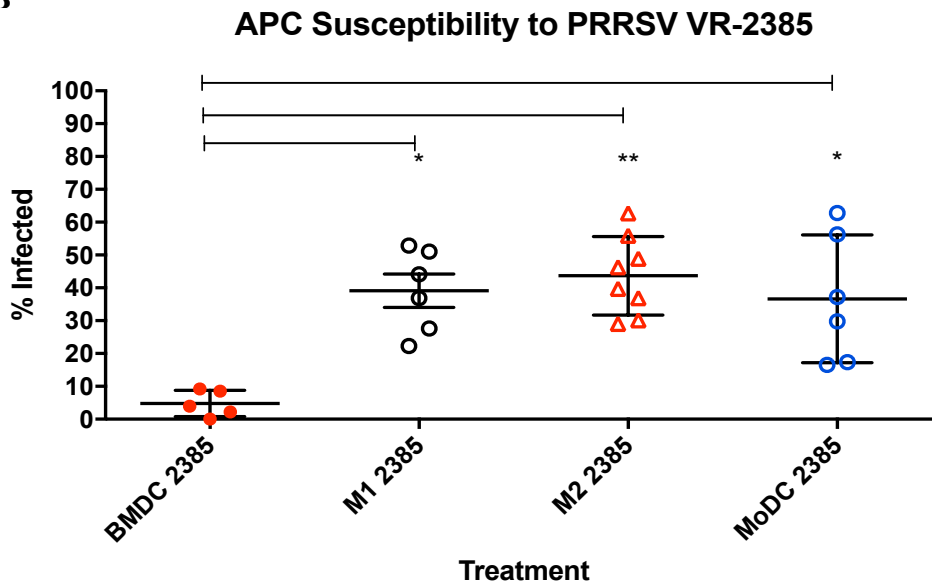
B

Figure 3-3: APC cell susceptibility to PRRSV infection. MoMΦs, MoDCs, and BMDCs were infected with two different strains of PRRSV (3a: VR-2332; 3b: VR-2385). Cells were fixed, permeabilized, and stained with SR30-FITC at 24 hours post infection. Data points were collected from unrelated animals, performed as single replicates. Statistical significance was determined comparing the groups to the BMDC infected population. $P < 0.05 = *$; $P < 0.005 = **$.

APC viability of PRRSV infected cells

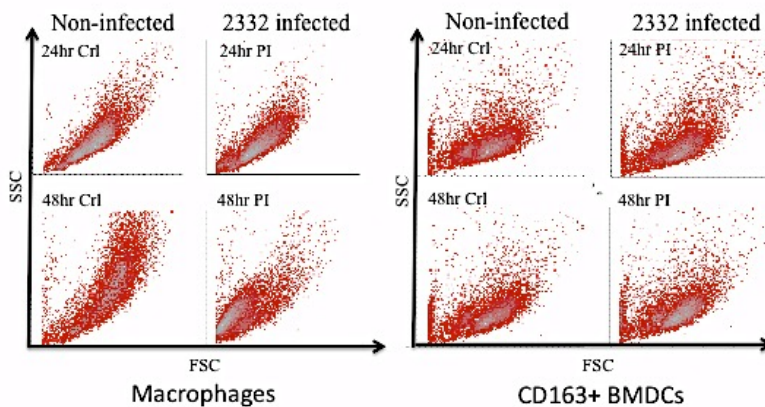


Figure 3-4: Antigen-presenting cell viability post infection. Forward scatter (FSC), side scatter (SSC) dot plots demonstrating cell viability of infected MoMΦs and infected BMDCs 24 hr and 48 hr post infection. Non-infected control (Ctrl) cells are on the left and the VR-2332 infected cells are shown on the right (PI-post infection).

Real time quantitative-PCR of PRRSV copies in supernatant of infected APCs:
 Viral RNA was isolated from the supernatants of APC cell cultures infected with PRRSV VR-2385 at 8 hours, 24 hours, and 48 hours post infection (PI). In order to quantify viral copies, a PRRSV stock of known TCID₅₀ was used to develop a standard curve (Supplementary figure 3-18). The results indicate that viral copies are detected earlier and at a higher concentration in the infected MoMΦs, and potentially MoDCs, in comparison to infected BMDCs (Figure 3-5).

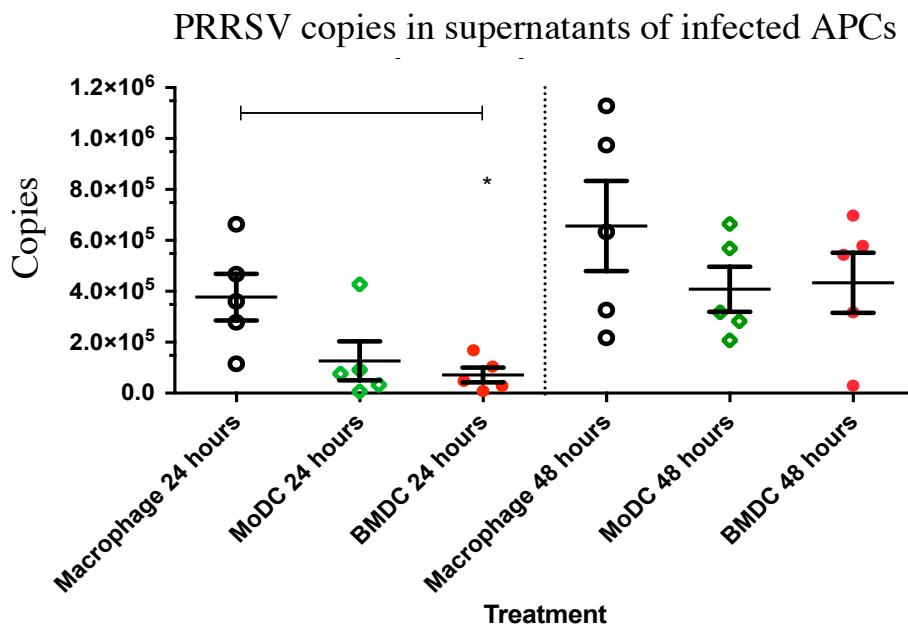


Figure 3-5: Real time quantitative PCR of PRRSV copies in the supernatant of infected cells. MoMΦs, MoDCs, and CD163⁺ BMDCs were infected with PRRSV VR-2385 (MOI 0.1) and supernatants were collected 8hr, 24hr, and 48hr post infection (PI). Data points were collected from unrelated animals, performed as single replicates. Reverse transcription reactions were performed in duplicate. A standard curve developed using known TCID₅₀ viral stock in order to quantify viral copies present in the supernatant of the infected cell cultures. $P = 0.0159$.

Expression of cell surface markers associated with antigen presentation:

The cell surface marker expression of MHCII (Figure 3-6) and MHCI (Figure 3-7) were analyzed in APCs infected with PRRSV using FCM. Change in expression was determined by calculating the difference between the mean fluorescence intensity (MFI) of the infected cells and their respective controls. There may be a trend in which M1

MΦs and both DC populations have increased MHCII and MHCII expression when exposed to PRRSV, but there was no statistical difference amongst the treatments. (FCM staining example in Supplementary Figure 3-19. Additional time points for the CD163-BMDCs and CD163⁺ BMDCs can be seen in supplementary Figures 3-20 and 3-21).

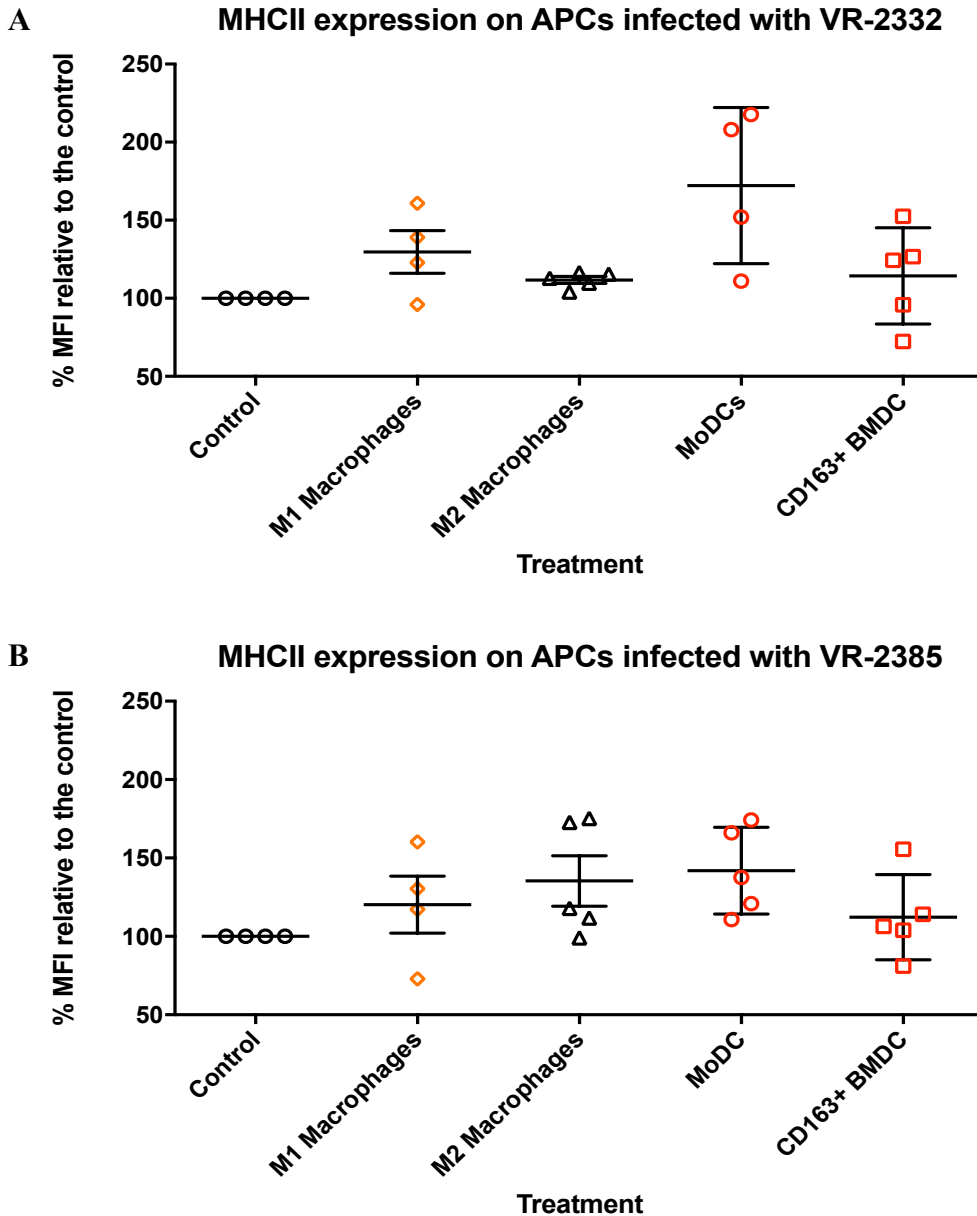


Figure 3-6: MHCII Cell surface expression on APCs infected with PRRSV. APCs were infected with VR-2332 (A) or VR-2385 (B). Change in cell surface expression of MHCII were determined by calculating the difference between the mean fluorescent intensity of the infected cells and their respective controls. The data was collected from non-related animals, performed as single replicates, and was determined to show no statistical significance.

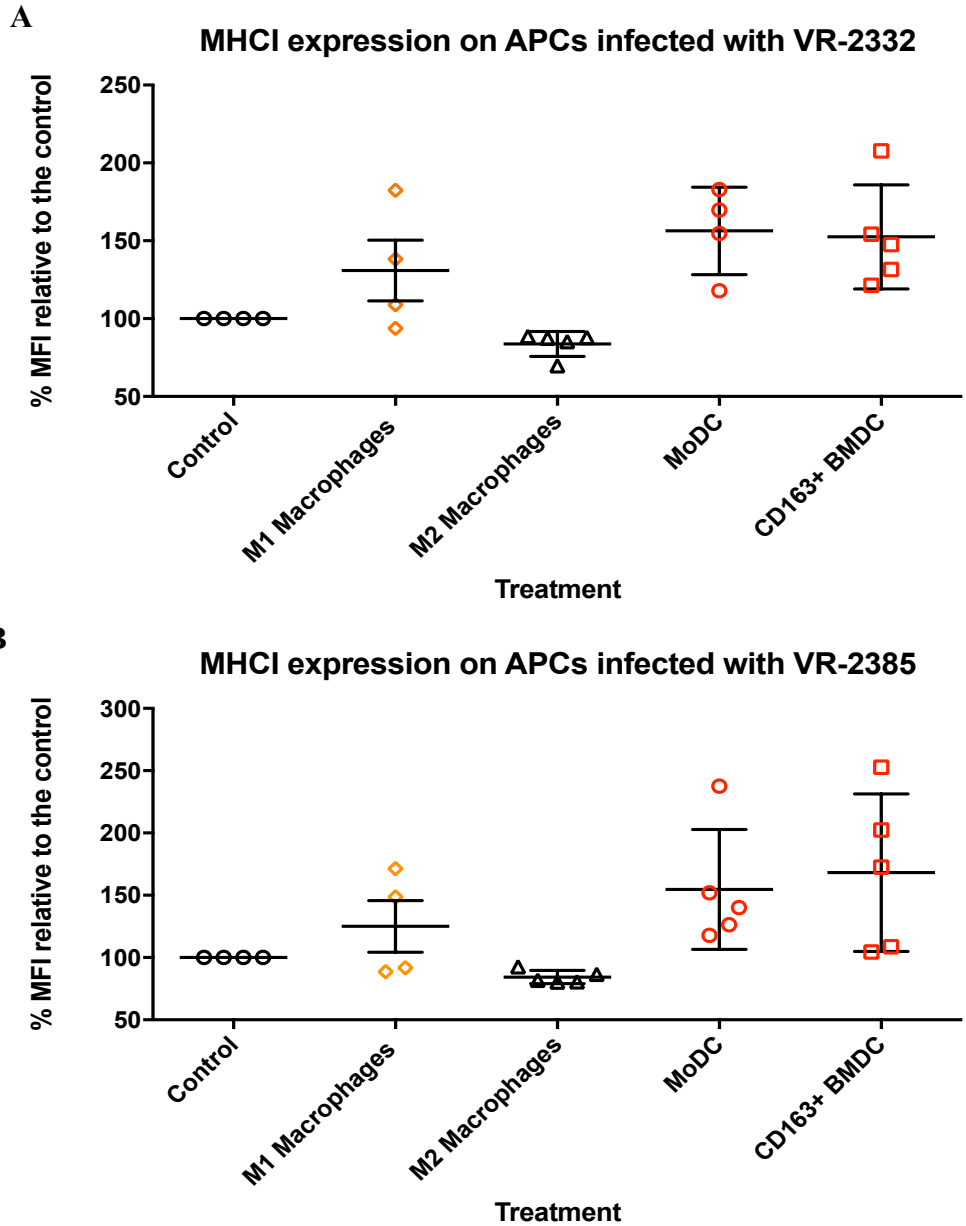


Figure 3-7: MHC I Cell surface expression on APCs infected with PRRSV. APCs were infected with VR-2332 (A) or VR-2385 (B). Changes in cell surface MHC I expression were determined by calculating the difference between the mean fluorescent intensity of the infected cells and their respective controls. The data was collected from non-related animals, performed as single replicates, and was determined to show no statistical significance.

Non-stimulated macrophage (M0) cell surface marker expression:

The MHC I and MHC II cell surface markers on non-stimulated MoMΦs infected with PRRSV VR-2385 and VR-2332 were assessed as previously performed in the other APC

populations. As Figure 3-8 indicates, there is a clear downregulation in the expression of both MHC I and MHC II on the surface of M0 MoMΦs infected with PRRSV.

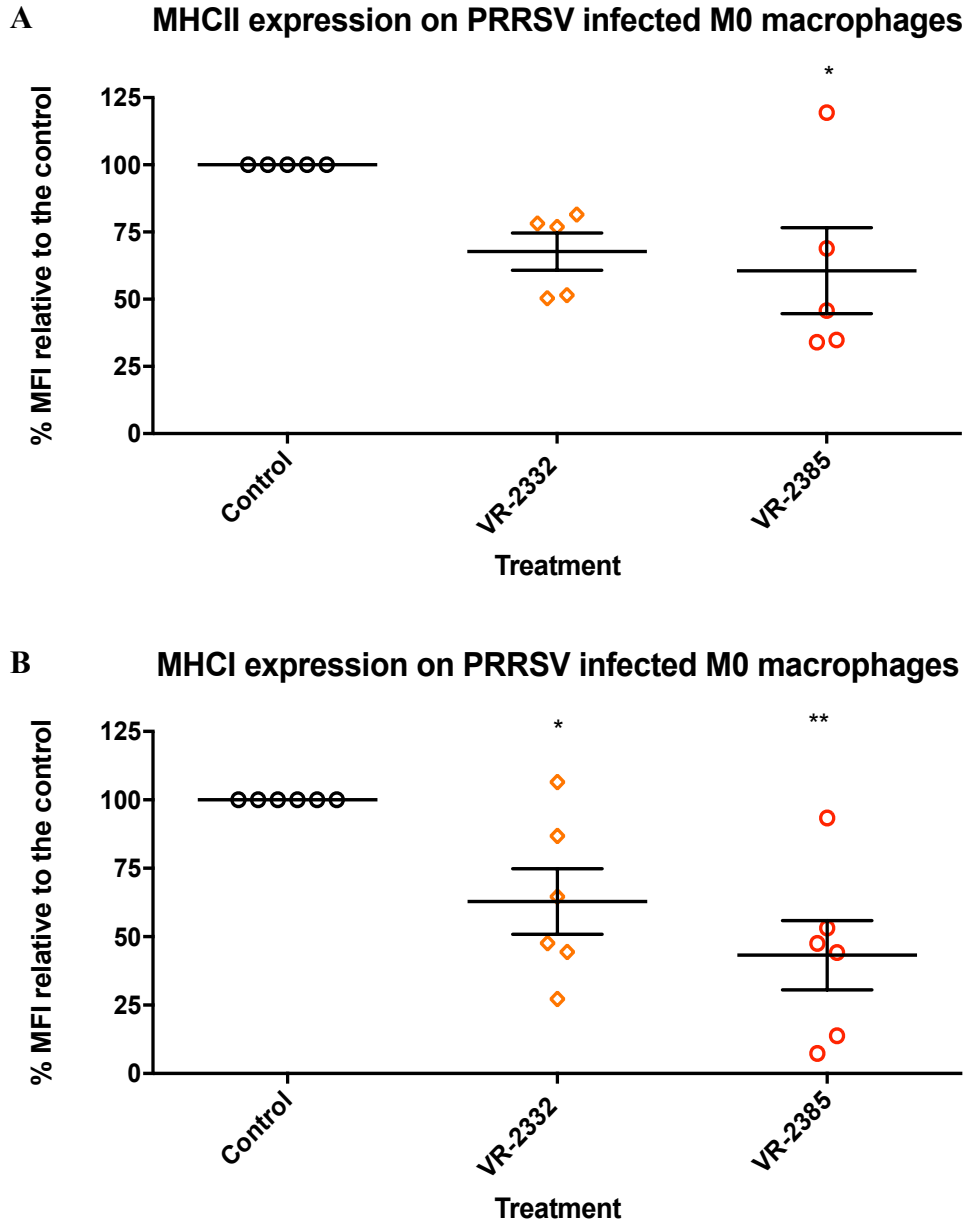


Figure 3-8: Cell surface expression of MHCII (A) and MHC I (B) on M0 MoMΦs infected with PRRSV VR-2332 and VR-2385. Changes in cell surface expression of MHC were determined by calculating the difference between the mean fluorescent intensity of the infected cells and their respective controls. Data points represent non-related animals, performed as single replicates, with VR-2332 and VR-2385 infections from non-related animals. $P < 0.05 = *$; $P < 0.005 = **$

T cell recall response from immunized animals in a macrophage-T cell co-culture: We were interested in how the expression of MHC molecules might influence T cell proliferation. Therefore, M0 MoMΦs were either: infected, treated with inactivated PRRSV, or mock-infected with media for 3 hours before being washed, and then cultured with T cells. The T cells were isolated from animals immunized with the PRRSV MLV and cultured with macrophages from syngeneic animals. As the results indicate in Figure 3-9, although there was a downregulation of MHC expression in MoMΦs infected with PRRSV (Figure 3.8), it did not abrogate their stimulatory capacity to promote lymphocyte proliferation. Lastly, inactivated PRRSV treatment of PBMCs promoted IFN- γ secretion in ELISpots. Which unlike the MoMΦ-T cell co-culture in which the inactivated virus treatment was applied, there was no lymphocyte proliferation potentially indicating a lack of stimulation (Supplementary Figure 3-23).

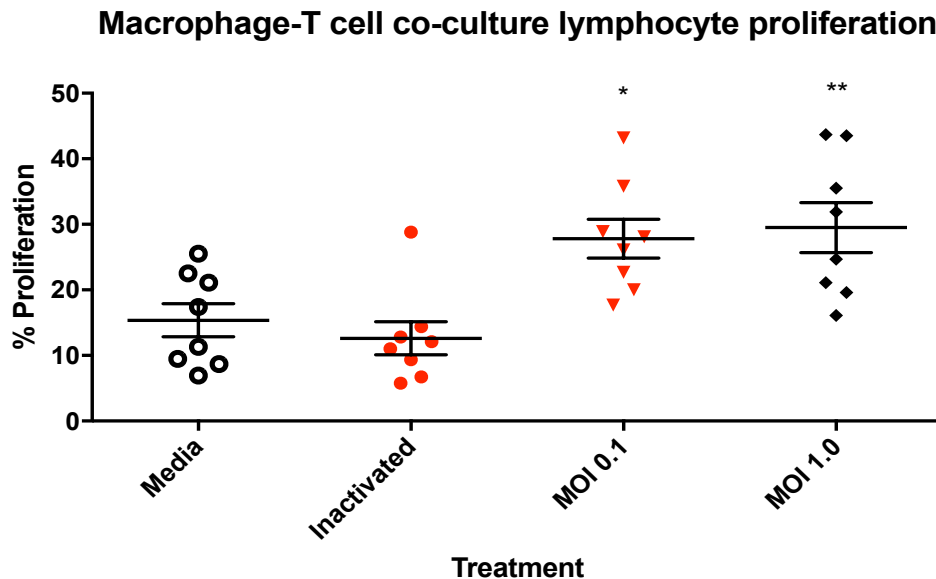


Figure 3-9: T cell recall-response from immunized animals via macrophage- T cell co-culture. Non-stimulated MoMΦs (M0) from immunized animals were infected with PRRSV VR-2385, and subsequently co-cultured with CFSE stained T cells from autologous animals to assay for lymphocyte proliferation. After 4 days in culture, proliferation was assessed with flow cytometry. Statistical significance was determined by comparing the treatments to the media alone treatment. $P < 0.05 = *$; $P < 0.005 = **$.

3.5 Discussion

The tropism of PRRSV is restricted to cells that express the hemoglobin/haptoglobin scavenger molecule CD163, which was identified as a necessary cellular receptor for viral entry into the cytoplasm (Calvert et al., 2007). In addition to CD163, sioladhesin 1 (CD169) and heparin-sulfate residues have been identified as attachment factors for PRRSV (Van Breedam et al., 2010; Van Gorp et al., 2008). Although it has been widely accepted that porcine alveolar macrophages (PAMs) are the primary target for PRRSV infection, dendritic cell (DC) susceptibility has been a subject of continuing debate. We feel that confusion surrounding DC permissibility to PRRSV exists as a result of utilizing inappropriate DC cultures to study the virus. The majority of DC research has been carried out in monocyte-derived DC (MoDC) cultures or granulocyte macrophage colony-stimulating factor (GM-CSF) bone marrow-derived DC (BMDC) cultures, which are both subject to MΦ and/or monocyte contaminants (Calzada-Nova et al., 2011; Chang et al., 2008; Flores-Mendoza et al., 2008; Peng et al., 2009; Silva-Campa et al., 2009; Subramaniam et al., 2011; Wang et al., 2007; Wongyanin et al., 2012; Wongyanin et al., 2010; Zhang et al., 2012). Because PRRSV is able to infect MΦs, the analysis of the DC innate response in these models may not be entirely accurate.

The *in vivo* differentiation of DCs from hematopoietic progenitor cells has been demonstrated to occur in response to FMS-related tyrosine kinase 3 ligand (Flt3L). Although GM-CSF and M-CSF have also been shown to play a role in DC differentiation, Flt3L knock out mice have shown markedly reduced levels of DCs. Furthermore, DCs obtained through *in vitro* differentiation utilizing Flt3L have been shown to contain multiple DC subsets, one of which is the plasmacytoid DCs (pDCs) (Belz and Nutt, 2012). Unfortunately, one of the major issues that exist in studying porcine DC immunology is obtaining cell surface markers that are specific for DCs. Unlike in mice and humans, porcine DCs cannot be identified based on the expression of CD11c. Furthermore, GM-CSF and MoDC cultures contain a specific subset of DCs, which is not representative of *in vivo* populations. As is demonstrated in supplementary Figure 3-11, the staining pattern of our BMDC populations appeared to correlate to those obtained in previous studies as being MHCII^{mid/high}, CD172a^{high}, and consisting of a

mixed population of CD163⁻ or CD163⁺ cells (Guzylack-Piriou et al., 2010). We feel confident in assuming the successful differentiation of our HSC precursors into DCs. The results obtained from the preliminary investigation with the highly virulent strain of PRRSV (VR-2385) indicate that BMDCs are infected by PRRSV (Figure 3-1). Furthermore, it was apparent that not every cell in the culture was infected, as the majority of the population (>80%) was negative for PRRSV 72 hours post-infection. It seemed logical to assume that the population being infected consisted of DCs expressing CD163. Additionally, we were interested in determining whether an avirulent strain (VR-2332) was also able to infect the CD163⁺ DCs. A major strategy that viruses have developed for immune evasion has been an interference with antigen presentation and maturation in DCs (Kruse et al., 2000; Mahanty et al., 2003; Wang et al., 2007). Thus, we isolated our BMDC population based on CD163 expression (Supplementary Figure 3-15). As expected, the CD163⁺ BMDCs were susceptible to infection and the CD163⁻ BMDCs were not susceptible (Figure 3-2). Considering there are multiple APC populations in pigs, we continued our investigation by comparing the susceptibility of CD163⁺ BMDCs to MoMΦs and MoDCs infected with PRRSV. Our results, as indicated in Figure 3-3 and Figure 3-5, show that PRRSV seems to infect MΦs more efficiently than the CD163⁺ BMDCs and potentially MoDCs. As mentioned previously, MoDC cultures are subject to MoMΦ contamination, which could explain the non-statistically significant difference in PRRSV transcripts between MoDCs and BMDCs or MoMΦs. At this time, it is difficult to conclude why there is a difference in APC susceptibility to PRRSV. Lastly, when comparing the forward scatter/side scatter profiles of the PRRSV infected APCs (Figure 3-4), it could be assumed that the CD163⁺ BMDCs remained healthy 48 hours post infection, whereas the MoDCs and MoMΦs were essentially dead after 48 hours. This difference in APC viability may be attributable to a less severe rate of infection, but it could also be an indication of a defense mechanism the CD163⁺ BMDCs possess not seen in the MoMΦs or MoDCs. An aspect of major interest in our lab is the progression to T cell immunity during PRRSV infection. Thus, we investigated the expression of cell surface markers associated with antigen presentation in the APC populations after PRRSV infection.

Antigen presenting cells utilize MHCI and MHCII to present peptide sequences derived from antigen to CD8 β ⁺ and CD4 α ⁺ T cells respectively. When comparing the levels of MHCI and MHCII expression on the APC populations (Figure 3-6 and Figure 3-7) there was no significant change in the expression of the molecules in PRRSV infected APCs. Furthermore, we were unable to detect any changes in CD80/86 expression (results not shown). On the other hand, non-stimulated MoM Φ s (M0) showed clear downregulations in both MHCI and MHCII cell surface expression when PRRSV infected (Figures 3-8). Ultimately, these results tell us little of what effect the changes in MHC expression have during antigen presentation to T cells. Thus, we chose to utilize M0 MoM Φ s to investigate whether PRRSV induced downregulation of MHC molecules had an effect of their capacity to stimulate T cell proliferation. Our results demonstrated that even though there is a downregulation of MHC molecules on the surface of MoM Φ s infected with PRRSV, it did not abrogate their stimulatory capacity, as the M0 MoM Φ s clearly retained their capacity to stimulate a recall response in T cells from immunized animals (Figure 3-9). Interestingly, the inactivated virus treatment in our IFN- γ ELISpot assay was able to stimulate IFN- γ secretion (Supplementary Figure 3-23) but we did not observe T cell proliferation in the M0 MoM Φ s treated with inactivated PRRSV in the T cell co-cultures. We speculate that this could be attributable to DCs not being present in our co-culture when they are present in the PBMC ELISpot assays. Overall, we can conclude that alteration of MHC expression on APCs does not necessarily correlate to their antigen-presenting ability, nor their T cell stimulatory capacity. This did not come as a surprise, as the MHC expression on the MoM Φ s was only down-regulated and not completely abrogated.

3.6 Supplementary figures

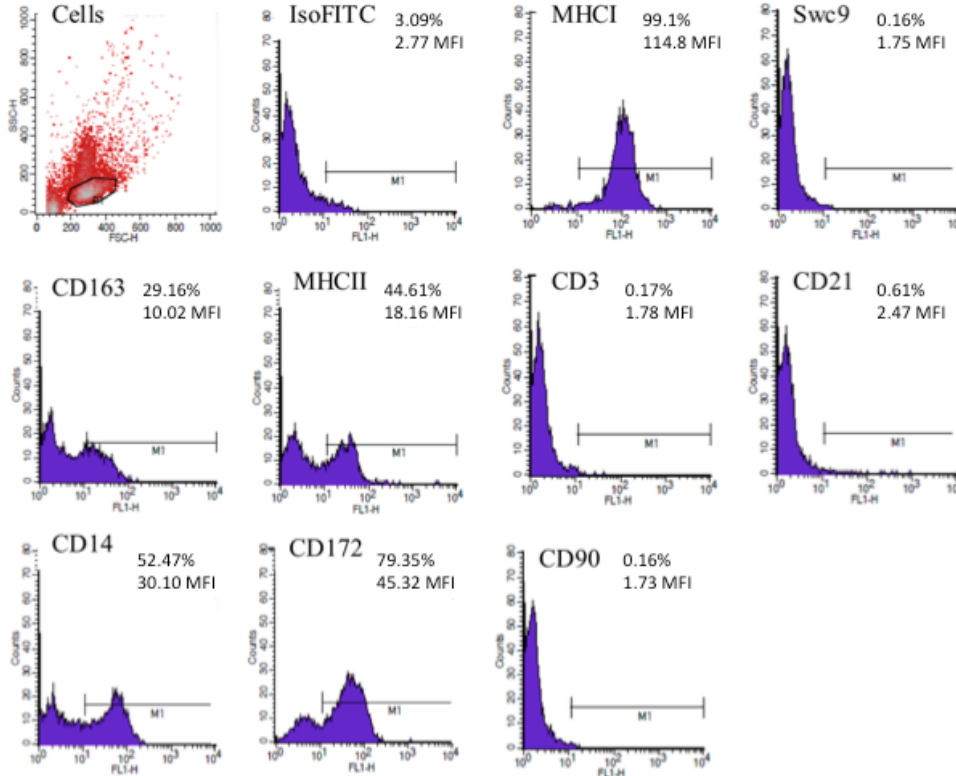


Figure 3-10: Bone marrow dendritic cell (BMDC) characterization. Flow cytometry demonstrating the cell surface markers of the stained BMDC population.

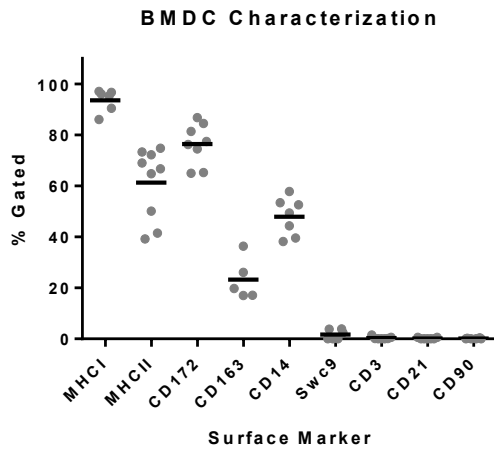


Figure 3-11: Summary of flow cytometry staining to characterize BMDC derived population. Each dot is representative of a different pig and the bars are representative of the mean staining for each marker. The mean % gated for each marker are as follows: MHCI (93.57%), MHCII (61.28%), CD172a (73.37%), CD163 (23.24%), and CD14 (47.89%). The cell population was devoid of macrophages (Swc9), T cells (CD3), B cells (CD21), and fibroblasts (CD90). Data points are from non-related animals.

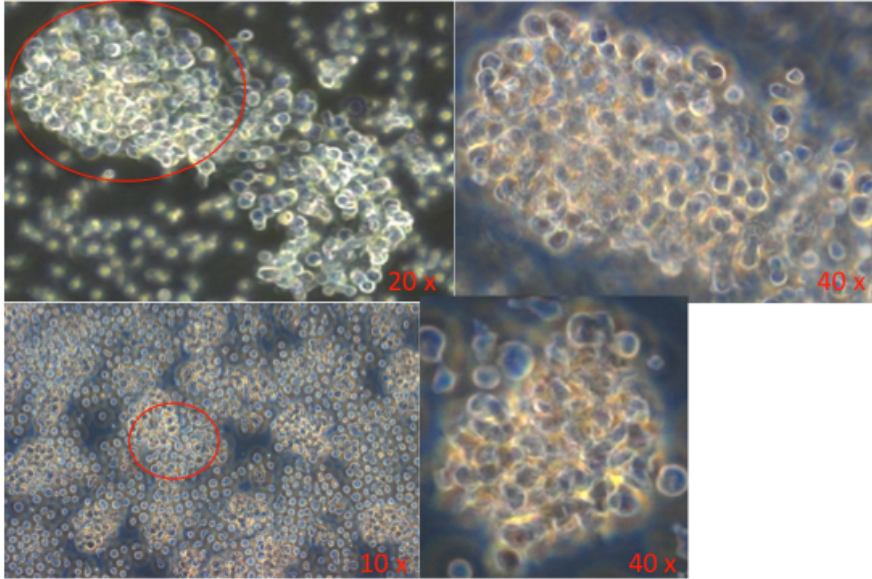


Figure 3-12: Light microscopy of BMDCs from 1 pig on day 7 of culture (6 well plates, 5.0×10^5 cells/mL).

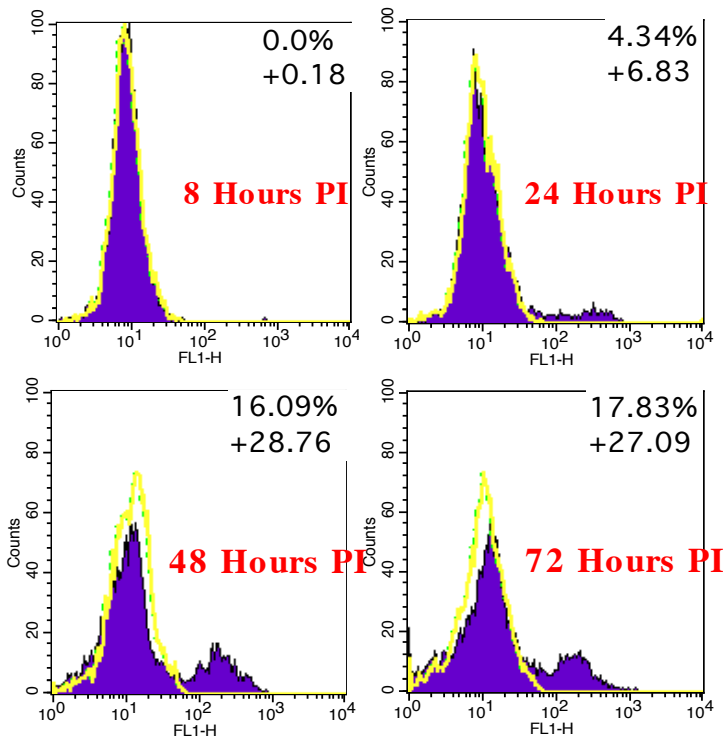


Figure 3-13: BMDC infection with VR-2385 over 72 hours. BMDCs were infected at an moi of 0.1 and harvested at the indicated time points. Flow cytometry of cells stained with the SR30-FITC ab against the PRRSV N protein. Yellow represents control cells stained with the SR30 ab; purple overlay represent infected cells stained with the SR30 ab

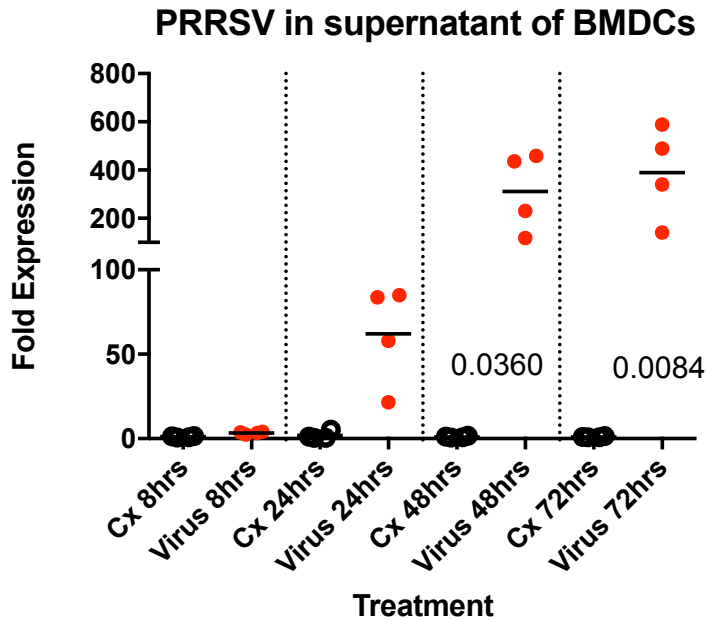


Figure 3-14: *PRRSV* replication in the supernatant. A 1 step reverse transcription was used to determine levels of *PRRSV* in the supernatant using the SuperScript® III Platinum® One-Step qRT-PCR Kit (Invitrogen) according to the manufacturer’s instructions. Fold expression was determined by comparing Ct values at indicated time points to their respective controls (non-infected cell supernatants). (Cx = non-infected, control cells). Data points are representative of BMDCs from non-related animals.

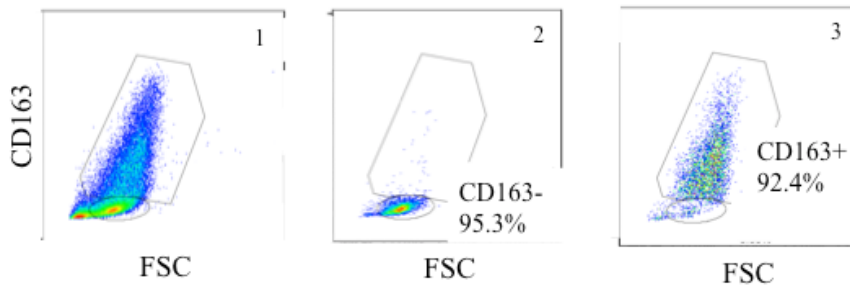


Figure 3-15: *Fluorescence activated cell-sorting* images to show gating strategy for the $CD163^+$ sort of the BMDC population.

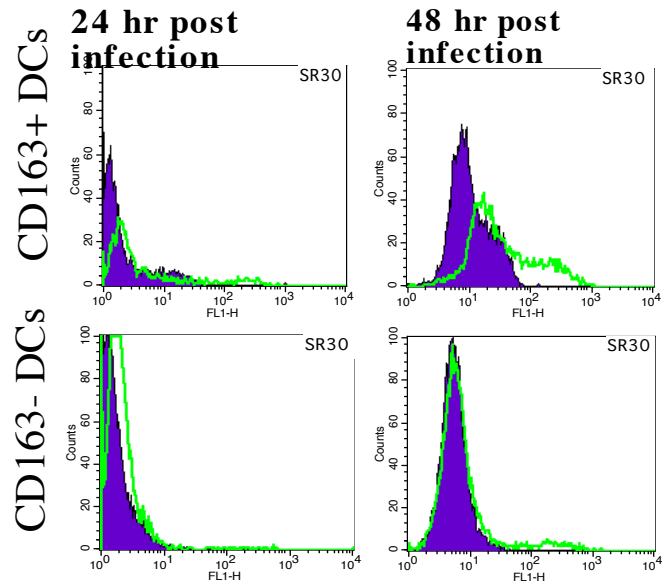


Figure 3-16: BMDCs sorted for CD163 expression were infected with PRRSV and stained intracellularly for PRRSV N protein. (Infected cells-Green; Non-infected cells-purple). Both populations were stained with SR30-FITC.

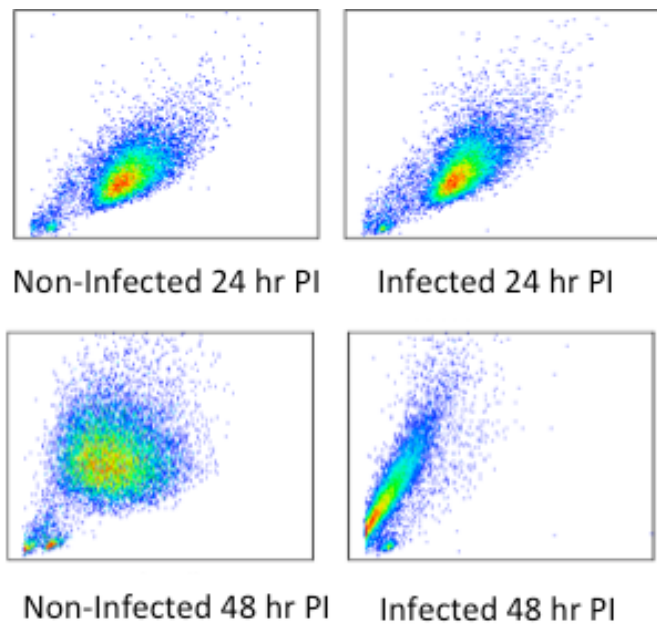


Figure 3-17: MoDC forward scatter/side scatter plots demonstrating cell viability 24 and hours post infection with PRRSV VR-2332. Non-infected cells are on the left side and the infected cells are on the right side.

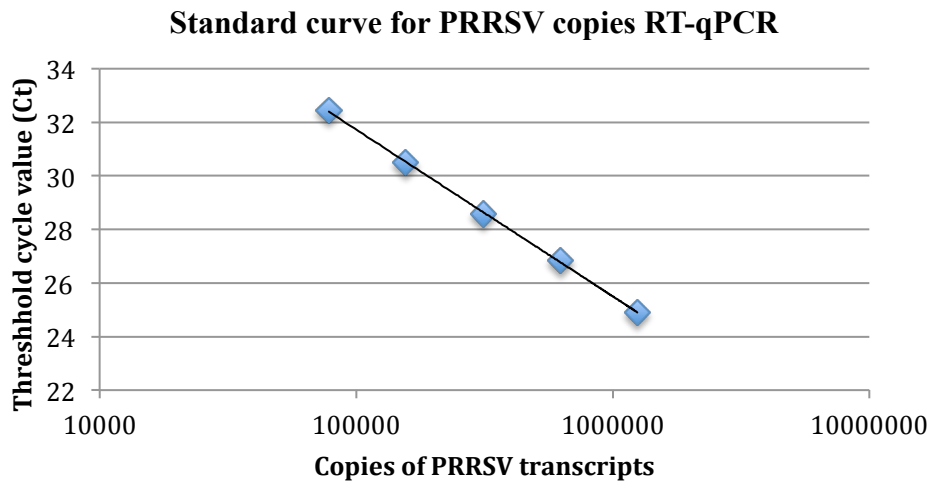


Figure 3-18: Standard curve utilized to demonstrate primer efficiency and quantification of PRRSV transcripts. $Y = -2.704\ln(x) + 62.863$. $R^2 = 0.99971$

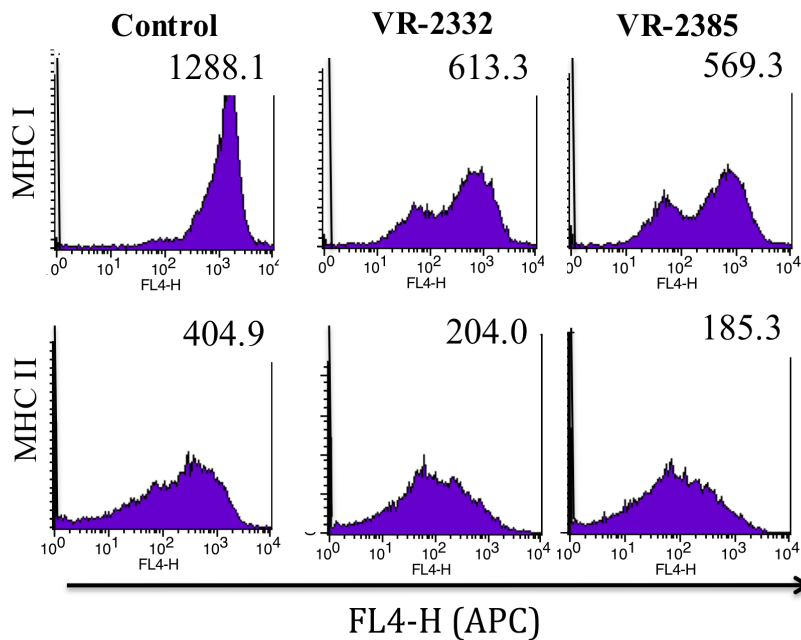


Figure 3-19: Representation of the flow cytometry staining of antigen-presenting cells for cell surface marker expression. Above, macrophages infected with PRRSV VR-2385 or VR-2332 were stained with anti-MHCI or anti-MHCII antibodies. Numbers a representative of the mean fluorescence intensity.

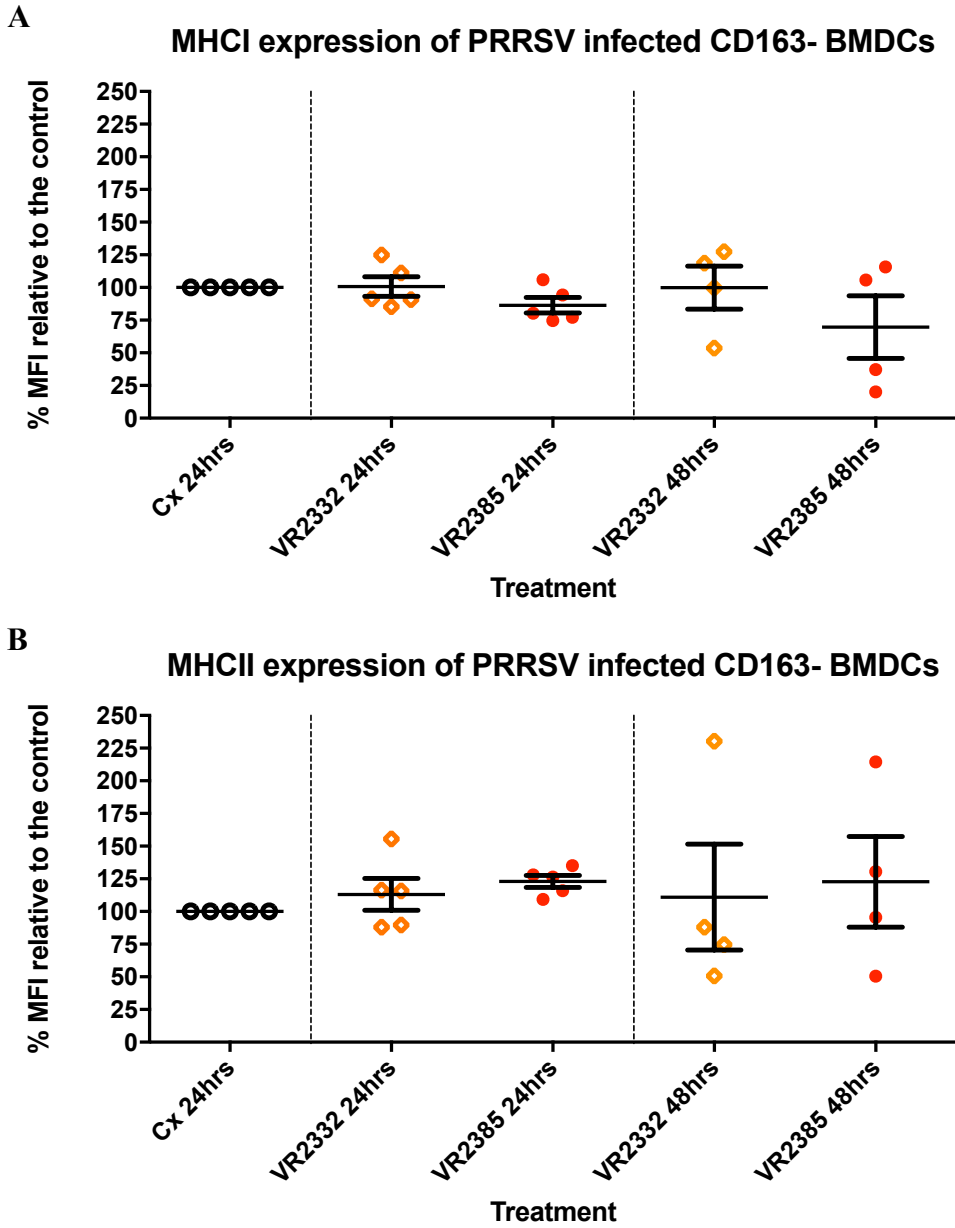


Figure 3-20: Flow cytometry demonstrating MFI of MHC I and MHC II expression on CD163- BMDCs treated with PRRSV. (Cx= non-infected control). Changes in the MFI of MHC I and MHC II cell surface expression was determined as previously indicated. The data was collected from non-related animals, performed as single replicates, and was determined to show no statistical significance.

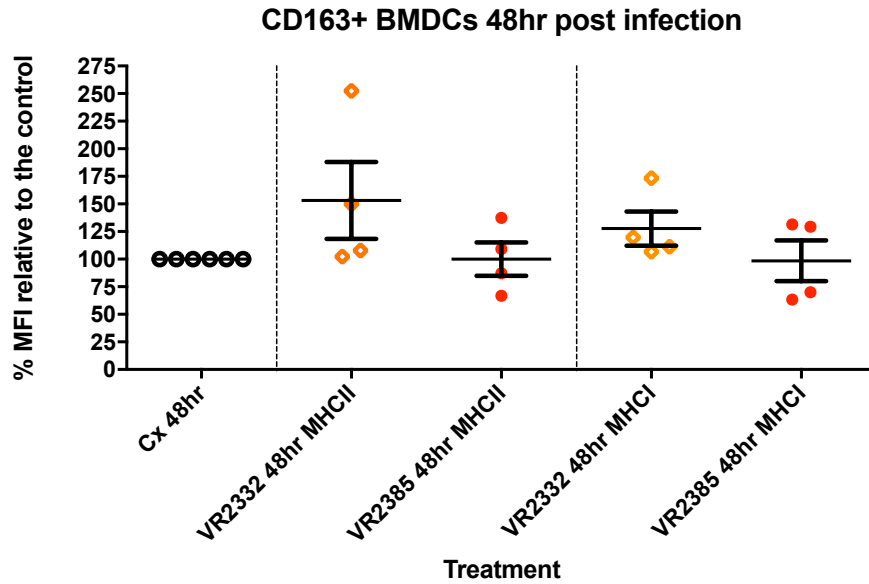


Figure 3-21: Flow cytometry data demonstrating MHC I and MHC II expression from the 48 hour time points of PRRSV infected CD163⁺ BMDCs. The data was collected from non-related animals, performed as single replicates, and was determined to show no statistical significance. (Cx= non-infected control)

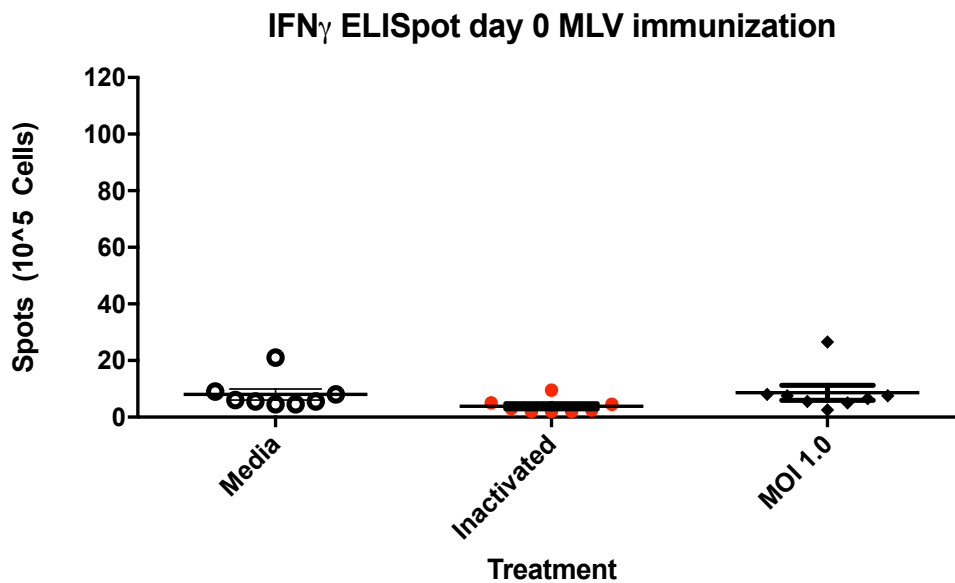


Figure 3-22: Interferon-gamma ELISpots from PRRSV immunized animals on day 0. Peripheral blood mononuclear cells (PBMCs) were plated at 5.0x10⁵ cells per well and stimulated with either live or inactivated PRRSV VR-2385 for 24 hours before IFN- γ ELISpot plates were developed.

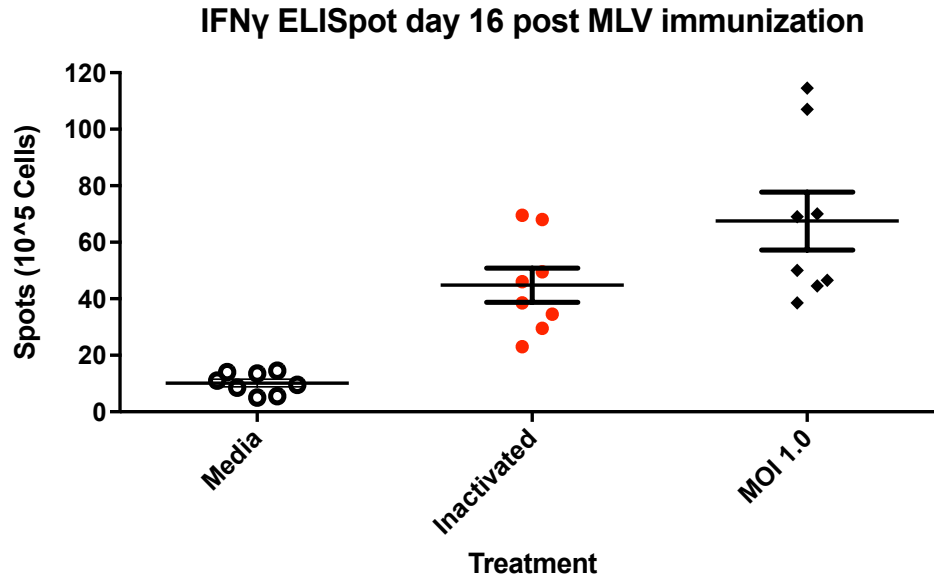


Figure 3-23: Interferon-gamma ELISpots from PRRSV immunized animals on day 16 post immunization. Peripheral blood mononuclear cells (PBMCs) were plated at 5.0×10^5 cells per well and stimulated with either live or inactivated PRRSV VR-2385 for 24 hours before IFN- γ ELISpot plates were developed.

Contributions: JD and JVK isolated PBMCs and monocytes. JD isolated hematopoietic stem cells. JD performed cell macrophage and MoDC cell differentiation cultures. JD performed the flow cytometry. JD isolated viral RNA and performed rt-qPCR. JD performed microscopy. JD did statistical analysis. JD and VG designed experiments.

3.7 Conclusion

Bone marrow-derived DCs were successfully differentiated and characterized using Flt3L. Antigen presenting cell susceptibility to PRRSV is restricted to cells that express CD163. The PRRSV replicates more efficiently in MoM Φ s than in CD163⁺ BMDCs, and potentially MoDCs. Lastly, the downregulation of surface MHCII in PRRSV infected M0 MoM Φ s did not abrogate their immunostimulatory capacity to induce CD4 α ⁺ Th cell proliferation, when co-cultured with T cells from MLV immunized animals. To further investigate PRRSV's influence on antigen presentation, in Chapter 4 we investigated the maturation of the invariant chain in MoDCs and PAMs infected with PRRSV.

Chapter 4 PRRSV INFECTION ALTERS THE ASSOCIATION OF GAMMA ACTIN 1 WITH MHCII IN MONOCYTE-DERIVED DENDRITIC CELLS

4.1 Abstract

Trafficking of peptide loaded MHCII molecules to the plasma membrane is an integral step during antigen presentation, driving the progression to CD4⁺ Th cell mediated immunity. The mechanism by which peptide loaded MHCII molecules are trafficked to the plasma membrane is unresolved, although the utilization of the actin cytoskeleton is likely. Additionally, it is relatively common for enveloped RNA viruses to hijack the actin cytoskeleton to mediate their entry, replication, and assembly within susceptible cells. Very little is known regarding the role of the actin cytoskeleton during infection with the porcine reproductive and respiratory syndrome virus (PRRSV) and an explanation for the delayed induction of T cell immunity to PRRSV is unknown. Porcine alveolar macrophages (PAMs) and monocyte-derived dendritic cells (MoDCs) were infected with PRRSV and MHCII was immunoprecipitated to determine whether PRRSV had an effect on antigen processing/presentation. Shotgun mass spectrophotometry indicated that the infection of porcine MoDCs by PRRSV alters the association of gamma actin 1 with MHCII. Furthermore, PRRSV did not alter the expression of gamma actin 1 in PAMs. PRRSV interference of antigen processing and presentation in MoDCs could influence the progression to T cell immunity.

4.2 Introduction

The eukaryotic cytoskeleton has both structural and functional roles. Structurally, within antigen-presenting cells (APCs), the actin cytoskeleton localizes just below the plasma membrane and is a major factor in podosome formation (Skruber et al., 2018).

Podosomes, a characteristic of immature dendritic cells (DCs), play a crucial role in cellular attachment, motility, and in sampling the external environment. Upon maturation,

the actin cytoskeleton is rearranged and DC podosomes are no longer apparent. Additional hallmarks of DC maturation include loss of phagocytic capacity, upregulation of co-stimulatory molecules, increased MHCII expression on the surfaces of cells, and halting the synthesis of new MHCII molecules, as the DCs prepare for antigen presentation (Kleijmeer et al., 2001; West et al., 2004). Functionally within eukaryotic cells, the actin cytoskeleton is utilized to traffic proteins and molecules throughout the cytoplasm. Concerning APCs, it has been shown that inhibition of the actin cytoskeleton prevented the maturation of the invariant chain in B cells, but this may not be the case with DCs (Barois et al., 1998). An additional role of the actin cytoskeleton in APC is during the formation of the immunological synapse between DCs and T cells, by sequestering co-stimulatory molecules and adhesion molecules to the site of antigen presentation (Comrie et al., 2015; Girard et al., 2012).

Viral infections are often associated with rearrangements of the actin cytoskeleton. It has been demonstrated that viruses, like respiratory syncytial virus (RSV), adenoviruses, reoviruses, and picornaviruses, utilize the actin cytoskeleton for entry, migration, replication, and egress. In particular, it has been shown that viral entry via clathrin-coated pits utilizes the actin cytoskeleton for trafficking (Jans et al., 2016; Wang et al., 2018). The role of the actin cytoskeleton during a PRRSV infection has gone largely unstudied. Manipulation of the rearrangement of the actin cytoskeleton in APCs by the PRRSV could influence multiple factors, including the following: cellular locomotion (migration of APCs to the draining lymph node); antigen processing (influencing the peptide repertoire being presented); antigen presentation (interfering with peptide loaded MHCII (pMHCII) trafficking to the plasma membrane). Although multiple theories have been postulated for the delayed induction of T cell immunity to PRRSV, like the necrosis and apoptosis in the thymus and lymph nodes leading to an overall lymphocyte depletion or the potential suppression of immunity by regulatory T cells early during infection, there has not yet been a definitive explanation (Manickam et al., 2013; Silva-Campa et al., 2009; Weesendorp et al., 2013; Wongyanin et al., 2010). Given that PRRSV is able to infect APCs, it may be plausible that the virus could be interfering with the processing and/or presentation of antigenic peptide sequences to T cells. Interrupting antigen

presentation in APCs could potentially offer an explanation for the delayed induction of T cell mediated immunity to the PRRSV.

Here, we sought to investigate the maturation of the invariant chain in response to PRRSV infection. MoDCs and porcine alveolar macrophages (PAMS) were infected with PRRSV (VR-2385) and cells were lysed 24 hours post infection. MHCII was immunoprecipitated from whole cell lysates and separated on a polyacrylamide gel. Bands on the gel were identified using shotgun mass spectrometry. Our results indicate that PRRSV does not have an influence on the maturation of the invariant chain. Mass spectrometry analysis indicated that PRRSV infection influences the association of gamma actin 1 with MHCII in MoDCs. Lastly, we show that the expression levels of proteins associated with MHCII in PAMs and MoDCs are different, potentially highlighting the professional antigen-presenting capability associated with DCs.

4.3 Materials and methods

Animals:

Six to eight-week old Dutch Landrace pigs were purchased from the pathogen free herd at the Prairie Swine Centre (Saskatchewan). All experiments were conducted in accordance with the ethical guidelines of the University of Saskatchewan and Canadian Council of Animal Care.

Cells and viruses:

Monocytes were isolated from whole blood as previously described (Auray *et al.*, 2013). Briefly, PBMCs were isolated on a FICOLL-PAQUE® Plus gradient (GE Healthcare, Uppsala Sweden). Monocytes were labeled with anti-human CD14 beads and selected for on LS columns using a magnetic isolated cell sorter (Miltenyi Biotec, Auburn, CA). To obtain MoDCs, monocytes were plated at 1.0×10^6 cells/mL in RPMI complete with recombinant porcine (rp) IL-4 (100 ng/mL – R&D 654-P4) and rpGM-CSF (20 ng/mL – R&D 711-PG) for 6 days at 37 °C with 5% carbon dioxide, and media was changed every 3rd day as performed previously (Facci *et al.*, 2010). Dendritic cells are susceptible to PRRSV infection and are often referred to as the professional APCs of the immune

system, thus we chose to investigate PRRSV effect on antigen presentation in MoDCs. Porcine alveolar macrophages (PAMs) are easily accessible and readily infected by PRRSV. PAMs were isolated via bronchoalveolar lavage, as described previously (Zhang et al., 2009). Briefly, lungs were removed from animals and 500 ml of PBS, at 4°C supplemented with 10% fetal bovine serum + gentamycin (100 µg/ml, Gibco) and 2x Antibiotic/Antimycotic (Sigma Aldrich), was poured into the lung using an endotracheal tube. The lung was massaged and cells were poured into a collection vessel. The effluent from the lung collection was filtered through 40 µm filters (Falcon) to remove debris. Cells were then pelleted (400xg) and washed twice before culturing in Dulbecco's Modified Eagle's Medium (Sigma Aldrich) + 2% FBS, 14 mM HEPES (Gibco), 0.1 mM non-essential amino acids (Gibco), 100 µg/ml Gentamycin (Gibco), 1x Antibiotic/Antimycotic (Gibco). PRRSV strain VR2385 (ATCC, Manassas, VA, USA) was used in the study.

Antigen presenting cell infections and sample preparation:

Briefly, ten million antigen-presenting cells were infected with PRRSV (MOI 0.1), or cells were non-infected for 3 hours at 37°, 5% CO₂. Cells were pelleted at 350 g, resuspended in fresh media, and seeded on 12 well plates. Cells were harvested 24 hours post infection, cells were then pelleted and washed before lysing in RIPA lysis buffer + 0.1mM PMSF protease inhibitor. Cells were incubated for 20 minutes at 4°C with shaking and sonicated for 2 minutes. Cellular debris was removed by centrifuging samples at 10,000xg for 5 minutes (twice) and the supernatant was placed into a new microcentrifuge tube. Protein concentration was determined using a Pierce BCA Protein Assay Kit (Thermo Fisher) and concentrations were normalized across samples.

MHCII Immunoprecipitation:

Dynabeads Magnetic Beads, Protein A, were utilized to immunoprecipitate MHCII according to the manufacturer's instructions. We identified an appropriate antibody to immunoprecipitate MHCII and silver stained a polyacrylamide gel. Briefly, fifty microliters of Dynabeads Protein A were incubated with 20.0 µg of MHCII (MSA3, King Fisher) for 20 minutes at room temperature with rotation. The dynabead-MHCII complex

was washed utilizing the magnet and washing buffer supplied by the manufacturer, before combining MHCII-dynabeads with the cellular lysates prepared previously. The lysates were left to immunoprecipitate overnight at 4°C with shaking, before following the manufacturer's instructions in completing the immunoprecipitation.

Polyacrylamide Gel Electrophoresis:

Samples were loaded into wells of a 12.5% polyacrylamide gel with a stack. The ProteoSilver™ Silver Stain Kit (SIGMA) was used according to the manufacturer's instructions. A band appeared at 40-45 kDa in the non-infected control cell sample but not in the PRRSV infected MoDC sample lane. The band was extracted with a razor blade, stored in ultra distilled water, and sent for shotgun mass spectrometry sequencing at the Proteomics Platform of the CHU de Québec Research Center (Quebec, Qc, Canada).

Tryptic digest:

Bands of interest were extracted from gels and placed in 96-well plates and then washed with water. Tryptic digestion was performed on a liquid handling robot (MultiProbe, Perkin Elmer) according to the manufacturer's specifications. Briefly, proteins were reduced with 10mM DTT and alkylated with 55mM iodoacetamide. Trypsin digestion was performed using 126nM of modified porcine trypsin (Sequencing grade, Promega, Madison, WI) at 37°C for 18h. Digestion products were extracted using 1% formic acid, 2% acetonitrile followed by 1% formic acid, 50% acetonitrile. The recovered extracts were pooled, vacuum centrifuge dried and then resuspended into 12 µl of 0.1% formic acid and 5 µl were analyzed by mass spectrometry.

Mass spectrometry:

Peptide samples were injected and separated by online reversed-phase (RP) nanoscale capillary liquid chromatography (nanoLC) and analyzed by electrospray mass spectrometry (ESI MS/MS). The experiments were performed with a Dionex UltiMate 3000 nanoRSLC chromatography system (Thermo Fisher Scientific / Dionex Softron GmbH, Germering, Germany) connected to an Orbitrap Fusion mass spectrometer

(Thermo Fisher Scientific, San Jose, CA, USA) driving with Orbitrap Fusion Tune Application 2.0 and equipped with a nanoelectrospray ion source. Peptides were trapped at 20 $\mu\text{L}/\text{min}$ in loading solvent (2% acetonitrile, 0.05% TFA) on a 5 mm x 300 μm C18 pepmap cartridge pre-column (Thermo Fisher Scientific / Dionex Softron GmbH, Germering, Germany) during 5 minutes. Then, the pre-column was switched online with a self-made 50 cm x 75 μm internal diameter separation column packed with ReproSil-Pur C18-AQ 3- μm resin (Dr. Maisch HPLC GmbH, Ammerbuch-Entringen, Germany) and the peptides were eluted with a linear gradient from 5-40% solvent B (A: 0,1% formic acid, B: 80% acetonitrile, 0.1% formic acid) in 30 minutes at 300 nL/min. Mass spectra were acquired using a data dependent acquisition mode using Thermo XCalibur software version 3.0.63. Full scan mass spectra (350 to 1800 m/z) were acquired in the orbitrap using an AGC target of 4e5, a maximum injection time of 50 ms and a resolution of 120 000. Internal calibration using lock mass on the m/z 445.12003 siloxane ion was used. Each MS scan was followed by acquisition of fragmentation MSMS spectra of the most intense ions for a total cycle time of 3 seconds (top speed mode). The selected ions were isolated using the quadrupole analyzer in a window of 1.6 m/z and fragmented by Higher energy Collision-induced Dissociation (HCD) with 35% of collision energy. The resulting fragments were detected by the linear ion trap in rapid scan rate with an AGC target of 1e4 and a maximum injection time of 50ms. Dynamic exclusion of previously fragmented peptides was set for a period of 20 sec and a tolerance of 10 ppm.

Database searching:

All MS/MS peak lists (MGF files) were generated using Thermo Proteome Discoverer software (Thermo Fisher Scientific Inc., version 2.1.0). MGF sample files were then analyzed using Mascot (Matrix Science, London, UK; version 2.5.1). Mascot was set up to search the contaminants_thegpm_20170713.fasta;

AX_Desulfovibrio_CI_194924_20160714 database (unknown version, 104802 entries) assuming the digestion enzyme trypsin. Mascot was searched with a fragment ion mass tolerance of 0,60 Da and a parent ion tolerance of 10,0 PPM. Carbamidomethyl of cysteine was specified in Mascot as a fixed modification. Deamidated of asparagine and glutamine and oxidation of methionine were specified in Mascot as variable modifications. Two missed cleavages were allowed.

Criteria for protein identification:

Scaffold (version Scaffold_4.7.5, Proteome Software Inc., Portland, OR) was used to validate MS/MS based peptide and protein identifications. Peptide identifications were accepted if they could be established at greater than 95.0% probability by the Peptide Prophet algorithm (Keller et al., 2002) with Scaffold delta-mass correction. Protein identifications were accepted if they could be established at greater than 95.0% probability and contained at least 2 identified peptides. Protein probabilities were assigned by the Protein Prophet algorithm (Nesvizhskii et al., 2003). Proteins that contain similar peptides and could not be differentiated based on MS/MS analysis alone were grouped to satisfy the principles of parsimony.

4.4 Results

PRRSV infection alters protein association with immunoprecipitated MHCII:

Twenty-four hours post infection with PRRSV, PAMs and MoDCs were lysed and whole cell fractions were analyzed by immunoprecipitation of MHCII. Protein concentrations were normalized and equal amounts of protein were loaded into separate wells on a PAGE-gel before silver staining. Non-infected MoDCs had a band of 40-50 kDa in size that was prominent in comparison to PRRSV infected MoDCs (Band “A”). The band was faint in PAMs, and PRRSV infection did not alter the prominence of the band. The indicated bands (**A**- 42-45 kDa; **B**- 30-35 kDa; **C** – 28-30 kDa; Figure 4-1) were extracted for identification via mass spectrometry sequencing.

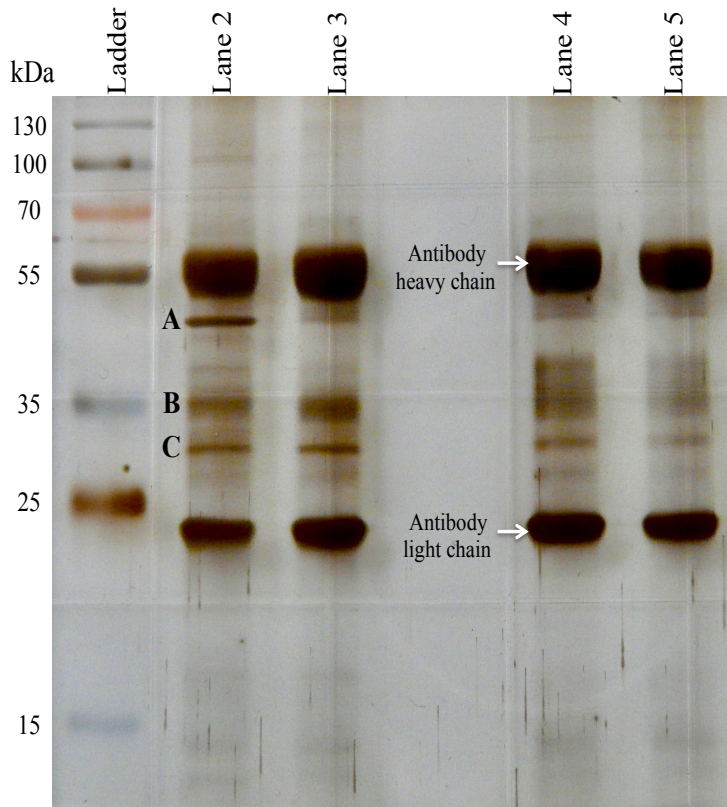


Figure 4-1: Silver stained SDS-PAGE-Gel of immunoprecipitated MHCII samples from PRRSV infected and non-infected APCs. MoDCs and PAMs were either infected or non-infected for 24 hours before immunoprecipitating MHCII. Protein concentrations were normalized before samples were loaded into their respective wells. Lane 2: Non-infected MoDCs; Lane 3: VR-2385 infected MoDCs; Lane 4: Non-infected PAMs; Lane 5: VR-2385 infected PAMs. Bands A, B, and C were extracted from Lane 2 and sent for mass spec sequencing. The experiment was repeated three times from non-related animals. The immunoprecipitation of MHCII from PAMs and MoDCs in the above image (isolated from the same animal) was performed simultaneously.

PRRSV infection alters the association of gamma actin 1 with MHCII:

The mass spectrometry data indicated that the missing band in the PRRSV infected MoDCs was gamma actin 1. Beyond gamma actin 1, there wasn't as remarkable of a difference in the expression pattern of the other protein bands amongst the other APC populations that were infected with PRRSV versus those that were not infected. The identification of the bands sent for mass spec sequencing were as follows: Band A - Actin gamma 1; Band B – SLA-DRA1; Band C – SLA-DRB1.

Table 4.1: Mass spectrometry identified proteins from the MHCII immunoprecipitation.

Identified Proteins	Accession Number	MW (kDa)	Quantitative Value (Normalized Spectra)			Total Spectrum Count		
			A	B	C	A	B	C
Actin gamma 1	I3LVD5_PIG	42	119	10	5	107	6	6
Sus scrofa SLA-DRB1	A0A287ARX3_PIG	30	2	15	23	2	9	26
Sus scrofa HLA-DRA1	A0A287AYL4_PIG	25	0	41	6	0	24	7
Cathepsin B	A0A287F94_PIG	41	0	0	7	0	0	8
Cathepsin Z	A5GFX7_PIG	34	0	0	7	0	0	8
Sus scrofa SLA-3	A0A287AJ58_PIG	40	8	0	0	7	0	0
SLA class II, DQ								
haplotype C beta chain	HB2C_PIG	30	0	0	5		0	6
Actin, beta like 2	A0A287A4R1_PIG	42	40	0	0	36	0	0
Sus scrofa CD74	A0A287B750_PIG	31	0	0	3	0	0	3
SLA class II, DQ								
haplotype C alpha chain	HA2C_PIG	28	0	5	0	0	3	0

Identified Proteins	Accession Number	Exclusive Unique Spectrum Count			Protein Identification Probability		
		A	B	C	A	B	C
Actin gamma 1	I3LVD5_PIG	49	6	6	100%	100%	100%
Sus scrofa SLA-DRB1	A0A287ARX3_PIG	2	7	10	100%	100%	100%
Sus scrofa HLA-DRA1	A0A287AYL4_PIG	0	9	5	0%	100%	100%
Cathepsin B	A0A287F94_PIG	0	0	8	0%	0%	100%
Cathepsin Z	A5GFX7_PIG	0	0	7	0%	0%	100%
Sus scrofa SLA-3	A0A287AJ58_PIG	7	0	0	100%	0%	0%
SLA class II, DQ							
haplotype C beta chain	HB2C_PIG	0	0	5	0%	0%	100%
Actin, beta like 2	A0A287A4R1_PIG	2	0	0	100%	0%	0%
Sus scrofa CD74	A0A287B750_PIG	0	0	3	0%	0%	100%
SLA class II, DQ							
haplotype C alpha chain	HA2C_PIG	0	3	0	0%	100%	0%

Extracted bands from the silver stained SDS-PAGE-Gel were identified using shotgun mass spectrophotometry as explained previously. Ten proteins, of 115, were identified as being relevant to the immunoprecipitation of MHCII using Scaffold 4 software. Quantitative value, total spectrum count, exclusive unique spectrum count, and protein identification probability indicate that the missing band is gamma actin 1. Bands B and C were identified as HLA-DRA1 and SLA-DRB1 respectively, confirming the successful immunoprecipitation of MHCII. A, B, C letter designations correspond to the extracted bands.

4.5 Discussion

Dendritic cells (DCs) are often referred to as the professional APCs of the immune system. This being attributable to their capability of processing antigens into peptide sequences for presentation on MHC molecules to stimulate naïve T cells, driving the adaptive immune response in a particular direction. Although macrophages are capable of stimulating T cell responses, the repertoire of peptide sequences being presented by DCs is likely more diverse. Studies have shown macrophages have higher proteolytic activity and a lower pH within late endosomes than DCs, theoretically resulting in increased

levels of proteolysis, which would in turn deplete the peptide repertoire for presentation (Delamarre et al., 2005]. When considering the immune response to a pathogen, a high degree of peptide diversity is favorable. The pathway in which MHCII is synthesized and loaded with peptide has been largely deduced, but the trafficking of peptide loaded MHCII to the plasma membrane in APCs has not been completely resolved (Blum et al., 2013; ten Broeke et al., 2013).

Originally we sought to investigate whether PRRSV has an influence on the maturation of the invariant chain. Referring to Figure 4.2 on the following page, shortly after translation, MHCII is trafficked to the endoplasmic reticulum (ER) for further modification. Within the ER, an invariant chain trimer acts as a scaffold to which three MHCII alpha chains and three MHCII beta chains bind. The MHCII nonamer is then trafficked through the trans-golgi network or to the plasma membrane, after which the MHCII-Invariant chain (I chain) complex can be found within early and late endosomes. Internalization of MHCII at the plasma membrane has been hypothesized to occur in response to poly-ubiquitination of a lysine residue on the cytoplasmic tail of the MHCII beta chain. This ubiquitination process has been showed to occur more readily in immature DCs than mature DCs, and may even be utilized as a differentiation marker of maturation. Within these endosomes, acidic conditions, in addition to cysteine proteases (Cathepsins S, F, and L), lead to the processing of the invariant chain into CLIP. CLIP occupies the binding groove of MHCII to prevent autonomic peptides from occupying the groove. An MHCII homologue, HLA-DM, is responsible for removing CLIP from the binding groove, thus facilitating the loading of a peptide sequence for antigen presentation. The peptide loaded MHCII heterodimer is then ready to be trafficked to the plasma membrane, where it localizes to lipid rafts for peptide presentation to CD4⁺ Th cells (Blum et al., 2013; Mellins and Stern, 2014). To determine whether PRRSV influences maturation of the invariant chain, we infected cells and immunoprecipitated MHCII.

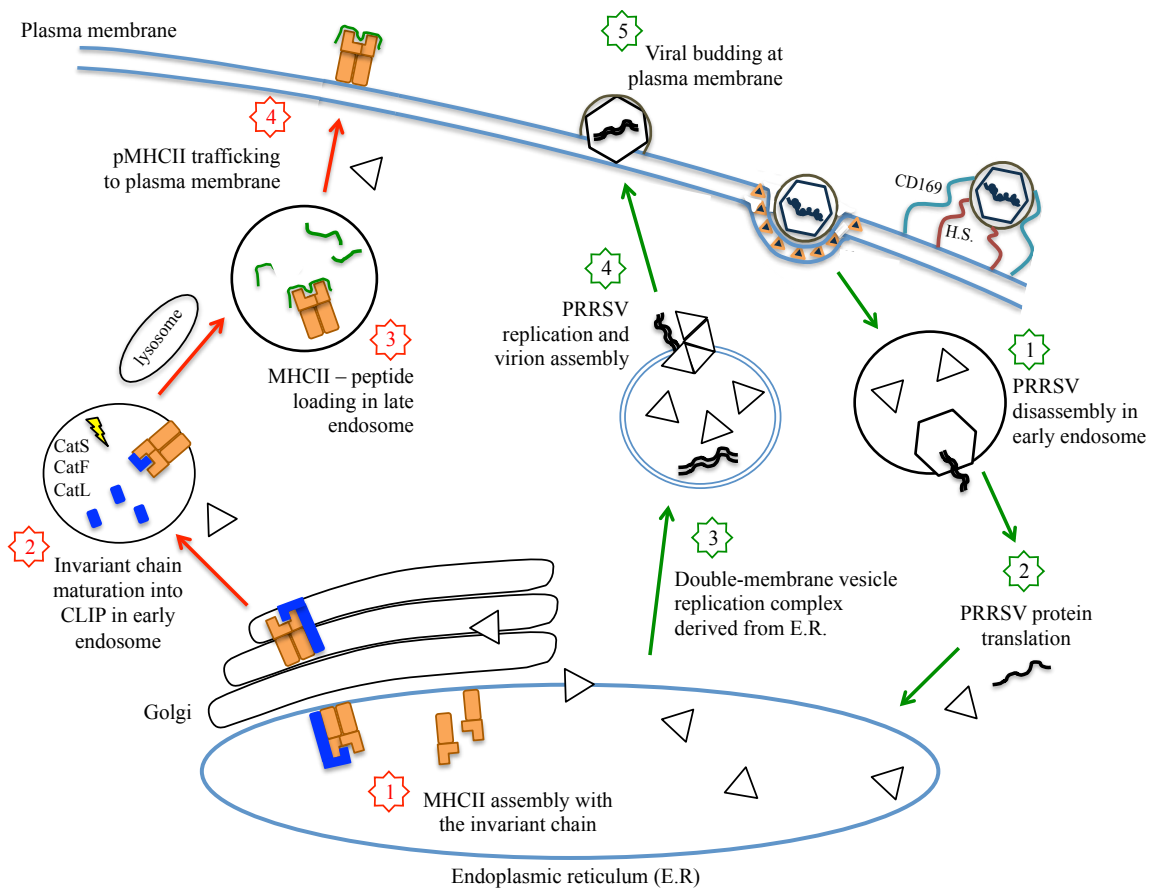


Figure 4-2: Schematic summarizing the replication and assembly of PRRSV, and the potential association of PRRSV with the maturation of the invariant chain and MHCII antigen processing and presentation. The schematic demonstrates the potential that PRRSV may interfere with the maturation of the invariant chain and/or with MHCII associated antigen processing/presentation. Arrows and numbers in green indicate the pathway of PRRSV replication and assembly. Arrows and numbers in red indicate the pathway of invariant chain maturation and MHCII peptide presentation; pMHCII = peptide loaded MHCII; CatS = Cathepsin S; CatF = Cathepsin F; CatL = Cathepsin L. Triangles = PRRSV proteins.

Our results coincide with what has been shown in the literature, as the alpha chain (HLA-DRA1) we identified was 33-35 kDa and the beta chain (SLA-DRB1) was 28-30 kDa (Schafer et al., 1998). Ultimately we observed one major discernable difference in the levels of MHCII associated molecules amongst the infected and non-infected cell populations. The size of the band did not correspond to that of the processed invariant chain (CD74 = 10 kDa) on the silver stained gel (Pierre and Mellman, 1998). At this time it is difficult to conclude whether PRRSV influences the maturation of the invariant chain, as there is no antibody available to detect the invariant chain in pigs. Considering

we have demonstrated that PRRSV infected macrophages and MoDCs were capable of stimulating antigen specific T cell proliferation (Chapter 6), we believe that PRRSV may not be suppressing invariant chain maturation. Interestingly a band within the PRRSV infected MoDCs was practically diminished, which was identified to be gamma actin 1. Upon maturation, DCs undergo several changes including but not limited to the following: a) increased MHCII on the plasma membrane; b) upregulation of co-stimulatory molecules; c) diminished phagocytic capacity; d) abrogation of new MHCII molecule synthesis; e) loss of podosomes as a result of cytoskeletal rearrangement (Kleijmeer et al., 2001; ten Broeke et al., 2013; West et al., 2004). As mentioned previously, little is known as to how pMHCII is trafficked to the plasma membrane, it has been shown that microtubules are utilized in transport, but it's also plausible that transport utilizes the cytoskeleton (Rocha and Neefjes, 2008).

Filamentous actin can be found underneath the plasma membranes of cells, providing a structural base in addition to aiding in cellular motility (Wang et al., 2018). Actin filaments accumulate at podosomes in APCs, enabling movement and sampling of the environment, and potentially playing a role in cellular migration. Upon activation, the actin filaments at podosomes are rearranged to favour endocytosis and phagocytosis of antigen, ultimately leading to the loss of podosomes in activated APCs (Burns et al., 2001). Gamma actin 1 and beta actin (twice as prominent in cells) are the predominant forms of actin that contribute to the actin cytoskeleton. Characterizing the roles of beta actin and gamma actin has proven to be challenging, owing to difficulty in purifying the actin filaments separately. It has been shown that beta-actin knockout mice do not survive embryogenesis, whereas gamma-actin knockouts survived into adulthood, although they struggled with morbidity throughout, suggesting gamma-actin's potential role in immunity (Skruber et al., 2018). Additionally it has been shown that the inhibition of the actin cytoskeleton prevents IFN- γ secretion in RSV infected cells (Jans et al., 2016). Furthermore, considering the localization of gamma actin has been to the cytoplasm it's plausible gamma actin could play a role in trafficking molecules to the plasma membrane, whereas beta actin filaments accumulate more so at lamellipodia, making beta actin more likely to serve as a structural component for cells.

Transport of MHCII to the plasma membrane potentially relies on the reorganization of the cytoskeleton. Late MHCII compartments (MIICs) have been shown to fuse together, by way of microtubules. It's plausible that vesicular bodies, budding from the MIICs, are responsible for carrying the peptide loaded MHCII molecules to the plasma membranes, by way of microtubules and cytoskeletal filaments. Microtubules extend from the MIICs, which have released vesicular bodies containing the peptide loaded MHCII molecules, to the plasma membrane (Chow et al., 2002; Kleijmeer et al., 2001; van Nispen tot Pannerden et al., 2010). It has been shown that microtubule formation can occur independently of antigen exposure, as a stimulus is the only necessary component. That being the case, stimulation of DCs by a TLR agonist into a mature phenotype will theoretically induce microtubule formation. Although, it seems that these microtubules appear to utilize kinesins and dyneins for movement, there was no association with actin filaments (Vyas et al., 2007). On the other hand, it has been shown that transport of MHCII in B cells occurs in association with the actin cytoskeleton. Trafficking of lysosomal vesicles containing either antigen or MHCII molecules within B cells appeared to be dependent on the activity of Myosin II in association with actin microfilaments (Vascotto et al., 2007). But these authors did not investigate the transport of MHCII to the plasma membrane. It's possible that MHCII transport to the plasma membrane could differ within APC populations and potentially differ between species. Overall, it seems that the rearrangement of the cytoskeleton is a characteristic of APC maturation and likely plays a role in trafficking of pMHCII to the plasma membrane. Trafficking of molecules within cells is highly dependent on utilizing the actin cytoskeleton, thus it comes as no surprise that viruses often rearrange the actin cytoskeleton for their own benefit.

Viral infections are often associated with rearrangements of the actin cytoskeleton. It has been demonstrated that viruses utilize the actin cytoskeleton for entry, migration, replication, and egress (Wang et al., 2018). Similar to actin cytoskeleton rearrangements, certain viruses utilize microtubules for entry or egress. It has been shown that successful entry, via endocytosis at clathrin-coated pits, of the respiratory syncytial virus in human monocytes is dependent on the actin cytoskeleton (Jans et al., 2016). Referring again to Figure 4.2, considering PRRSV entry via clathrin-coated pits, it's likely that PRRSV is

utilizing the actin cytoskeleton during viral entry. In the context of a PRRSV infection, the virus would be internalized via clathrin-coated pits into endosomes. Early endosomes mature into late endosomes, through acidification, eventually forming an MHCII class compartment (MIIC). The environment, specifically the low pH, within these late endosomes is relatively harsh, resulting in the proteolysis of antigen to generate peptide sequences, which are then loaded into the binding groove of MHCII, being under the regulation of HLA-DM. The pH of the late endosomes in DCs is much higher than that of macrophages, which theoretically would result in a more diverse repertoire of peptide sequences given the lower activity of proteolysis associated with a less harsh endocytic environment (Blum et al., 2013; Delamarre et al., 2005).

The role of the cytoskeleton during a PRRSV infection has gone largely unstudied. Our results seem to indicate that the association of gamma actin 1 with MHCII is present in MoDCs but not alveolar macrophages. Furthermore, the gamma actin 1 association with MHCII was largely diminished when MoDCs were infected with the PRRSV. We are thus left questioning why gamma actin 1 was immunoprecipitated with MHCII, and why gamma actin 1 was not as pronounced in the PRRSV infected MoDCs. Additionally, we are left questioning why the alveolar macrophages did not have gamma actin 1 in similar levels as the MoDCs. Our results seem to indicate that gamma actin 1 could play a prominent role during antigen presentation, although this is based on speculation.

Overall, there are a few potential explanations for the association of gamma actin 1 with MHCII in response to a PRRSV infection. They include but are not limited to the following: a) PRRSV induces rearrangement of the actin cytoskeleton to favor its replication, assembly, and/or egress; b) maturation of MoDCs induces rearrangement of the actin cytoskeleton for cellular locomotion (migration of APCs to the draining lymph node); c) trafficking of pMHCII to the plasma membrane is dependent on gamma actin filament reorganization; d) PRRSV influences the rearrangement of gamma actin 1 in MoDCs, potentially interfering with antigen presentation. If PRRSV does interfere with antigen processing and presentation, it could have drastic implications on the stimulation of naïve T helper cells and the progression to T cell immunity. In conclusion, the role of the actin cytoskeleton during a PRRSV infection and the potential role of gamma actin 1 during antigen presentation warrant further attention.

Contribution: JD isolated PBMCs and monocytes. JD performed MoDC differentiation cultures. JD isolated PAMs. JD performed MHCII immunoprecipitation. JD ran SDS-PAGE gels. The Proteomics Platform of the CHU de Québec Research Center (Quebec, Qc, Canada) ran the mass spec. JD and VG designed experiments.

4.6 Conclusion

Gamma actin 1 association with MHCII is more pronounced in MoDCs than in PAMs. Furthermore, PRRSV infection of MoDCs alters the association of actin gamma 1 with MHCII. The role of the actin cytoskeleton during a PRRSV infection, in addition to the role of the actin cytoskeleton in the trafficking of peptide loaded MHCII to the plasma membrane, should be investigated further. To investigate the interaction of APCs with T cells, in Chapter 5 we established an assay using a mixed leukocyte reaction (MLR) so that the MLR could be modified to assess antigen specific T cell responses to the PRRSV.

Chapter 5 PORCINE M1 MACROPHAGES ARE MORE POTENT INDUCERS OF LYMPHOCYTE PROLIFERATION THAN M2 OR M0 MACROPHAGES

5.1 Abstract

Antigen presenting cells (APCs) are responsible for the activation of naïve T lymphocytes in addition to playing a significant role in stimulating the proliferation of central memory and effector memory T cells. Dendritic cells are the professional APCs of the immune system, but monocytes, macrophages and B cells also possess the capacity to process and present antigen to T lymphocytes. It is not uncommon for macrophages to be characterized into an M1 (inflammatory) or M2 (non-inflammatory) phenotype. Thus, we were interested in the differential stimulatory capacity of phenotypically distinct macrophages in a mixed leukocyte reaction. Here we show a method to measure the differentiation of porcine macrophages into an M1 or M2 phenotype, and their differential ability to stimulate T cells in a mixed leukocyte reaction (MLR).

5.2 Introduction:

The mixed leukocyte reaction (MLR) is an immunological assay representative of a graft versus host disease response. Essentially, the MLR is exemplary in demonstrating alloreactivity of T lymphocytes. During the development of the T cell repertoire in the thymus, T cells undergo a process of positive and negative selection. During positive selection, CD4 α /CD8 β double-positive thymocytes migrate to the thymic cortex and interact with thymic epithelial cells. If the double positive thymocytes interact more strongly with MHCII they become CD4 α ⁺ and if they interact more with MHCI they acquire a CD8 lineage. If the thymocyte has undergone a poor rearrangement of its T cell receptor (TCR) and does not interact with either MHCI or MHCII, that thymocyte undergoes apoptosis and is eliminated from the T cell repertoire. The negative selection of T cells eliminates those lymphocytes that have acquired a T cell receptor (TCR) that is

reactive against self-MHC molecules in association with a self-peptide sequence. Those T cells that are self reactive, for the most part, undergo apoptosis and are eliminated from the repertoire, in turn preventing self-reactivity and auto-immunity. Alloreactivity can therefore be defined as T cells that recognize foreign MHC molecules, as they are non-self. This phenomenon becomes highly relevant when considering host rejection of graft tissue transplants (Colf et al., 2007; Nagy, 2012).

MLRs are typically performed using entire leukocyte populations from whole blood mixed with the leukocytes from the whole blood of another individual. Here, we have modified the traditional MLR to evaluate the capacity of macrophages to stimulate lymphocyte proliferation by culturing APCs with a T lymphocyte enriched population, with the intent of promoting increased levels of lymphocyte proliferation. Pigs are becoming an increasingly popular animal model to study human diseases, due to the similarity in anatomy, physiology, and genetics with humans (Bassols et al., 2014; Meurens et al., 2012; Summerfield et al., 2015). Additionally, pork is a primary protein source globally and limiting disease in pigs enhances food security. Taking this into consideration, investigating APC function and APC interactions with T cells will provide insight towards the induction of T cell immunity to pathogens.

Several different macrophage populations exist *in vivo* (Varol et al., 2015). For the most part, a resting macrophage can be characterized as having an M2 phenotype (homeostatic). When an M2 macrophage becomes activated, usually via cytokine stimulation or pattern recognition receptor activation, it acquires an M1 phenotype. The M1 macrophages have a lower endosomal pH, are more sensitive to stimulation via pattern recognition receptors, and respond with higher levels of inflammatory cytokine secretion in comparison to their M2 counterparts (Martinez and Gordon, 2014; Mills and Ley, 2014). Given the activation status of M1 macrophages, we hypothesized that M1 macrophages would possess a higher capacity to stimulate T cell proliferation in comparison to M2 macrophages. We were interested in determining whether the metabolic state of MΦs correlates to an APC's capability to stimulate lymphocyte proliferation in a MLR.

5.3 Materials and methods

Animals:

Six to eight week old Dutch Landrace pigs were purchased from the pathogen free herd at the Prairie Swine Centre (Saskatchewan). All experiments were conducted in accordance with the ethical guidelines of the University of Saskatchewan and Canadian Council of Animal Care.

Cell isolation and differentiation:

Monocytes were isolated from whole blood as previously described (Auray *et al.*, 2013). Briefly, PBMCs were isolated on a FICOLL-PAQUE® Plus gradient (GE Healthcare, Uppsala Sweden). Monocytes were labeled with anti-human CD14 (TUK4) directly conjugated to magnetic beads, and selected using LS columns with magnetic activated cell sorter (MACS; Miltenyi Biotec, Auburn, CA). To derive macrophages, monocytes were plated at 1.0×10^6 cells/mL, in 3 ml per well, of RPMI-1640 complete (Gibco®-BRL) (1% Antibiotic/antimycotic, 0.5 mM β -mercaptoethanol, 1% MEM non-essential amino acids (Gibco®-BRL), 1% HEPES (Gibco®-BRL), and 10% FBS) supplemented with rpGM-CSF (20 ng/ml - Biosource, Camarillo, CA) for 3 days at 37 °C with 5% CO₂. After the 3rd day in culture with rpGM-CSF, to derive an M1 phenotype, macrophages were cultured in RPMI supplemented with 20 ng/mL of rpIFN- γ (Ceiba Geigy) for 24 hours. To derive an M2 phenotype, macrophages were cultured in RPMI supplemented with 100 ng/mL of rpIL-4 (Gibco™ ThermoFisher) for 24 hours. The M0 macrophages were cultured without the addition of any cytokines. Macrophages were chosen to perform the MLRs because the differentiation time is only 3 days as opposed to 6 days with MoDCs. T-lymphocytes were enriched from PBMCs using a MACS sorter. Briefly, 3.0×10^7 PBMCs were incubated with 300 μ g of anti-CD172a antibody (BL1H7, BioRad) and 300 μ g of anti-CD21 antibody (BB6-11C9.6, Southern Biotech) in 300 μ l of PBS+2% FBS for 15 minutes at 4° C with shaking. Cells were washed twice, and anti-IgG1 bead conjugated antibody (Miltenyi Biotec) was added to the CD172a/CD21 labeled PBMCs according to manufacturer's recommendations. Cells were washed and resuspended in 1 ml of MACS buffer (Miltenyi Biotec), before capturing non-T cells on a MACS LS

column to obtain a T-lymphocyte enriched population. The enriched T cells were labeled with carboxyfluorescein succinimidyl ester (CFSE) according to the manufacturer's protocol (CFSE, Thermo Fisher), enumerated, and seeded at 3.0×10^5 cells/well on a 96 well U-bottom plate.

Macrophage – T cell mixed leukocyte reaction:

Monocyte-derived macrophages (MoMΦ) and T cells were co-cultured to investigate the stimulatory capacity of M1 and M2 MoMΦs, to promote T lymphocyte proliferation. After 3 days in culture and 24 hours after the addition of IL-4 or IFN- γ , 3.0×10^4 macrophages were co-cultured with 3.0×10^5 T cells from the same or from genetically non-related pigs. The macrophage-T cell co-cultures were incubated at 37° C, 5% CO₂ for 4 days before assessing proliferation with flow cytometry as described below. Concavalin A (5 μ g/mL) stimulated lymphocytes served as a positive control.

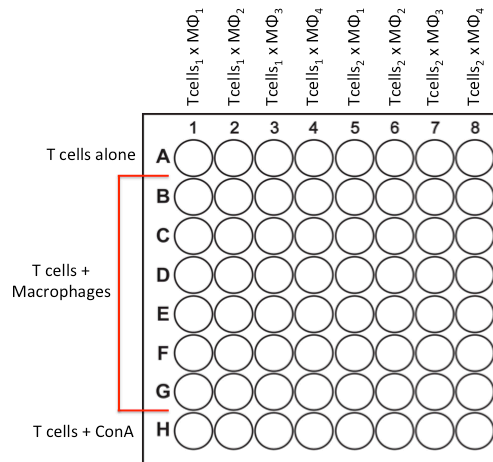


Figure 5-1: Figure demonstrating the plating schematic utilized in co-culturing APCs with an enriched T cell population for the MLRs.

Flow cytometry:

Briefly, recovered cells were incubated 20 min at 4°C with primary antibodies, then washed twice before incubation with their respective secondary antibody. The primary and secondary antibodies utilized were as follows: mouse anti-pig CD4 α (MIL17, BioRad); mouse anti-pig CD8 β (PG164a, Kingfisher Biotech); mouse anti-pig $\gamma\delta$ (PGBL31A, Kingfisher Biotech); Goat anti-mouse IgG1-PE (Southern Biotech, 1072-09); Goat anti-mouse IgG2a-A1647 (Southern Biotech, 1080-31); Goat anti-mouse

IgG2b-biotin (Southern Biotech, 1091-08); Streptavidin-PerCP-Cyanine 5.5 (eBioscience, 45-4317-80)

At least 50,000 events were collected on a FACSCALIBUR™ (BD Biosciences, Mountain View, CA) using the CELLQUEST™ software. Data were analyzed using FlowJo X (treestar) software. Populations were defined as follows: a) CTL: $\gamma\delta^-$ CD4 α^- CD8 β^+ ; b) CD4 α^+ Th cells: $\gamma\delta^-$ CD4 α^+ CD8 β^- ; c) gamma delta: $\gamma\delta^+$ CD4 α^- CD8 β^- .

Statistical Analysis:

All data points on graphs are representative of genetically unrelated individual animals. All the data were statistically analysed using GRAPHPAD PRISM™ 7 software (GraphPad Software, Inc., La Jolla, CA). Multiple comparisons between >2 groups were assessed using the Kruskal-Wallis test for non-paired, non-Gaussian data. For comparisons between 2 groups, the Mann-Whitney test for non-paired, non-Gaussian data was used. When $P \leq 0.05$, differences were considered significant.

5.4 Results

An enriched population of T lymphocytes (Supplementary Figure 5-7) was stained with CFSE in order to monitor proliferation in a mixed leukocyte reaction (MLR). After deriving macrophages from blood monocytes, cells were either non-stimulated (M0) with RPMI complete, IFN- γ stimulated (M1), or IL-4 stimulated (M2) for 24 hours before were culturing with T cells at a ratio of 1:10, either from the same animal (autologous) or from different animals (allogenic).

Our results indicate that the M1 MoM Φ s possess the highest capacity to stimulate T lymphocyte proliferation in a MLR. As shown in Figure 5-5, the CD4 α T cell population co-cultured with the M1 MoM Φ s had a mean proliferation of 46.2% in comparison to the M0 MoM Φ s which had 14.2% or M2 MoM Φ s which had 18.4% CD4 α mean proliferation. Similarly, as demonstrated in Figure 5-6, the CD8 β population in the M1 MLR had 34.1% mean proliferation while the M0 and M2 MLRs had 9.8% and 10.2% mean proliferation levels respectively. We did not record any significant difference in the proliferation levels of the gamma delta T cell populations.

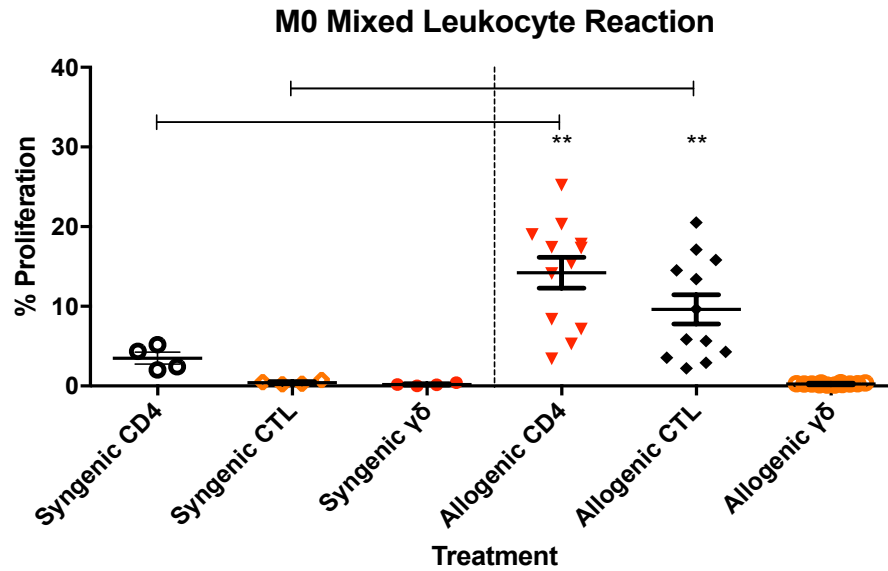


Figure 5-2: M0 mixed leukocyte reaction T cell proliferation. Non-stimulated MoMΦs (M0) were cultured with CFSE-labeled T lymphocytes, either autologous or allogenic, and stained for specific T lymphocyte subsets to monitor proliferation after 4 days in culture. Statistical analysis performed using Mann-Whitney test comparing the autologous versus allogenic T cell proliferations within each T cell subset. Data points are single replicates, from non-related animals (N=4).

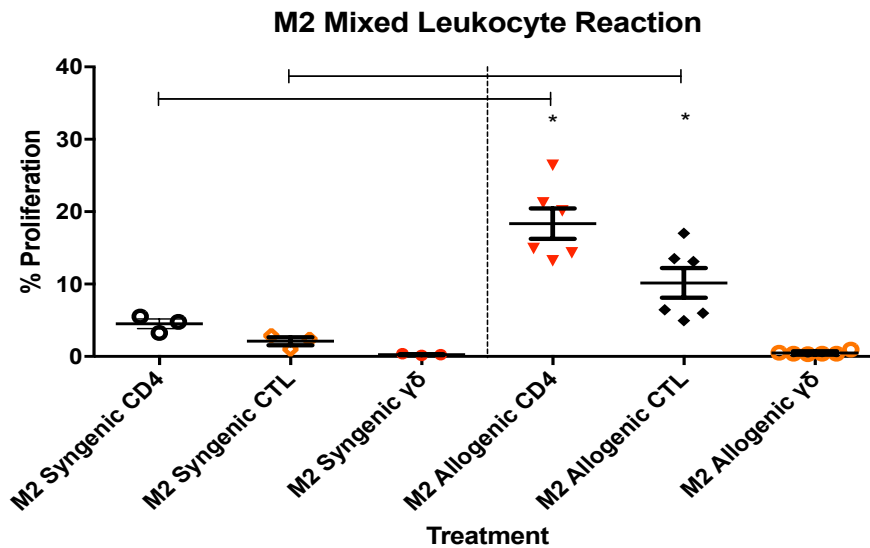


Figure 5-3: M2 mixed leukocyte reaction T cell proliferation. Interleukin-4 stimulated MoMΦs (M2) were cultured with CFSE-labeled T lymphocytes, either autologous or allogenic, and stained for specific T lymphocyte subsets to monitor proliferation after 4 days in culture. Statistical analysis performed using Mann-Whitney test comparing the autologous versus allogenic T cell proliferations within each T cell subset. Data points are from non-related animals performed as single replicates (N=3).

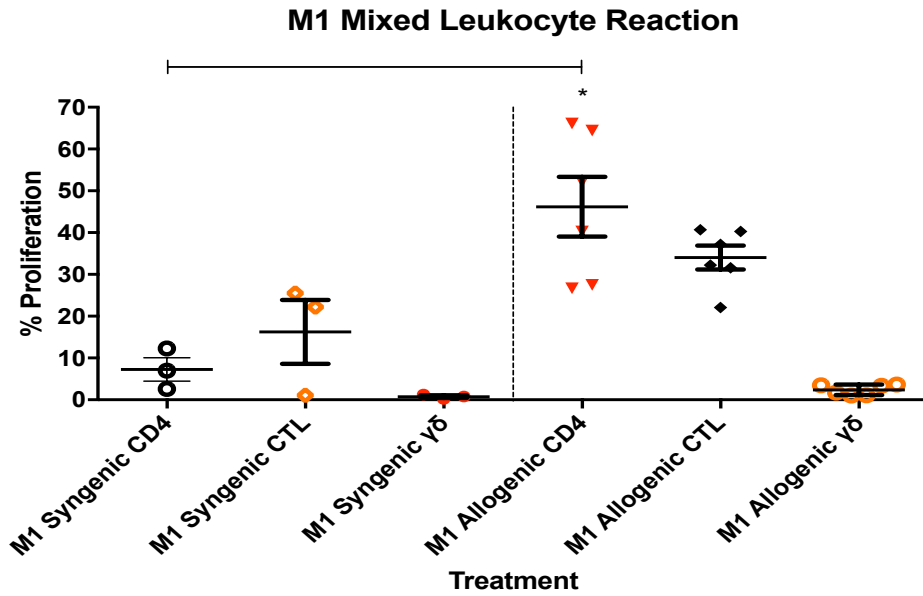


Figure 5-4: *M1 mixed leukocyte reaction T cell proliferation.* Interferon-gamma stimulated MoMΦs (M1) were cultured with CFSE-labeled T lymphocytes, either autologous or allogenic and stained for specific T lymphocyte subsets to monitor proliferation after 4 days in culture. Statistical analysis performed using Mann-Whitney test comparing the autologous versus allogenic T cell proliferations within each T cell subset. Data points are from non-related animals performed as single replicates (N=3).

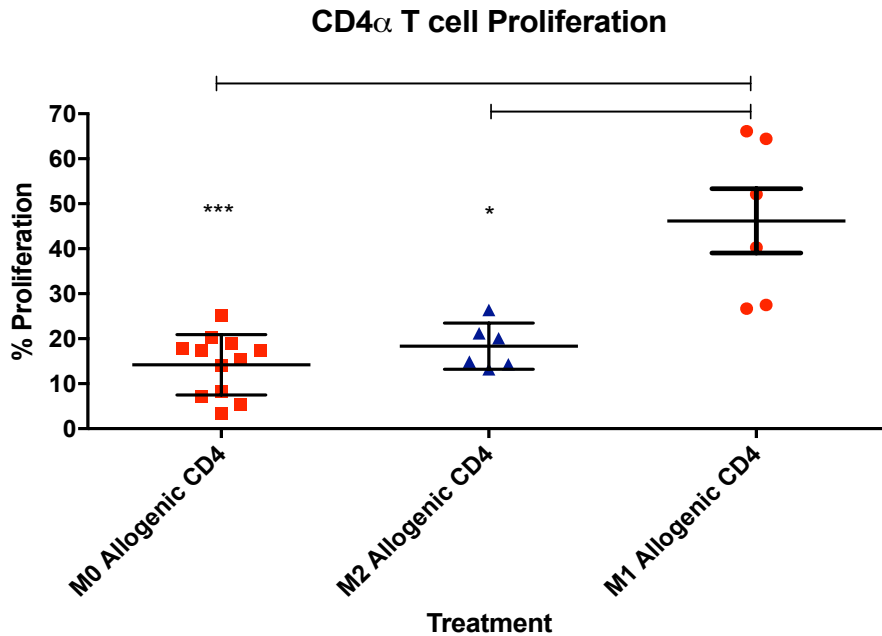


Figure 5-5: *CD4 α T cell proliferation.* Comparison of the level of CD4 α T cell proliferation amongst the M0, M2, and M1 MoMΦ mixed leukocyte reactions. Statistical analysis performed using Kruskal-Wallis test of multiple comparisons. $P < 0.05 = *$; $P < 0.005 = **$; $P < 0.0005 = ***$. Data points are from non-related animals performed as single replicates (N=3), with M1 and M2 MoMΦs from the same animals.

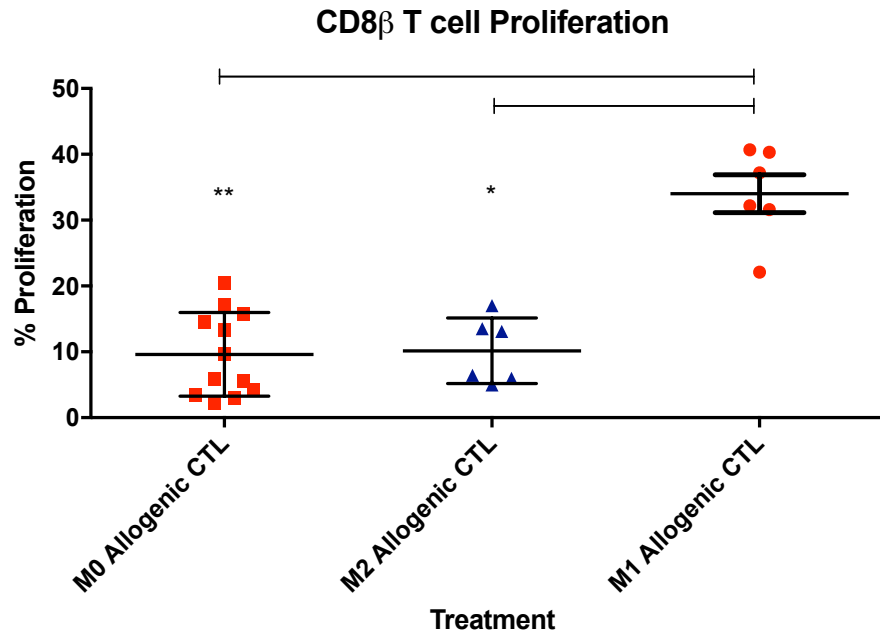


Figure 5-6: CD8 β T cell proliferation. Comparison of the level of CD8 β T cell proliferation amongst the M0, M2, and M1 MoM Φ mixed leukocyte reactions. Statistical analysis performed using Kruskal-Wallis test of multiple comparisons. $P < 0.05 = *$; $P < 0.005 = **$; $P < 0.0005 = ***$. Data points are from non-related animals performed as single replicates (N=3), with M1 and M2 MoM Φ s from the same animals.

5.5 Discussion

Macrophages have an indispensable role during tissue development, in the regulation of homeostasis, and in providing a first line of defense against invading pathogens (Varol et al., 2015). Multiple organs have tissue resident macrophages that are seeded during gestation. The origin of tissue resident macrophages has been traced to progenitor cells arising mainly from the fetal liver or yolk sac (Perdiguero and Geissmann, 2016). Interestingly, resident macrophage populations, such as Kupfer cells in the liver, are self-replenishing throughout adulthood and do not arise from blood monocytes (Krenkel and Tacke, 2017). The complexity associated with different stimuli and the diverse microenvironments that macrophages may encounter within specific tissues makes it difficult to characterize the numerous subsets that exist, particularly when considering the phenotypic state of the macrophage (Hoeffel and Ginhoux, 2015). Furthermore, mimicking diverse tissue microenvironments *in vitro* is nearly impossible. During an infection, blood monocytes are recruited to sites of inflammation where they differentiate

into MoDCs or MoMΦs (Epelman et al., 2014; Lutz et al., 2017). Thus, deriving macrophages from blood monocytes *in vitro* provides insight as to how MoMΦs may be functioning *in vivo*. In addition, discrepancies exist when comparing *in vitro* mouse studies of macrophages to humans, making pig monocyte/macrophages potentially more comparable in studying human APC population dynamics (Murray et al., 2014). Thus, for the purpose of simplicity, in this study we have chosen to analyze macrophages derived from blood monocytes in two classical states, those being the M1 or M2 phenotype. As mentioned in the introduction, M2 macrophages exhibit a steady-state phenotype, being most prominent in the absence of a pathogen or inflammatory state. They are non-inflammatory, have high phagocytic capacity, and play a role in tissue regeneration and tissue maintenance. Macrophages display plasticity, switching from an M2 to M1 phenotype, and vice versa (Mantovani et al., 2013). Immune stimulation, such as IFN- γ or lipopolysaccharide, can drive an M2 macrophage into an M1 phenotype. The M1 macrophages are inflammatory, more sensitive to pattern recognition receptor stimulation, and have lower pH in their endosomes making M1 macrophages ideal to kill invading pathogens. Once an infection has been resolved, M1 macrophages are fully capable of returning to their original resting state (M2) via cytokine stimulation (IL-4, IL-13, or IL-10) (Martinez and Gordon, 2014). We utilized non-stimulated MoMΦs as a comparison to the M1 and M2 phenotypes to determine whether non-stimulated MoMΦs were more similar to resting M2 MΦs or to the inflammatory M1 MΦs. Given the phenotypic differences between M1 and M2 macrophages, we hypothesized that IFN- γ stimulated (M1) MoMΦs would stimulate increased T lymphocyte proliferation when compared non-stimulated (M0) or IL-4 stimulated (M2) MoMΦs. Using an MLR, our results confirmed that M1 MoMΦs were more proficient in promoting T lymphocyte proliferation in both CD4 α and CD8 β T cell populations. The macrophages and T cells being from pigs becomes relevant when considering the increased utilization of pigs to study human pathologies and human infectious diseases, as responses in pigs are more similar to humans than what has been seen in mice (Fairbairn et al., 2011; Meurens et al., 2012). We did not see any difference in the proliferation of gamma delta ($\gamma\delta$) T cells in the MLRs, but $\gamma\delta$ T cells proliferated in response to ConA stimulation (Supplementary Figure 5-9). The role of $\gamma\delta$ T cells during graft rejection has not been entirely elucidated.

It has been hypothesized that $\gamma\delta$ T cells play a secondary role during tissue rejection, being dependent on the alloreactivity of $CD4\alpha^+$ Th cells (Tsuji et al., 1996). Furthermore, it has been hypothesized that $\gamma\delta$ T cells have immunosuppressive qualities during host vs graft tissue rejection, benefiting the host (Nagai et al., 1998). Another possible explanation for the lack of $\gamma\delta$ T cell proliferation may be attributable to a secreted inhibitory molecule by monocytes, or potentially through the proliferative suppression exhibited by IL-2 on $\gamma\delta$ T cells (Okragly et al., 1995). We feel that because alloreactivity seems to be dependent on $\alpha\beta$ TCR recognition, and $\gamma\delta$ T cells do not interact directly with MHCI or MHCII, it could explain why we did not observe proliferation in the $\gamma\delta$ T cell population.

In conclusion, we have demonstrated that M1 macrophages possess a greater capacity to promote T lymphocyte proliferation than M0 or M2 macrophages derived from blood monocytes. Furthermore, we have demonstrated that $\gamma\delta$ T cells do not directly participate in the mixed leukocyte reaction. Lastly, we conclude that the stimulation of APCs towards specific phenotypes has clear implications on both the magnitude of T cell proliferation and type of T cell effectors induced to proliferate.

5.6 Supplementary Figures

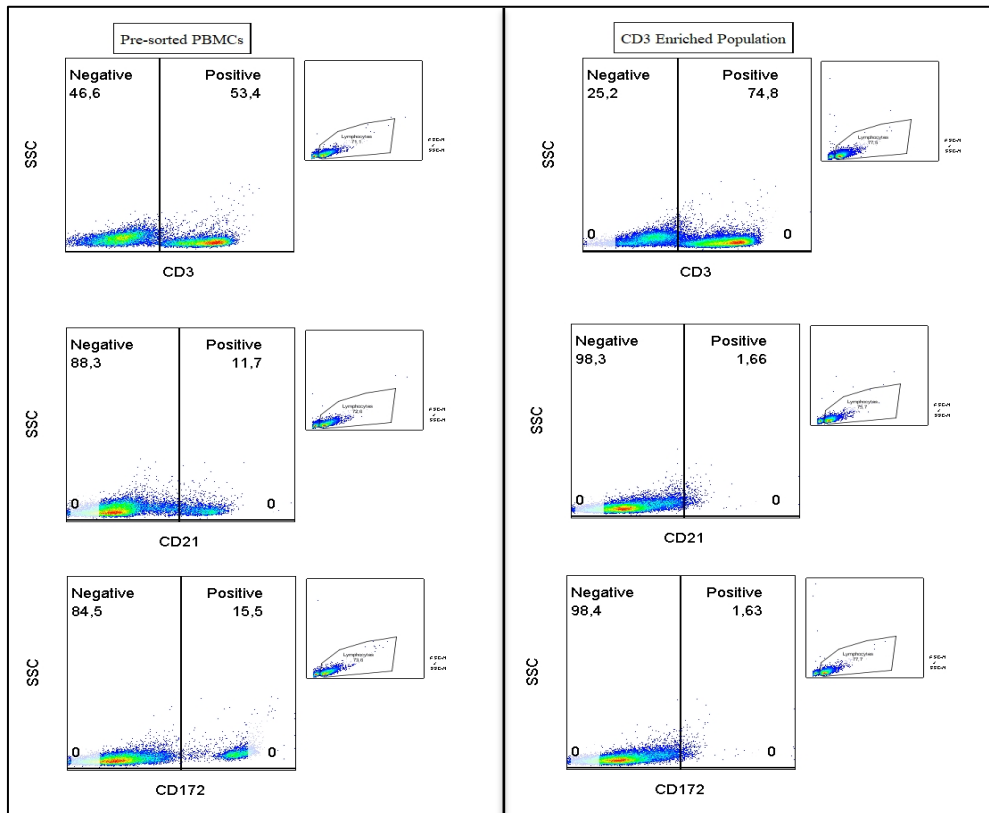


Figure 5-7: FlowJo schematic demonstrating the purity of the enriched T cell population. CD21⁺ B cells and CD172a⁺ APCs were depleted from the PBMC population to obtain an enriched CD3⁺ T cell population for the APC-T cell co-culture assays.

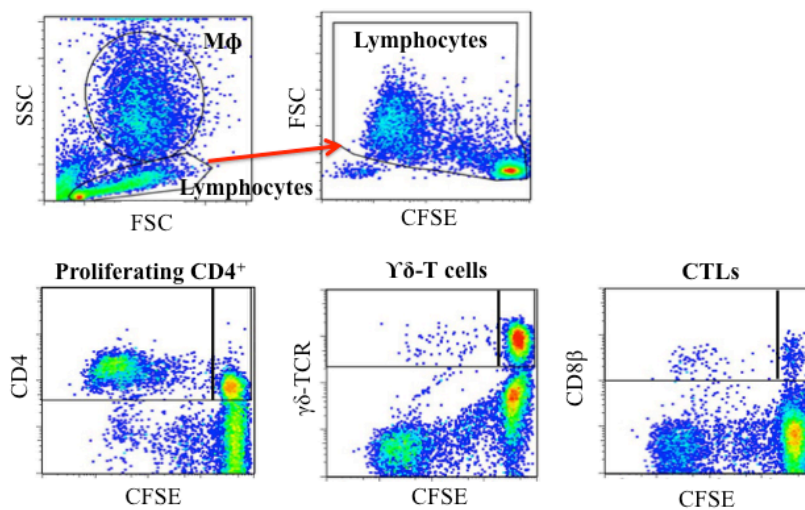


Figure 5-8: Schematic representing the gating strategy for analysis of T cell proliferation in the MLR co-culture assay.

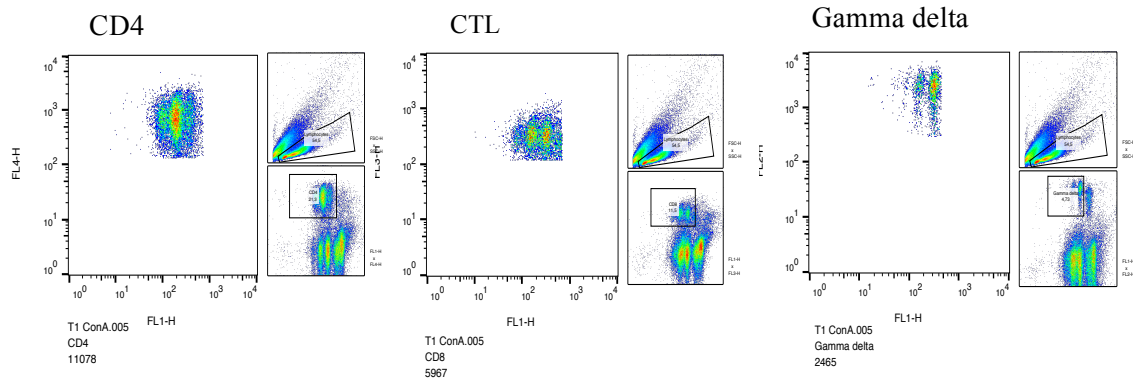


Figure 5-9: Schematic demonstrating T cell proliferation in response to ConA stimulation in the MLR. All three of the T cell subsets ($CD4\alpha^+$, CTL, gamma delta T cells) proliferated in response to the ConA positive control.

Contributions: JD and JVK isolated PBMCs and monocytes. JD performed macrophage and MoDC cell differentiation cultures. JD performed the flow cytometry and analysis. JD established the MLR. JD did statistical analysis. JD and VG designed experiments.

5.7 Conclusion

Interferon-gamma stimulated (M1) monocyte-derived macrophages (MoMΦs) possess a higher capacity to stimulate lymphocyte proliferation than non-stimulated (M0) or IL-4 stimulated (M2) MoMΦs, as evidence in the increased proliferation of CTLs and $CD4\alpha^+$ T cells. Gamma-delta T cells ($\gamma\delta$) do not proliferate in the MLR, likely being attributable to a lack of $\gamma\delta$ T cell receptor interaction with MHCI or MHCII molecules. To investigate the antigen-specific T cell response to PRRSV, in Chapter 6 we modified the MLR and co-cultured MoDCs and MoMΦs over the course of a PRRSV infection with T cells from PRRSV infected animals.

Chapter 6 T-CELL IMMUNE RESPONSE TO PRRSV INFECTION

6.1 Abstract

The T cell adaptive immune response to the porcine reproductive and respiratory syndrome virus (PRRSV) is delayed. Previous studies indicate that IFN- γ secreting cells in peripheral blood, detected 2 weeks post infection, and neutralizing antibodies, detected 4 weeks post infection, are correlates of protection. Research surrounding immune regulation by the PRRSV has generally focused on identifying viral mechanisms of innate immune regulation. Little is known regarding the T cell immune response to PRRSV and the delayed induction of T cell immunity. Considering the tropism of PRRSV is restricted to antigen-presenting cells (APCs) of the porcine immune, it's plausible that PRRSV could be regulating antigen processing/presentation in APCs. Thus, we chose to investigate the T cell immune response to PRRSV in animals over the course of an infection, utilizing a commercial, swine-influenza A virus vaccine (FluSure XP) as a comparison. Here, we show that the infection of monocyte-derived dendritic cells (MoDCs) and monocyte-derived macrophages (MoM Φ) by PRRSV does not abrogate their immunostimulatory capacity to induce T cell proliferation, the T cell immune response to PRRSV is geared towards Th1 type immunity, PRRSV infection may increase the T cell immune response to the FluSure XP vaccine, and lastly we highlight potential differences in the T cell immunostimulatory capacity of MoM Φ s and MoDCs, specifically showing that MoDCs may be more potent inducers of central memory T helper cell proliferation.

6.2 Introduction:

The porcine reproductive and respiratory syndrome virus (PRRSV) is a positive sense, single-stranded, enveloped RNA virus that causes disease in swine worldwide. The virus is classed under the order Nidovirales from the *Arteriviridae* family and was first

identified in the early 1990s (Shi et al., 2010). Today, the PRRSV is the most significant pathogen in the swine industry causing losses upwards of \$650 million dollars in the United States alone (Holtkamp, 2012). Outcomes of disease include respiratory difficulty, spontaneous abortions and fetus mummification in sows, weight loss, and death under certain circumstances (Reeth, 1997; Tong et al., 2007). The demand for an efficacious vaccine and the development of strategies for disease control are top priorities for producers and consumers alike.

PRRSV infects both MΦs and DCs, with its viral tropism being restricted to cells that express the hemoglobin/haptoglobin scavenger molecule CD163 (Calvert et al., 2007). The PRRSV spreads rapidly after an infection, being detectable in peripheral lymphoid organs within the first few days of infection. Hallmarks of a PRRSV infection include a general immune suppression of innate cytokine secretion (Type 1 IFNs and pro-inflammatory cytokines), although this appears to be strain specific as some of the highly pathogenic Chinese strains seem to induce a cytokine storm, resulting in increased rates of mortality in herds (Yoo et al., 2010) (Guo et al., 2013). The adaptive immune response to PRRSV can be characterized by an early appearance of non-neutralizing antibodies (within 9 days) and a delayed induction of IFN- γ secreting cells (2 weeks post infection) in peripheral blood mononuclear cells (PBMCs). Shortly after the appearance of IFN- γ secreting cells in PBMCs, neutralizing antibodies become prominent, correlating with the resolution of the infection, although PRRSV persists in the tonsils of pigs for up to year (Loving et al., 2015). There has not yet been an explanation for the delayed appearance of neutralizing antibodies, and even less is known regarding the delayed induction of T cell immunity. A subject of continuing debate is whether the delayed induction of immunity is attributable to PRRSV specific regulatory T cells (Tregs) (Nedumpun et al., 2018; Rodriguez-Gomez et al., 2015; Silva-Campa et al., 2009; Wongyanin et al., 2012; Wongyanin et al., 2010). Another potential explanation for the delayed induction of immunity could be attributable to the atrophy and apoptosis of lymphocytes in the thymus and peripheral lymphoid organs of infected animals (Gomez-Laguna et al., 2013a; He et al., 2012). Considering PRRSV infects APCs, we believe this could also have a detrimental impact on the progression to T cell immunity, potentially having an effect on the skewed humoral immune response.

Our previous investigation indicated that the susceptibility of MoDCs and MoMΦs are comparable. Furthermore, results indicated that the cell surface expression of MHC I and MHC II on non-stimulated MoMΦs is downregulated in response to a PRRSV infection, while a potential slight upregulation on the surface of MoDCs was observed. Here, we chose to compare the immunostimulatory capacity of MoDCs and MoMΦs to induce T cell proliferation in response to a PRRSV infection in animals. A previous study investigating the pathogenesis of swIAV in the pig lung found that there was a marked increase in the migration of MoDCs into the parenchyma surrounding the lungs after pigs were infected with swIAV. Additionally, the authors demonstrated that MoDCs possessed a high capacity to induce the proliferation of CD4α⁺ and CD4α⁻ CD8α⁺ T cells (Maisonnette et al., 2016). Thus we chose to immunize animals with a swIAV, and induce a T cell recall response with live-swIAV (H1N1) as a positive control in our study. In total 24 animals were separated into three groups of 8 and were either infected with PRRSV, immunized with FluSure XP and infected with PRRSV, or housed separately and immunized with the FluSure XP vaccine as a control. Over the course of a month we utilized an APC-T cell co-culture assay to monitor PRRSV-antigen specific and swIAV-antigen specific T cell recall responses. We accomplished this by isolating monocytes from animals using a Multi-MACS sorter and, after differentiating monocytes into MoMΦ or MoDCs, on the appropriate days T cells were isolated from the same animals and the differentiated APCs were co-cultured with T cells from autologous animals. This allowed us to monitor the progression to T cell immunity over the course of an infection to PRRSV while comparing the immune response to animals that were either immunized with FluSure XP or animals that received the FluSure XP vaccine in addition to being infected with PRRSV. Lastly, using 6-colour flow cytometry we compared the immunostimulatory capacity of MoMΦs and MoDCs to induce specific T cell subsets in response to either PRRSV or swIAV.

6.3 Materials and methods

Animals:

Twenty-four, 3-week old Dutch Landrace pigs were purchased from the high health herd at the Last Mountain Lake (Saskatchewan). Animals were confirmed to be free of Swine Influenza and PRRSV via serum samples (IDEXX Influenza A ab; IDEXX PRRS X3 ab Test). All experiments were conducted in accordance with the ethical guidelines of the University of Saskatchewan and Canadian Council of Animal Care.

Trial Design:

Animals were separated into three groups and acclimatized for a week. Immunizations were delivered intramuscularly (2.0 ml). Group A received the FluSure XP vaccine (Zoetis) and was housed separately from Group B and Group C. Group B received the FluSure vaccine, and Group C received a PBS mock immunization. Animals received a boost immunization two weeks later. The FluSure XP vaccine was prepared according to the manufacturer's instructions and adjuvanted with Emulsigen D (20:80 ratio of ED to total volume). On the same day as the boost (animals at 6 weeks of age), Groups B and C were infected with PRRSV VR-2385 intranasally (1 ml in each nostril, 5.0×10^5 TCID₅₀/mL) and Group A received a PBS mock infection intranasally. Three weeks after the PRRSV infection, Groups A and B received an additional FluSure XP booster immunization. Antigen presenting cells and T cells were co-cultured to investigate the stimulatory capacity of PRRSV infected MoMΦs and MoDCs, to promote T lymphocyte proliferation. As a comparison, PBMCs from each animal were treated in the same manner as the APC-T cell co-cultures. Monocytes were isolated from animals and cultured into MoMΦs or MoDCs. The enriched T cell population was isolated either 3 days later (MoMΦ co-culture) or 6 days later (MoDC co-culture).

Serum ELISAs:

Serum was collected from animals to confirm seroconversion in response to the influenza immunization and the PRRSV infection. The IDEXX Porcine Reproductive and Respiratory Syndrome Virus Antibody X3 Test Kit (IDEXX Laboratories) was utilized to

assess seroconversion to PRRSV infection and the IDEXX Swine Influenza Antibody Test Kit (IDEXX Laboratories) was utilized to assess seroconversion to swIAV. Briefly, serum from animals of each group were collected and diluted according to manufacturer's protocol. Serum ELISAs were performed in triplicate according to the manufacturer's instructions. The absorption spectrums were measured at A650, and after fulfilling the validity criteria, the average of the triplicate samples were interpreted as positive or negative according to the manufacturer's instructions. To further interpret the data, test samples were compared to the negative control, as the baseline of 1.0, in order to obtain a "titre" index.

Cells and viruses:

Peripheral blood mononuclear cells (PBMCs) were isolated from 50 ml of fresh pig blood using Sepmate™ tubes and Lymphoprep™ according to the manufacturer's instructions (StemCell Technologies). Prior to monocyte isolation, 1.5×10^7 PBMCs were removed for the PBMC proliferation assay and for the IFN- γ ELISpots. PBMCs intended for the cell proliferation assay were labeled with Cell Trace Violet (Cell Trace Violet, Thermo Fisher) according to the manufacturer's protocol prior to infection with PRRSV or swIAV. The remaining PBMCs were labeled with anti-human CD14 beads (Miltenyi Biotec) and selected for on LS columns using a Multi-MACS (Miltenyi Biotec, Auburn, CA). To obtain MoM Φ s, monocytes were plated at 1.0×10^6 cells/mL in RPMI complete supplemented with rpGM-CSF (20 ng/ml - Invitrogen) for 3 days at 37 °C with 5% carbon dioxide. To obtain MoDCs, monocytes were plated at 1.0×10^6 cells/mL in RPMI complete with recombinant porcine (rp) IL-4 (100 ng/mL – Gibco™ ThermoFisher) and rpGM-CSF (20 ng/mL – R&D 711-PG) for 6 days at 37 °C with 5% carbon dioxide, and media was changed every 3rd day as shown previously (Facci *et al.*, 2010). Enriched populations of CD3⁺ T cells were isolated from PBMCs using a Multi-MACS sorter. Briefly, 3.0×10^7 PBMCs were isolated as previously from 20 ml of fresh blood. PBMCs incubated with 300 μ g of anti-CD172a antibody (BL1H7, BioRad) and 300 μ g of anti-CD21 antibody (BB6-11C9.6, Southern Biotech) in 300 μ l of PBS+2% FBS for 15 minutes at 4° C with shaking. Cells were washed twice, and anti-IgG1 MACS beads (Miltenyi Biotec) were added to the CD172a/CD21 labeled PBMCs according to the

manufacturer's protocol. Cells were washed and resuspended in 1.0 ml of MACS buffer (Miltenyi Biotec), before sorting on a Multi-MACS block to obtain a T-lymphocyte enriched population. The enriched T cell population was stained with Cell Trace Violet according to the manufacturer's protocol (Cell Trace Violet, Thermo Fisher) before being plated at 2.0×10^5 cells/well on a 96 well U bottom plate. After the addition of APCs (1:10 ratio to T cells), the APC-T cell co-culture was incubated at 37° C, 5% CO₂ for 4 days before assessing proliferation with FCM.

PRRSV strain VR2385 (ATCC, Manassas, VA, USA) was used in the study. Virus was grown up on MARC-145 cells and titers were calculated as the TCID_{50/mL} (Reed and Muench, 1938). Swine influenza, strain A/SW/SK 02 H1N1, was propagated on MDCK cells and titres were calculated as plaque forming units/mL (Dulbecco et al 1953).

PBMC, APC infection, and T cell proliferation assay:

Cell Trace Violet labeled PBMCs were infected with PRRSV strain VR-2385 at a 1.0 MOI for 3 hours at 37°, 5% CO₂. Similarly, cells were treated with swIAV (H1N1) at an MOI of 10.0. PBMCs were left in culture to proliferate for 4 days and Concavalin A (5 µg/mL) was administered to cell cultures as a positive control. MoMΦs, and MoDCs were infected with PRRSV strain VR-2385 at a 1.0 MOI for 3 hours at 37°, 5% CO₂. Similarly, cells were treated with swIAV (H1N1) at an MOI of 10.0. After 3 hours, APCs were washed and pelleted at 350 g, resuspended in fresh media, and plated with their respective autologous population of enriched T cells at a ratio of 1-APC: 10-T cells. Prior to culture, T cells were labeled with Cell Trace Violet according to the manufacturer's protocol as indicated previously. Cells were left to proliferate in culture for 4 days (PBMCs), (MoDCs and MoMΦs with T cells). Cell proliferation was measured as the percent of Cell Trace Violet labeled cells that proliferated in response to each treatment. Comparisons of percent proliferation were performed within groups, according to each treatment relative to the control (media alone treated cells). Supernatants were removed from cell cultures on the 4th day for cytokine ELISAs and the cells were pooled for flow cytometry staining.

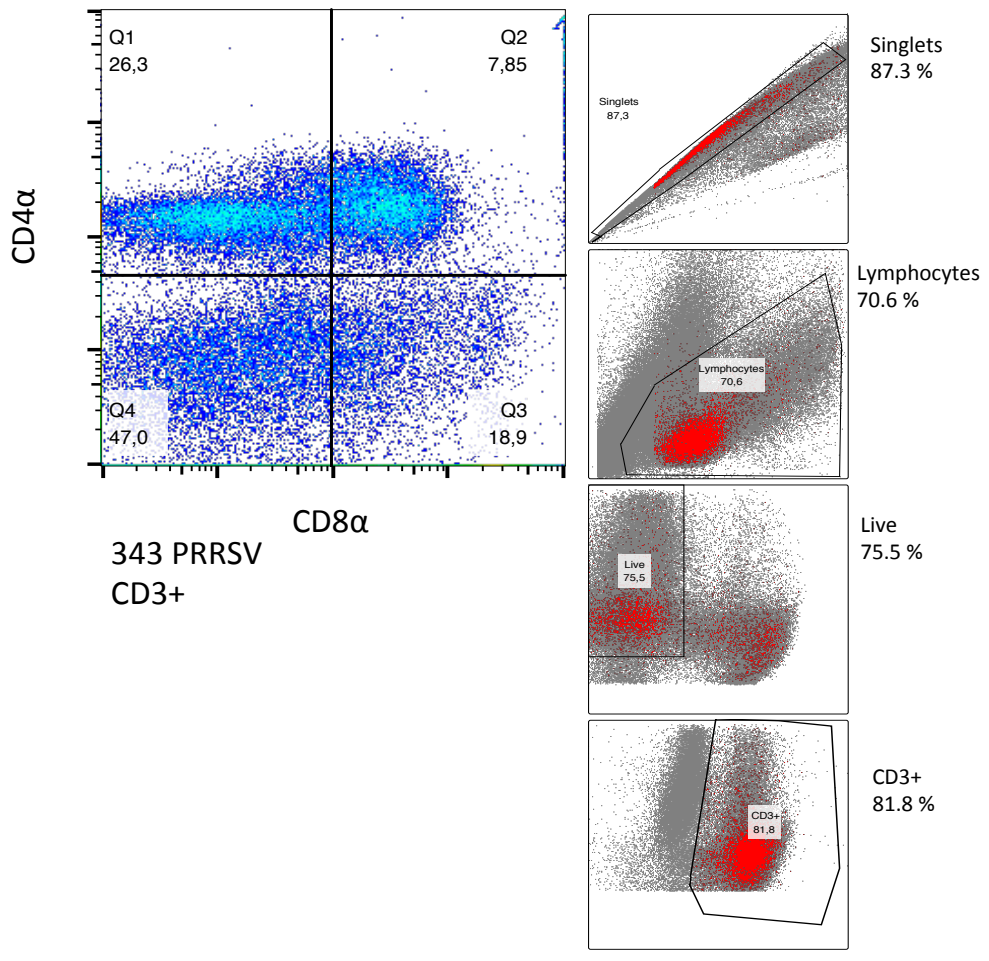
Flow cytometry:

After 4 days in culture, the PBMC cell cultures and APC-T cell co-cultures were pooled from 8 wells into one well and stained to assess cell surface marker expression by flow cytometry. Briefly, cells were stained with the LIVE/DEAD™ Fixable Near-IR Dead Cell Stain Kit (Thermo Fisher) according to the manufacturer's instructions. After live/dead staining, cells were incubated for 8 minutes at room temperature with primary antibodies, then washed twice (PBS + 2% FBS) before incubation with their respective secondary antibody. At least 100,000 events within the gated population (lymphocytes) were collected on a CyanADP (BD Biosciences, Mountain View, CA) and data was analyzed using FlowJo X software. To normalize the data, the percentage of cells within the proliferating cell subset was cross-multiplied with the total percentage of proliferating CD3⁺ cells. Thus, the frequencies of cell subsets presented in the results below are representative of the total amount of cells that proliferated in within the entire CD3⁺ T cell population.

Table 6.1: *Table indicating the primary and secondary antibodies, including their clone numbers and suppliers, utilized for the multicolour flow cytometry staining.*

Antibody	Clone/Cat #	Working dilution	Fluorochrome	Manufacturer
Anti-pig CD27 (g1)	B307	1/33	APC	BD
Anti-pig CD3	PPT3	1/10	FITC	Abcam
Anti-pig CD4a	74-12-04	1/20	PerCP-Cy5.5	BD
Anti-pig CD8a	76-2-11	1/80	PE	Southern Biotech
Anti-g1 APC	1070-11s	1/400	Anti-g1 APC	Southern Biotech

A



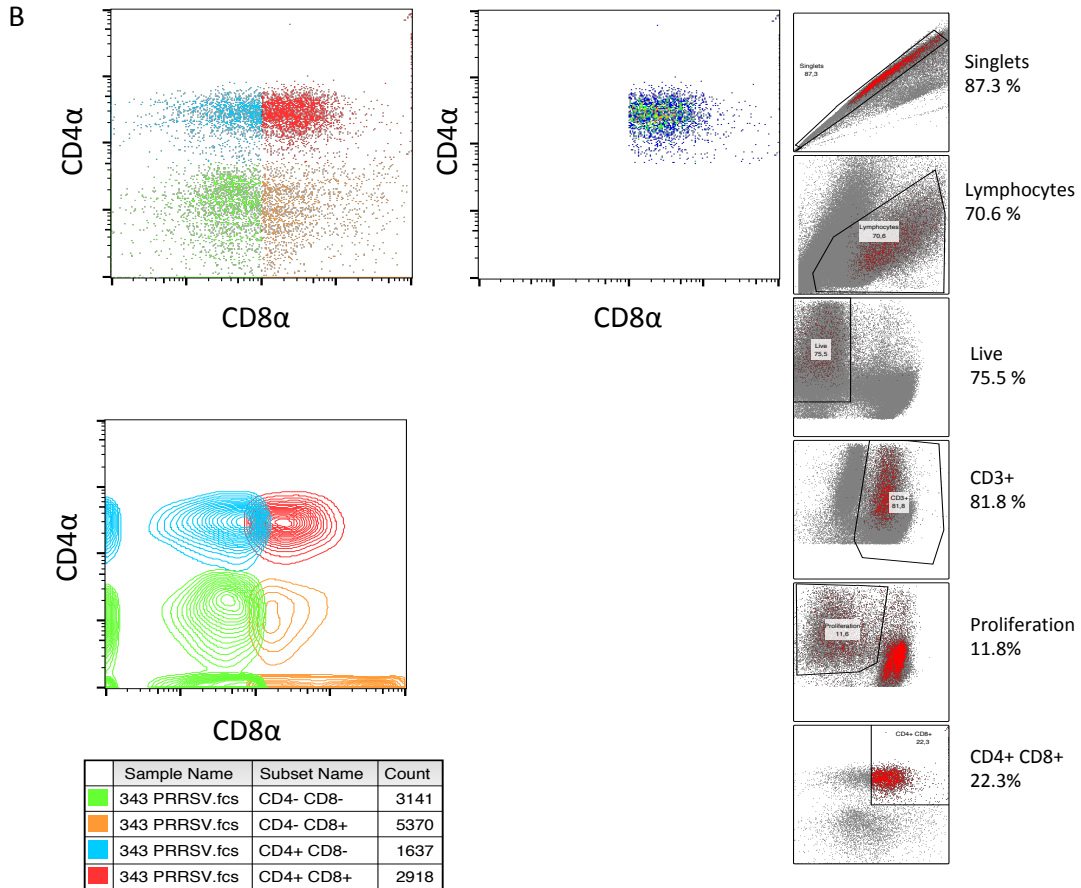


Figure 6-1: Schematic demonstrating the gating strategy applied for the analysis of $CD4\alpha^+ CD8\alpha^+$ T cells (red), $CD4\alpha^+ CD8\alpha^-$ T cells (blue), and $CD4\alpha^- CD8\alpha^+$ T cells (orange) (6-1A) from a PBMC cell culture treated with PRRSV. The gating schematic shown was from PBMCs of pig 343 (Group B) that were stimulated with PRRSV. Briefly, a gate was established around singlets before drawing a gate surrounding lymphocytes. A gate was then drawn on live cells, before gating on $CD3^+$ T cells and then gates were established for the T cell subsets (Figure 6-1A). After establishing appropriate gates for the subsets, we then drew a gate surrounding the proliferating cell population and the previously established gates for T cell subsets were used to assess proliferation of the specific T cell subsets (Fig 6-1B). Gating strategies for $CD4\alpha^+ CD8\alpha^+ CD27^+/CD27^-$ T cells can be found in the supplemental figures. The percentage of cells within the proliferating cell subset is representative of the total percentage of proliferating $CD3^+$ T cells, within the entire $CD3^+$ T cell population.

Interferon-gamma ELISpots:

Peripheral blood mononuclear cells (PBMCs) were isolated using Sepmate tubes and lymphoprep according to the manufacturer's instructions. ELISpots were performed as demonstrated previously (Dar et al., 2012). Briefly, nitrocellulose microtiter plates (UNIFILTER[®] 350, Whatmann, Florham Park, NJ, USA) were coated with 0.5 µg/100 µl of anti-porcine IFN-γ monoclonal antibodies solution (Thermo Fisher Scientific, Inc., Nepean, ON, Canada). 5.0x10⁵ PBMC were added to each well and cells were stimulated with PRRSV (VR-2385, MOI 1.0) or H1N1 influenza virus (MOI 1.0). After 24 hr incubation at 37 °C, rabbit anti-porcine IFN-γ antibody solution (0.2 µg/100 µl in phosphate buffer saline with 0.05% tween[®] 20) was added and plates were incubated for 4 hours at room temperature. Biotin-conjugated goat ant-rabbit IgG (Invitrogen-Zymed, Burlington, ON, Canada) was added (1/5000 dilution) for 2 hours at room temp before the addition of 1/5000 diluted streptavidin alkaline phosphatase solution for 1.5 hours at room temp. Lastly, spots were developed with NBT/BCIP (Sigma-Aldrich, St. Louis, MO, USA). Spots were counted with an AID ELISpot Reader Classic.

Multiplex fluorescent microsphere immunoassay (FMIA):

To measure cytokine secretion, supernatant samples were collected on the 4th day of the lymphocyte proliferation cell culture assays. A six-plex assay was developed as previously described (Laidnig 2014). Briefly, capture antibodies (Table 2) were coupled to magnetic beads (Biorad, Mississauga ON, Canada). All reactions took place at room temperature. Beads (1200 beads/µl) were diluted 1:50 in PBSA + 1% New Zealand Pig Serum (Sigma P3484) + 0.05% Na Azide and 50 µl of diluted beads was added to each well on a Grenier Bio-One Fluotrac 200 96F black plate (VWR catalogue #82050-754). Beads were washed with PBST in BioPlex plate washer before adding samples and standards. Fifty microliters of standard and cell supernatants (diluted 1:2) were added to their respective wells and incubated in the dark for 1 hour, shaking at 800 rpm. The plates were washed 3x as previously before adding 50 µL of the appropriately diluted secondary antibodies coupled to biotin. Plates were incubated for 40 minutes with shaking before washing as previously. Fifty µL of prozyme Streptavidin RPE (Cedarlane cat # PJRS20), diluted to 5 µg/mL in PBS-NZ, was added to each well and incubated for 30 minutes with

shaking. Plates were washed as previously in PBST and 100 µl of TE buffer was added to each well and placed on a shaker for 5 minutes before reading. Cytokine samples were analyzed on a Bio-Plex® 200 system and subsequently analyzed with the Bio-Plex Manager software version 6.1 (Biorad, Mississauga, ON, Canada).

Table 6.2: Table indicating the primary and secondary antibodies, including their concentrations and suppliers, utilized in the FMIA.

Protein	Supplier	Concentration	Biotin	Supplier	Concentration
rPorc IFN-alpha	GeneTex GTX11408	200 pg/mL	Porc IFN-alpha	PBL	1/5000
rPorc IFN-gamma	Fisher PIMP700	2000 pg/mL	Porc IFN-gamma	Fisher (Endogen)	1/400
rPorc IL-10	Invitrogen ASC0104	5000 pg/mL	Porc IL-10	Invitrogen	0.5 µg/ml
rPorc IL-12	Kingfisher MA0413S	5000 pg/mL	Porc IL-12	R&D	0.5 µg/ml
rPorc IL-13	Kingfisher PB0094S-100	5000 pg/mL	Porc IL-13	Kingfisher	0.5 µg/ml
rPorc IL-17A	Kingfisher KP0498S-100	500 pg/mL	Porc IL-17A	Kingfisher	0.1 µg/ml

Table 6.3: Table indicating the standards utilized in the FMIA along with the suppliers.

Standard	Supplier	Standard	Supplier
rPorc IFN-alpha	Genetech	rPorc IL-12	R&D 912PL025
rPorc IFN-gamma	Ceiba Geigy	rPorc IL-13	Kingfisher RP0007S-005
rPorc IL-10	Invitrogen PSC0104	rPorc IL-17A	Kingfisher RP0128S-005

Statistical Analysis:

All data points on graphs are representative of genetically unrelated individual animals.

All the data were statistically analysed using GRAPHPAD PRISM™ 7 software

(GraphPad Software, Inc., La Jolla, CA). Differences between groups were assessed using the Mann-Whitney U test for non-paired, non-Gaussian data unless otherwise indicated. When $P \leq 0.05$, differences were considered significant

6.4 Results:

Animal trial design:

The animals in all three of the groups did not exhibit any clinical symptoms to the PRRSV infection. There was no remarkable difference in recorded body temperatures or behavior. Additionally, there was no adverse reaction to the FluSure-XP immunization. Animals from Group A were housed separately from animals of Groups B and C, which were housed together, to prevent passive exposure to PRRSV. The trial design is demonstrated in the table below:

Table 6.4: Table indicating the groups and their immunization with the FluSure-XP vaccine of exposure to PRRSV strain VR-2385

Group	FluSure XP immunization	VR-2385 PRRSV
Group A	Three doses	PBS inoculation (1x)
Group B	Three doses	5.0×10^5 TCID ₅₀ per nostril (1x)
Group C	PBS inoculation (3x)	5.0×10^5 TCID ₅₀ per nostril (1x)

Animals from Groups A and B received 2 ml immunizations according to the manufacturer's instructions of the FluSure-XP vaccine (Zoetis). Animals from Groups B and C were infected with PRRSV VR-2385 via nasal inoculation with 5.0×10^5 TCID₅₀ in 1 ml per nostril for a total of 1.0×10^6 TCID₅₀.

Sero-conversion in response to swIAV immunization and PRRSV infection:

Serum ELISAs were utilized to demonstrate that the animals underwent seroconversion in response to the swIAV immunization and the PRRSV infection. Serum was collected on days 9, 18, and 32 post PRRSV challenge. Figure 6-2a demonstrates that antibodies to PRRSV were present 9 days post challenge and continued to increase over the course of the trial. The antibody response to the influenza immunizations followed a similar trend, increasing as the trial progressed. Of note, on day 32 post-PRRSV infection the swIAV

titres increased in response to the booster immunization (Figure 6-2b). The increase could be attributable to animals receiving a double dosage of the vaccine (2 ml in each side of the neck) with the intention of increasing the T cell response in the lymphocyte proliferation cell culture assays.

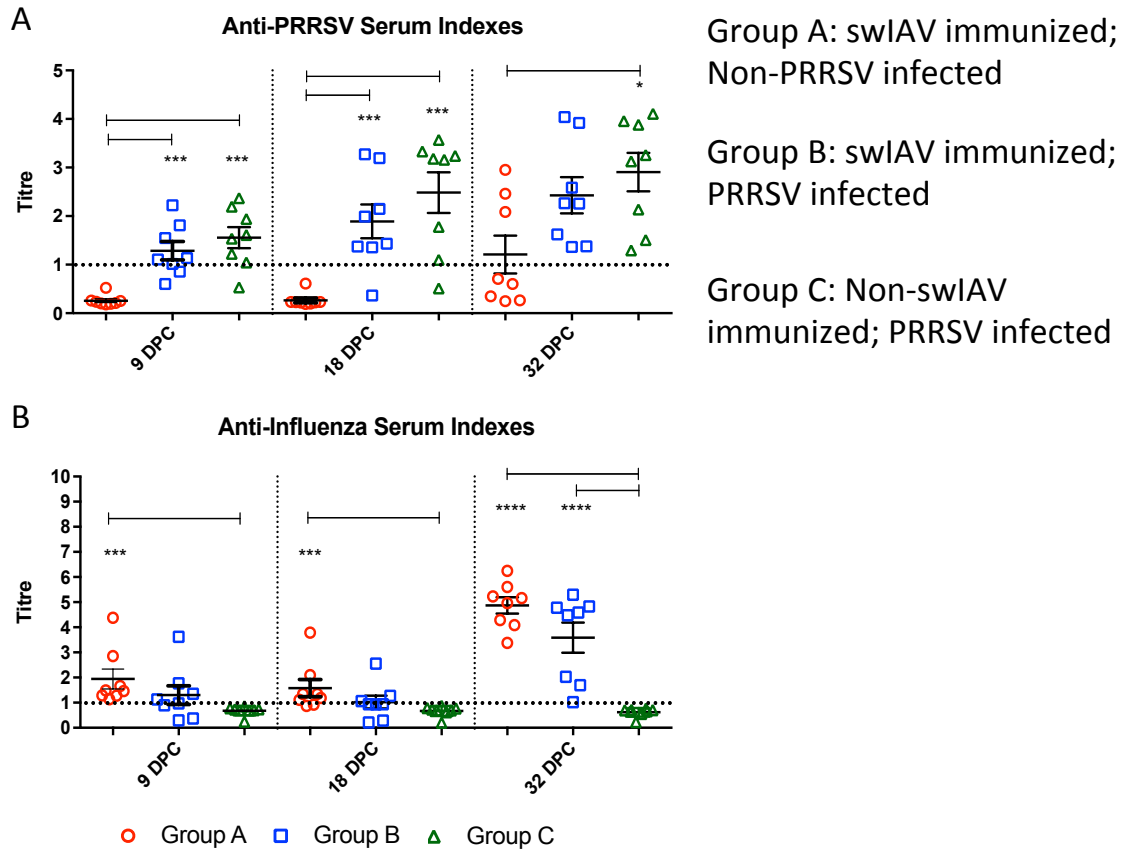


Figure 6-2: Serum ELISAs measured utilizing the commercial IDEXX ELISA kits for PRRSV (Fig 2a) or swIAV (Fig 2b) to demonstrate seroconversion and compare the humoral immune response amongst the treatments. The IDEXX ELISA kits for both PRRSV and swIAV give a read out of seroconversion as positive or negative. Serum indice calculations are described previously. Statistical significance was determined in the PRRSV ELISAs by comparing Groups B and C to Group A. And similarly in the swIAV ELISAs, Groups A and B were compared to Group C. Group A – swIAV immunized & non-PRRSV infected. Group B – swIAV immunized & PRRSV infected. Group C – non-swIAV immunized & PRRSV infected. ELISAs were performed in duplicate and the average was used to calculate the absorbance value. Values were reported with statistical significance if $P < 0.05 = *$; $P < 0.005 = **$; $P < 0.0005 = ***$.

Interferon-gamma secreting cells in PBMCs:

The IFN- γ secreting cells were measured in PBMCs on the days indicated below (Figure 6-3). Briefly, 5.0×10^5 PBMCs were plated per well and swIAV (MOI 10) or PRRSV (MOI 1.0) was subsequently added. After 20 hours in culture, the ELISPOTs were developed to assay for IFN- γ secretion. As shown in the graphs below, IFN- γ secretion to PRRSV became apparent in Group B and Group C 14 days post challenge and increased as the trial progressed. This indicates a successful conversion to T cell immunity. We detected IFN- γ secreting cells in response to the swIAV treatment on Day 0 PRRSV challenge in Groups A and B, and IFN- γ secreting cells to swIAV remained detectable throughout the trial, although it was much less prominent than the IFN- γ response to PRRSV (Figure 6-3).

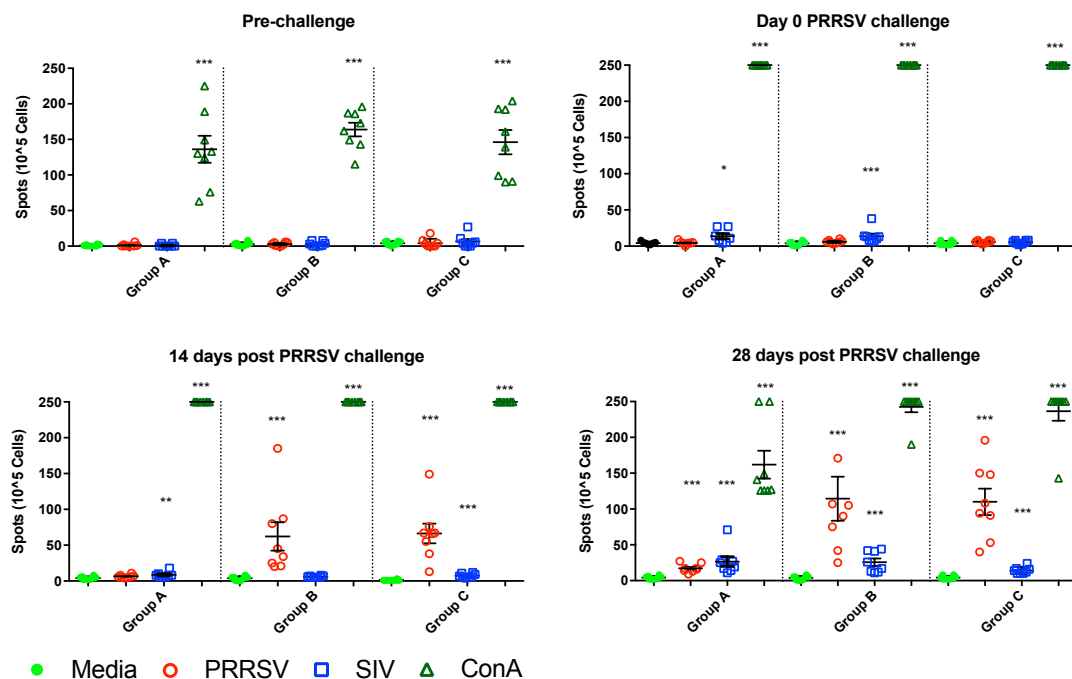


Figure 6-3: Peripheral blood mononuclear cell (PBMC) interferon-gamma ELISPOTs from the different treatment groups over the course of the trial. Briefly, 5.0×10^5 PBMCs were isolated on the respective dates listed. Cells were treated with PRRSV (MOI 1.0) or swIAV (MOI 10.0) and the IFN- γ ELISPOT plates were developed 20 hours post treatment. ELISPOTs were performed in triplicate, from which the average number of spots was calculated. Statistical significance was determined by comparing the swIAV or PRRSV treated samples to the negative control (non-stimulated cells). Values were reported with statistical significance if $P < 0.05 = *$; $P < 0.005 = **$; $P < 0.0005 = ***$.

Total lymphocyte proliferation:

We were interested in comparing the immunostimulatory capacity of MoMΦs and MoDCs to determine whether a difference existed in their ability to induce T cell proliferation. In order to perform this comparison, monocytes were isolated from the PBMCs of the animals and subsequently derived into MoMΦs or MoDCs (as described in the materials and methods section), after which they were co-cultured with an enriched T cell population from autologous animals. The co-culture assays were compared to the T cell proliferation in PBMCs.

First, we measured the overall level of lymphocyte proliferation in the PBMC and the antigen-presenting cell–T cell (APC-T cell) co-culture assays. On day 0 of the PRRSV challenge, there was no proliferation in PBMCs in response to any treatments. Therefore, we increased the MOI of swIAV to 10.0. Similarly, we did not detect proliferation in the APC-T cell co-culture assays during the first week of PRRSV infection. During the second week of infection, lymphocyte proliferation was prominent in response to both the PRRSV and swIAV treatments. The highest level of lymphocyte proliferation to PRRSV was seen in the PBMC cultures (Group C – 27.44%) while the highest level of proliferation to the swIAV treatment was observed in the MoMΦ-T cell co-culture (Group B – 16.83%) (Figure 6-5a, and Supplementary Table 6.6). These results were reflected at a later time point with the highest level of lymphocyte proliferation to PRRSV in the PBMCs of Group C (44.30%) and the highest level of lymphocyte proliferation to swIAV in Group B of the MoMΦ-T cell co-culture (16.60%) (Figure 6-5b, and Supplementary Table 6.6). Lastly, lymphocyte proliferation was detected in the media alone treatments in the MoMΦ and MoDC-T cell co-culture assays during the second week of infection (Figure 6-5a) of Groups B and C, but not Group A. During the third week of infection, we did not detect lymphocyte proliferation in the media alone treatments within Groups A, B, or C (Figure 6-5b). Data showing the proliferation of lymphocytes in response to swIAV or PRRSV, within respective Groups and different cell culture proliferation assays, can be found in Supplementary Table 6.6 .

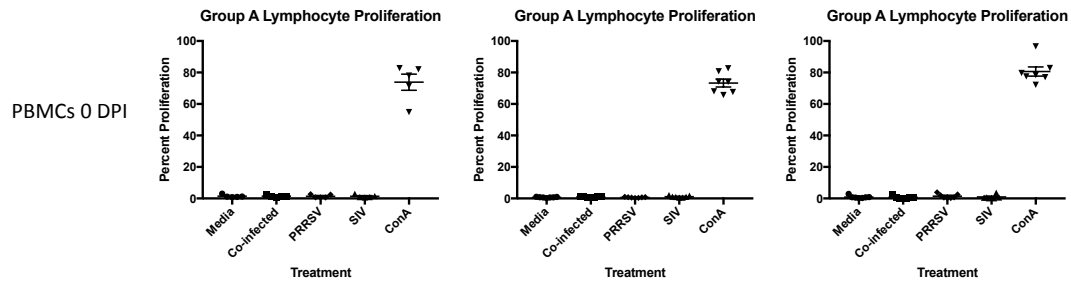
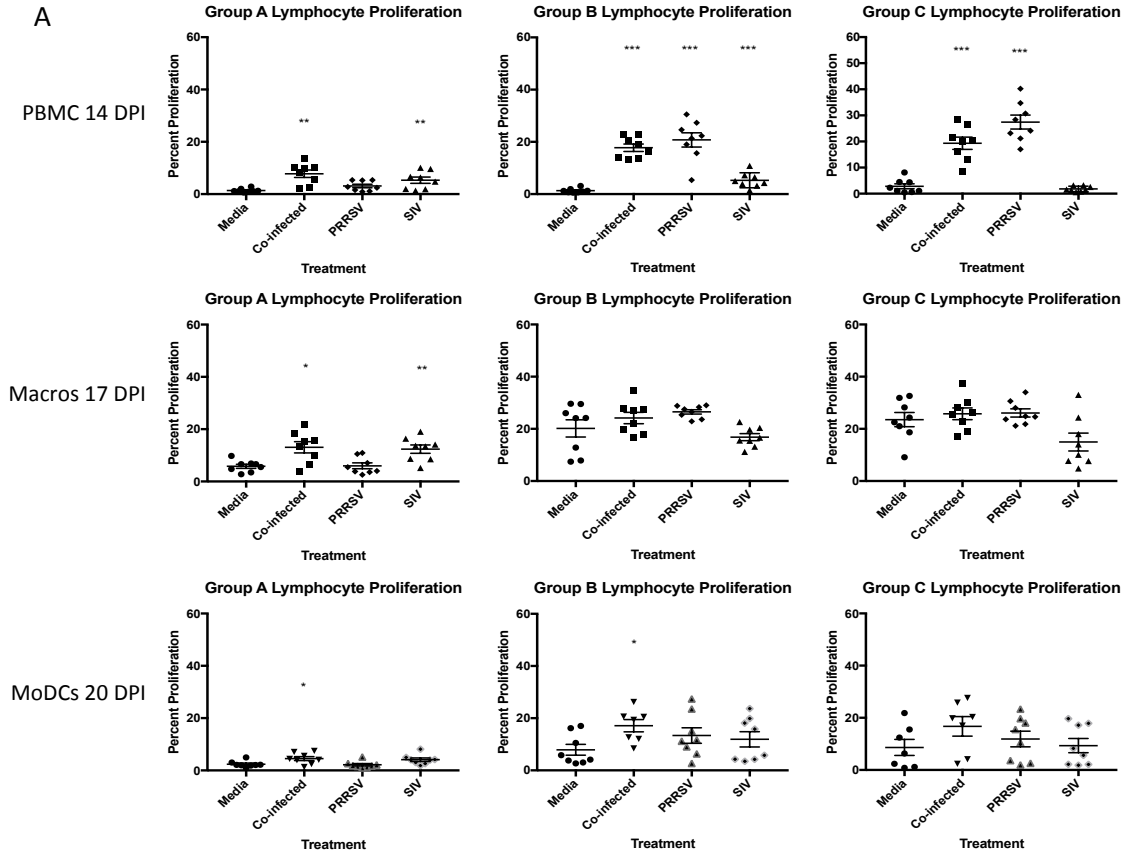


Figure 6-4: The level of total lymphocyte proliferation in PBMC cell culture assays in response to PRRSV (MOI 1.0), swIAV (MOI 1.0), or co-infected treatments on day 0 from their respective animal groups. PBMCs were stained with Cell Trace Violet prior to treatment. After treatment, PBMCs were left in culture for 4 days before measuring cell proliferation using flow cytometry. Proliferation of lymphocytes was based on the entire population of Cell Trace Violet labeled cells, acquired as single replicates (n=6-8). (gating previously on singlets and dead cell exclusion).



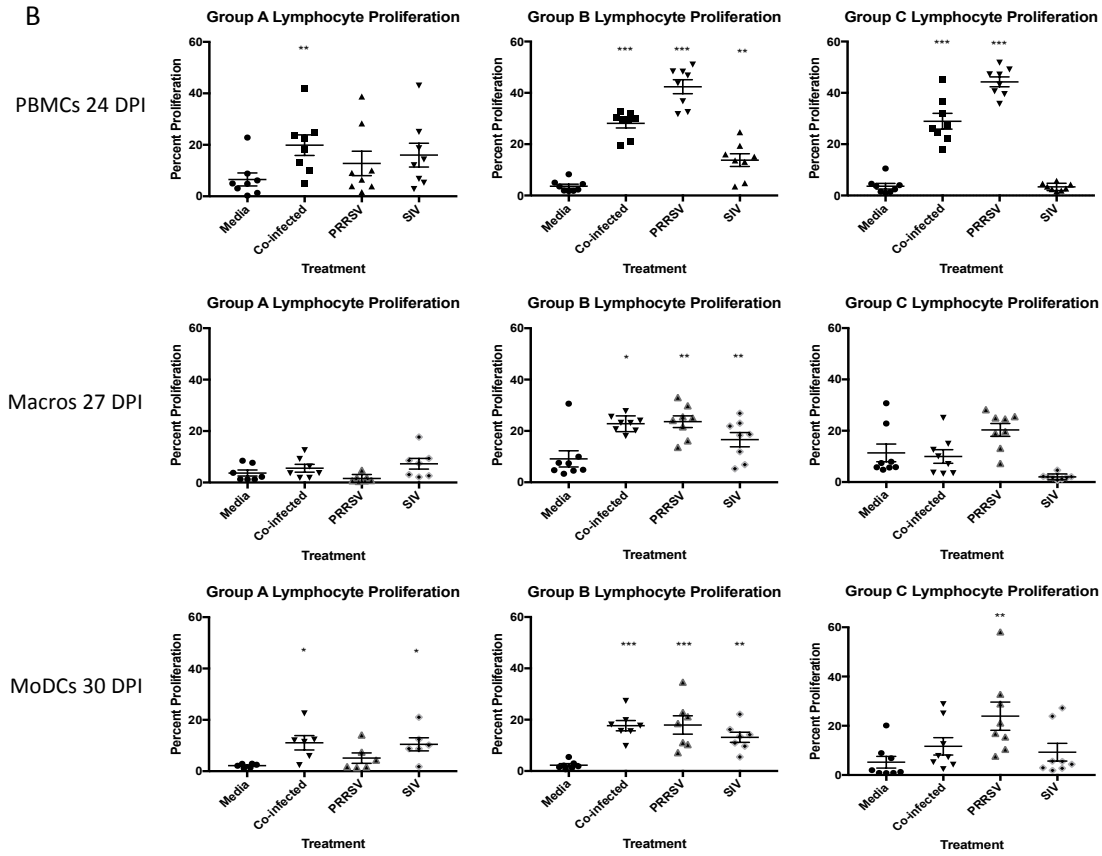
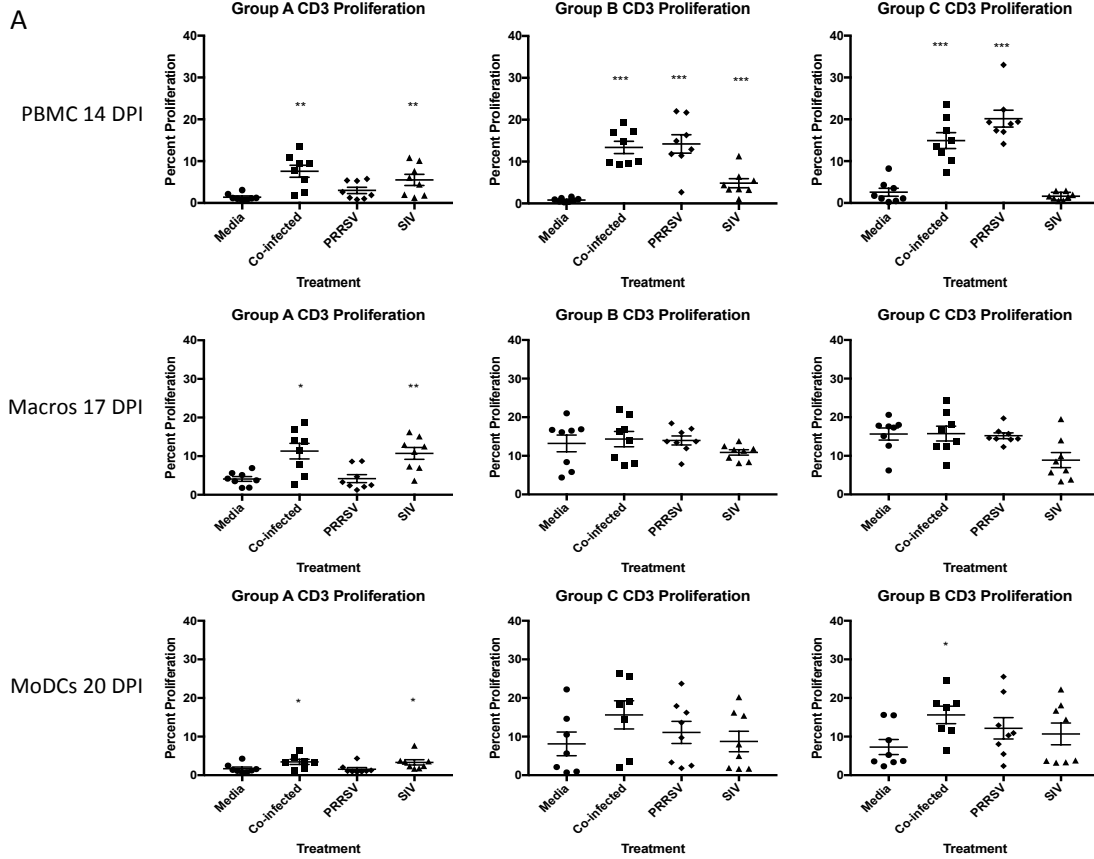


Figure 6-5: The percentages of total lymphocyte proliferation from PBMC, MoMΦ-T cell co-cultures, and MoDC-T cell co-cultures in response to PRRSV (MOI 1.0), swIAV (MOI 10.0), or co-infected treatments from their respective groups on the indicated days post PRRSV challenge. After treatment, lymphocytes were left in culture for 4 days before measuring proliferation using flow cytometry. Proliferation of lymphocytes was based on the entire population of Cell Trace Violet labeled cells (gating previously on singlets and dead cell exclusion), acquired as single replicates (n=6-8). Statistical significance was determined by comparing the co-infected, swIAV, or PRRSV treated samples to the negative control (non-stimulated cells). Values were reported with statistical significance if $P < 0.05 = *$; $P < 0.005 = **$; $P < 0.0005 = ***$. *MoMΦs were added at a 1:5 ratio to T cells on day 17.

CD3⁺ T cell proliferation:

The proliferation of CD3⁺ T cells was measured in response to the treatments. Figure 6-6a demonstrates that we detected T cell proliferation in response to the swIAV immunization in Groups A (PBMCs – 5.51%; MoMΦ – 10.72 %; MoDC – 3.33%) and Groups B (PBMCs – 4.83%; MoMΦs – 10.88%; MoDCs – 10.69%) during the second week post PRRSV infection. The percent of CD3⁺ T cell proliferation data reflects those

results observed in the lymphocyte proliferation assay with the highest level of proliferation to PRRSV being in the PBMC culture in Group C (20.16%, 14 DPI and 27.23%, 24 DPI) and to swIAV in the MoMΦ-T cell co-cultures in Group B (10.88%, 17 DPI and 13.76%, 27 DPI). The mean proliferation percent between the MoDC and MoMΦ-T cell co-cultures were comparable (Supplementary Table 6.7).



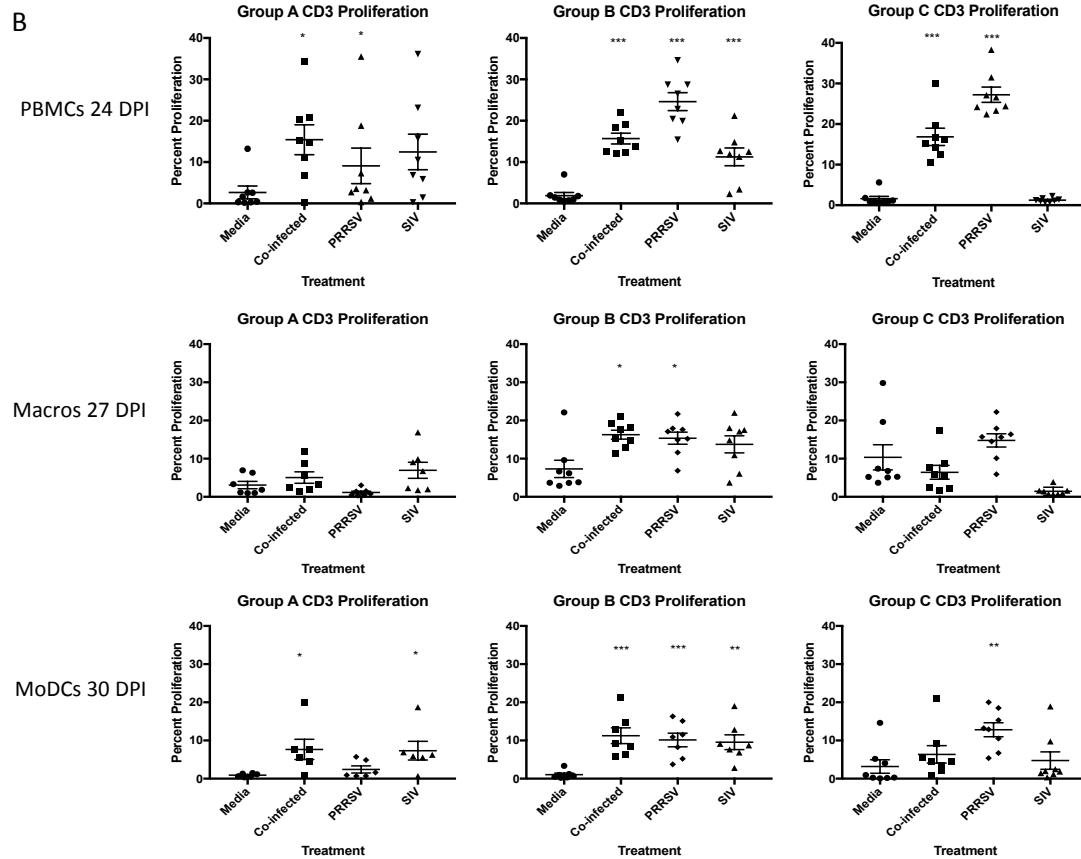
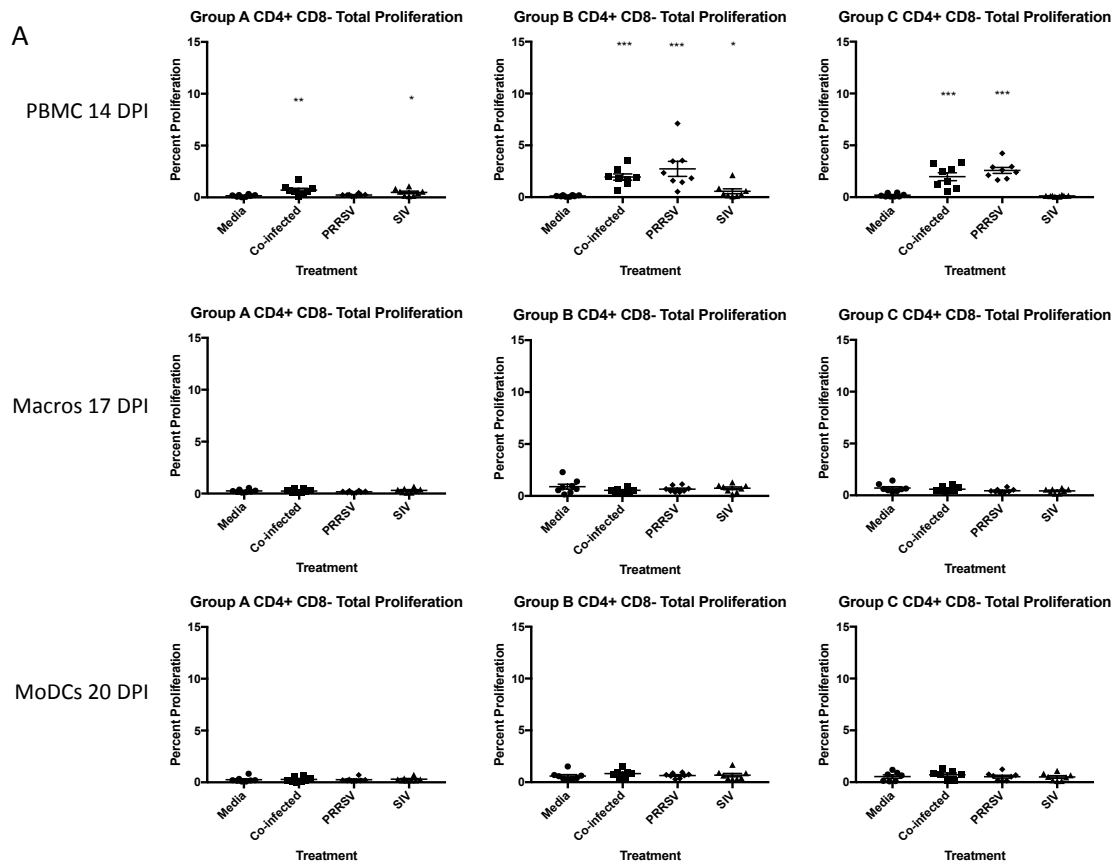


Figure 6-6: The percentages of CD3⁺ T cell proliferation from PBMC, MoMΦ-T cell co-cultures, and MoDC-T cell co-cultures in response to PRRSV (MOI 1.0), swIAV (MOI 10.0), or co-infected treatments from their respective groups on the indicated days post PRRSV challenge. After treatment, lymphocytes were left in culture for 4 days before measuring proliferation using flow cytometry, acquired as single replicates (n=6-8). Statistical significance was determined by comparing the co-infected, swIAV, or PRRSV treated samples to the negative control (non-stimulated cells) within each group. Values were reported with statistical significance if $P < 0.05 = *$; $P < 0.005 = **$; $P < 0.0005 = ***$. *MoMΦs were added at a 1:5 ratio to T cells on day 17.

Naïve T cell proliferation:

The indicated percentage of proliferation in the T cell subsets was determined by cross-multiplying the level of proliferation of the entire CD3⁺ T cell population with the percentage of proliferation from the specific subset. Thus, the percentages indicated in the following figures are an indication of the percent of T cell subset proliferation within the entire CD3⁺ T cell population. We were interested in comparing the immunostimulatory capacity of MoMΦs and MoDCs to induce the proliferation of different T cell populations. Here we show the proliferation of naïve T cells (defined as

CD4 α^+ CD8 α^-) in response to different treatments (Figure 6-7). There was no comparable difference in the level of proliferation between the APC-T cell co-culture assays. A slight proliferation of naïve T cells was observed in the PBMC cultures over the course of the trial (Figure 6-7a and 6-7b; Supplementary Table 6.8). It's plausible that the proliferating naïve T cells are CD8 α low/dim T cells trending towards becoming activated, as it would be unexpected to see antigen specific recall proliferation in a naïve T cell.



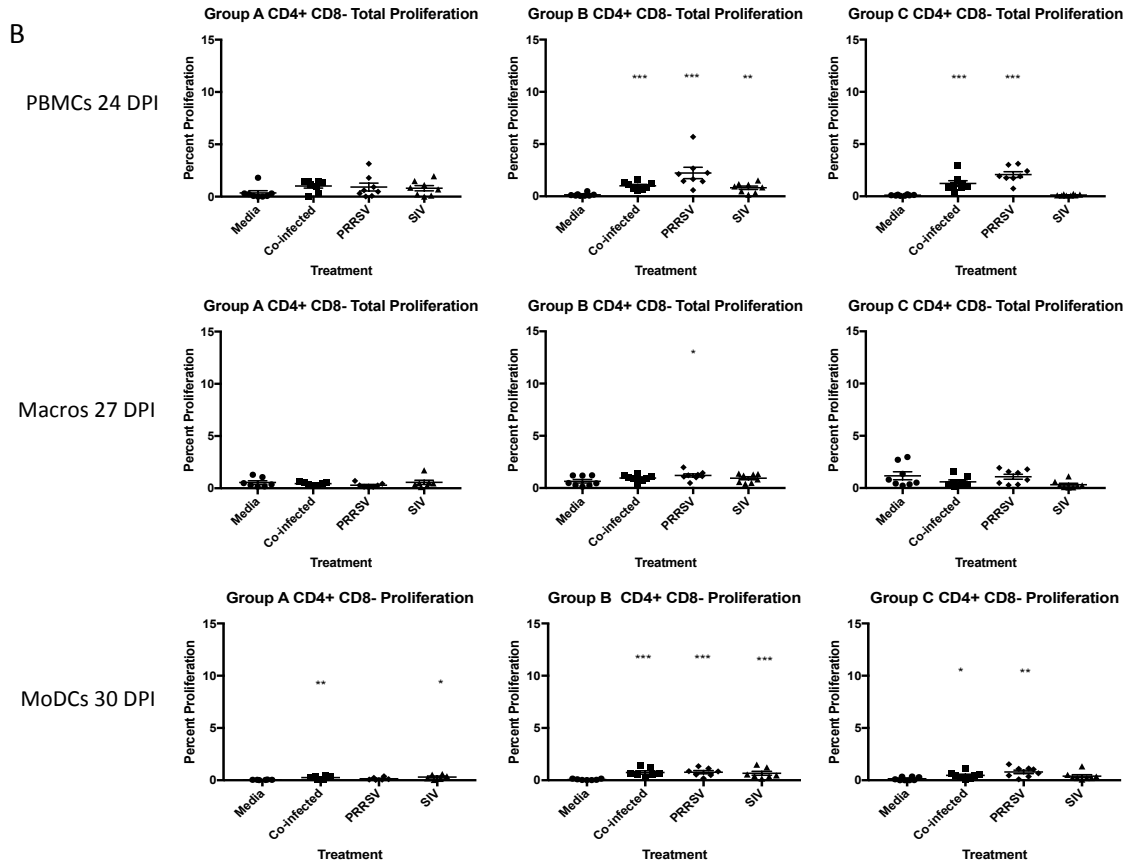
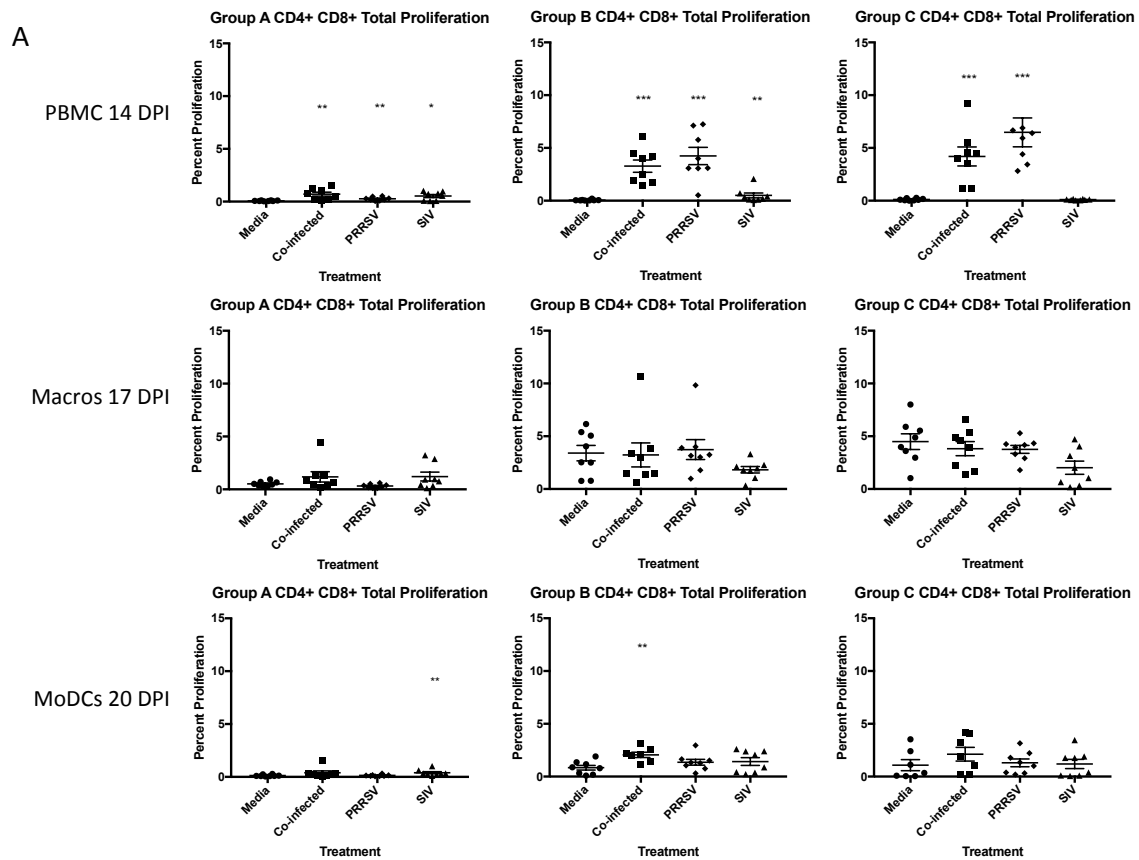


Figure 6-7: The percentages of total $CD4\alpha^+$ $CD8\alpha^-$ T cell (naïve) proliferation from PBMC, MoMΦ-T cell co-cultures, and MoDC-T cell co-cultures in response to PRRSV (MOI 1.0), swIAV (MOI 10.0), or co-infected treatments from their respective groups on the indicated days post PRRSV challenge. After treatment, cell cultures were left to proliferate for 4 days before measuring proliferation using flow cytometry, acquired as single replicates (n=6-8). Statistical significance was determined by comparing the co-infected, swIAV, or PRRSV treated samples to the negative control (non-stimulated cells) within each group. Values were reported with statistical significance if $P < 0.05 = *$; $P < 0.005 = **$; $P < 0.0005 = ***$. *MoMΦs were added at a 1:5 ratio to T cells on day 17.

Activated T helper cell proliferation:

To measure the levels of activated, antigen specific, T helper cell (Th cell) proliferation, cells were gated on $CD4\alpha^+$ $CD8\alpha^+$ expression (Figure 6-1). There was an increase in Th cell proliferation as the trial progressed in all of the cell culture assays (Figure 6-8a vs 6-8b). At 24 days post PRRSV challenge, the highest mean proliferation of activated Th cells in response to PRRSV treatment was detected in the PBMC cultures in Group C (6.720%). The mean proliferation of activated Th cells in the APC-T cell co-cultures to PRRSV treatment was higher in MoDCs (Group C – 4.947%) than in MoMΦs (3.116%)

as indicated in Supplementary Table 6.9. Lastly, the mean percent of activated Th cell proliferation in response to swIAV treatment was higher in Groups B than in Groups A in the PBMC cell cultures (Group A – 1.746%; Group B – 1.948%) and in the APC-T cell co-cultures (MoMΦs: Group A-1.14%; Group B - 2.36%. MoDCs: Group A – 2.27%; Group B – 3.60%,) as indicated in Supplementary Table 6.9. The mean proliferation of activated Th cells was highest in the MoDC-T cell co-culture assay.



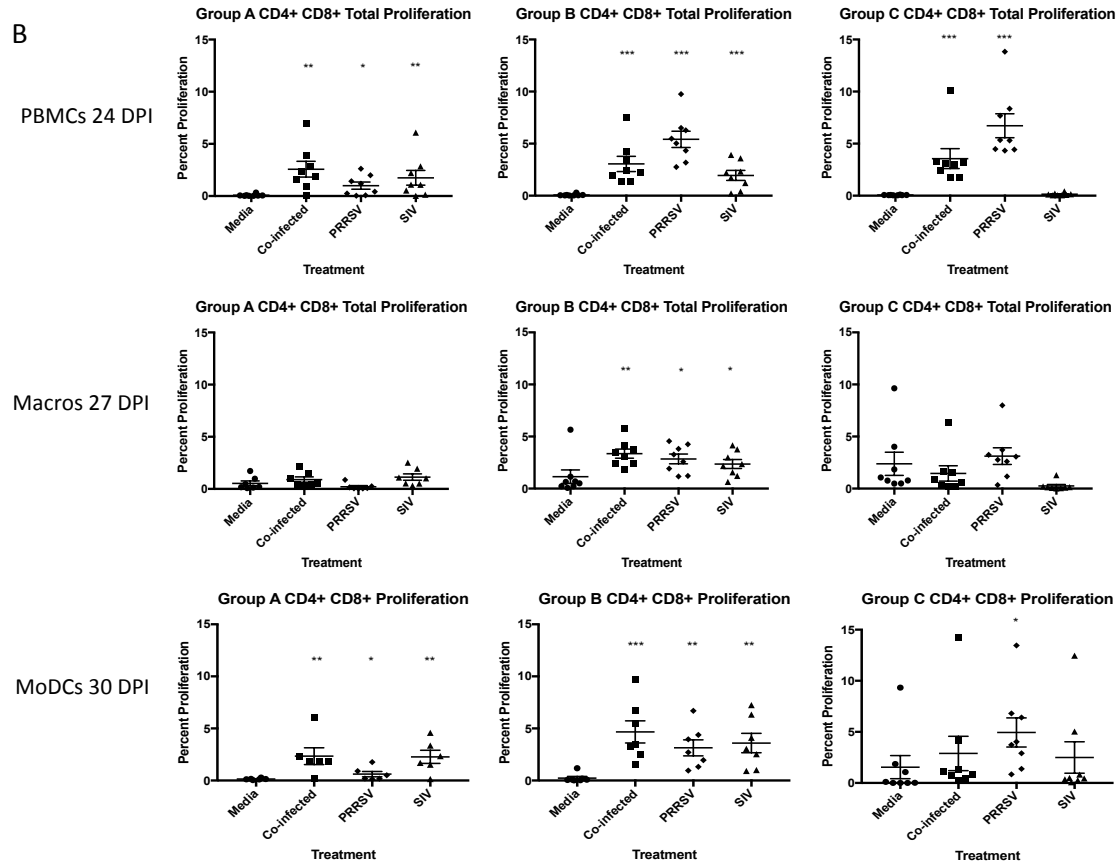
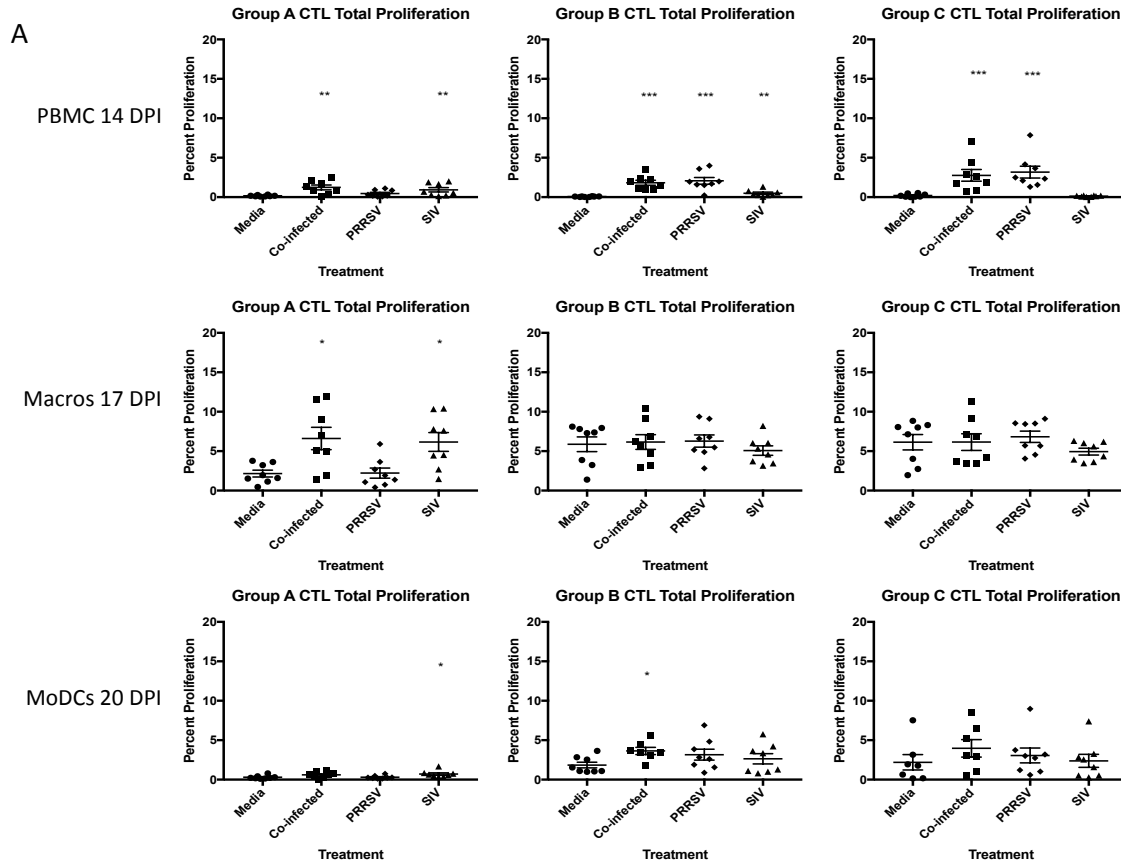


Figure 6-8: The percentages of total $CD4\alpha^+$ $CD8\alpha^+$ T cell (activated) proliferation from PBMC, MoM Φ -T cell co-cultures, and MoDC-T cell co-cultures in response to PRRSV (MOI 1.0), swIAV (MOI 10.0), or co-infected treatments from their respective groups on the indicated days post PRRSV challenge. After treatment, lymphocytes were left in culture for 4 days before measuring proliferation using flow cytometry, acquired as single replicates (n=6-8). Statistical significance was determined by comparing the co-infected, swIAV, or PRRSV treated samples to the negative control (non-stimulated cells) within each group. Values were reported with statistical significance if $P < 0.05 = *$; $P < 0.005 = **$; $P < 0.0005 = ***$. *MoM Φ s were added at a 1:5 ratio to T cells on day 17.

Cytotoxic lymphocyte proliferation:

To measure the proliferation of cytotoxic lymphocytes (CTLs), cells were gated as $CD3^+$ $CD4\alpha^-$ $CD8\alpha^+$ (Figure 6-1). Proliferation of CTLs in response to PRRSV was evident in the media alone treatment in Groups B and C, from the APC-T cell co-culture assays, during the second week post PRRSV challenge (Figure 6-9a). At the later time point during the trial, CTL proliferation was not detected in the media alone treatments of the APC-T cell co-culture assays (Figure 6-9b). The highest level of CTL proliferation was observed in response to PRRSV treatment, 24 days post-PRRSV infection, in the

PBMC culture in Group C (11.59%). The mean percent of CTL proliferation to PRRSV treatment in the APC-T cell co-cultures was highest in Group C as well. The level of CTL proliferation was higher in the MoM Φ -T cell co-culture (6.44%) than in the MoDC-T cell co-culture (4.89%) as indicated in Supplementary Table 6.10. The mean proliferation of CTLs in response to swIAV treatment was comparable amongst the PBMC and APC-T cell co-culture assays. The highest level of CTL proliferation in response to swIAV treatment during the later time point of the trial was observed in the MoM Φ -T cell co-culture, in Group B (5.72%), followed by the PBMCs in Group A (4.46%), and lastly the MoDC-T cell co-culture in Group A (3.391%). The overall highest level of CTL proliferation amongst the cultures was observed in the MoM Φ s 17 days post infection (6.82% in response to PRRSV treatment in Group C) as indicated in Supplementary Table 6.10.



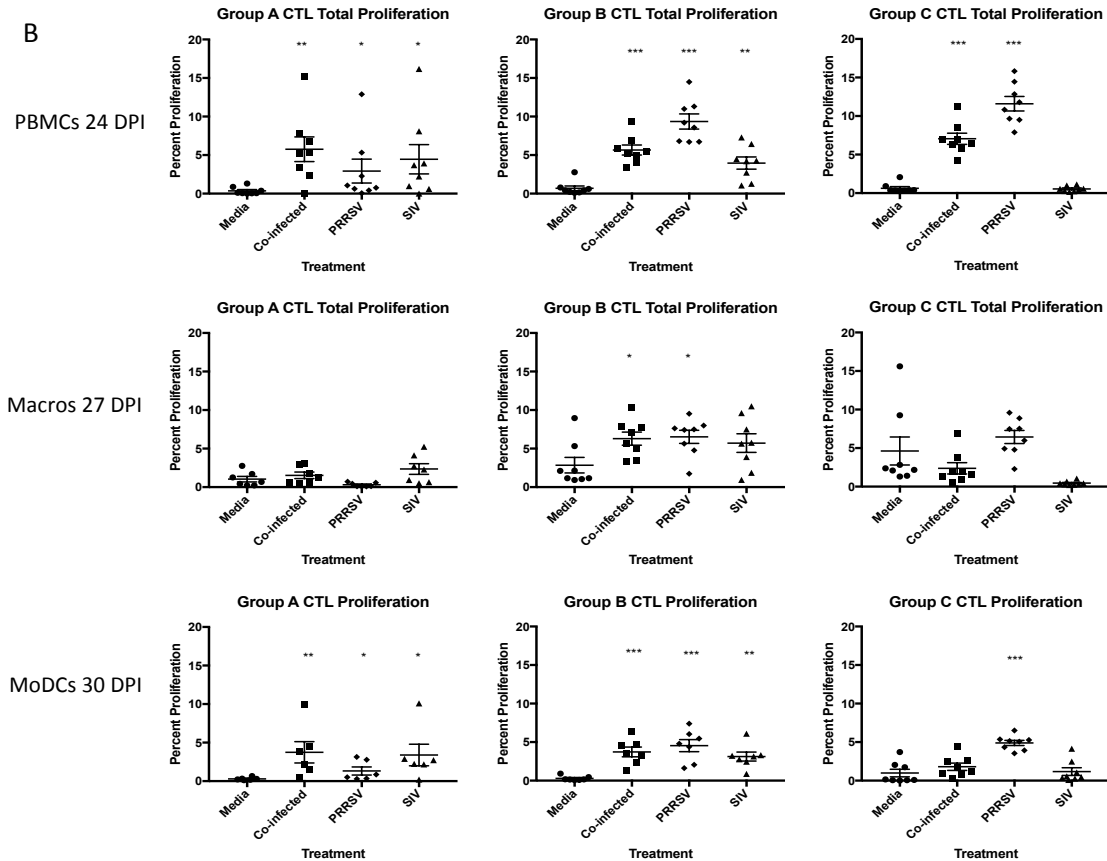
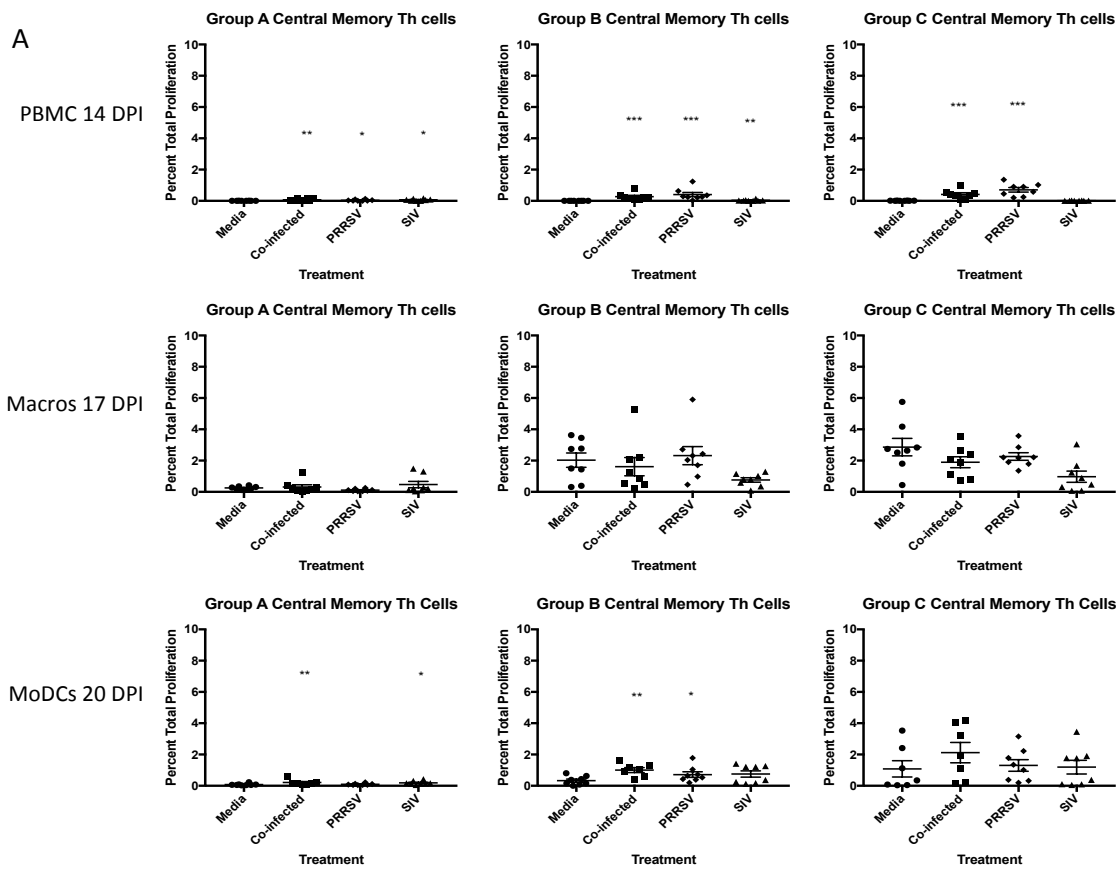


Figure 6-9: The percentages of total $CD3^+ CD4^- CD8\alpha^+$ T cell (CTL) proliferation from PBMC, MoM Φ -T cell co-cultures, and MoDC-T cell co-cultures in response to PRRSV (MOI 1.0), swIAV (MOI 10.0), or co-infected treatments from their respective Groups, on the indicated days post-PRRSV infection. After treatment, lymphocytes were left to proliferate in cell cultures for 4 days before measuring proliferation using flow cytometry, performed as single replicates (n=6-8). Statistical significance was determined by comparing the co-infected, swIAV, or PRRSV treated samples to the negative control (non-stimulated cells) within each group. Values were reported with statistical significance if $P < 0.05 = *$; $P < 0.005 = **$; $P < 0.0005 = ***$. *MoM Φ s were added at a 1:5 ratio to T cells on day 17.

Central memory T helper (Th) cell proliferation:

Central memory Th cells were defined as being $CD3^+ CD4\alpha^+ CD8\alpha^+$ and $CD27^+$. Central memory Th cells were detectable as early as 14 days post infection in the PBMC and APC-T cell co-culture assays in response to the PRRSV treatment (Figure 11a). The highest level of central memory Th cell proliferation over the course of the animal trial, in response to PRRSV treatment, was detected in Groups C. During the earlier time point of the trial, the highest levels of central memory Th cell proliferation were observed in

the MoM Φ -T cell co-cultures (2.26%), then the MoDC-T cell co-cultures (1.30%), followed by the PBMC cultures (0.79%) as indicated in Supplementary Table 6.12. During the later time point, the highest level of central memory Th cell proliferation to PRRSV was recorded in the PBMC cultures (3.60%) compared to the MoDC-T cell co-culture (2.96%) or to the MoM Φ T-cell co-culture (1.60%) as shown in Supplementary Table 6.12. In response to the swIAV treatment, the highest mean proliferation of central memory Th cells was observed in the MoDC-T cell co-cultures, at both the early and later time points during the animal trial, although the difference was more pronounced in the later time point (Figure 6-11). The mean percent proliferation of Group B (MoDCs – 1.06%; MoM Φ s – 0.738%) in response to swIAV in the APC-T cell co-cultures was higher than that of Group A (MoDCs - 0.86%; MoM Φ s - 0.36%). The percent proliferation of central memory Th cells in the PBMCs was similar to the MoM Φ -T cell co-culture (Group A – 0.425%; Group B – 0.502%) as indicated in Supplementary Table 6.12.



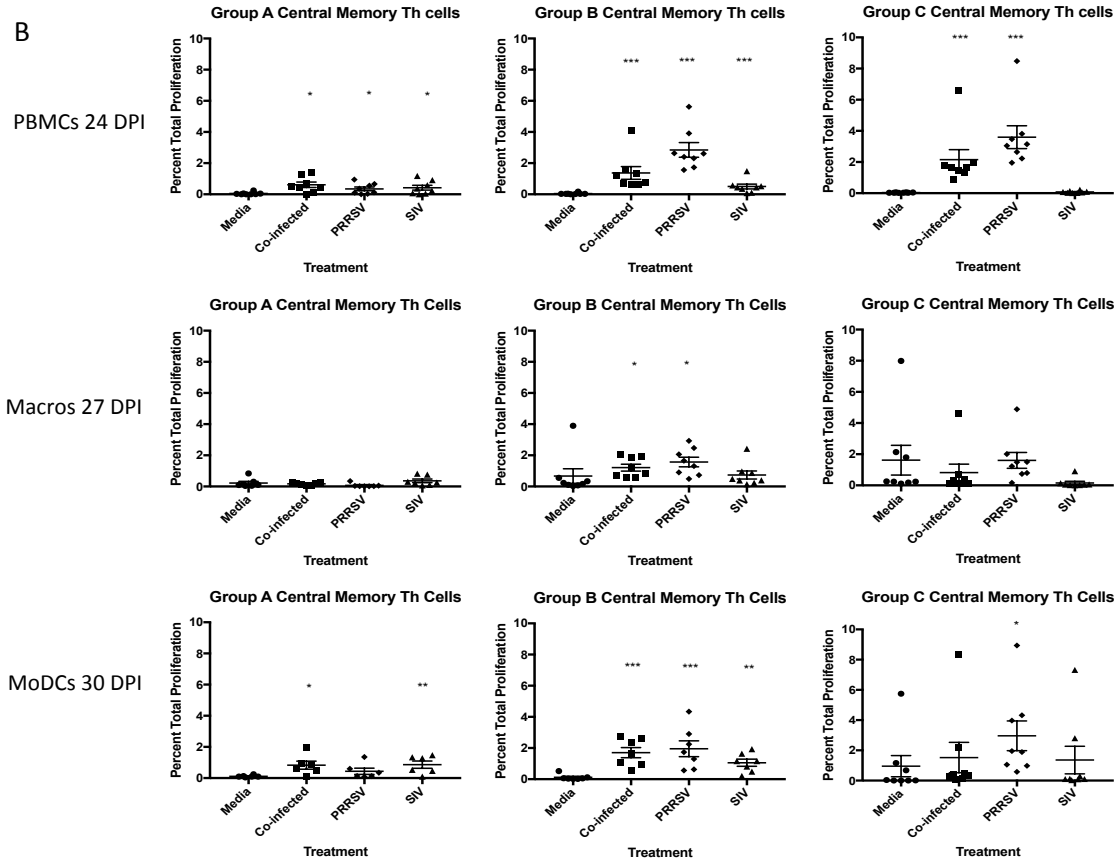
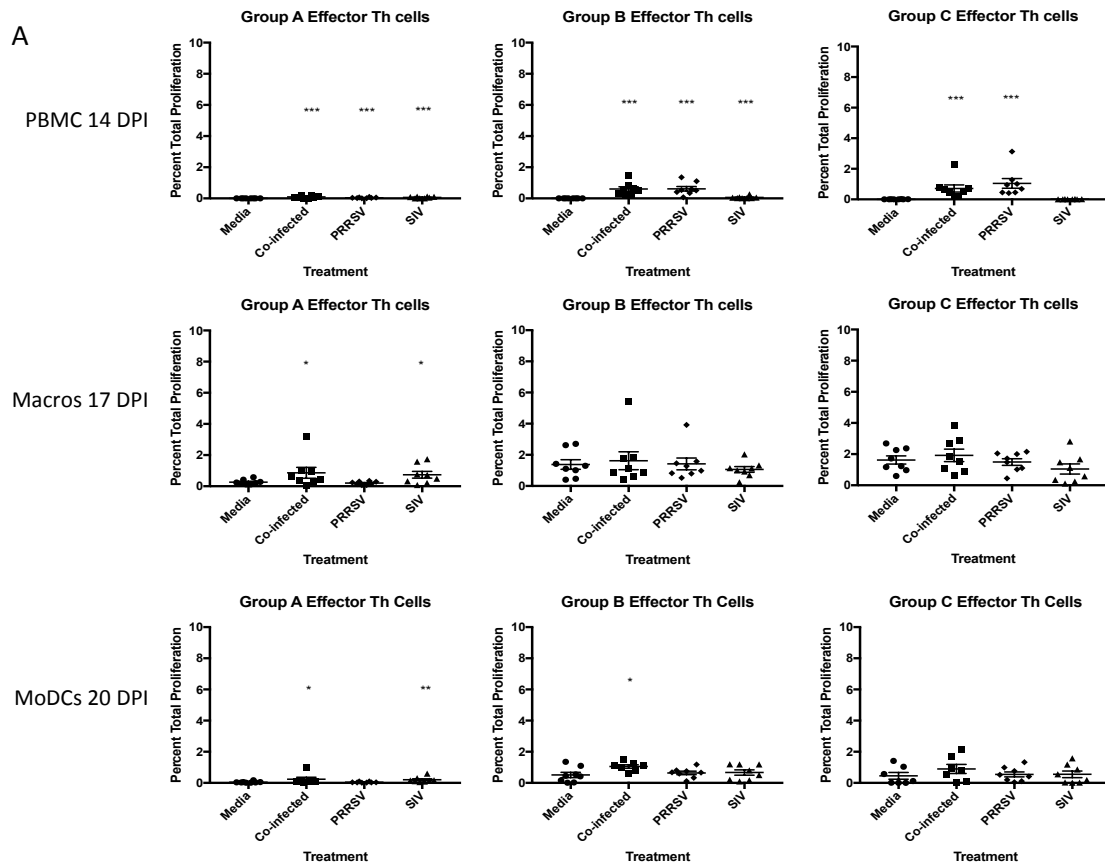


Figure 6-10: The percentages of $CD4\alpha^+$ $CD8\alpha^+$ $CD27^+$ Th cell (central memory T helper cell) proliferation from PBMC, MoM Φ -T cell co-cultures, and MoDC-T cell co-cultures in response to PRRSV (MOI 1.0), swIAV (MOI 10.0), or co-infected treatments from their respective groups at the indicated time points post-PRRSV infection. After treatment, lymphocytes were left to proliferate in culture for 4 days before measuring proliferation using flow cytometry, performed as single replicates (n=6-8). Statistical significance was determined by comparing the co-infected, swIAV, or PRRSV treated samples to the negative control (non-stimulated cells) within each group. Values were reported with statistical significance if $P < 0.05 = *$; $P < 0.005 = **$; $P < 0.0005 = ***$. *MoM Φ s were added at a 1:5 ratio to T cells on day 17.

Effector T helper cell proliferation:

Effector Th cells were defined as being $CD3^+$ $CD4\alpha^+$ $CD8\alpha^+$ $CD27^-$. The results are similar to the other T cell proliferation profiles measured previously. Effector Th cells were detected as early as 14 days post infection in the PBMC cultures and APC-T cell co-cultures. During the earlier time point of the animal trial, the highest mean percentages of effector Th cell proliferation were recorded in the MoM Φ -T cell co-culture to both PRRSV and swIAV (Figure 6-12a and Supplementary Table 6.13). During the later time

point, the highest level of effector Th cell proliferation in response to PRRSV treatment was observed in Group C for the PBMC culture (3.12%), followed by the MoDC-T cell co-culture (1.99%), and the least in the MoM Φ -T cell co-culture (1.410%) as indicated in Supplementary Table 6.13 and show in Figure 12b. In response to the swIAV treatment, during the early time point of the trial, the mean percent proliferation reflects those recorded for the PRRSV treatment with the highest level of proliferation being recorded in the MoM Φ -T cell co-culture (1.16%), followed by the MoDC-T cell co-culture (0.67%), and finally the PBMC culture (0.06%). During the later time point of the trial, higher levels of effector Th cell proliferation to swIAV were seen in Groups B (MoDC – 2.54%; MoM Φ – 1.67%; PBMC – 1.45%) than in Groups A (MoDC – 1.41%; MoM Φ – 0.77%; PBMC – 1.32 %) as shown in Supplementary Table 6.13, and the highest level of proliferation were recorded in the MoDC-T cell co-cultures.



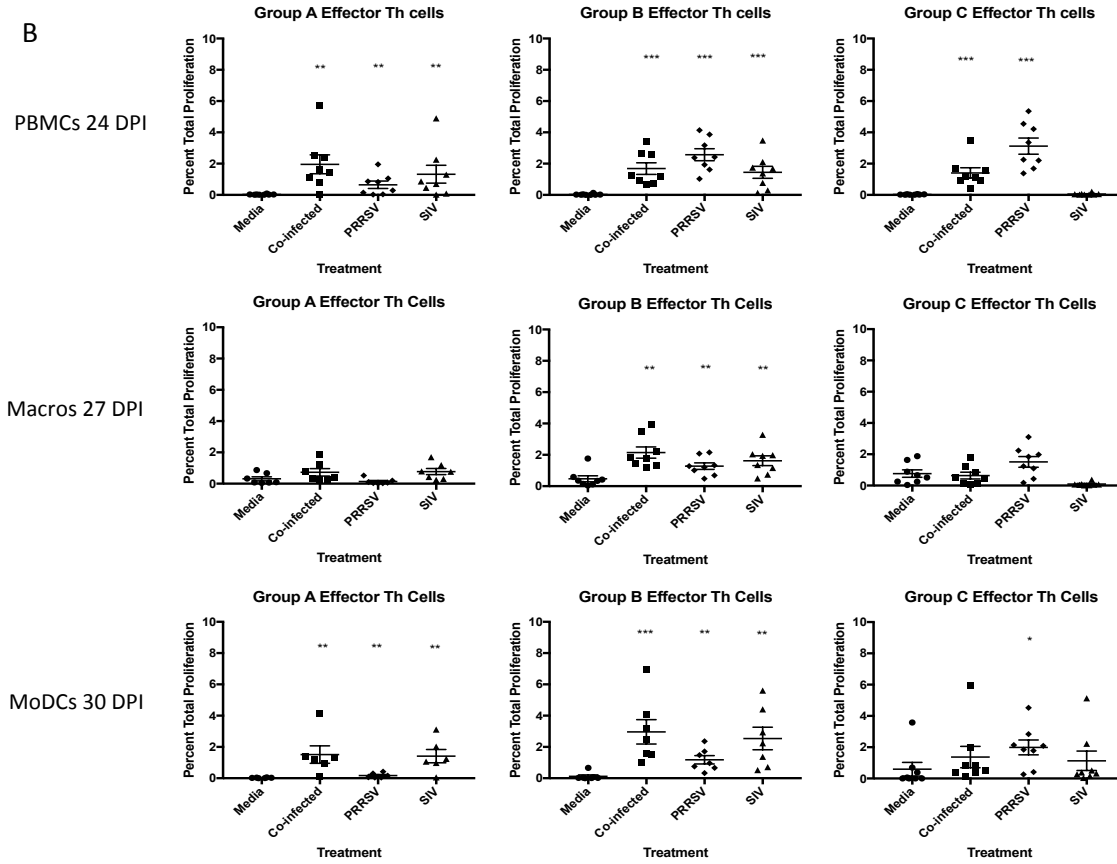


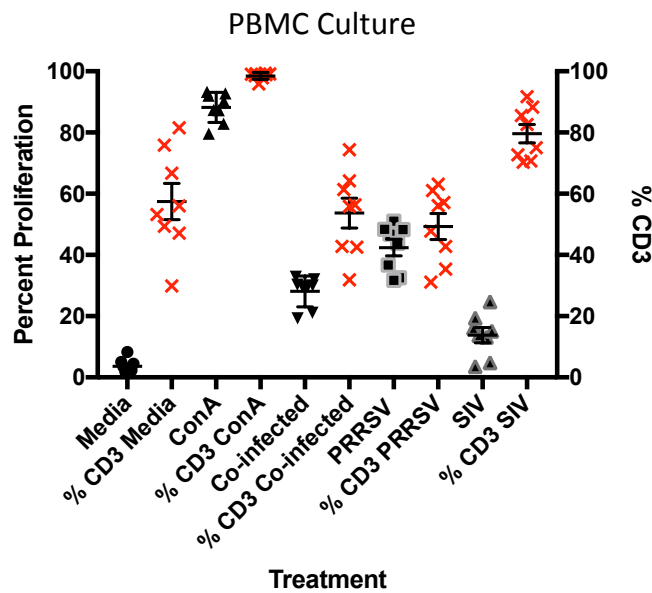
Figure 6-11: The percentages of $CD4\alpha^+$ $CD8\alpha^+$ $CD27^+$ T cell (effector memory T helper cell) proliferation from PBMC, MoMΦ-T cell co-cultures, and MoDC-T cell co-cultures in response to PRRSV (MOI 1.0), swIAV (MOI 10.0), or co-infected treatments from their respective groups at the indicated time points post PRRSV-challenge. After treatment, lymphocytes were left to proliferate in culture for 4 days before measuring proliferation using flow cytometry, performed as single replicates (n=6-8). Statistical significance was determined by comparing the co-infected, swIAV, or PRRSV treated samples to the negative control (non-stimulated cells) within each group. Values were reported with statistical significance if $P < 0.05 = *$; $P < 0.005 = **$; $P < 0.0005 = ***$. *MoMΦs were added at a 1:5 ratio to T cells on day 17.

Proliferation of an uncharacterized lymphocyte population:

During the analysis of the lymphocyte and $CD3^+$ T cell proliferation levels, we noticed a difference in the percentage of cells that were $CD3^+$ within the proliferating populations depending on the administered treatment (Figure 14a, 14b, 14c). We chose to show results from Group B, from the later time point of the infection, in order to have a comparison to the level of proliferation to both swIAV and PRRSV within the same group. Levels of $CD3^+$ T cell proliferation in the cell culture assays are indicated in Table

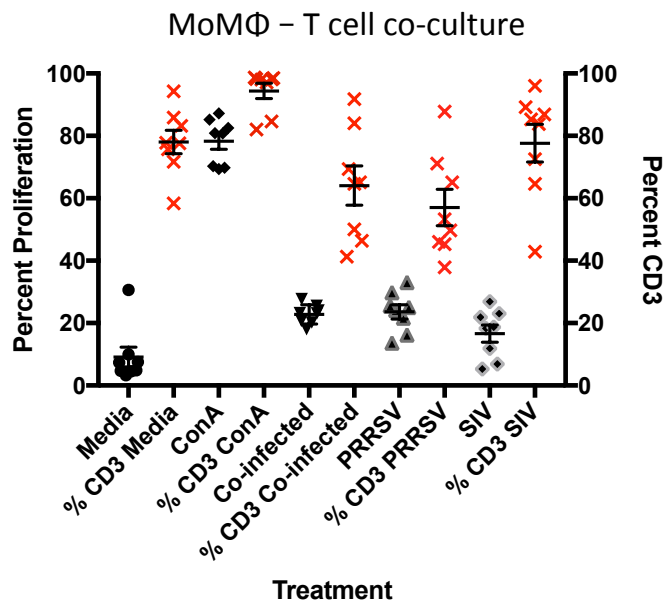
5 below. The results indicate that over 50% of the proliferating lymphocyte population in Group B (from the PBMC culture) in response to the PRRSV treatment, were not CD3⁺ T cells. Similarly, in the swIAV+PRRSV co-infected treated PBMCs, nearly 47% of the proliferating lymphocyte population was not CD3⁺, as indicated in Table 6.5. On the other hand, in the swIAV treated PBMCs less than 20% of the proliferating population was not CD3⁺. These results, although not as statistically significant as those in the PBMC cell culture, were reflected in the MoMΦ-T cell and MoDC-T cell co-cultures (Table 6.5).

A



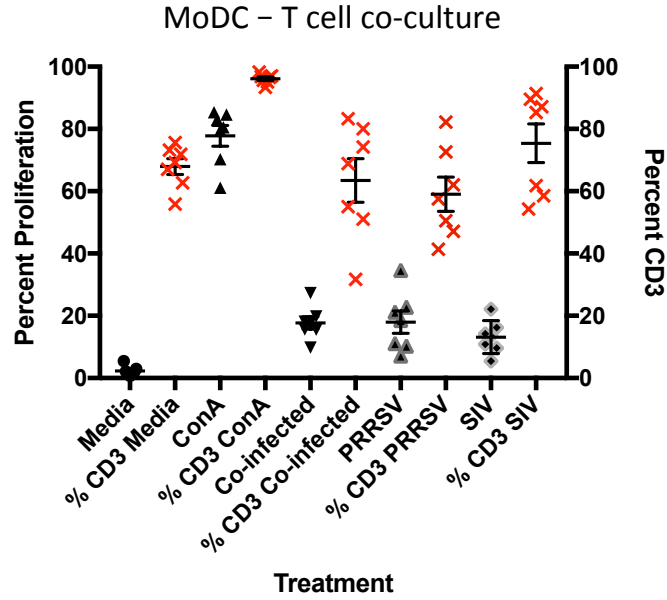
Holm-Sidak's multiple comparisons test	Mean Diff.	Significant?	Summary	Adjusted P Value
% CD3 ConA vs. % CD3 Co-infected	44.8	Yes	****	<0.0001
% CD3 PRRSV vs. % CD3 Co-infected	-4.388	No	ns	0.3912
% CD3 SIV vs. % CD3 Co-infected	25.91	Yes	****	<0.0001
% CD3 PRRSV vs. % CD3 ConA	-49.19	Yes	****	<0.0001
% CD3 SIV vs. % CD3 ConA	-18.89	Yes	**	0.0016
% CD3 SIV vs. % CD3 PRRSV	30.3	Yes	****	<0.0001

B



Holm-Sidak's multiple comparisons test	Mean Diff.	Significant?	Summary	Adjusted P Value
% CD3 ConA vs. % CD3 Co-infected	30.33	Yes	**	0.0022
% CD3 PRRSV vs. % CD3 Co-infected	-7.05	No	ns	0.3633
% CD3 SIV vs. % CD3 Co-infected	13.58	No	ns	0.1646
% CD3 PRRSV vs. % CD3 ConA	-37.38	Yes	***	0.0002
% CD3 SIV vs. % CD3 ConA	-16.75	No	ns	0.1057
% CD3 SIV vs. % CD3 PRRSV	20.63	Yes	*	0.0453

C



	Mean Diff.	Significant?	Summary	Adjusted P Value
Holm-Sidak's multiple comparisons test				
% CD3 ConA vs. % CD3 Co-infected	32.66	Yes	**	0.0013
% CD3 PRRSV vs. % CD3 Co-infected	-4.4	No	ns	0.5709
% CD3 SIV vs. % CD3 Co-infected	11.97	No	ns	0.2450
% CD3 PRRSV vs. % CD3 ConA	-37.06	Yes	***	0.0004
% CD3 SIV vs. % CD3 ConA	-20.69	Yes	*	0.0490
% CD3 SIV vs. % CD3 PRRSV	16.37	No	ns	0.1233

Figure 6-12: The percentages of CD3⁺ T cells (right y-axis) that proliferated within the total lymphocyte population (left y-axis) of the PBMC (Figure 14A), MoMΦ-T cell co-culture (Figure 14B), and MoDC-T cell co-culture (Figure 14C), from Group B, in response to either media, ConA, Co-infected, PRRSV, or swIAV treatments. The percent proliferation of CD3⁺ T cells is represented as red “X”s while the percent proliferation of the entire lymphocyte population is represented as black triangles. The Shapiro-Wilk normality test confirmed Gaussian distribution and an ordinary one-way ANOVA of multiple comparisons was utilized to describe statistical significance. Data was acquired as single replicates (n=8). Values were reported with statistical significance as $P = 0.0453 = *$; $P < 0.0001 = ****$; ns = not significant.

Table 6.5: *The mean percentage of CD3⁺ lymphocytes that proliferated in response to the indicated administered treatments in the PBMC or APC-T cell co-culture assays from Group B animals.*

	PBMCs (CD3)	MoMΦs (CD3)	MoDCs (CD3)
ConA	98.5%	94.4%	96.1%
Co-infected	53.7%	64.1%	63.4%
PRRSV	49.3%	57.0%	59.0%
swIAV	79.6%	77.7%	75.4%

6.4 Discussion:

The adaptive immune response to PRRSV can be characterized by the early appearance of non-neutralizing antibodies (within a week), a delayed appearance of IFN- γ secreting cells in PBMCs (2 weeks), which is likely associated with a delayed induction of T cell immunity, and a delayed appearance of neutralizing antibodies (3-4 weeks) (Loving et al., 2015). The resolution of an infection is attributable to both IFN- γ secreting cells and the induction of neutralizing antibodies, although PRRSV persists in the tonsils of pigs for up to a year. As of late, the T cell response to PRRSV has garnered more attention, with studies indicating T cell epitope cross-reactivity amongst strains, and it seems to be generally accepted that the T cell response is being geared towards Th1 type immunity (Correas et al., 2017; Rahe and Murtaugh, 2017). But, there has not yet been an explanation for the delayed induction of T cell immunity. A potential explanation for the delayed induction of T cell immunity has been proposed to be associated with the induction of PRRSV specific regulatory T cells (Silva-Campa et al., 2009; Wongyanin et al., 2012; Wongyanin et al., 2010), but this is under debate (Rodriguez-Gomez et al., 2015). In addition to atrophy and apoptosis in observed in peripheral lymphoid organs, and the thymus, of PRRSV infected animals, another potential explanation for the delayed induction of T cell immunity could be associated with the manipulation of antigen processing and presentation in the target cells of PRRSV infection, CD163⁺ myeloid derived APCs (Calvert et al., 2007) (Gomez-Laguna et al., 2013b). Therefore, we chose to investigate the induction of T cell immunity over the course of an infection to PRRSV, comparing the immune response to animals immunized with a commercially distributed swine-influenza A vaccine (FluSure XP), in addition to comparing the

immunostimulatory capacity of MoDCs and MoMΦs to induce the proliferation of specific T cell subsets in response to PRRSV infection or swIAV (H1N1) stimulation.

Humoral response and IFN- γ secreting cells:

To confirm the immunization with FluSure XP and the infection with PRRSV of the animals, we first tested for antibodies in the serum of the animals. As expected, PRRSV antibodies were detectable 9 days post challenge and increased over the course of the trial (Figure 6-2a). The antibody response to swIAV immunization was apparent throughout the course of the trial. Of note, in order to increase the level of T lymphocyte proliferation to swIAV, animals received a booster (double dose) of the FluSure vaccine 21 days post-PRRSV infection. On day 32 post-PRRSV infection the levels of antibodies against swIAV increased drastically (Figure 6-2b). Additionally, it's possible that PRRSV infection may have an effect on the antibody response to swIAV, as the antibody titres in Group A to swIAV are slightly higher than in Group B, although these differences were not found to be statistically significant. Lastly, Group A may have been exposed to PRRSV later during the trial, as antibody titres to PRRSV became detectable 32 days post-PRRSV infection. In addition to serum ELISAs to measure antibody secretion, we utilized IFN- γ ELISpots to detect IFN- γ secreting cells in PBMCs. Our results indicate that IFN- γ secreting cells to PRRSV are detectable 14 days post infection and the amount of IFN- γ secreting cells in PBMCs increased at 28 days post-PRRSV infection (Figure 6-3). The detection of IFN- γ secreting cells to PRRSV 2 weeks post infection reflects results from a recent study (Correas et al., 2017). Although IFN- γ secretion to swIAV was detectable over the course of the trial, the amount of IFN- γ secreting cells was not as prominent as that PRRSV. The lower IFN- γ response to the swIAV immunization could be an efficacy issue associated the vaccine formulation, being attributable to a weak T cell stimulation. It doesn't seem that PRRSV infection influenced the level of IFN- γ secretion to swIAV in the immunized animals (Group A vs Group B, Figure 6-3). Similarly, the swIAV immunization did not have an effect on the IFN- γ response to PRRSV (Group B vs Group C, Figure 6-3). Overall, based on these results, the T cell response to PRRSV is functional and there may be a slight delay in the induction of T cell immunity.

Lymphocyte and CD3⁺ T cells:

We first measured the overall levels of lymphocyte proliferation in response to either swIAV, PRRSV, or a combination of both PRRSV and swIAV within PBMCs or MoMΦs or MoDCs co-cultured with an enriched population of T cells. During the first week of infection, we were unable to detect any T cell or lymphocyte proliferation in PBMCs in response to any of the viral treatments administered to the cell cultures (Figure 6-4). As a result, we decided to increase the MOI of swIAV from 1.0 to 10.0 in the PBMC cell cultures, and in the APC treatments prior to co-culturing with the enriched T cells. As Figure 6-5a demonstrates, we were able to induce lymphocyte proliferation in response to the swIAV, PRRSV, and co-infection treatments in the lymphoproliferation assay cell cultures during the second week of PRRSV infection. Overall, there wasn't a noteworthy difference in the level of lymphocyte proliferation between the MoMΦ-T cell or MoDC-T cell co-cultures. The highest percentage of lymphocyte proliferation was recorded in the PBMC cell culture, while the MoDC-T cell co-culture had the lowest percentage of lymphocyte proliferation (Figure 6-5a, Supplementary Table 6.6). These results were reflected later in the animal trial, as the percentage of lymphocyte proliferation to PRRSV was higher in the PBMCs than in the APC-T cell co-cultures, with an overall increase as the trial continued (Figure 6-5a vs 6-5b). A recent study indicates that plasmacytoid DCs (pDCs) may have a role in up-regulating the expression of co-stimulatory molecules on DC subsets, including MoDCs (in response to TLR-7 and TLR-9 stimulation) (Auray et al., 2016). This could potentially explain the higher level of lymphocyte proliferation in our PBMC proliferation cultures in comparison to the APC-T cell co-cultures. The percentage of CD3⁺ T cell proliferation, in response to the viral treatments, reflects the proliferation profiles recorded in the previous total lymphocyte proliferation figures (Figures 6-6a and 6-6b). During the earlier time point of the animal trial, we observed lymphocyte and T cell proliferation in response to the media alone treatments in Groups B and C in the APC-T cell co-cultures, but not in the PBMCs. During the later time point of the animal trial, we did not record any proliferation in the media alone treatments in the APC-T cell co-cultures (Figure 6-6b).

Monocytes are potentially infected *in vivo*:

To address the lymphocyte proliferation in the APC-T cell co-culture assays, in Groups B and C, in the media alone treatments, we hypothesize that the animals were viremic during the first few weeks of infection. If that were the case, a portion of monocytes that we isolated from whole blood of the PRRSV infected pigs may have been infected with PRRSV. As a result, while the monocytes were differentiating into MoMΦs or MoDCs, PRRSV would have been replicating within the cell cultures. This could have had an impact on the differentiation of monocytes into MoDCs and MoMΦs during the viremic stage of infection. In order to confirm whether or not monocytes are infected *in vivo*, future experiments are needed. A recent study indicates that the monocyte population in the peripheral blood of pigs infected with PRRSV decreases, potentially indicating the susceptibility of monocytes to infection (Ferrari et al., 2018). Based on our results, it is possible that monocytes are infected by PRRSV, lending an explanation to the proficiency by which PRRSV is able to migrate to peripheral lymphoid organs and to the uterus.

Naïve and activated CD4 α^+ Th cells:

The purpose of the trial was to compare the immunostimulatory capacity of MoMΦs and MoDCs. In particular, we aimed to determine whether MoMΦs or MoDCs preferentially induced the proliferation of specific T lymphocyte subsets. The profiles of proliferation amongst the subsets reflect those results from the CD3 $^+$ T cell proliferation assays. We detected naïve Th cell proliferation mostly in the PBMC cell cultures, but it's likely that these cells had a low/dim expression of CD8 α and could have been transitioning towards an “activated” state, as we would not anticipate observing antigen specific proliferation within a naïve population of T cells (Figures 6-7a and 6-7b). The percentages of CD4 α^+ CD8 α^+ activated Th cell proliferation reflected previous results. Essentially, the PBMCs had a higher percentage of proliferation than the APC-T cell co-cultures and the amounts of Th cell proliferation increased over the course of the trial. The highest level of proliferation to PRRSV was observed in the Group C lymphocyte proliferation assays. And the highest level of activated Th cell proliferation to swIAV was observed in Group B from all three of the lymphocyte proliferation assays. Lastly, the MoDC-T cell co-

cultures had higher levels of activated Th cell proliferation in response to both PRRSV and swIAV treatments than in the MoMΦ-T cell co-cultures. This may be attributable to MoDCs presenting a greater diversity of MHCII associate peptide sequences to T cells than MoMΦ as a result of the lower pH and higher protease activity in the endosomes of macrophages during antigen processing (Blum et al., 2013; Delamarre et al., 2005). This could explain the higher capacity of MoDCs to stimulate CD4⁺ Th cell proliferation. When comparing the level of Th cell proliferation to swIAV in Group A vs Group B (Figure 6-8), the level of Th cell proliferation was higher in the animals infected with PRRSV. Furthermore, we saw similar results in the gamma delta T cells (Figure 6-9b), in the central memory Th cells (6-11b) and the effector Th cells (6-12b). It's possible that the PRRSV infection could be “training” monocytes to acquire an M1 phenotype (Bordon, 2014; Saeed et al., 2014).

CD4⁻ CD8⁺ T cells (CTL) response:

The induction of CTL mediated immunity to a virus is highly important towards overcoming an infection (Elemans et al., 2014). Overall, the CTL proliferation profiles follow a similar trend as the other T cell subsets, in that CTL proliferation was recorded as early as 14 days post infection in the cell culture assays and continued to increase as the trial progressed (Figures 6-9a and 6-9b). The highest levels of CTL proliferation were observed in the PBMC cell cultures, and Group C had the highest mean percent CTL proliferation to PRRSV treatment, while Group B had the highest mean percent CTL proliferation to swIAV treatment. Upon further analysis, the differences between the treatments within the MoDC and MoMΦ- T cell co-cultures were not shown to be statistically significant. Overall, the induction of CTL proliferation seems to indicate that immunity to the PRRSV and the FluSure immunization are being directed towards a Th1 type immune response.

Central memory CD4⁺ Th cells and effector CD4⁺ Th cells:

Central memory Th cells (CD4⁺ CD8⁺ CD27⁺) were detectable 14 days post PRRSV challenge in PBMCs, and in the APC-T cell co-cultures on days 17 and 20 (Figure 6-11a). This was somewhat surprising, as we did not anticipate seeing central memory Th

cells until later during the infection (MacLeod et al., 2010; Pepper and Jenkins, 2011b). But, these results are relatively similar to those obtained in a recent study in which memory Th cells began to increase 17 days post infection (Ferrari et al., 2018). The highest level of central memory Th cell proliferation in response to PRRSV was recorded in Group C from the cell culture assays. Furthermore, the highest of level central memory Th cell proliferation to PRRSV was in the PBMC cell culture assay. In addition, higher levels of central memory Th cell proliferation were observed in the MoDC-T cell co-culture assays compared to the MoMΦ-T cell co-cultures (Supplementary Table 6.12). These results indicate that MoDCs may possess a higher capacity to stimulate central memory Th cell proliferation than MoMΦs. This was also reflected in the proliferation profiles of the swIAV treatments, in which the highest level of central memory Th cell proliferation was again recorded in Group B for the cell culture assays (Supplementary Table 6.12). Statistically significant results indicating that MoDCs possessed a higher capacity than MoMΦs to stimulate central memory Th cell proliferation was found in Group C, in response to the PRRSV treatment (Supplementary Figure 6-33). The mean percent proliferation profiles of the effector Th cell responses to PRRSV and swIAV were very similar to that observed for the central memory Th cell proliferation profiles. The highest level of effector Th cell proliferation to PRRSV was recorded in the PBMC cultures, followed by the MoDC-T cell co-culture, and then the MoMΦ-T cell co-culture, all in Group C. And the highest proliferations in the effector Th cell population to swIAV were recorded in Groups B, with the MoDC-T cell co-cultures having higher levels of proliferation than both the PBMC and MoMΦ-T cell cultures (Supplementary Table 6.13), although this was not found to be statistically significant.

Comparing the mean percentage of lymphocyte proliferation amongst the T cell subsets, it becomes apparent that MoDCs may be more potent inducers of central memory Th cells. It's plausible that this difference in immunostimulatory preference between MoDCs and MoMΦs highlights their attributes. Dendritic cells are often considered the professional APCs of the immune system, for many reasons including migration to the lymph node for antigen presentation to naïve T cells, and having a more diverse repertoire of peptide sequences than macrophages. In this case, DCs could play a crucial role in the induction of CD4 α^+ Th cells, aiding in the progression of the entire T cell

immune response and directly influencing the humoral immune response (Luckheeram et al., 2012b); (Swain, McKinstry, & Strutt, 2012a). In comparison, macrophages are often considered to be the sentinels of the immune system, being involved in the maintenance of homeostasis and tissue regeneration under non-pathogenic conditions, or playing significant roles in search and destroy phagocytosis when encountering a pathogen (Mills and Ley, 2014) (Varol et al., 2015). In the case of PRRSV, the induction of CTLs would be critical in overcoming an infectious state (Barry and Bleackley, 2002). The evidence thus far implies that the T cell response is being geared towards Th1 type immunity. To further support this, we assayed cell culture supernatants after the 4th day in culture for various cytokines.

Cytokine response:

We assayed for cytokine expression after 4 days and for the most part we were unable to detect cytokines in the majority of the supernatants from the cell cultures, reflecting results obtained previously (Reutner et al., 2013). Taking into consideration a viral infection and Th1 type immunity, we were particularly interested in type 1-interferons (IFN- α , IFN- β), IL-12, and IFN- γ . Our results indicate that both swIAV and to a lesser extent PRRSV stimulated IFN- α secretion (Supplementary Figures 6-19 and 6-20), although IFN- α was detected in some of the media alone treatments as well. More importantly, IFN- γ was detected in the cell cultures in response to swIAV, PRRSV, and the co-infection treatments. There wasn't a notable difference amongst the treatments or the groups (Supplementary Figures 6-21 and 6-22). Lastly, there was an inconsistency in the detection of IL-12, IL-10, IL-13, and IL-17 α amongst the various treatments and the different groups making it difficult to form any definitive conclusions regarding the aforementioned cytokines expressions (Supplementary Figures 6-23 to 6-29). Overall, the detection of IFN- γ in the cell culture supernatants in response to both swIAV and PRRSV, in addition to the induced CTL proliferation, we feel that a protective immune response to PRRSV is associated with Th1 type immunity.

Unidentified lymphocyte population:

Lastly, we noticed that the percentages of T cells within the total population of proliferating lymphocytes differed, depending on the treatment administered. Specifically, there was an unidentified population of lymphocytes that proliferated in response to the PRRSV treatment in all three of the cell culture assays, being most pronounced in the PBMC population (Figure 6-14). Furthermore, this was not the case in the ConA stimulated positive control treatment and to a much lesser extent in the swIAV treated lymphocyte proliferative cell culture assays. Today there is no anti-pig anti-CD19 antibody available, as such we could only enrich the T cell population for our co-culture assays by depleting B cells that express CD21. Thus, we hypothesize that the unidentified lymphocyte population are CD19⁺ B cells in the APC-T cell co-cultures, and a mix of CD21⁺ and CD19⁺ B cells in the PBMC cell cultures. There is a robust non-NA response seen early during infection with PRRSV (within 3 days antibodies are detectable), and this may be attributable to hypergammaglobulinemia. It has been shown that the amount of immunoglobulin present in bronchoalveolar lavages (BAL) during a PRRSV infection was increased more than 10 fold in comparison to pigs infected with swIAV and porcine circovirus-2 (PCV-2). The study showed that the majority of the B cells, during the viremic stage of a PRRSV infection, express different isotypes (IgM, IgG, IgA) but nearly identical sequences in their 3rd complementarity-determining region (HCDR3) of the antibody heavy chain. In other words, the authors showed that the non-NA response to PRRSV originated from similar B cell clones that had not undergone somatic hypermutation (Schroeder et al., 1998). If this is the case, it supports our hypothesis as to the portion of the lymphocytes proliferating in response to PRRSV in the PBMC cultures (Figure 6-14) being B cells. Further experiments are needed to identify the proliferating population of unidentified cells.

6.5 Conclusion:

In conclusion, there does not seem to be an overly remarkable difference between the immunostimulatory capacity of MoMΦs and MoDCs to induce CD3⁺ T cell proliferation. That being stated, our results indicate that MoDCs may be more potent stimulators of

central memory Th cell proliferation in response to both PRRSV. A major question in PRRSV immunology, considering the delayed induction of T cell immunity and skewed humoral response, has been what effect PRRSV has on the antigen-presenting/processing capability of APCs. Our results indicate that even though MoMΦs and MoDCs are being infected by PRRSV, they are able to present antigen to induce a robust T cell response. This response was markedly stronger than that to the swIAV treatment, which was administered at 10x the dose in comparison to PRRSV. And lastly, we have shown that it is plausible that PRRSV infects monocytes *in vivo* providing some clarity regarding the pathogenesis of the virus. Furthermore, the lymphoproliferative T cell response to swIAV in the animals infected with PRRSV was consistently stronger than the response to swIAV in the animals not exposed to PRRSV, hinting that PRRSV infection increased the immunostimulatory capacity of the monocyte population within those PRRSV infected animals. Our results indicate that there might be a slight delay in the induction of T cell immunity to PRRSV. Reasons for the delay could be attributable to PRRSV interfering with antigen processing/presentation in DCs or MΦs, atrophy and apoptosis of lymphoid populations in the lymph nodes, the induction of PRRSV specific Tregs, or potentially a combination of the three explanations. A recent study indicated that PRRSV specific Tregs are most prominent in peripheral lymphoid organs and tissue surrounding the lung (Nedumpun et al., 2018). Based on our results, CTLs and effector T cells are induced 14 days post-PRRSV infection. It's plausible that these tissue specific Tregs could suppress T cell function at sites of infection, and once the T cell response breaches a threshold, the CTLs and effector T cells would be able to overcome the immune suppression by the Tregs. Overall we can conclude that the T cell immune response to PRRSV is functional, it is even more robust than the T cell response to the FluSure XP immunization, and it is being geared towards Th1 type immunity.

6.6 Supplementary Figures:

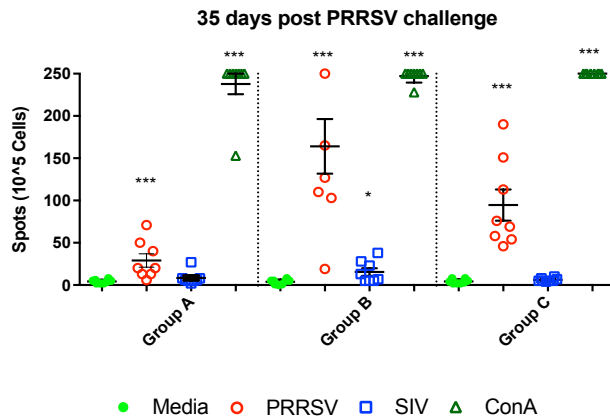


Figure 6-13: Figure representing the peripheral blood mononuclear cell (PBMC) interferon-gamma ELISPOTs from the different treatment groups in the fifth week of PRRSV infection. Briefly, 5.0×10^5 PBMCs were isolated on the respective dates listed. Cells were treated with PRRSV (MOI 1.0) or swIAV (MOI 10.0) and the IFN- γ ELISpot plates were developed 20 hours post treatment. Statistical significance was determined by comparing the swIAV or PRRSV treated samples to the negative control (non-stimulated cells). Values were reported with statistical significance if $P < 0.05 = *$; $P < 0.005 = **$; $P < 0.0005 = ***$.

Table 6.6: Mean percentage of lymphocyte proliferation in the indicated treatments, groups, cell cultures, on specific days post infection (DPI).

PBMCs	14 DPI				24 DPI			
	Media	Co-infected	PRRSV	SIV	Media	Co-infected	PRRSV	SIV
Group A	1.40	7.78	3.11	5.33	6.54	19.88	12.76	16.00
Group B	1.31	17.74	20.76	5.30	3.64	28.11	42.40	13.79
Group C	2.80	19.34	27.44	1.83	3.63	28.94	44.30	3.35

Macrophages	17 DPI				27 DPI			
	Media	Co-infected	PRRSV	SIV	Media	Co-infected	PRRSV	SIV
Group A	5.81	13.07	5.99	12.37	3.69	5.56	1.59	7.28
Group B	20.19	24.16	26.50	16.83	9.12	22.80	23.60	16.60
Group C	23.54	25.78	26.09	14.95	11.37	9.99	20.31	2.05

MoDCs	20 DPI				30 DPI			
	Media	Co-infected	PRRSV	SIV	Media	Co-infected	PRRSV	SIV
Group A	2.39	4.54	2.17	4.11	2.16	11.08	5.12	10.48
Group B	7.89	17.13	13.35	11.91	2.27	17.68	17.95	13.15
Group C	8.63	16.71	11.88	9.35	5.20	11.66	23.90	9.27

Table 6.7: Mean percentage of CD3⁺ T cell proliferation in the indicated treatments, groups, cell cultures, on specific days post infection (DPI).

PBMCs	14 DPI				24 DPI			
	Media	Co-infected	PRRSV	SIV	Media	Co-infected	PRRSV	SIV
Group A	1.39	7.58	3.00	5.51	2.66	15.40	9.08	12.46
Group B	0.83	13.38	14.21	4.83	1.90	15.68	24.63	11.27
Group C	2.58	14.92	20.16	1.63	1.61	16.84	27.23	1.26

Macrophages	17 DPI				27 DPI			
	Media	Co-infected	PRRSV	SIV	Media	Co-infected	PRRSV	SIV
Group A	4.10	11.30	4.19	10.72	3.09	5.05	1.14	6.95
Group B	13.22	14.34	13.99	10.88	7.32	16.28	15.36	13.76
Group C	15.65	15.76	15.20	8.89	10.35	6.43	14.79	1.44

MoDCs	20 DPI				30 DPI			
	Media	Co-infected	PRRSV	SIV	Media	Co-infected	PRRSV	SIV
Group A	1.69	3.44	1.56	3.33	0.92	7.66	2.42	7.32
Group B	7.30	15.62	12.14	10.69	1.02	11.57	10.02	9.88
Group C	8.10	15.62	11.09	8.75	4.06	7.18	12.73	5.72

Table 6.8: Mean percentage of naïve (CD3⁺ CD4⁺ CD8⁻) T cell proliferation in the indicated treatments, groups, cell cultures, on specific days post infection (DPI).

PBMCs	14 DPI				24 DPI			
	Media	Co-infected	PRRSV	SIV	Media	Co-infected	PRRSV	SIV
Group A	0.226	1.265	0.437	0.898	0.350	1.016	0.917	0.806
Group B	0.178	4.385	5.973	0.989	0.149	1.011	2.234	0.819
Group C	0.300	5.075	7.347	0.206	0.107	1.227	2.080	0.124

Macrophages	17 DPI				27 DPI			
	Media	Co-infected	PRRSV	SIV	Media	Co-infected	PRRSV	SIV
Group A	0.254	0.249	0.169	0.307	0.551	0.445	0.292	0.565
Group B	0.895	0.543	0.656	0.740	0.650	0.957	1.206	0.942
Group C	0.702	0.597	0.444	0.435	1.172	0.597	1.078	0.324

MoDCs	20 DPI				30 DPI			
	Media	Co-infected	PRRSV	SIV	Media	Co-infected	PRRSV	SIV
Group A	0.259	0.282	0.255	0.304	0.044	0.261	0.145	0.311
Group B	0.589	0.723	0.647	0.684	0.073	0.741	0.774	0.668
Group C	0.477	0.632	0.532	0.501	0.141	0.469	0.797	0.394

Table 6.9: Mean percentage of activated ($CD3^+ CD4^+ CD8^+$) T helper cell proliferation in the indicated treatments, groups, cell cultures, on specific days post infection (DPI).

PBMCs	14 DPI				24 DPI			
	Media	Co-infected	PRRSV	SIV	Media	Co-infected	PRRSV	SIV
Group A	0.010	0.171	0.081	0.130	0.079	2.570	0.997	1.746
Group B	0.007	0.871	1.022	0.096	0.075	3.052	5.417	1.948
Group C	0.015	1.124	1.755	0.020	0.064	3.561	6.720	0.138

Macrophages	17 DPI				27 DPI			
	Media	Co-infected	PRRSV	SIV	Media	Co-infected	PRRSV	SIV
Group A	0.516	1.178	0.315	1.208	0.534	0.897	0.210	1.135
Group B	3.405	3.231	3.737	1.824	1.144	3.355	2.848	2.360
Group C	4.488	3.819	3.754	2.017	2.384	1.456	3.116	0.250

MoDCs	20 DPI				30 DPI			
	Media	Co-infected	PRRSV	SIV	Media	Co-infected	PRRSV	SIV
Group A	0.129	0.388	0.139	0.394	0.142	2.341	0.613	2.274
Group B	0.838	1.800	1.356	1.422	0.235	4.670	3.138	3.598
Group C	0.947	1.857	1.301	1.192	1.550	2.893	4.947	2.492

Table 6.10: Mean percentage of cytotoxic lymphocyte ($CD3^+ CD4^- CD8^+$) proliferation in the indicated treatments, groups, cell cultures, on specific days post infection (DPI).

PBMCs	14 DPI				24 DPI			
	Media	Co-infected	PRRSV	SIV	Media	Co-infected	PRRSV	SIV
Group A	0.171	1.234	0.465	0.933	0.357	5.759	2.925	4.460
Group B	0.068	1.826	2.071	0.492	0.691	5.658	9.355	3.965
Group C	0.215	2.764	3.182	0.133	0.627	7.053	11.598	0.548

Macrophages	17 DPI				27 DPI			
	Media	Co-infected	PRRSV	SIV	Media	Co-infected	PRRSV	SIV
Group A	2.162	6.606	2.217	6.162	1.040	1.532	0.307	2.352
Group B	5.877	6.155	6.277	5.069	2.850	6.286	6.527	5.715
Group C	6.137	6.152	6.821	4.942	4.628	2.377	6.435	0.450

MoDCs	20 DPI				30 DPI			
	Media	Co-infected	PRRSV	SIV	Media	Co-infected	PRRSV	SIV
Group A	0.301	0.600	0.306	0.713	0.298	3.740	1.317	3.391
Group B	1.850	3.181	3.165	2.646	0.289	3.728	4.538	3.126
Group C	1.924	3.475	3.062	2.377	0.985	1.802	4.895	1.173

Table 6.11: Mean percentage of gamma delta T cell ($CD3^+ \gamma\delta^+$) proliferation in the indicated treatments, groups, cell cultures, on specific days post infection (DPI).

PBMCs	14 DPI				24 DPI			
	Media	Co-infected	PRRSV	SIV	Media	Co-infected	PRRSV	SIV
Group A	0.420	2.629	0.764	1.800	0.183	1.745	0.945	1.147
Group B	0.242	3.485	2.217	1.586	0.169	1.642	2.231	1.187
Group C	0.511	1.942	1.723	0.462	0.094	1.473	2.165	0.091

Macrophages	17 DPI				27 DPI			
	Media	Co-infected	PRRSV	SIV	Media	Co-infected	PRRSV	SIV
Group A	2.797	9.386	3.415	8.755	0.145	0.243	0.076	0.579
Group B	7.345	8.899	7.797	7.406	0.575	0.947	0.804	1.129
Group C	6.980	8.276	7.868	6.720	0.919	0.334	0.571	0.118

MoDCs	20 DPI				30 DPI			
	Media	Co-infected	PRRSV	SIV	Media	Co-infected	PRRSV	SIV
Group A	0.266	0.248	0.127	0.333	0.203	0.860	0.233	0.837
Group B	2.032	3.130	3.402	2.503	0.232	1.266	1.039	1.289
Group C	1.842	2.643	2.607	1.972	0.314	0.433	0.963	0.305

Table 6.12: Mean percentage of central memory T helper cell ($CD3^+ CD4\alpha^+ CD8\alpha^+ CD27^+$) proliferation in the indicated treatments, groups, cell cultures, on specific days post infection (DPI).

PBMCs	14 DPI				24 DPI			
	Media	Co-infected	PRRSV	SIV	Media	Co-infected	PRRSV	SIV
Group A	0.008	0.088	0.049	0.073	0.050	0.612	0.348	0.425
Group B	0.005	0.267	0.440	0.039	0.044	1.369	2.850	0.502
Group C	0.011	0.452	0.797	0.011	0.038	2.153	3.597	0.081

Macrophages	17 DPI				27 DPI			
	Media	Co-infected	PRRSV	SIV	Media	Co-infected	PRRSV	SIV
Group A	0.251	0.315	0.112	0.468	0.225	0.170	0.071	0.361
Group B	2.029	1.611	2.319	0.763	0.673	1.209	1.570	0.738
Group C	2.863	1.896	2.259	0.973	1.618	0.820	1.603	0.157

MoDCs	20 DPI				30 DPI			
	Media	Co-infected	PRRSV	SIV	Media	Co-infected	PRRSV	SIV
Group A	0.080	0.208	0.094	0.191	0.116	0.828	0.438	0.863
Group B	0.329	0.878	0.716	0.753	0.118	1.704	1.958	1.057
Group C	1.082	2.122	1.301	1.192	0.957	1.524	2.960	1.360

Table 6.13: Mean percentage of effector T helper cell ($CD3^+ CD4^+ CD8\alpha^+ CD27$) proliferation in the indicated treatments, groups, cell cultures, on specific days post infection (DPI).

PBMCs	14 DPI				24 DPI			
	Media	Co-infected	PRRSV	SIV	Media	Co-infected	PRRSV	SIV
Group A	0.002	0.082	0.033	0.058	0.029	1.957	0.649	1.322
Group B	0.003	0.604	0.582	0.057	0.031	1.684	2.568	1.446
Group C	0.004	0.673	0.958	0.010	0.026	1.407	3.123	0.057

Macrophages	17 DPI				27 DPI			
	Media	Co-infected	PRRSV	SIV	Media	Co-infected	PRRSV	SIV
Group A	0.285	0.839	0.212	0.740	0.309	0.727	0.139	0.774
Group B	1.198	1.730	1.414	1.024	0.487	2.190	1.164	1.687
Group C	1.518	1.791	1.416	1.159	0.870	0.653	1.410	0.096

MoDCs	20 DPI				30 DPI			
	Media	Co-infected	PRRSV	SIV	Media	Co-infected	PRRSV	SIV
Group A	0.048	0.235	0.045	0.203	0.026	1.513	0.175	1.411
Group B	0.509	1.053	0.640	0.669	0.117	2.966	1.180	2.541
Group C	0.452	0.896	0.546	0.554	0.593	1.369	1.987	1.132

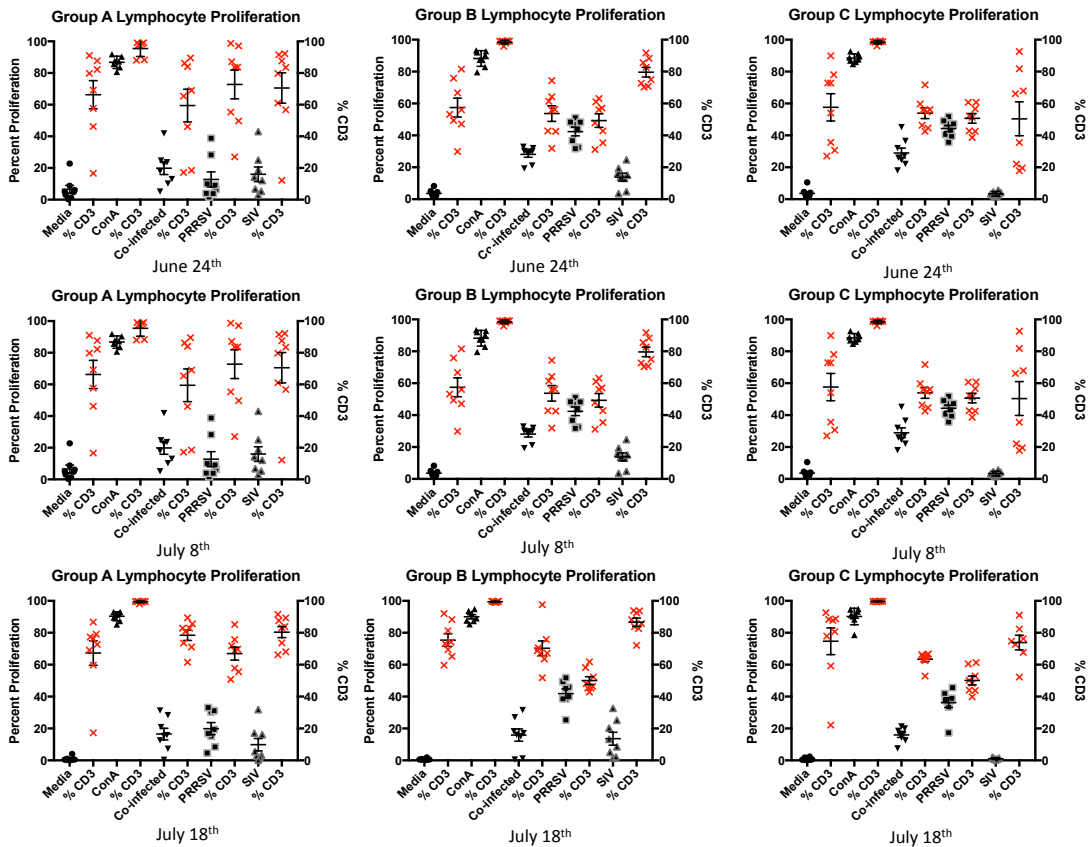


Figure 6-14: Figure indicating the percentage of $CD3^+$ T cells that proliferated within the total lymphocyte population of the PBMC cultures from all of the groups over the course of the trial.

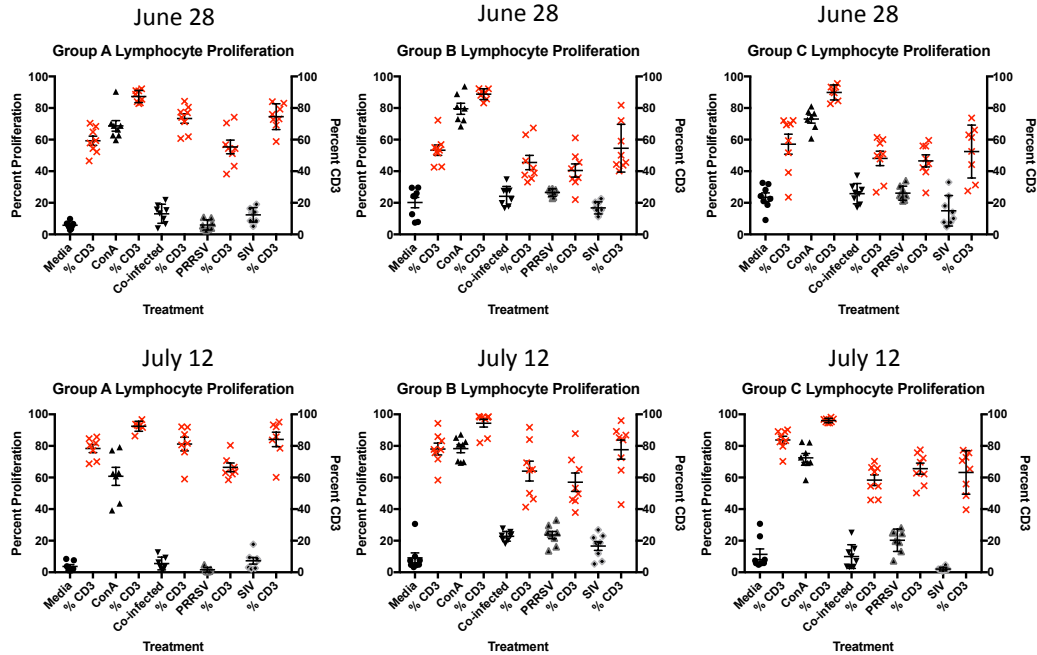


Figure 6-15: Figure indicating the percentage of CD3⁺ T cells that proliferated within the total lymphocyte population of the MoMΦ-T cell co-cultures from all of the groups over the course of the trial.

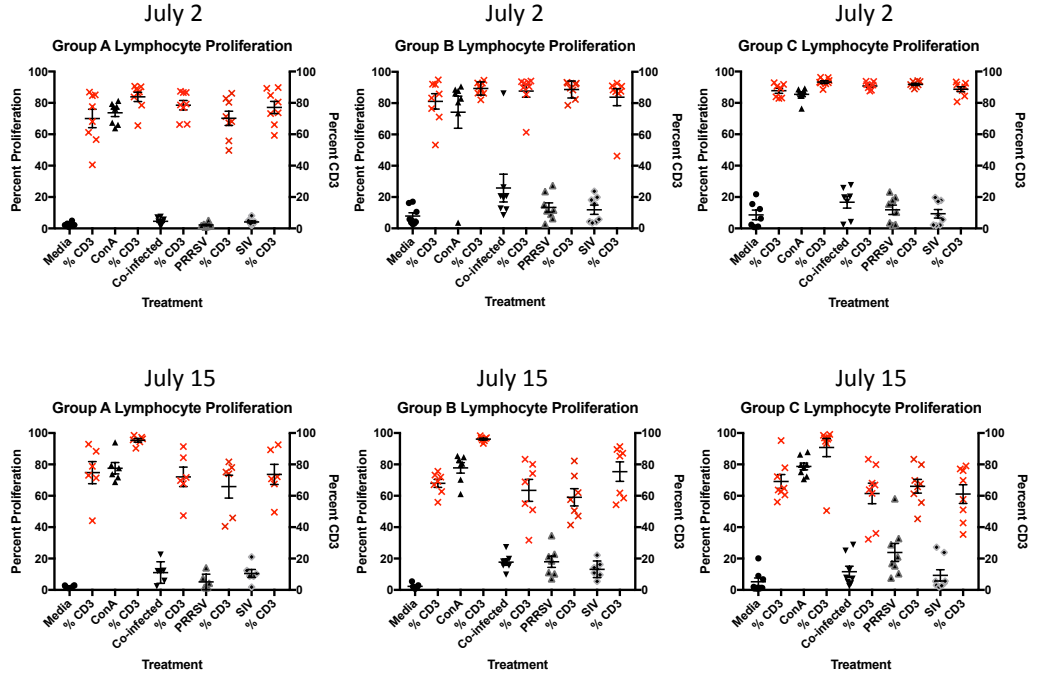


Figure 6-16: Figure indicating the percentage of CD3⁺ T cells that proliferated within the total lymphocyte population of the MoDC-T cell co-cultures from all of the groups over the course of the trial.

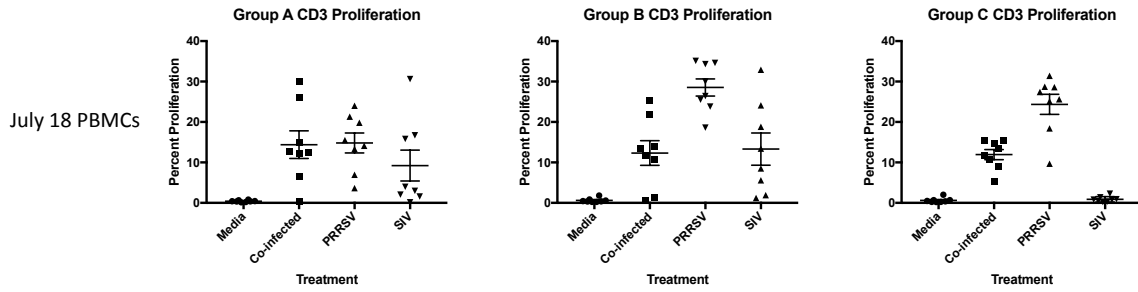


Figure 6-17: Figure indicating the level of CD3⁺ T cell proliferation from PBMC cultures in response to PRRSV (MOI 1.0), swIAV (MOI 10.0), or co-infected treatments from their respective groups during the fifth week of infection. After treatment, lymphocytes were left in culture for 4 days before measuring proliferation using flow cytometry. Statistical significance was determined by comparing the co-infected, swIAV, or PRRSV treated samples to the negative control (non-stimulated cells). Values were reported with statistical significance if $P < 0.05 = *$; $P < 0.005 = **$; $P < 0.0005 = ***$.

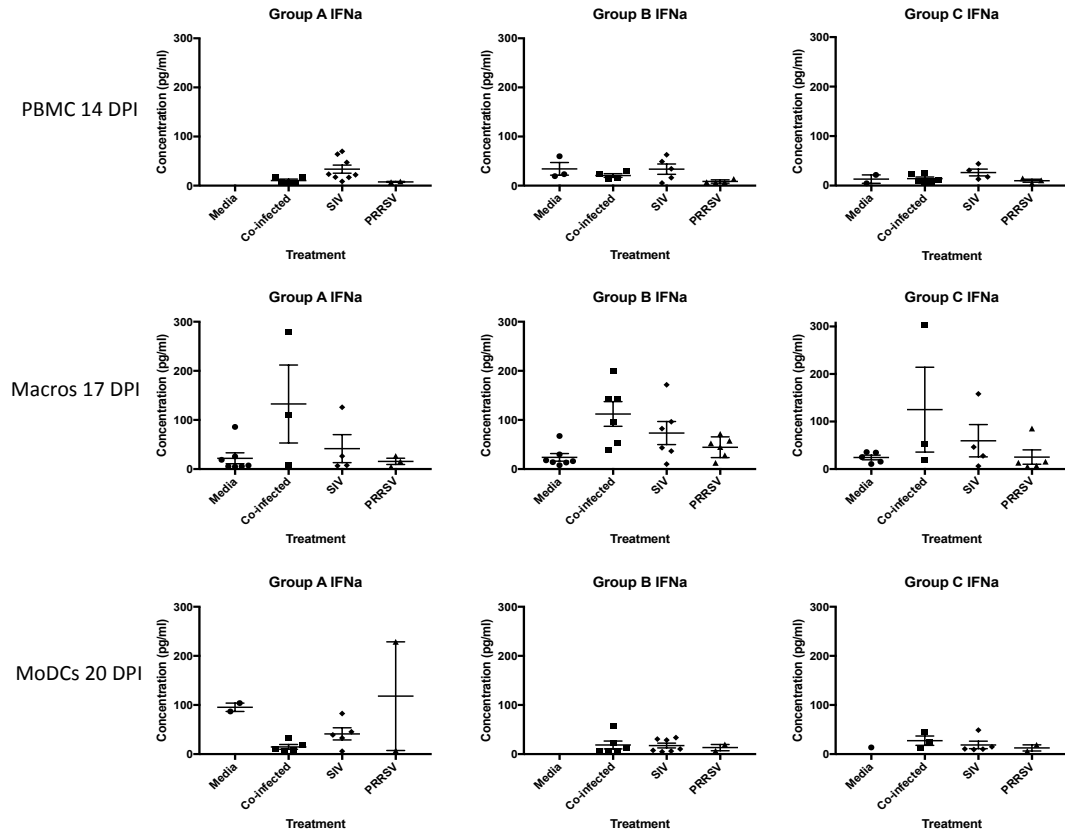


Figure 6-18: Representation of the FRIA cytokine ELISAs measuring IFN- α during the 2nd week post-PRRSV infection. Supernatants from the cell culture assays were removed after 4 days in culture to measure cytokine secretion in response to the administered treatments indicated in the graphs. Samples were analyzed in duplicate.

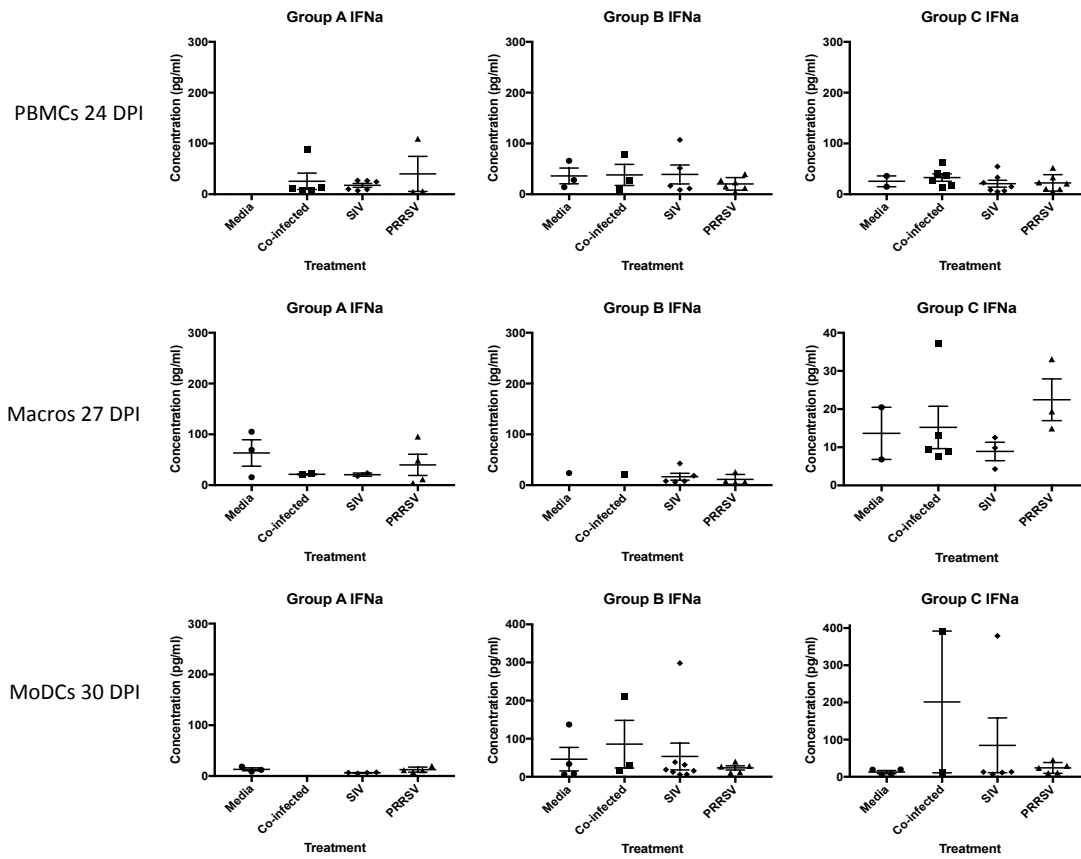


Figure 6-19: Representation of the FMIA cytokine ELISAs measuring IFN- α during the 3rd week post-PRRSV infection. Supernatants from the cell culture assays were removed after 4 days in culture to measure cytokine secretion in response to the administered treatments indicated in the graphs. Samples were analyzed in duplicate.

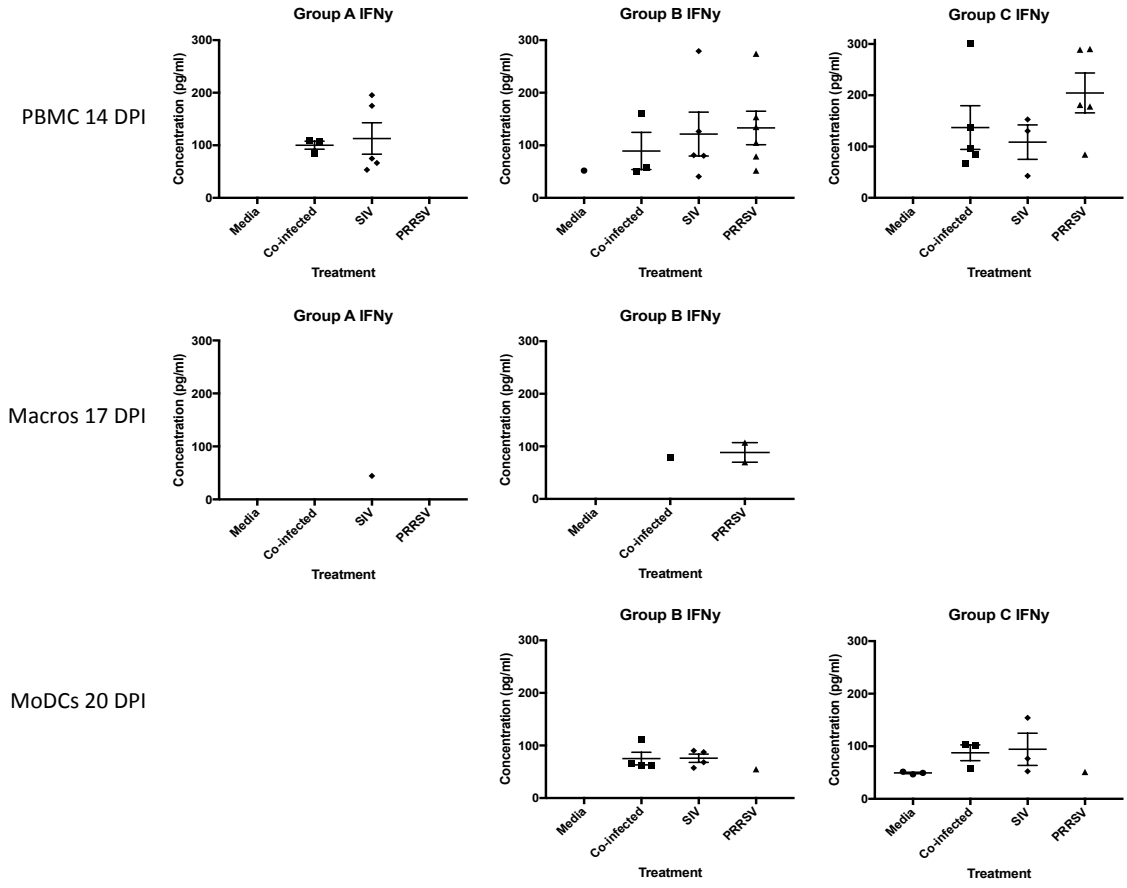


Figure 6-20: Representation of the FMIA cytokine ELISAs measuring IFN- γ during the 2nd week post-PRRSV infection. Supernatants from the cell culture assays were removed after 4 days in culture to measure cytokine secretion in response to the administered treatments indicated in the graphs. Samples were analyzed in duplicate.

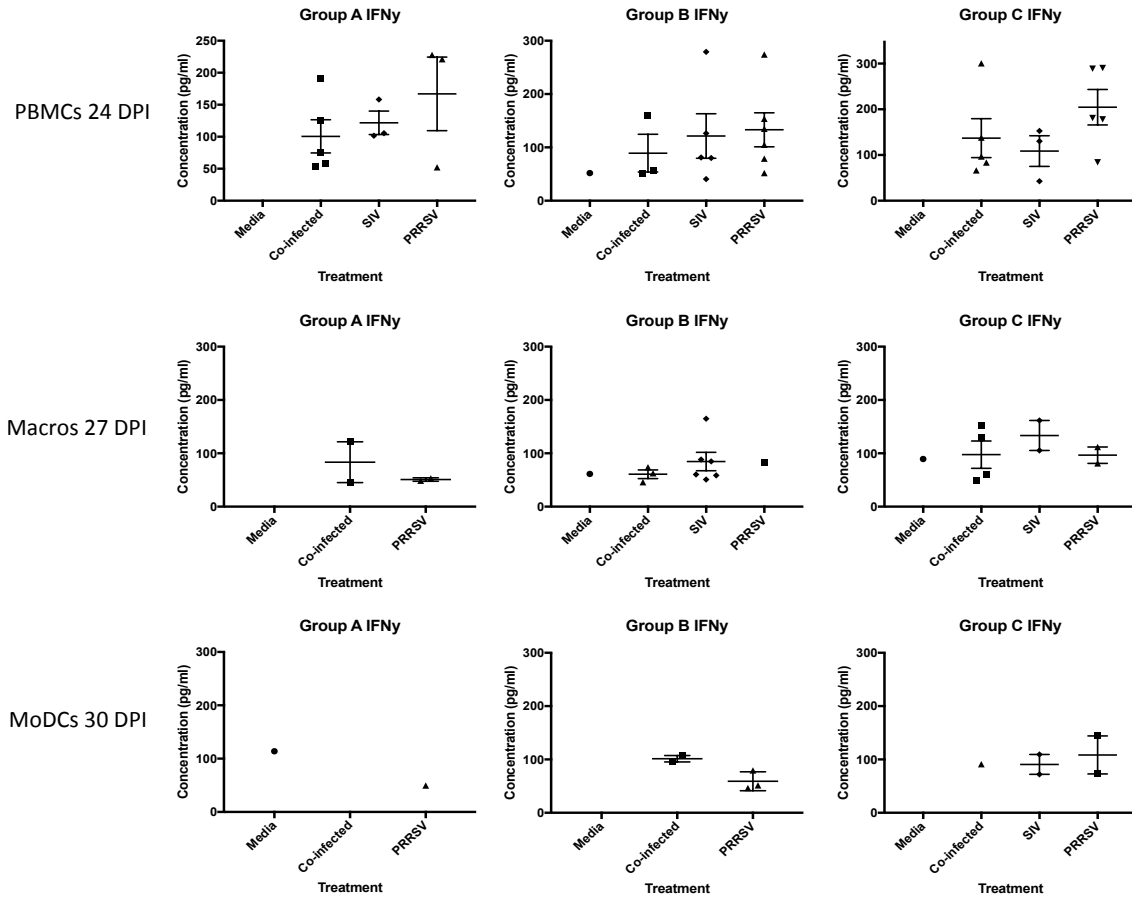


Figure 6-21: Representation of the FMIA cytokine ELISAs measuring IFN- γ during the 3rd week post-PRRSV infection. Supernatants from the cell culture assays were removed after 4 days in culture to measure cytokine secretion in response to the administered treatments indicated in the graphs. Samples were analyzed in duplicate.

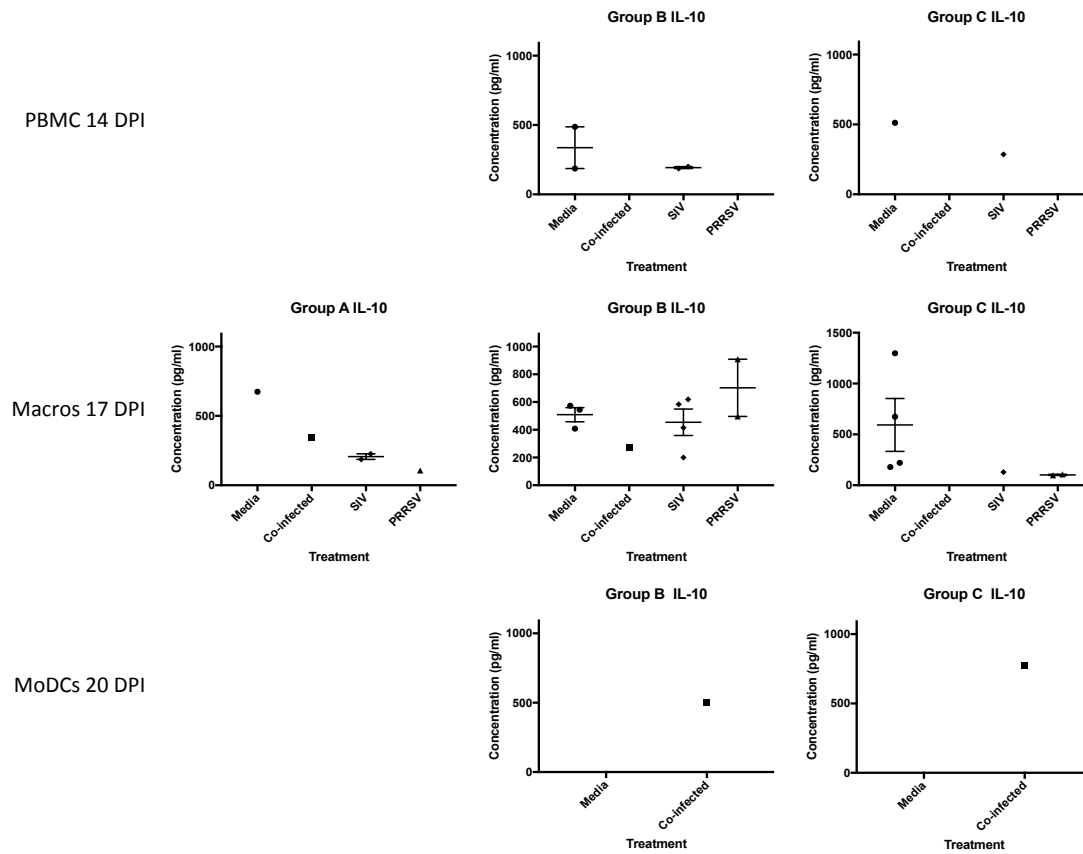


Figure 6-22: Representation of the FMIA cytokine ELISAs measuring IL-10 during the 2nd week post-PRRSV infection. Supernatants from the cell culture assays were removed after 4 days in culture to measure cytokine secretion in response to the administered treatments indicated in the graphs. Samples were analyzed in duplicate.

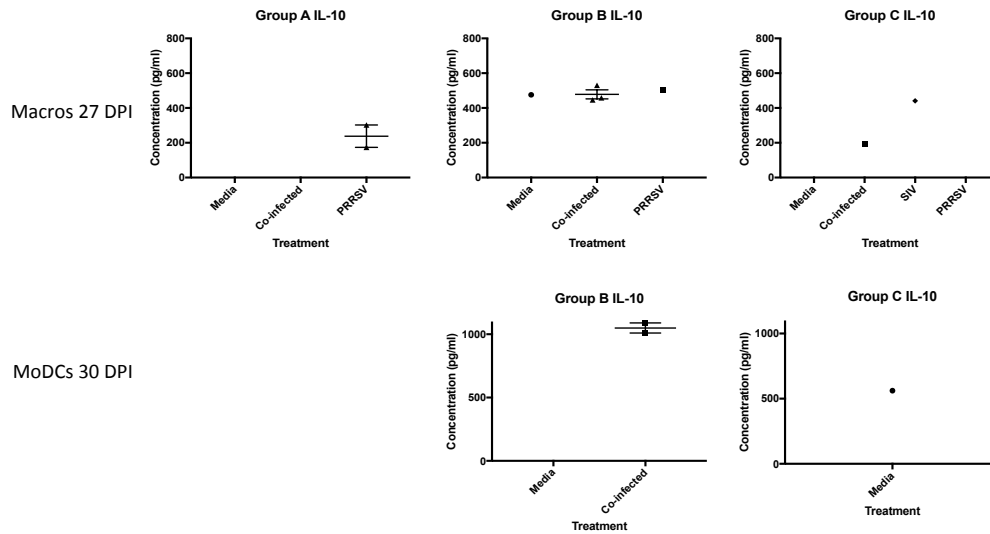


Figure 6-23: Representation of the FMIA cytokine ELISAs measuring IL-10 during the 3rd week post-PRRSV infection. Supernatants from the cell culture assays were removed after 4 days in culture to measure cytokine secretion in response to the administered treatments indicated in the graphs. Samples were analyzed in duplicate.

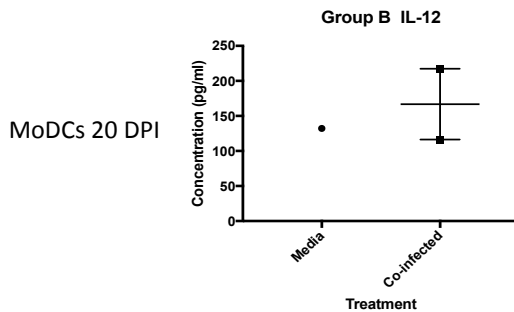


Figure 6-24: Representation of the FMIA cytokine ELISAs measuring IL-12 during the 2nd week post-PRRSV infection. Supernatants from the cell culture assays were removed after 4 days in culture to measure cytokine secretion in response to the administered treatments indicated in the graphs. Samples were analyzed in duplicate.

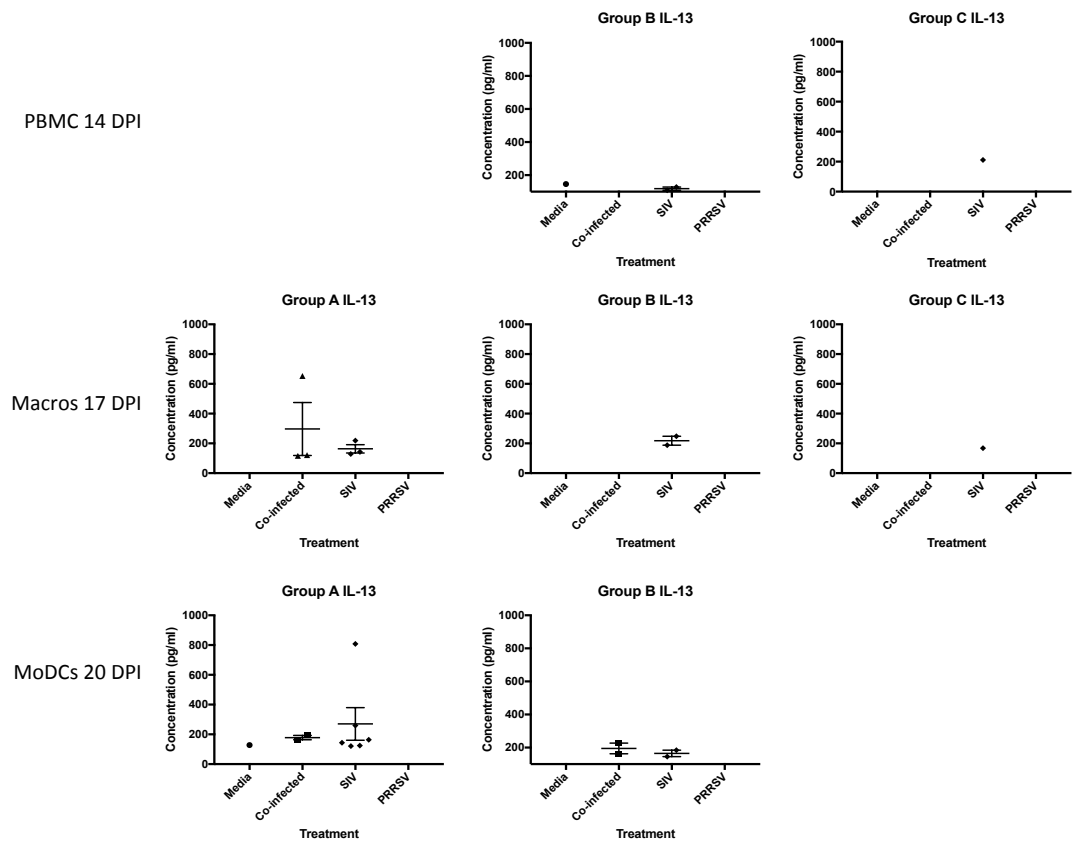


Figure 6-25: Representation of the FMIA cytokine ELISAs measuring IL-13 during the 2nd week post-PRRSV infection. Supernatants from the cell culture assays were removed after 4 days in culture to measure cytokine secretion in response to the administered treatments indicated in the graphs. Samples were analyzed in duplicate.

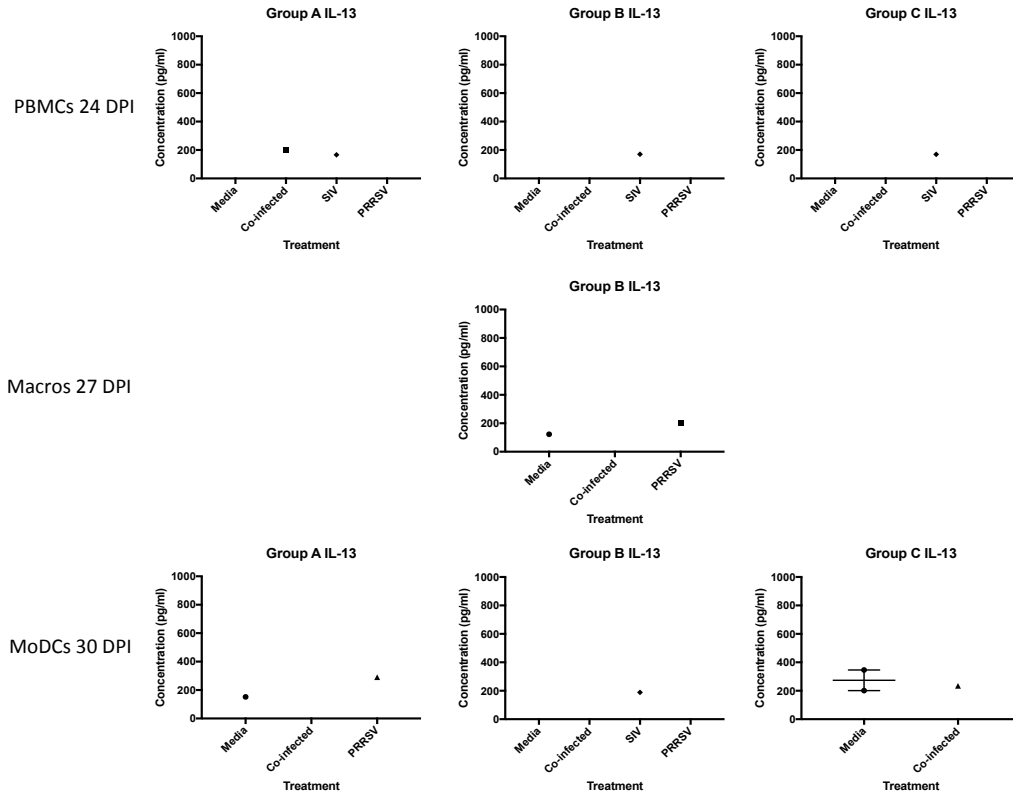


Figure 6-26: Representation of the FMIA cytokine ELISAs measuring IL-13 during the 3rd week post-PRRSV infection. Supernatants from the cell culture assays were removed after 4 days in culture to measure cytokine secretion in response to the administered treatments indicated in the graphs. Samples were analyzed in duplicate.

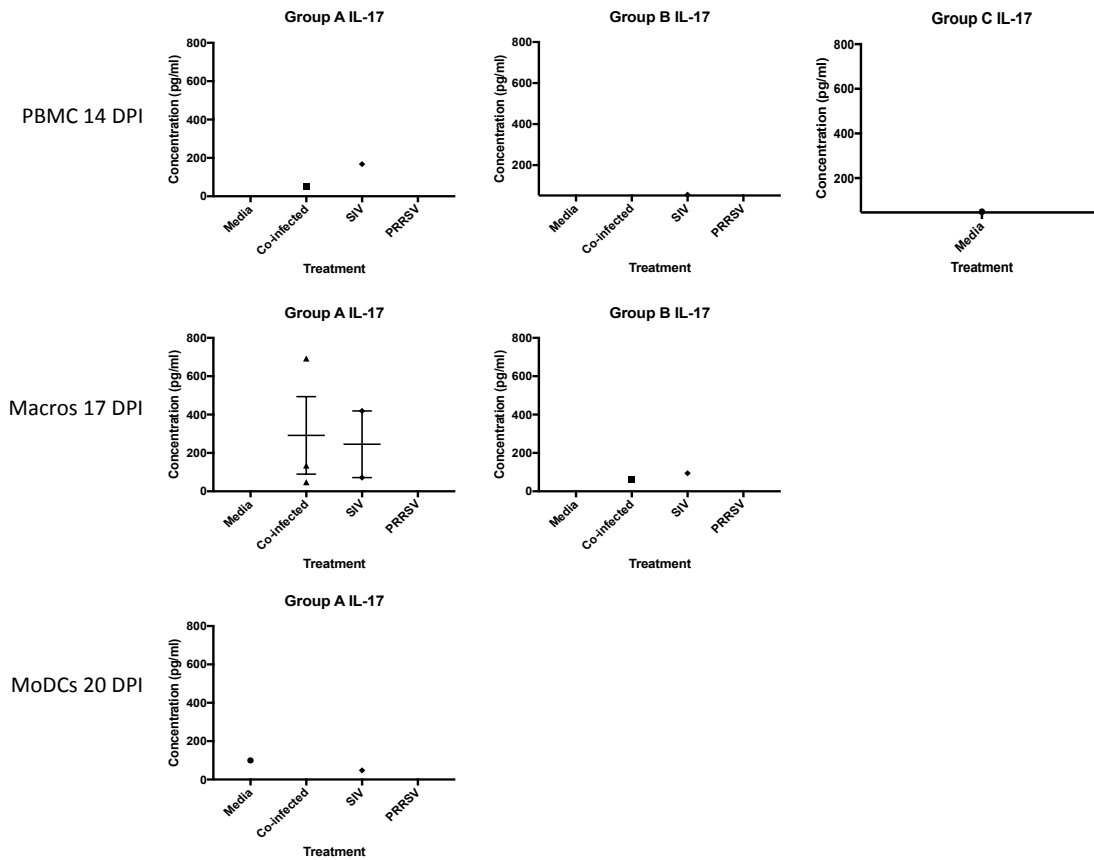


Figure 6-27: Representation of the FMIA cytokine ELISAs measuring IL-17 α during the 2nd week post-PRRSV infection. Supernatants from the cell culture assays were removed after 4 days in culture to measure cytokine secretion in response to the administered treatments indicated in the graphs. Samples were analyzed in duplicate.

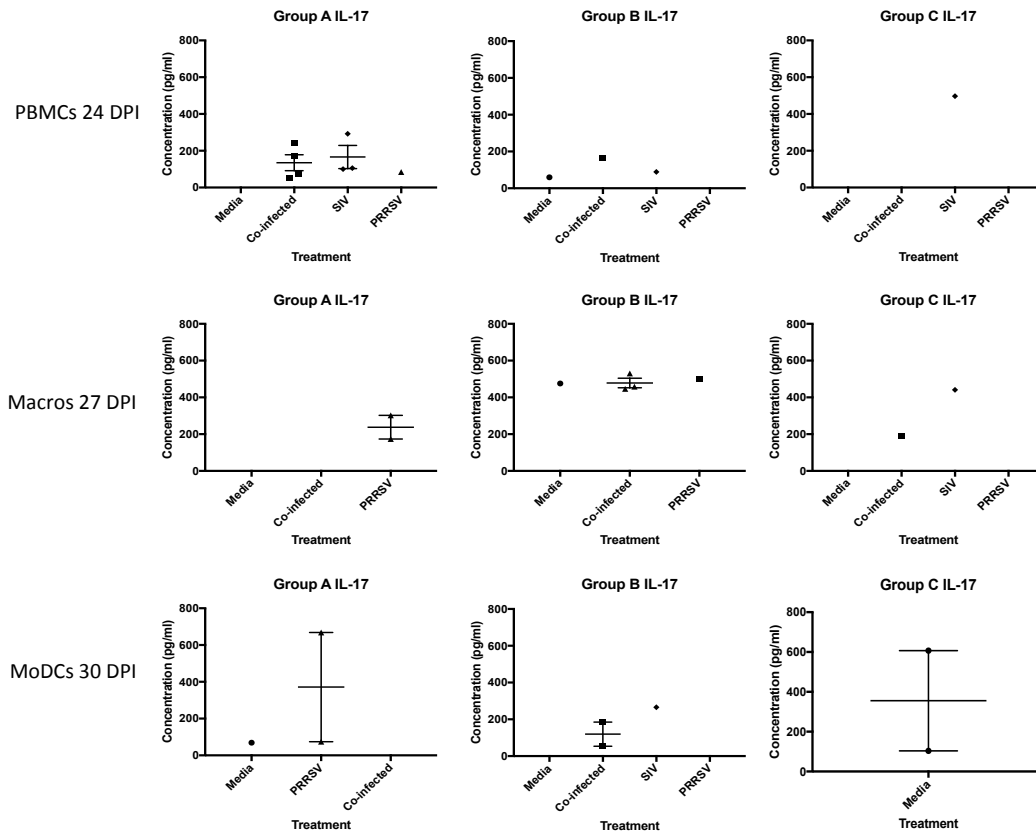


Figure 6-28: Representation of the FMIA cytokine ELISAs measuring IL-17 α during the 3rd week post-PRRSV infection. Supernatants from the cell culture assays were removed after 4 days in culture to measure cytokine secretion in response to the administered treatments indicated in the graphs. Samples were analyzed in duplicate.

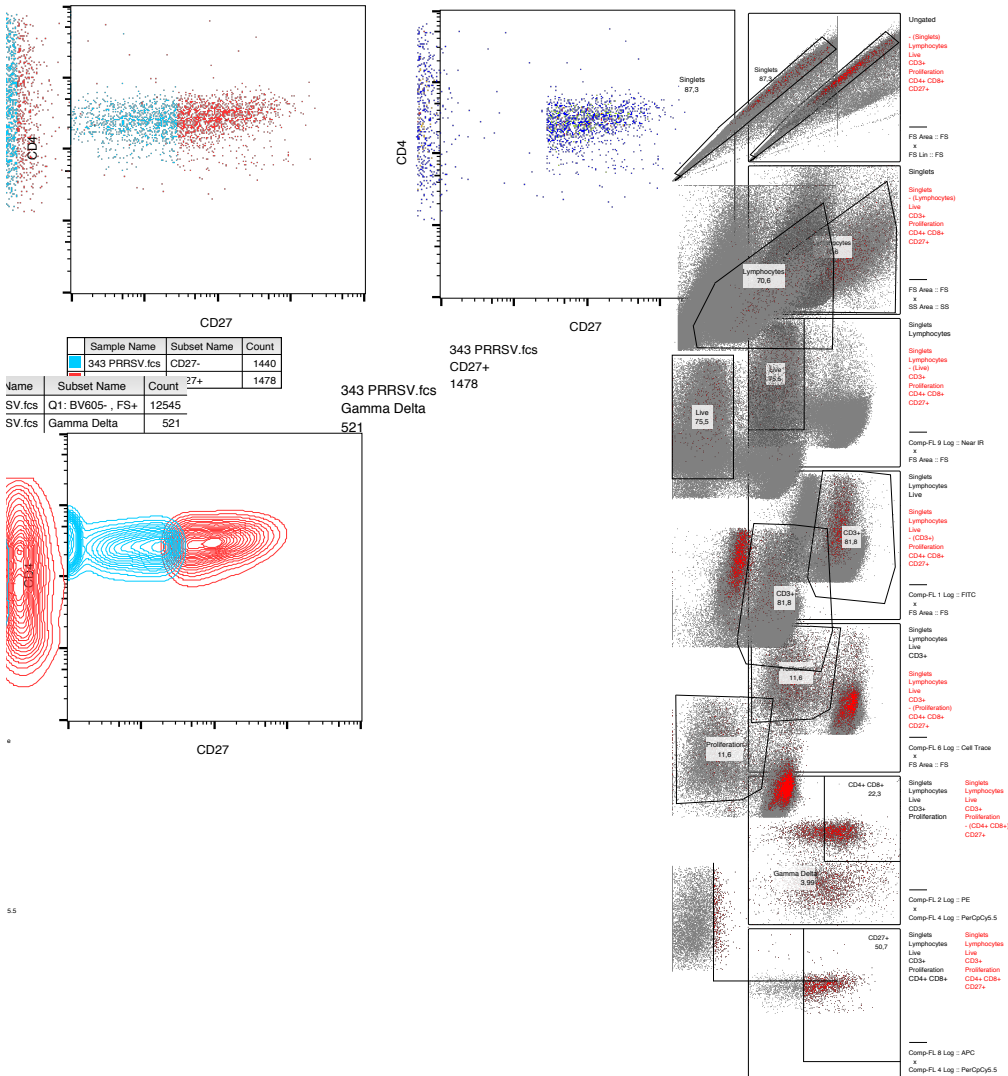


Figure 6-29: Schematic demonstrating the gating strategy utilized for $CD4\alpha^+ CD8\alpha^+ CD27^+$ T cells from a PRRSV treated PBMC cell culture (pig 343). Briefly, a gate was established around singlets before drawing a gate surrounding lymphocytes. A gate was then drawn on live cells, before gating on $CD3^+$ T cell expression. After gating on the proliferating cell population, a gate established for the $CD4\alpha^+ CD8\alpha^+$ T cell subset, before gating on $CD27^-$ (Effector Th cells, in blue) and $CD27^+$ (Central memory Th cells, in red) to measure Th cell subset proliferation.

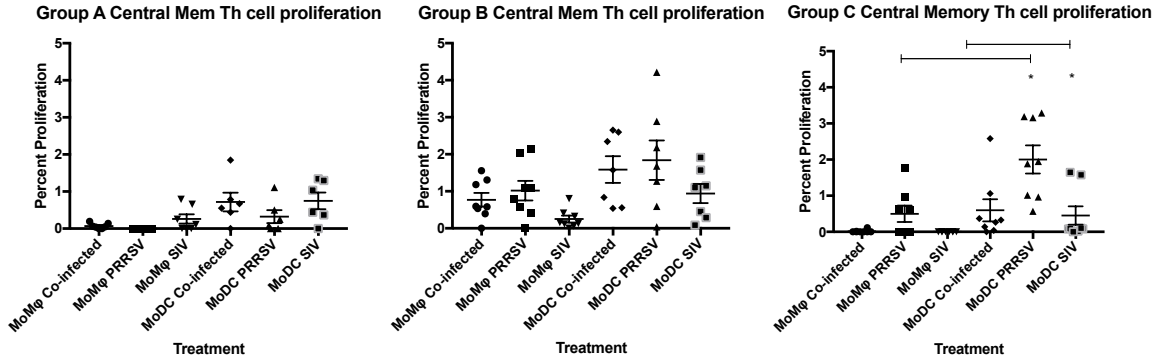


Figure 6-30: Comparison between the immunostimulatory capacity of MoDCs and MoM Φ s to stimulate central memory Th cell proliferation during the later time point of the animal trial to the specific treatments within their respective groups. The mean percent proliferation of the indicated treatment was subtracted from the mean proliferation of the media alone treatment, according to each separate animal. The percent proliferation was then compared between MoM Φ s and MoDCs according to each treatment. Statistical analysis was based on non-Gaussian distribution and the Kruskal-Wallis test of multiple comparisons was used to test for significance. $P < 0.05 = *$; $P < 0.005 = **$; $P < 0.0005 = ***$.

Contributions: JD, Stacy Strom, and JVK isolated PBMCs, monocytes, and T cells. JVK and JD cell trace violet stained the T cells. Stacy Strom, JVK, and JD performed the ELISpot assays. JD performed serum ELISAs. JD and Donna Dent performed FMIA ELISAs. JD performed macrophage and MoDC cell differentiation cultures. JD performed the flow cytometry. JD, JVK, and Stacy Strom co-cultured APCs with T cells. JD did statistical analysis. JD and VG designed experiments.

Chapter 7 GENERAL DISCUSSION

The PRRSV is an enveloped, positive sense, single stranded, RNA virus that infects APCs of the porcine immune system. Cell susceptibility is restricted to cells that express the hemoglobin/haptoglobin scavenger molecule CD163 (Calvert et al., 2007). Animals infected with PRRSV are subject to an array of clinical syndromes such as respiratory difficulty and pneumonia, weight loss, and the infection of the fetus leading to spontaneous abortions and fetal mummification, accounting for the majority of the economic losses (Butler et al., 2014). Outcomes of disease range from being asymptomatic to upwards of 100% mortality in pig herds, being largely attributable to the pathogenicity of the PRRSV strain, secondary co-infections with opportunistic pathogens, in addition to the age, sex, and breed of the pig. The initial site of PRRSV replication is within PAMs in the alveolar space (Chen, Triple, Kerrigan, Tian, & Rowland, 2016). Shortly after which PRRSV becomes viremic spreading to peripheral lymphoid organs and establishing a persistent state in the tonsils (Lunney et al., 2016). The innate immune system is subject to regulation by PRRSV in a strain specific manner, according to pathogenicity. The highly virulent Chinese strains of PRRSV seem to induce a cytokine storm, whereas the less virulent strains suppress the expression of innate immune cytokines. Innate immune suppression and a depletion of the myeloid phagocyte population lead to an immunocompromised state, leaving animals susceptible to secondary infections. Regarding the adaptive immune response, antibodies to the PRRSV are detected within a week of infection, although the antibodies are non-neutralizing. There is a delayed induction of T cell immunity to the PRRSV and roughly 4 weeks post infection, neutralizing antibodies become detectable leading to the resolution of the infection (Loving et al., 2015). There is a high demand for novel vaccines as the currently live attenuated vaccines are limited in cross-protectiveness and pose a risk of reverting to virulence. Understanding the delayed induction of T cell immunity and the dysregulated humoral immune response will be critical in the development of novel vaccine platforms. The aim of this thesis was to understand the role that APCs play during the pathogenesis of the virus and to shed light upon the interaction of PRRSV infected APCs with T cells.

We hypothesized that specific subsets of DCs were susceptible to PRRSV. We decided to utilize FMS-related tyrosine kinase 3 ligand (Flt3L) to differentiate DCs from hematopoietic progenitor cells, isolated from the bone marrow. In chapter 3, we successfully differentiated BMDCs and we showed that CD163⁺ BMDCs were susceptible to PRRSV infection and that the CD163⁻ BMDCs were not susceptible. We continued our investigation by comparing the susceptibility of CD163⁺ BMDCs to MΦs and MoDCs infected with PRRSV. Our results indicated that PRRSV infects MoDCs and MoMΦs more efficiently than CD163⁺ BMDCs. Lastly, our results indicated that the CD163⁺ BMDCs remained healthy 48 hours post infection, whereas the MoMΦs and MoDCs were essentially dead after 48 hours. This difference in APC viability may be attributable to a less severe rate of infection, but it could also be an indication of a defense mechanism that CD163⁺ BMDCs possess not seen in the myeloid derived MΦs or MoDCs.

An aspect of major interest in our lab is the progression to T cell immunity during a PRRSV infection, and a major strategy that viruses have developed for immune evasion has been the compromise of antigen presentation and maturation of DCs (Kruse et al., 2000; Mahanty et al., 2003; Wang et al., 2007). Thus, in chapter 3 we investigated the expression of cell surface markers associated with antigen presentation in the APC populations. When comparing the levels of MHCI and MHCII expression on the APC populations, PRRSV infected, non-stimulated MoMΦs showed clear downregulations in both MHCI and MHCII cell surface expression. Our results demonstrated that even though there is a downregulation of MHC molecules on the surface of MoMΦs infected with PRRSV, it did not abrogate their stimulatory capacity, as the MoMΦs clearly retained their capacity to stimulate a recall response in T cells from PRRSV immunized animals. Ultimately, we were left questioning why there was a delayed induction of T cell immunity to PRRSV. To further address the delayed induction of T cell immunity after PRRSV infection, we decided to investigate the maturation of the invariant chain in MoDCs and PAMs.

Dendritic cells (DCs) are often referred to as the professional APCs of the immune system, being largely attributable to their capacity to stimulate naïve T cells, driving the adaptive immune response in a particular direction. The pathway in which MHCII is

synthesized and loaded with peptide has been largely deduced, but the trafficking of peptide loaded MHCII to the plasma membrane in APCs is not completely resolved (Blum et al., 2013; ten Broeke et al., 2013). Originally we sought to investigate whether PRRSV has an influence on the maturation of the invariant chain. Theoretically, if PRRSV were to interfere with the maturation of the invariant chain, it would result in the occupation of the MHCII binding groove with CLIP. This in turn would prevent the loading of a PRRSV peptide sequences into the MHCII binding groove for antigen presentation (Blum et al., 2013; Mellins and Stern, 2014). To determine whether PRRSV influences the maturation of the invariant chain, in chapter 4 we infected cells and immunoprecipitated MHCII.

We successfully immunoprecipitated MHCII from infected and non-infected MoDCs and PAMs, as we identified the alpha chain (SLA-DRA1) and the beta chain (SLA-DRB1) of MHCII. There was one major discernable difference in the levels of MHCII associated molecules amongst the infected and non-infected cell populations, and it was not associated with the invariant chain. At this time, it is difficult to conclude whether PRRSV infection alters the maturation of the invariant chain, as we could not identify an antibody for its identification in pigs. Interestingly the band of interest within the infected cell population was practically diminished, which we identified to be gamma actin 1. The role of the cytoskeleton during a PRRSV infection has gone largely unstudied. Our results seem to indicate that the association of gamma actin 1 with MHCII is present in MoDCs and to a much lesser extent in PAMs. Furthermore, the gamma actin 1 association with MHCII was largely diminished when MoDCs were infected with PRRSV. We are thus left questioning why gamma actin 1 was immunoprecipitated with MHCII, and why gamma actin 1 was not as pronounced in the PRRSV infected MoDCs or the PAMs, regardless of infection status. It's plausible that gamma actin 1 could play a prominent role during antigen presentation, potentially in the transport of peptide loaded MHCII molecules (pMHCII) to the cell surface, or possibly in sequestering pMHCII to lipid rafts at immunological synaptic junctions during T cell stimulation. Further studies investigating the role of the actin cytoskeleton during a PRRSV infection, and during antigen presentation in MoDCs, could be beneficial towards understanding the pathogenesis of PRRSV. To draw any sort of conclusions regarding the relationship of

APCs with T cells during a PRRSV infection, it was essential to develop a method to culture the APCs with T cells, so we established an assay by modifying the mixed leukocyte reaction (MLR) in chapter 5.

We hypothesized that IFN- γ stimulated (M1) macrophages would possess a greater capacity to stimulate T lymphocyte proliferation than non-stimulated (M0) or IL-4 stimulated (M2) macrophages. Using an MLR, we demonstrated that M1 macrophages possessed a greater capability to promote T lymphocyte proliferation than M0 or M2 macrophages derived from blood monocytes. Furthermore, we modified the MLR in Chapter 6 to assess antigen specific T cell responses. Overall, the stimulation of APCs towards specific phenotypes had clear implications on both the robustness of the T cell response and type of T cell immunity that will be induced. The results obtained from the MLR gave us the confidence to study the stimulation of antigen specific T lymphocyte populations *in vitro* isolated from PRRSV infected animals.

The purpose of the animal trial in Chapter 6 was to investigate and characterize the T cell response to PRRSV infection, and to compare the immunostimulatory capacity of MoM Φ s and MoDCs to promote the proliferation of specific T cell subsets. We utilized the FluSure XP vaccine to swine-influenza as a positive control and a comparative measure of immunity to PRRSV infection. We detected IFN- γ secreting cells in PBMCs from PRRSV infected animals 2 weeks post infection, in addition to T cell proliferation in both the PBMC and APC-T cell co-cultures in all of the Groups to both PRRSV and swIAV treatments. For the most part, the highest level of T lymphocyte proliferation to both PRRSV infection and swIAV treatment was detected in the PBMC lymphoproliferation cell cultures. Overall, our main findings included the following: A) PRRSV infection of animals in Group B may have enhanced the T cell response to swIAV immunization in the MoM Φ -T cell co-culture and MoDC-T cell co-culture, being potentially attributable to monocyte training in PRRSV infected animals. B) The stimulatory capacity between MoM Φ s and MoDCs to induce overall lymphocyte proliferation did not differ significantly. Although MoDCs may be more potent inducers of central memory Th cells as exhibited in response to both PRRSV and swIAV treatments. C) During the second week of infection, we observed proliferation in the media alone treatments in the APC-T cell co-cultures from the animal groups that were

infected with PRRSV. We hypothesize that the monocytes that we isolated for the MoM Φ and MoDC differentiation were infected with PRRSV. D) Lastly, more than 50% the population of cells that proliferated in response to PRRSV which were not CD3⁺ T cells in the PBMC culture. We hypothesize that the unidentified population of cells could be CD19⁺/CD21⁺ B cells. If the population consists of B cells it lends support to our overall theory regarding PRRSV induction of hypergammaglobulinemia, which will be discussed in more detail below.

In conclusion, we have shown that the susceptibility of APCs is restricted to those cells that express CD163. Furthermore, the rate of replication of PRRSV is slower in CD163⁺ BMDCs, and potentially in MoDCs, than in MoM ϕ s. The infection of APCs by PRRSV does not abrogate their antigen-presenting and immunostimulatory capacity to promote T lymphocyte proliferation. Furthermore PRRSV infection appears to be altering the association of gamma actin 1 with MHCII. We are unable to draw a definitive conclusion as to whether the lack of gamma actin 1 association is attributable to the maturation of DCs and the transport of peptide loaded MHCII to the plasma membrane, or is occurring as a result of PRRSV hijacking the actin cytoskeleton for its own replication and assembly. Regarding the induction of T cell immunity to PRRSV, although the induction of T cell immunity may be delayed, the T cell response is functional. We demonstrated that both MoM ϕ s and MoDCs were capable of stimulating Th cell and CTL proliferation in an antigen specific manner to PRRSV and swIAV. Lastly, a distinguishing feature of MoDCs in comparison to MoM Φ s could be an increased potency to induce central memory Th cell proliferation.

Theory regarding the delayed induction of T cell immunity to PRRSV:

This thesis in its entirety allowed us to propose a theory regarding the delayed induction of T cell immunity and the dysregulated humoral immune response (being the induction of non-neutralizing antibodies and delayed appearance of neutralizing antibodies). We believe that a specific subset of DCs, those being derived from hematopoietic progenitor cells with Flt3L, is responsible for the initiation of the CD4 α ⁺ T cell response to PRRSV. Our results indicate that the pathogenesis of the virus or the rate of replication within MoM Φ s and DCs is different. The virus replicates more quickly in MoM Φ s than CD163⁺

BMDCs, and the virus seems to kill the MoMΦs and MoDCs more quickly than it does the CD163⁺ BMDCs. Theoretically, APCs would need around 24 hours to stimulate a naïve T cell to become activated for its particular antigen (Jelley-Gibbs et al., 2000). We feel that macrophages and MoDCs may simply not have enough time to present antigen to the T cell specific for its specific derived viral peptide sequence. Given the likelihood that the BMDC population isn't as prominent as MoDCs and MoMΦs *in vivo*, the CD163⁺ BMDCs could be the APC population responsible for driving T cell immunity. Thus, the delayed induction of T cell immunity could be attributable to the rarity of this specific DC population in addition to time constraint of that DC population reaching the lymph node for antigen presentation to naïve T cells. The delayed induction of CD4α⁺ Th cells would also result in a lack of follicular Th cell induction. A recent report indicates that γδ T cells play a significant role during the differentiation of follicular Th cells (Rezende et al., 2018). Therefore the induction of γδ T cells could be relevant when considering the induction of follicular Th cells. Overall, in the absence of follicular Th cells, B cells would not be able to undergo proper somatic hypermutation. Additionally, B cells would enter a state of hypergammaglobulinemia in which they would proliferate and plasma cell synthesis of antibodies would go undirected, as discussed in the humoral immunity section of the literature review. Thus, once follicular Th cells are active (likely 2 weeks post infection when IFN-γ secreting cells become detectable in PBMCs and γδ T cell proliferation is at its highest point) the B cells would undergo somatic hypermutation (roughly a week's time) and the synthesis of neutralizing antibodies would follow (4 weeks post infection), which is what we see *in vivo* (Loving et al., 2015).

7.1 Future work

There are several directions that the work from this thesis can take. Investigating the pathogenesis of PRRSV within Flt3L-derived CD163⁺ BMDCs could provide useful information into the mechanisms surrounding the decreased susceptibility to PRRSV of the CD163⁺ BMDCs. Additionally, investigating the peptide sequences being presented in association with MHCII by the CD163⁺ BMDC population, if our theory is correct, has the potential to aid in the development of a novel vaccine. Continuing, the mechanisms surrounding the transport of peptide loaded MHCII to the plasma membrane are not completely understood. Understanding the role of the cytoskeleton during MHCII trafficking to the plasma membrane would contribute to the general knowledge surrounding antigen presentation and processing for the field of immunology. Furthermore, investigating the role of the actin cytoskeleton during a PRRSV infection, and whether PRRSV manipulates the cytoskeleton, could provide a deeper understanding of the pathogenesis of virus and would contribute to the general knowledge for the field of virology. Lastly, explanations for the delayed induction of T cell immunity and the delayed induction of neutralizing antibodies do not exist. Although it would be difficult to investigate, determining the point in time that follicular T helper cells migrate into germinal centers could provide insight into the process of somatic hypermutation in B cells during a PRRSV infection. Ultimately, this could provide an answer as to whether or not the delayed induction of neutralizing antibodies is attributable to a lack of follicular Th cells coordinating somatic hypermutation.

REFERENCES

- Akira, S., Uematsu, S., Takeuchi, O., 2006. Pathogen Recognition and Innate Immunity. *Cell* 124, 783-801.
- Allende, R., Lewis, T.L., Lu, Z., Rock, D.L., Kutish, G.F., Ali, A., Doster, A.R., Osorio, F.A., 1999. North American and European porcine reproductive and respiratory syndrome viruses differ in non-structural protein coding regions. *The Journal of general virology* 80 (Pt 2), 307-315.
- Auray, G., Keller, I., Python, S., Gerber, M., Bruggmann, R., Ruggli, N., Summerfield, A., 2016. Characterization and Transcriptomic Analysis of Porcine Blood Conventional and Plasmacytoid Dendritic Cells Reveals Striking Species-Specific Differences. *Journal of immunology* 197, 4791-4806.
- Banchereau, J., Steinman, R.M., 1998. Dendritic cells and the control of immunity. *Nature* 392, 245-252.
- Barois, N., Forquet, F., Davoust, J., 1998. Actin microfilaments control the MHC class II antigen presentation pathway in B cells. *Journal of cell science* 111 (Pt 13), 1791-1800.
- Barry, M., Bleackley, R.C., 2002. Cytotoxic T lymphocytes: all roads lead to death. *Nature reviews. Immunology* 2, 401-409.
- Bassols, A., Costa, C., Eckersall, P.D., Osada, J., Sabria, J., Tibau, J., 2014. The pig as an animal model for human pathologies: A proteomics perspective. *Proteomics. Clinical applications* 8, 715-731.
- Baumann, A., Mateu, E., Murtaugh, M.P., Summerfield, A., 2013. Impact of genotype 1 and 2 of porcine reproductive and respiratory syndrome viruses on interferon-alpha responses by plasmacytoid dendritic cells. *Veterinary research* 44, 33.
- Belz, G.T., Nutt, S.L., 2012. Transcriptional programming of the dendritic cell network. *Nat Rev Immunol* 12, 101-113.
- Beura, L.K., Sarkar, S.N., Kwon, B., Subramaniam, S., Jones, C., Pattnaik, A.K., Osorio, F.A., 2010. Porcine reproductive and respiratory syndrome virus nonstructural protein 1beta modulates host innate immune response by antagonizing IRF3 activation. *Journal of virology* 84, 1574-1584.
- Bevan, M.J., 2004. Helping the CD8(+) T-cell response. *Nature reviews. Immunology* 4, 595-602.
- Blum, J.S., Wearsch, P.A., Cresswell, P., 2013. Pathways of antigen processing. *Annual review of immunology* 31, 443-473.
- Bordet, E., Blanc, F., Tired, M., Crisci, E., Bouguyon, E., Renson, P., Maisonnasse, P., Bourge, M., Leplat, J.J., Giuffra, E., Jouneau, L., Schwartz-Cornil, I., Bourry, O., Bertho, N., 2018. Porcine Reproductive and Respiratory Syndrome Virus Type 1.3 Lena Triggers Conventional Dendritic Cells 1 Activation and T Helper 1 Immune Response Without Infecting Dendritic Cells. *Frontiers in immunology* 9, 2299.
- Bordon, Y., 2014. Macrophages: innate memory training. *Nature reviews. Immunology* 14, 713.
- Bouso, P., 2008. T-cell activation by dendritic cells in the lymph node: lessons from the movies. *Nature reviews. Immunology* 8, 675-684.

- Brar, M.S., Shi, M., Murtaugh, M.P., Leung, F.C., 2015. Evolutionary diversification of type 2 porcine reproductive and respiratory syndrome virus. *The Journal of general virology* 96, 1570-1580.
- Brockmeier, S.L., Loving, C.L., Eberle, K.C., Hau, S.J., Buckley, A., Van Geelen, A., Montiel, N.A., Nicholson, T., Lager, K.M., 2017a. Interferon alpha inhibits replication of a live-attenuated porcine reproductive and respiratory syndrome virus vaccine preventing development of an adaptive immune response in swine. *Veterinary microbiology* 212, 48-51.
- Brockmeier, S.L., Loving, C.L., Palmer, M.V., Spear, A., Nicholson, T.L., Faaberg, K.S., Lager, K.M., 2017b. Comparison of Asian porcine high fever disease isolates of porcine reproductive and respiratory syndrome virus to United States isolates for their ability to cause disease and secondary bacterial infection in swine. *Veterinary microbiology* 203, 6-17.
- Burns, S., Thrasher, A.J., Blundell, M.P., Machesky, L., Jones, G.E., 2001. Configuration of human dendritic cell cytoskeleton by Rho GTPases, the WAS protein, and differentiation. *Blood* 98, 1142-1149.
- Burton, D.R., 2002. Antibodies, viruses and vaccines. *Nature reviews. Immunology* 2, 706-713.
- Butler, J.E., Lager, K.M., Golde, W., Faaberg, K.S., Sinkora, M., Loving, C., Zhang, Y.I., 2014. Porcine reproductive and respiratory syndrome (PRRS): an immune dysregulatory pandemic. *Immunologic research* 59, 81-108.
- Butler, J.E., Sun, J., Weber, P., Ford, S.P., Rehakova, Z., Sinkora, J., Lager, K., 2001. Antibody repertoire development in fetal and neonatal piglets. IV. Switch recombination, primarily in fetal thymus, occurs independent of environmental antigen and is only weakly associated with repertoire diversification. *Journal of immunology* 167, 3239-3249.
- Butler, J.E., Weber, P., Sinkora, M., Baker, D., Schoenherr, A., Mayer, B., Francis, D., 2002. Antibody repertoire development in fetal and neonatal piglets. VIII. Colonization is required for newborn piglets to make serum antibodies to T-dependent and type 2 T-independent antigens. *Journal of immunology* 169, 6822-6830.
- Butler, J.E., Wertz, N., Weber, P., Lager, K.M., 2008. Porcine reproductive and respiratory syndrome virus subverts repertoire development by proliferation of germline-encoded B cells of all isotypes bearing hydrophobic heavy chain CDR3. *Journal of immunology* 180, 2347-2356.
- Calvert, J.G., Slade, D.E., Shields, S.L., Jolie, R., Mannan, R.M., Ankenbauer, R.G., Welch, S.K., 2007. CD163 expression confers susceptibility to porcine reproductive and respiratory syndrome viruses. *Journal of virology* 81, 7371-7379.
- Calzada-Nova, G., Schnitzlein, W., Husmann, R., Zuckermann, F.A., 2010. Characterization of the cytokine and maturation responses of pure populations of porcine plasmacytoid dendritic cells to porcine viruses and toll-like receptor agonists. *Vet Immunol Immunopathol* 135, 20-33.
- Calzada-Nova, G., Schnitzlein, W.M., Husmann, R.J., Zuckermann, F.A., 2011. North American porcine reproductive and respiratory syndrome viruses inhibit type I

- interferon production by plasmacytoid dendritic cells. *Journal of virology* 85, 2703-2713.
- Canelli, E., Catella, A., Borghetti, P., Ferrari, L., Ogno, G., De Angelis, E., Bonilauri, P., Guazzetti, S., Nardini, R., Martelli, P., 2018. Efficacy of a modified-live virus vaccine in pigs experimentally infected with a highly pathogenic porcine reproductive and respiratory syndrome virus type 1 (HP-PRRSV-1). *Veterinary microbiology* 226, 89-96.
- Cao, J., Grauwet, K., Vermeulen, B., Devriendt, B., Jiang, P., Favoreel, H., Nauwynck, H., 2013. Suppression of NK cell-mediated cytotoxicity against PRRSV-infected porcine alveolar macrophages in vitro. *Veterinary microbiology* 164, 261-269.
- Chang, H.C., Peng, Y.T., Chang, H.L., Chaung, H.C., Chung, W.B., 2008. Phenotypic and functional modulation of bone marrow-derived dendritic cells by porcine reproductive and respiratory syndrome virus. *Vet Microbiol* 129, 281-293.
- Chaung, H.C., Chen, C.W., Hsieh, B.L., Chung, W.B., 2010. Toll-Like Receptor expressions in porcine alveolar macrophages and Dendritic Cells in responding to poly IC stimulation and porcine reproductive and respiratory syndrome virus (PRRSV) infection. *Comparative immunology, microbiology and infectious diseases* 33, 197-213.
- Chen, N., Tribble, B.R., Kerrigan, M.A., Tian, K., Rowland, R.R.R., 2016. ORF5 of porcine reproductive and respiratory syndrome virus (PRRSV) is a target of diversifying selection as infection progresses from acute infection to virus rebound. *Infection, genetics and evolution : journal of molecular epidemiology and evolutionary genetics in infectious diseases* 40, 167-175.
- Chow, A., Toomre, D., Garrett, W., Mellman, I., 2002. Dendritic cell maturation triggers retrograde MHC class II transport from lysosomes to the plasma membrane. *Nature* 418, 988-994.
- Chung, C.J., Cha, S.H., Grimm, A.L., Ajithdoss, D., Rzepka, J., Chung, G., Yu, J., Davis, W.C., Ho, C.S., 2018. Pigs that recover from porcine reproduction and respiratory syndrome virus infection develop cytotoxic CD4+CD8+ and CD4+CD8- T-cells that kill virus infected cells. *PloS one* 13, e0203482.
- Colf, L.A., Bankovich, A.J., Hanick, N.A., Bowerman, N.A., Jones, L.L., Kranz, D.M., Garcia, K.C., 2007. How a single T cell receptor recognizes both self and foreign MHC. *Cell* 129, 135-146.
- Comrie, W.A., Li, S., Boyle, S., Burkhardt, J.K., 2015. The dendritic cell cytoskeleton promotes T cell adhesion and activation by constraining ICAM-1 mobility. *The Journal of cell biology* 208, 457-473.
- Correas, I., Osorio, F.A., Steffen, D., Pattnaik, A.K., Vu, H.L.X., 2017. Cross reactivity of immune responses to porcine reproductive and respiratory syndrome virus infection. *Vaccine* 35, 782-788.
- Crotty, S., 2015. A brief history of T cell help to B cells. *Nature reviews. Immunology* 15, 185-189.
- Dar, A., Lai, K., Dent, D., Potter, A., Gerdts, V., Babiuk, L.A., Mutwiri, G.K., 2012. Administration of poly[di(sodium carboxylatoethylphenoxy)]phosphazene (PCEP) as adjuvant activated mixed Th1/Th2 immune responses in pigs. *Veterinary immunology and immunopathology* 146, 289-295.

- Delamarre, L., Pack, M., Chang, H., Mellman, I., Trombetta, E.S., 2005. Differential lysosomal proteolysis in antigen-presenting cells determines antigen fate. *Science* 307, 1630-1634.
- Dokland, T., 2010. The structural biology of PRRSV. *Virus research* 154, 86-97.
- Dotti, S., Guadagnini, G., Salvini, F., Razzuoli, E., Ferrari, M., Alborali, G.L., Amadori, M., 2013. Time-course of antibody and cell-mediated immune responses to Porcine Reproductive and Respiratory Syndrome virus under field conditions. *Research in veterinary science* 94, 510-517.
- Durfee, L.A., Huibregtse, J.M., 2010. Identification and Validation of ISG15 Target Proteins. *Sub-cellular biochemistry* 54, 228-237.
- Elemans, M., Florins, A., Willems, L., Asquith, B., 2014. Rates of CTL killing in persistent viral infection in vivo. *PLoS computational biology* 10, e1003534.
- Embgenbroich, M., Burgdorf, S., 2018. Current Concepts of Antigen Cross-Presentation. *Frontiers in immunology* 9, 1643.
- Epelman, S., Lavine, K.J., Randolph, G.J., 2014. Origin and functions of tissue macrophages. *Immunity* 41, 21-35.
- Facci, M.R., Auray, G., Buchanan, R., van Kessel, J., Thompson, D.R., Mackenzie-Dyck, S., Babiuk, L.A., Gerdts, V., 2010. A comparison between isolated blood dendritic cells and monocyte-derived dendritic cells in pigs. *Immunology* 129, 396-405.
- Fairbairn, L., Kapetanovic, R., Sester, D.P., Hume, D.A., 2011. The mononuclear phagocyte system of the pig as a model for understanding human innate immunity and disease. *Journal of leukocyte biology* 89, 855-871.
- Fang, Y., Fang, L., Wang, Y., Lei, Y., Luo, R., Wang, D., Chen, H., Xiao, S., 2012. Porcine reproductive and respiratory syndrome virus nonstructural protein 2 contributes to NF-kappaB activation. *Virology Journal* 9, 83.
- Ferrari, L., Canelli, E., De Angelis, E., Catella, A., Ferrarini, G., Ogno, G., Bonati, L., Nardini, R., Borghetti, P., Martelli, P., 2018. A highly pathogenic porcine reproductive and respiratory syndrome virus type 1 (PRRSV-1) strongly modulates cellular innate and adaptive immune subsets upon experimental infection. *Veterinary microbiology* 216, 85-92.
- Flores-Mendoza, L., Silva-Campa, E., Resendiz, M., Osorio, F.A., Hernandez, J., 2008. Porcine reproductive and respiratory syndrome virus infects mature porcine dendritic cells and up-regulates interleukin-10 production. *Clin Vaccine Immunol* 15, 720-725.
- Garcia-Nicolas, O., Auray, G., Sautter, C.A., Rappe, J.C., McCullough, K.C., Ruggli, N., Summerfield, A., 2016. Sensing of Porcine Reproductive and Respiratory Syndrome Virus-Infected Macrophages by Plasmacytoid Dendritic Cells. *Frontiers in microbiology* 7, 771.
- Girard, T., El-Far, M., Gaucher, D., Acuto, O., Beaulé, G., Michel, F., Mourad, W., Sekaly, R.P., 2012. A conserved polylysine motif in CD86 cytoplasmic tail is necessary for cytoskeletal association and effective co-stimulation. *Biochemical and biophysical research communications* 423, 301-307.
- Gomez-Laguna, J., Salguero, F.J., Fernandez de Marco, M., Barranco, I., Rodriguez-Gomez, I.M., Quezada, M., Carrasco, L., 2013a. Type 2 Porcine Reproductive and Respiratory Syndrome Virus infection mediated apoptosis in B- and T-cell

- areas in lymphoid organs of experimentally infected pigs. *Transboundary and emerging diseases* 60, 273-278.
- Gomez-Laguna, J., Salguero, F.J., Pallares, F.J., Carrasco, L., 2013b. Immunopathogenesis of porcine reproductive and respiratory syndrome in the respiratory tract of pigs. *Veterinary journal* 195, 148-155.
- Guo, B., Lager, K.M., Henningson, J.N., Miller, L.C., Schlink, S.N., Kappes, M.A., Kehrli, M.E., Jr., Brockmeier, S.L., Nicholson, T.L., Yang, H.C., Faaberg, K.S., 2013. Experimental infection of United States swine with a Chinese highly pathogenic strain of porcine reproductive and respiratory syndrome virus. *Virology* 435, 372-384.
- Guzylack-Piriou, L., Alves, M.P., McCullough, K.C., Summerfield, A., 2010. Porcine Flt3 ligand and its receptor: generation of dendritic cells and identification of a new marker for porcine dendritic cells. *Developmental and comparative immunology* 34, 455-464.
- Haiwick, G., Hermann, J., Roof, M., Fergen, B., Philips, R., Patterson, A., 2018. Examination of viraemia and clinical signs after challenge with a heterologous PRRSV strain in PRRS Type 2 MLV vaccinated pigs: A challenge-dose study. *PloS one* 13, e0209784.
- Hanada, K., Suzuki, Y., Nakane, T., Hirose, O., Gojobori, T., 2005. The origin and evolution of porcine reproductive and respiratory syndrome viruses. *Mol Biol Evol* 22, 1024-1031.
- Hangartner, L., Zinkernagel, R.M., Hengartner, H., 2006. Antiviral antibody responses: the two extremes of a wide spectrum. *Nature reviews. Immunology* 6, 231-243.
- He, Y., Wang, G., Liu, Y., Shi, W., Han, Z., Wu, J., Jiang, C., Wang, S., Hu, S., Wen, H., Dong, J., Liu, H., Cai, X., 2012. Characterization of thymus atrophy in piglets infected with highly pathogenic porcine reproductive and respiratory syndrome virus. *Veterinary microbiology* 160, 455-462.
- Hoeffel, G., Ginhoux, F., 2015. Ontogeny of Tissue-Resident Macrophages. *Frontiers in immunology* 6, 486.
- Holtkamp, D.J.K., James B.; Zimmerman, Jeffrey J.; Neumann, Eric; Rotto, Hans; Yoder, Tiffany K.; Wang, Chong; Yeske, Paul; Mowrer, Christine L.; and Haley, Charles 2012. Economic Impact of Porcine Reproductive and Respiratory Syndrome Virus on U.S. Pork Producers. In *Animal Industry Report* (Iowa State University, AS 658, ASL R2671.).
- Hou, J., Wang, L., Quan, R., Fu, Y., Zhang, H., Feng, W.H., 2012. Induction of interleukin-10 is dependent on p38 mitogen-activated protein kinase pathway in macrophages infected with porcine reproductive and respiratory syndrome virus. *Virol J* 9, 165.
- Huang, Y., Li, Z., Li, J., Yibo, K., Yang, L., Mah, C.K., Liu, G., Yu, B., Wang, K., 2019. Efficacy evaluation of three modified-live PRRS vaccines against a local strain of highly pathogenic porcine reproductive and respiratory syndrome virus. *Veterinary microbiology* 229, 117-123.
- Hume, D.A., 2008. Macrophages as APC and the dendritic cell myth. *Journal of immunology* 181, 5829-5835.
- Jans, J., elMoussaoui, H., de Groot, R., de Jonge, M.I., Ferwerda, G., 2016. Actin- and clathrin-dependent mechanisms regulate interferon gamma release after

- stimulation of human immune cells with respiratory syncytial virus. *Virology journal* 13, 52.
- Jelley-Gibbs, D.M., Lepak, N.M., Yen, M., Swain, S.L., 2000. Two distinct stages in the transition from naive CD4 T cells to effectors, early antigen-dependent and late cytokine-driven expansion and differentiation. *Journal of immunology* 165, 5017-5026.
- Jeong, J., Park, C., Oh, T., Park, K.H., Yang, S., Kang, I., Park, S.J., Chae, C., 2018. Cross-protection of a modified-live porcine reproductive and respiratory syndrome virus (PRRSV)-2 vaccine against a heterologous PRRSV-1 challenge in late-term pregnancy gilts. *Veterinary microbiology* 223, 119-125.
- Kappes, M.A., Faaberg, K.S., 2015. PRRSV structure, replication and recombination: Origin of phenotype and genotype diversity. *Virology* 479-480, 475-486.
- Kappes, M.A., Miller, C.L., Faaberg, K.S., 2013. Highly divergent strains of porcine reproductive and respiratory syndrome virus incorporate multiple isoforms of nonstructural protein 2 into virions. *Journal of virology* 87, 13456-13465.
- Karniyuchuk, U., Geldhof, M., Vanhee, M., Van Doorselaere, J., Saveleva, T., Nauwynck, H., 2010. Pathogenesis and antigenic characterization of a new East European subtype 3 porcine reproductive and respiratory syndrome virus isolate. *BMC Veterinary Research* 6, 30.
- Kaser, T., Mair, K.H., Hammer, S.E., Gerner, W., Saalmuller, A., 2015. Natural and inducible Tregs in swine: Helios expression and functional properties. *Developmental and comparative immunology* 49, 323-331.
- Keller, A., Nesvizhskii, A.I., Kolker, E., Aebersold, R., 2002. Empirical statistical model to estimate the accuracy of peptide identifications made by MS/MS and database search. *Analytical chemistry* 74, 5383-5392.
- Kim, O., Sun, Y., Lai, F.W., Song, C., Yoo, D., 2010. Modulation of type I interferon induction by porcine reproductive and respiratory syndrome virus and degradation of CREB-binding protein by non-structural protein 1 in MARC-145 and HeLa cells. *Virology* 402, 315-326.
- Kimman, T.G., Cornelissen, L.A., Moormann, R.J., Rebel, J.M., Stockhofe-Zurwieden, N., 2009. Challenges for porcine reproductive and respiratory syndrome virus (PRRSV) vaccinology. *Vaccine* 27, 3704-3718.
- Kittawornrat, A., Engle, M., Panyasing, Y., Olsen, C., Schwartz, K., Rice, A., Lizano, S., Wang, C., Zimmerman, J., 2013. Kinetics of the porcine reproductive and respiratory syndrome virus (PRRSV) humoral immune response in swine serum and oral fluids collected from individual boars. *BMC veterinary research* 9, 61.
- Kleijmeer, M., Ramm, G., Schuurhuis, D., Griffith, J., Rescigno, M., Ricciardi-Castagnoli, P., Rudensky, A.Y., Ossendorp, F., Melief, C.J., Stoorvogel, W., Geuze, H.J., 2001. Reorganization of multivesicular bodies regulates MHC class II antigen presentation by dendritic cells. *The Journal of cell biology* 155, 53-63.
- Klein, L., Kyewski, B., Allen, P.M., Hogquist, K.A., 2014. Positive and negative selection of the T cell repertoire: what thymocytes see (and don't see). *Nature reviews. Immunology* 14, 377-391.
- Krenkel, O., Tacke, F., 2017. Liver macrophages in tissue homeostasis and disease. *Nature reviews. Immunology* 17, 306-321.

- Kristensen, C.S., Bøtner, A., Takai, H., Nielsen, J.P., Jorsal, S.E., 2004. Experimental airborne transmission of PRRS virus. *Veterinary Microbiology* 99, 197-202.
- Kruse, M., Rosorius, O., Kratzer, F., Stelz, G., Kuhnt, C., Schuler, G., Hauber, J., Steinkasserer, A., 2000. Mature dendritic cells infected with herpes simplex virus type 1 exhibit inhibited T-cell stimulatory capacity. *J Virol* 74, 7127-7136.
- Lalor, S.J., McLoughlin, R.M., 2016. Memory gammadelta T Cells-Newly Appreciated Protagonists in Infection and Immunity. *Trends in immunology* 37, 690-702.
- Li, H., Zheng, Z., Zhou, P., Zhang, B., Shi, Z., Hu, Q., Wang, H., 2010. The cysteine protease domain of porcine reproductive and respiratory syndrome virus non-structural protein 2 antagonizes interferon regulatory factor 3 activation. *The Journal of general virology* 91, 2947-2958.
- Liu, P., Bai, Y., Jiang, X., Zhou, L., Yuan, S., Yao, H., Yang, H., Sun, Z., 2018. High reversion potential of a cell-adapted vaccine candidate against highly pathogenic porcine reproductive and respiratory syndrome. *Veterinary microbiology* 227, 133-142.
- Lopez, O.J., Osorio, F.A., 2004. Role of neutralizing antibodies in PRRSV protective immunity. *Veterinary immunology and immunopathology* 102, 155-163.
- Loving, C.L., Osorio, F.A., Murtaugh, M.P., Zuckermann, F.A., 2015. Innate and adaptive immunity against Porcine Reproductive and Respiratory Syndrome Virus. *Veterinary immunology and immunopathology* 167, 1-14.
- Lu, Z.H., Wang, X., Wilson, A.D., Dorey-Robinson, D.L.W., Archibald, A.L., Ait-Ali, T., Frossard, J.P., 2017. Quasispecies evolution of the prototypical genotype 1 porcine reproductive and respiratory syndrome virus early during in vivo infection is rapid and tissue specific. *Archives of virology* 162, 2203-2210.
- Luckheeram, R.V., Zhou, R., Verma, A.D., Xia, B., 2012a. CD4(+)T Cells: Differentiation and Functions. *Clin Dev Immunol*.
- Luckheeram, R.V., Zhou, R., Verma, A.D., Xia, B., 2012b. CD4(+)T cells: differentiation and functions. *Clinical & developmental immunology* 2012, 925135.
- Lunney, J.K., Fang, Y., Ladinig, A., Chen, N., Li, Y., Rowland, B., Renukaradhya, G.J., 2016. Porcine Reproductive and Respiratory Syndrome Virus (PRRSV): Pathogenesis and Interaction with the Immune System. *Annual review of animal biosciences* 4, 129-154.
- Luo, R., Fang, L., Jiang, Y., Jin, H., Wang, Y., Wang, D., Chen, H., Xiao, S., 2011. Activation of NF- κ B by nucleocapsid protein of the porcine reproductive and respiratory syndrome virus. *Virus Genes* 42, 76-81.
- Lutz, M.B., Strobl, H., Schuler, G., Romani, N., 2017. GM-CSF Monocyte-Derived Cells and Langerhans Cells As Part of the Dendritic Cell Family. *Frontiers in immunology* 8, 1388.
- Ma, Z.T., Wang, Y.L., Zhao, H.Y., Xu, A.T., Wang, Y.Q., Tang, J., Feng, W.H., 2013. Porcine Reproductive and Respiratory Syndrome Virus Nonstructural Protein 4 Induces Apoptosis Dependent on Its 3C-Like Serine Protease Activity. *PloS one* 8.
- MacLeod, M.K., Kappler, J.W., Marrack, P., 2010. Memory CD4 T cells: generation, reactivation and re-assignment. *Immunology* 130, 10-15.

- Mahanty, S., Hutchinson, K., Agarwal, S., McRae, M., Rollin, P.E., Pulendran, B., 2003. Cutting edge: impairment of dendritic cells and adaptive immunity by Ebola and Lassa viruses. *J Immunol* 170, 2797-2801.
- Maisonasse, P., Bouguyon, E., Piton, G., Ezquerro, A., Urien, C., Deloizy, C., Bourge, M., Leplat, J.J., Simon, G., Chevalier, C., Vincent-Naulleau, S., Crisci, E., Montoya, M., Schwartz-Cornil, I., Bertho, N., 2016. The respiratory DC/macrophage network at steady-state and upon influenza infection in the swine biomedical model. *Mucosal immunology* 9, 835-849.
- Manickam, C., Dwivedi, V., Patterson, R., Papenfuss, T., Renukaradhya, G.J., 2013. Porcine reproductive and respiratory syndrome virus induces pronounced immune modulatory responses at mucosal tissues in the parental vaccine strain VR2332 infected pigs. *Vet Microbiol* 162, 68-77.
- Mantovani, A., Biswas, S.K., Galdiero, M.R., Sica, A., Locati, M., 2013. Macrophage plasticity and polarization in tissue repair and remodelling. *The Journal of pathology* 229, 176-185.
- Martinez, F.O., Gordon, S., 2014. The M1 and M2 paradigm of macrophage activation: time for reassessment. *F1000prime reports* 6, 13.
- Mellins, E.D., Stern, L.J., 2014. HLA-DM and HLA-DO, key regulators of MHC-II processing and presentation. *Current opinion in immunology* 26, 115-122.
- Meurens, F., Summerfield, A., Nauwynck, H., Saif, L., Gerdt, V., 2012. The pig: a model for human infectious diseases. *Trends in microbiology* 20, 50-57.
- Miguel, J.C., Chen, J., Van Alstine, W.G., Johnson, R.W., 2010. Expression of inflammatory cytokines and Toll-like receptors in the brain and respiratory tract of pigs infected with porcine reproductive and respiratory syndrome virus. *Veterinary immunology and immunopathology* 135, 314-319.
- Mildner, A., Jung, S., 2014. Development and function of dendritic cell subsets. *Immunity* 40, 642-656.
- Miller, L.C., Lager, K.M., Kehrli, M.E., Jr., 2009. Role of Toll-like receptors in activation of porcine alveolar macrophages by porcine reproductive and respiratory syndrome virus. *Clin Vaccine Immunol* 16, 360-365.
- Mills, C.D., Ley, K., 2014. M1 and M2 macrophages: the chicken and the egg of immunity. *Journal of innate immunity* 6, 716-726.
- Molina, R.M., Cha, S.H., Chittick, W., Lawson, S., Murtaugh, M.P., Nelson, E.A., Christopher-Hennings, J., Yoon, K.J., Evans, R., Rowland, R.R., Wu, W., Zimmerman, J.J., 2008. Immune response against porcine reproductive and respiratory syndrome virus during acute and chronic infection. *Veterinary immunology and immunopathology* 126, 283-292.
- Murray, P.J., Allen, J.E., Biswas, S.K., Fisher, E.A., Gilroy, D.W., Goerdts, S., Gordon, S., Hamilton, J.A., Ivashkiv, L.B., Lawrence, T., Locati, M., Mantovani, A., Martinez, F.O., Mege, J.L., Mosser, D.M., Natoli, G., Saeij, J.P., Schultze, J.L., Shirey, K.A., Sica, A., Suttles, J., Udalova, I., van Ginderachter, J.A., Vogel, S.N., Wynn, T.A., 2014. Macrophage activation and polarization: nomenclature and experimental guidelines. *Immunity* 41, 14-20.
- Murtaugh, M.P., Stadejek, T., Abrahante, J.E., Lam, T.T., Leung, F.C., 2010. The ever-expanding diversity of porcine reproductive and respiratory syndrome virus. *Virus research* 154, 18-30.

- Nagai, M., Azuma, E., Qi, J., Kumamoto, T., Hiratake, S., Hirayama, M., Umemoto, M., Komada, Y., Sakurai, M., 1998. Suppression of alloreactivity with gamma delta T-cells: relevance to increased gamma delta T-cells following bone marrow transplantation. *Biomedicine & pharmacotherapy = Biomedecine & pharmacotherapie* 52, 137-142.
- Nagy, Z.A., 2012. Alloreactivity: an old puzzle revisited. *Scandinavian journal of immunology* 75, 463-470.
- Nan, Y., Wu, C., Gu, G., Sun, W., Zhang, Y.J., Zhou, E.M., 2017. Improved Vaccine against PRRSV: Current Progress and Future Perspective. *Frontiers in microbiology* 8, 1635.
- Nauwynk, U.U.K.a.H.J., 2013. Pathogenesis and prevention of placental and transplacental porcine reproductive and respiratory syndrome virus infection. *Vet Research* 44.
- Nedumpun, T., Sirisereewan, C., Thanmuan, C., Techapongtada, P., Puntarotairung, R., Naraprasertkul, S., Thanawongnuwech, R., Suradhat, S., 2018. Induction of porcine reproductive and respiratory syndrome virus (PRRSV)-specific regulatory T lymphocytes (Treg) in the lungs and tracheobronchial lymph nodes of PRRSV-infected pigs. *Veterinary microbiology* 216, 13-19.
- Nelsen, C.J., Murtaugh, M.P., Faaberg, K.S., 1999. Porcine reproductive and respiratory syndrome virus comparison: divergent evolution on two continents. *J Virol* 73, 270-280.
- Nesvizhskii, A.I., Keller, A., Kolker, E., Aebersold, R., 2003. A statistical model for identifying proteins by tandem mass spectrometry. *Analytical chemistry* 75, 4646-4658.
- Niebling, W.L., Pierce, S.K., 1993. Antigen Entry into Early Endosomes Is Insufficient for Mhc Class-II Processing. *Journal of immunology* 150, 2687-2697.
- Niederwerder, M.C., Bawa, B., Seroo, N.V., Tribble, B.R., Kerrigan, M.A., Lunney, J.K., Dekkers, J.C., Rowland, R.R., 2015. Vaccination with a Porcine Reproductive and Respiratory Syndrome (PRRS) Modified Live Virus Vaccine Followed by Challenge with PRRS Virus and Porcine Circovirus Type 2 (PCV2) Protects against PRRS but Enhances PCV2 Replication and Pathogenesis Compared to Results for Nonvaccinated Cochallenged Controls. *Clinical and vaccine immunology : CVI* 22, 1244-1254.
- Okragly, A.J., Hanby-Florida, M., Baldwin, C.L., 1995. Monocytes control gamma/delta T-cell responses by a secreted product. *Immunology* 86, 599-605.
- Osorio, F.A., Galeota, J.A., Nelson, E., Brodersen, B., Doster, A., Wills, R., Zuckermann, F., Laegreid, W.W., 2002. Passive transfer of virus-specific antibodies confers protection against reproductive failure induced by a virulent strain of porcine reproductive and respiratory syndrome virus and establishes sterilizing immunity. *Virology* 302, 9-20.
- Patel, D., Nan, Y., Shen, M., Ritthipichai, K., Zhu, X., Zhang, Y.J., 2010. Porcine reproductive and respiratory syndrome virus inhibits type I interferon signaling by blocking STAT1/STAT2 nuclear translocation. *Journal of virology* 84, 11045-11055.
- Peng, Y.T., Chaung, H.C., Chang, H.L., Chang, H.C., Chung, W.B., 2009. Modulations of phenotype and cytokine expression of porcine bone marrow-derived dendritic

- cells by porcine reproductive and respiratory syndrome virus. *Vet Microbiol* 136, 359-365.
- Pennock, N.D., White, J.T., Cross, E.W., Cheney, E.E., Tamburini, B.A., Kedl, R.M., 2013. T cell responses: naive to memory and everything in between. *Advances in physiology education* 37, 273-283.
- Pepper, M., Jenkins, M.K., 2011a. Origins of CD4(+) effector and central memory T cells. *Nature immunology* 12, 467-471.
- Pepper, M., Jenkins, M.K., 2011b. Origins of CD4(+) effector and central memory T cells. *Nature immunology* 12, 467-471.
- Perdiguero, E.G., Geissmann, F., 2016. The development and maintenance of resident macrophages. *Nature immunology* 17, 2-8.
- Petry, D.B., Lunney, J., Boyd, P., Kuhar, D., Blankenship, E., Johnson, R.K., 2007. Differential immunity in pigs with high and low responses to porcine reproductive and respiratory syndrome virus infection. *J Anim Sci* 85, 2075-2092.
- Pierre, P., Mellman, I., 1998. Developmental regulation of invariant chain proteolysis controls MHC class II trafficking in mouse dendritic cells. *Cell* 93, 1135-1145.
- Pitkin, A., Deen, J., Dee, S., 2009. Further assessment of fomites and personnel as vehicles for the mechanical transport and transmission of porcine reproductive and respiratory syndrome virus. *Can J Vet Res* 73, 298-302.
- Rahe, M.C., Murtaugh, M.P., 2017. Mechanisms of Adaptive Immunity to Porcine Reproductive and Respiratory Syndrome Virus. *Viruses* 9.
- Randolph, G.J., Angeli, V., Swartz, M.A., 2005. Dendritic-cell trafficking to lymph nodes through lymphatic vessels. *Nat Rev Immunol* 5, 617-628.
- Reeth, K.V., 1997. Pathogenesis and clinical aspects of a respiratory porcine reproductive and respiratory syndrome virus infection. *Veterinary Microbiology* 55, 223-230.
- Reutner, K., Leitner, J., Müllebnner, A., Ladinig, A., Essler, S.E., Duvalgneau, J.C., Ritzmann, M., Steinberger, P., Saalmuller, A., Gerner, W., 2013. CD27 expression discriminates porcine T helper cells with functionally distinct properties. *Veterinary research* 44, 18.
- Rezende, R.M., Lanser, A.J., Rubino, S., Kuhn, C., Skillin, N., Moreira, T.G., Liu, S., Gabriely, G., David, B.A., Menezes, G.B., Weiner, H.L., 2018. gammadelta T cells control humoral immune response by inducing T follicular helper cell differentiation. *Nature communications* 9, 3151.
- Riese, R.J., Mitchell, R.N., Villadangos, J.A., Shi, G.P., Palmer, J.T., Karp, E.R., De Sanctis, G.T., Ploegh, H.L., Chapman, H.A., 1998. Cathepsin S activity regulates antigen presentation and immunity. *Journal of Clinical Investigation* 101, 2351-2363.
- Rocha, N., Neefjes, J., 2008. MHC class II molecules on the move for successful antigen presentation. *The EMBO journal* 27, 1-5.
- Rodriguez-Gomez, I.M., Gomez-Laguna, J., Barranco, I., Pallares, F.J., Ramis, G., Salguero, F.J., Carrasco, L., 2012. Downregulation of Antigen-Presenting Cells in Tonsil and Lymph Nodes of Porcine Reproductive and Respiratory Syndrome Virus-Infected Pigs. *Transboundary and emerging diseases*.
- Rodriguez-Gomez, I.M., Kaser, T., Gomez-Laguna, J., Lamp, B., Sinn, L., Rumenapf, T., Carrasco, L., Saalmuller, A., Gerner, W., 2015. PRRSV-infected monocyte-derived dendritic cells express high levels of SLA-DR and CD80/86 but do not

- stimulate PRRSV-naive regulatory T cells to proliferate. *Veterinary research* 46, 54.
- Rosendahl Huber, S., van Beek, J., de Jonge, J., Luytjes, W., van Baarle, D., 2014. T cell responses to viral infections - opportunities for Peptide vaccination. *Frontiers in immunology* 5, 171.
- Rowland, R.R., 2010. The interaction between PRRSV and the late gestation pig fetus. *Virus research* 154, 114-122.
- Rowland, R.R., Kervin, R., Kuckleburg, C., Sperlich, A., Benfield, D.A., 1999. The localization of porcine reproductive and respiratory syndrome virus nucleocapsid protein to the nucleolus of infected cells and identification of a potential nucleolar localization signal sequence. *Virus research* 64, 1-12.
- Rowland, R.R., Lawson, S., Rossow, K., Benfield, D.A., 2003. Lymphoid tissue tropism of porcine reproductive and respiratory syndrome virus replication during persistent infection of pigs originally exposed to virus in utero. *Veterinary microbiology* 96, 219-235.
- Rowland, R.R., Yoo, D., 2003. Nucleolar-cytoplasmic shuttling of PRRSV nucleocapsid protein: a simple case of molecular mimicry or the complex regulation by nuclear import, nucleolar localization and nuclear export signal sequences. *Virus research* 95, 23-33.
- Saeed, S., Quintin, J., Kerstens, H.H., Rao, N.A., Aghajani-refah, A., Matarese, F., Cheng, S.C., Ratter, J., Berentsen, K., van der Ent, M.A., Sharifi, N., Janssen-Megens, E.M., Ter Huurne, M., Mandoli, A., van Schaik, T., Ng, A., Burden, F., Downes, K., Frontini, M., Kumar, V., Giamarellos-Bourboulis, E.J., Ouwehand, W.H., van der Meer, J.W., Joosten, L.A., Wijmenga, C., Martens, J.H., Xavier, R.J., Logie, C., Netea, M.G., Stunnenberg, H.G., 2014. Epigenetic programming of monocyte-to-macrophage differentiation and trained innate immunity. *Science* 345, 1251086.
- Sang, Y., Rowland, R.R., Blecha, F., 2011. Interaction between innate immunity and porcine reproductive and respiratory syndrome virus. *Anim Health Res Rev* 12, 149-167.
- Schafer, P.H., Malapati, S., Hanfelt, K.K., Pierce, S.K., 1998. The assembly and stability of MHC class II-(alpha beta)₂ superdimers. *Journal of immunology* 161, 2307-2316.
- Schroeder, H.W., Jr., Ippolito, G.C., Shiokawa, S., 1998. Regulation of the antibody repertoire through control of HCDR3 diversity. *Vaccine* 16, 1383-1390.
- Sercarz, E.E., Maverakis, E., 2003. MHC-guided processing: Binding of large antigen fragments. *Nature Reviews Immunology* 3, 621-629.
- Shi, G.P., Bryant, R.A.R., Riese, R., Verhelst, S., Driessen, C., Li, Z.Q., Bromme, D., Ploegh, H.L., Chapman, H.A., 2000. Role for cathepsin F in invariant chain processing and major histocompatibility complex class II peptide loading by macrophages. *Journal of Experimental Medicine* 191, 1177-1185.
- Shi, G.P., Villadangos, J.A., Dranoff, G., Small, C., Gu, L.J., Haley, K.J., Riese, R., Ploegh, H.L., Chapman, H.A., 1999. Cathepsin S required for normal MHC class II peptide loading and germinal center development. *Immunity* 10, 197-206.

- Shi, M., Lam, T.T.-Y., Hon, C.-C., Hui, R.K.-H., Faaberg, K.S., Wennblom, T., Murtaugh, M.P., Stadejek, T., Leung, F.C.-C., 2010. Molecular epidemiology of PRRSV: A phylogenetic perspective. *Virus research* 154, 7-17.
- Shi, X., Wang, L., Li, X., Zhang, G., Guo, J., Zhao, D., Chai, S., Deng, R., 2011. Endoribonuclease activities of porcine reproductive and respiratory syndrome virus nsp11 was essential for nsp11 to inhibit IFN-beta induction. *Molecular immunology* 48, 1568-1572.
- Silva-Campa, E., Flores-Mendoza, L., Resendiz, M., Pinelli-Saavedra, A., Mata-Haro, V., Mwangi, W., Hernandez, J., 2009. Induction of T helper 3 regulatory cells by dendritic cells infected with porcine reproductive and respiratory syndrome virus. *Virology* 387, 373-379.
- Singer, A., Adoro, S., Park, J.H., 2008. Lineage fate and intense debate: myths, models and mechanisms of CD4- versus CD8-lineage choice. *Nature reviews. Immunology* 8, 788-801.
- Skruber, K., Read, T.A., Vitriol, E.A., 2018. Reconsidering an active role for G-actin in cytoskeletal regulation. *Journal of cell science* 131.
- Song, C., Krell, P., Yoo, D., 2010. Nonstructural protein 1 α subunit-based inhibition of NF- κ B activation and suppression of interferon- β production by porcine reproductive and respiratory syndrome virus. *Virology* 407, 268-280.
- Stadejek, T., Stankevicius, A., Murtaugh, M.P., Oleksiewicz, M.B., 2013. Molecular evolution of PRRSV in Europe: current state of play. *Veterinary microbiology* 165, 21-28.
- Subramaniam, S., Sur, J.H., Kwon, B., Pattnaik, A.K., Osorio, F.A., 2011. A virulent strain of porcine reproductive and respiratory syndrome virus does not up-regulate interleukin-10 levels in vitro or in vivo. *Virus research* 155, 415-422.
- Summerfield, A., Meurens, F., Ricklin, M.E., 2015. The immunology of the porcine skin and its value as a model for human skin. *Molecular immunology* 66, 14-21.
- Sun, Z., Chen, Z., Lawson, S.R., Fang, Y., 2010. The cysteine protease domain of porcine reproductive and respiratory syndrome virus nonstructural protein 2 possesses deubiquitinating and interferon antagonism functions. *Journal of virology* 84, 7832-7846.
- Sun, Z., Li, Y., Ransburgh, R., Snijder, E.J., Fang, Y., 2012. Nonstructural protein 2 of porcine reproductive and respiratory syndrome virus inhibits the antiviral function of interferon-stimulated gene 15. *Journal of virology* 86, 3839-3850.
- Swain, S.L., McKinstry, K.K., Strutt, T.M., 2012a. Expanding roles for CD4(+) T cells in immunity to viruses. *Nature Reviews Immunology* 12, 136-148.
- Swain, S.L., McKinstry, K.K., Strutt, T.M., 2012b. Expanding roles for CD4(+) T cells in immunity to viruses. *Nature reviews. Immunology* 12, 136-148.
- Swenson, S.L., Hill, H.T., Zimmerman, J.J., Evans, L.E., Landgraf, J.G., Wills, R.W., Sanderson, T.P., McGinley, M.J., Brevik, A.K., Ciszewski, D.K., et al., 1994. Excretion of porcine reproductive and respiratory syndrome virus in semen after experimentally induced infection in boars. *J Am Vet Med Assoc* 204, 1943-1948.
- Takamatsu, H.H., Denyer, M.S., Stirling, C., Cox, S., Aggarwal, N., Dash, P., Wileman, T.E., Barnett, P.V., 2006. Porcine gammadelta T cells: possible roles on the innate and adaptive immune responses following virus infection. *Veterinary immunology and immunopathology* 112, 49-61.

- Talker, S.C., Kaser, T., Reutner, K., Sedlak, C., Mair, K.H., Koinig, H., Graage, R., Viehmann, M., Klingler, E., Ladinig, A., Ritzmann, M., Saalmuller, A., Gerner, W., 2013. Phenotypic maturation of porcine NK- and T-cell subsets. *Developmental and comparative immunology* 40, 51-68.
- ten Broeke, T., Wubbolts, R., Stoorvogel, W., 2013. MHC class II antigen presentation by dendritic cells regulated through endosomal sorting. *Cold Spring Harbor perspectives in biology* 5, a016873.
- Tong, G.Z., Zhou, Y.J., Hao, X.F., Tian, Z.J., An, T.Q., Qiu, H.J., 2007. Highly pathogenic porcine reproductive and respiratory syndrome, China. *Emerging infectious diseases* 13, 1434-1436.
- Tsuji, S., Char, D., Bucy, R.P., Simonsen, M., Chen, C.H., Cooper, M.D., 1996. Gamma delta T cells are secondary participants in acute graft-versus-host reactions initiated by CD4+ alpha beta T cells. *European journal of immunology* 26, 420-427.
- Turk, V., Stoka, V., Vasiljeva, O., Renko, M., Sun, T., Turk, B., Turk, D., 2012. Cysteine cathepsins: From structure, function and regulation to new frontiers. *Bba-Proteins Proteom* 1824, 68-88.
- Ulferts, R., Ziebuhr, J., 2011. Nidovirus ribonucleases: Structures and functions in viral replication. *RNA biology* 8, 295-304.
- Van Breedam, W., Delputte, P.L., Van Gorp, H., Misinzo, G., Vanderheijden, N., Duan, X., Nauwynck, H.J., 2010. Porcine reproductive and respiratory syndrome virus entry into the porcine macrophage. *The Journal of general virology* 91, 1659-1667.
- Van Gorp, H., Van Breedam, W., Delputte, P.L., Nauwynck, H.J., 2008. Sialoadhesin and CD163 join forces during entry of the porcine reproductive and respiratory syndrome virus. *The Journal of general virology* 89, 2943-2953.
- van Nispen tot Pannerden, H.E., Geerts, W.J., Kleijmeer, M.J., Heijnen, H.F., 2010. Spatial organization of the transforming MHC class II compartment. *Biology of the cell* 102, 581-591.
- Vantourout, P., Hayday, A., 2013. Six-of-the-best: unique contributions of gammadelta T cells to immunology. *Nature reviews. Immunology* 13, 88-100.
- Varol, C., Mildner, A., Jung, S., 2015. Macrophages: Development and Tissue Specialization. *Annual review of immunology* 33, 643-675.
- Vascotto, F., Lankar, D., Faure-Andre, G., Vargas, P., Diaz, J., Le Roux, D., Yuseff, M.I., Sibarita, J.B., Boes, M., Raposo, G., Mougneau, E., Glaichenhaus, N., Bonnerot, C., Manoury, B., Lennon-Dumenil, A.M., 2007. The actin-based motor protein myosin II regulates MHC class II trafficking and BCR-driven antigen presentation. *The Journal of cell biology* 176, 1007-1019.
- Veit, M., Matczuk, A.K., Sinhadri, B.C., Krause, E., Thaa, B., 2014. Membrane proteins of arterivirus particles: structure, topology, processing and function. *Virus research* 194, 16-36.
- Vignali, D.A., Collison, L.W., Workman, C.J., 2008. How regulatory T cells work. *Nature reviews. Immunology* 8, 523-532.
- Vivier, E., Tomasello, E., Baratin, M., Walzer, T., Ugolini, S., 2008. Functions of natural killer cells. *Nature immunology* 9, 503-510.

- Vyas, J.M., Kim, Y.M., Artavanis-Tsakonas, K., Love, J.C., Van der Veen, A.G., Ploegh, H.L., 2007. Tubulation of class II MHC compartments is microtubule dependent and involves multiple endolysosomal membrane proteins in primary dendritic cells. *Journal of immunology* 178, 7199-7210.
- Vyas, J.M., Van der Veen, A.G., Ploegh, H.L., 2008a. The known unknowns of antigen processing and presentation. *Nature Reviews Immunology* 8, 607-618.
- Vyas, J.M., Van der Veen, A.G., Ploegh, H.L., 2008b. The known unknowns of antigen processing and presentation. *Nature reviews. Immunology* 8, 607-618.
- Wang, G., Song, T., Yu, Y., Liu, Y., Shi, W., Wang, S., Rong, F., Dong, J., Liu, H., Cai, X., Zhou, E.M., 2011. Immune responses in piglets infected with highly pathogenic porcine reproductive and respiratory syndrome virus. *Veterinary immunology and immunopathology* 142, 170-178.
- Wang, I.H., Burckhardt, C.J., Yakimovich, A., Greber, U.F., 2018. Imaging, Tracking and Computational Analyses of Virus Entry and Egress with the Cytoskeleton. *Viruses* 10.
- Wang, X., Eaton, M., Mayer, M., Li, H., He, D., Nelson, E., Christopher-Hennings, J., 2007. Porcine reproductive and respiratory syndrome virus productively infects monocyte-derived dendritic cells and compromises their antigen-presenting ability. *Archives of virology* 152, 289-303.
- Weesendorp, E., Morgan, S., Stockhofe-Zurwieden, N., Popma-De Graaf, D.J., Graham, S.P., Rebel, J.M., 2013. Comparative analysis of immune responses following experimental infection of pigs with European porcine reproductive and respiratory syndrome virus strains of differing virulence. *Veterinary microbiology* 163, 1-12.
- Wen, K., Bui, T., Li, G., Liu, F., Li, Y., Kocher, J., Yuan, L., 2012. Characterization of immune modulating functions of gammadelta T cell subsets in a gnotobiotic pig model of human rotavirus infection. *Comparative immunology, microbiology and infectious diseases* 35, 289-301.
- West, M.A., Wallin, R.P., Matthews, S.P., Svensson, H.G., Zaru, R., Ljunggren, H.G., Prescott, A.R., Watts, C., 2004. Enhanced dendritic cell antigen capture via toll-like receptor-induced actin remodeling. *Science* 305, 1153-1157.
- Wills, R.W., Zimmerman, J.J., Yoon, K.J., Swenson, S.L., Hoffman, L.J., McGinley, M.J., Hill, H.T., Platt, K.B., 1997. Porcine reproductive and respiratory syndrome virus: routes of excretion. *Vet Microbiol* 57, 69-81.
- Wongyanin, P., Buranapraditkul, S., Yoo, D., Thanawongnuwech, R., Roth, J.A., Suradhat, S., 2012. Role of porcine reproductive and respiratory syndrome virus nucleocapsid protein in induction of interleukin-10 and regulatory T-lymphocytes (Treg). *J Gen Virol* 93, 1236-1246.
- Wongyanin, P., Buranapraditkun, S., Chokeshai-Usaha, K., Thanawongnuwech, R., Suradhat, S., 2010. Induction of inducible CD4+CD25+Foxp3+ regulatory T lymphocytes by porcine reproductive and respiratory syndrome virus (PRRSV). *Vet Immunol Immunopathol* 133, 170-182.
- Yoo, D., Song, C., Sun, Y., Du, Y., Kim, O., Liu, H.C., 2010. Modulation of host cell responses and evasion strategies for porcine reproductive and respiratory syndrome virus. *Virus research* 154, 48-60.
- Zhang, H., Guo, X., Ge, X., Chen, Y., Sun, Q., Yang, H., 2009. Changes in the cellular proteins of pulmonary alveolar macrophage infected with porcine reproductive

- and respiratory syndrome virus by proteomics analysis. *Journal of proteome research* 8, 3091-3097.
- Zhang, H., Guo, X., Nelson, E., Christopher-Hennings, J., Wang, X., 2012. Porcine reproductive and respiratory syndrome virus activates the transcription of interferon alpha/beta (IFN- α/β) in monocyte-derived dendritic cells (Mo-DC). *Veterinary Microbiology* 159, 494-498.
- Zheng, J., Liu, Y., Lau, Y.L., Tu, W., 2013. gammadelta-T cells: an unpolished sword in human anti-infection immunity. *Cellular & molecular immunology* 10, 50-57.
- Zhou, L., Yang, H., 2010. Porcine reproductive and respiratory syndrome in China. *Virus research* 154, 31-37.
- Zhou, L., Zhang, J., Zeng, J., Yin, S., Li, Y., Zheng, L., Guo, X., Ge, X., Yang, H., 2009. The 30-amino-acid deletion in the Nsp2 of highly pathogenic porcine reproductive and respiratory syndrome virus emerging in China is not related to its virulence. *Journal of virology* 83, 5156-5167.